The University Of Sheffield.

The effect of osmolytes on the protein barnase

By:

Yashwanth Kumar Demakethepalli Ramamurthy

A thesis submitted in partial fulfilment of the requirements for the degree of Doctor of Philosophy

The University of Sheffield

Faculty of Science

Department of Molecular Biology and Biotechnology Firth Court, Western Bank, Sheffield S10 2TN

September 2021

PREFACE

This thesis describes the work conducted at the Department of Molecular Biology and Biotechnology of the University of Sheffield for the degree of Doctor of Philosophy. Some part of this thesis was conducted at the department of Chemical and Biological Engineering. This work was conducted between October 2017 and September 2021 under the supervision of Prof. Mike P Williamson. This thesis is my original work, and no part of this thesis is conducted at any other place or submitted for the award of any diploma/degree anywhere.

Yashwanth Kumar D R

Department of MBB,

September 2021

ACKNOWLEDGEMENT

I would like to thank my supervisor Mike P Williamson for his constant guidance and encouragement without which this PhD thesis would not have been possible.

I am grateful to the Faculty of Science for providing full scholarship for 3.5 years to pursue my PhD degree.

I am thankful to Dr. Robert Falconer for guidance and Department of Chemical and Biological Engineering for allowing me to conduct my DSC experiments.

I would like to thank Dr. Clare Trevitt, who was a postdoc in our group for her guidance and teaching. I also acknowledge her work in my thesis.

I am thankful to Dr. Andrea Hounslow who was our NMR manager for her constant help and support in conducting NMR experiments.

I would like to thank my fellow PhD students Dr. Henry P Wood and Dr. Francisco Aarón Cruz Navarrete for their constant help and motivation in me learning various techniques.

I would like to thank my other fellow PhD students Dr. Mahreen Hassan and Adam Flinders for their help and support during my PhD. I thank all the members of BioNMR group for their cooperation.

Finally, I would like to thank my parents, family, friends, and teachers back home in India for their constant support and encouragement.

Abstract

Studying the role of various factors like pressure both osmotic and hydrostatic, temperature, and chemical denaturants on protein structure, function, solubility and stability is very helpful in understanding many biochemical processes. Franz Hofmeister has studied the salting out properties of salts on proteins and has derived a lyotropic series of ions. According to the structure maker/breaker theory, kosmotropes withdraw water from the protein decreasing solubility and increasing stability, whilst chaotropes are weak in withdrawing water, increasing solubility and decreasing stability. Jordan Bye and coworkers refined the structure maker/breaker theory and focused on the water organizing ability of ions rather than direct interactions with protein surfaces. Their findings confirm that sulphate stabilizes whilst thiocyanate destabilizes proteins. It is believed that osmolytes like TMAO, ectoine, and betaine that are produced and accumulated by marine organisms as an intracellular solute, to counteract the destabilizing effects of osmotic stress, denaturants such as urea, and high pressure can counteract protein destabilizing effects and enable the cells to carry out cellular functions without affecting protein structure. We have tested the hypothesis that osmolytes work in a similar manner to Hofmeister series ions: that they interact strongly with water and compete with the protein for water binding, which is how they counteract the effect of urea. To find this we have studied the effect of TMAO, ectoine, and betaine on barnase by ^{15}N HSQC, ^{13}C HSQC, and 2D-HNCO experiments and compared them to the effect of sodium thiocyanate on barnase. We have also studied the effects of osmolytes on protein denaturants like urea by ^{1}H NMR. DSC results suggest that TMAO may not strongly stabilize the protein by itself but can counteract the destabilizing effects of urea. NMR data show that the effects of osmolytes on NMR spectra of the protein barnase are smaller than those of typical Hofmeister ions such as sulphate and thiocyanate. NMR $\Delta\delta$ also show that ectoine binds very weakly and betaine does not bind, TMAO binds stronger than other osmolytes and chloride but weaker than sulphate and thiocyanate. Osmolytes have a clear influence on protein stability, but they clearly do this without significant protein binding. Data from mixed osmolyte solutions also suggest that osmolytes do not bind to urea either. All this data suggests that binding may not be necessary to cause chemical shift changes and effects of ions on protein is independent of their ability to bind. All this implies that osmolytes affect the protein stability by their ability to withdraw water from the protein surface – and therefore counteract the perturbations induced by other solutes.

Table of Contents

List of Figures

1 Chapter 1: Introduction to Hofmeister series anions and osmolytes

1.1 What are Hofmeister effects?

Protein solubility and stability play a major role in biochemical processes of all living organisms. Understanding the factors affecting solvation of hydrophobic surfaces and nonpolar molecules is critical. Franz Hofmeister studied the salting out properties of salts on proteins and derived a lyotropic series of ions based on their ability to withdraw water and precipitate egg white protein (Hofmeister, 1888) as seen in Figure 1.1. Lyotropy describes the effect of solutes on surface tension of solutions and their ability to precipitate (Melander and Horvath, 1977). He published this in German literature which was translated to English very recently by Jungwirth and Cremer (2014) and Jungwirth (2015). He distinguished the effects of anions and cations in two Hofmeister series.

Figure 1.1. Plaque in memory of Hofmeister at the building of the Charles University (Jungwirth and Cremer, 2014). "Reprinted with permission from Springer Nature: Nature Chemistry, Beyond Hofmeister, Pavel Jungwirth et al 2014."

Arrhenius and Ostwald's theory of electrolytic dissociation explains how salts dissociate into ions in water (Jungwirth and Cremer, 2014, Okur et al., 2017). This also played

a major role in Hofmeister's work. He studied salting out of not just proteins but also gelatin, ferric oxide and sodium oleate (Okur et al., 2017). This led to the structure maker/breaker theory on the ability of salts to solubilize proteins (Hofmeister, 1888, Jungwirth and Cremer, 2014, Jungwirth, 2015).

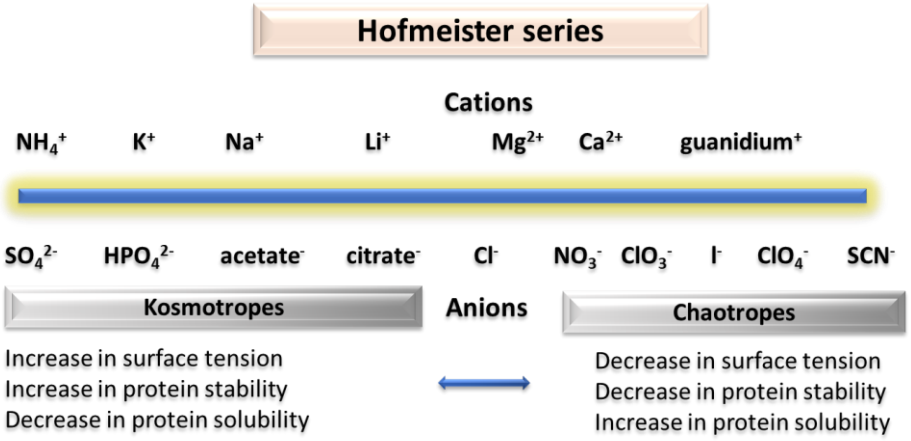

Figure 1.2. Hofmeister series of cations and anions and their properties. Anions on the left i.e., sulfate to citrate are kosmotropes and anions on the right i.e., from nitrate to thiocyanate are chaotropes. Chloride is in the middle of kosmotropes and chaotropes. "Adapted with permission from OKUR, H. I., HLADILKOVA, J., REMBERT, K. B., CHO, Y., HEYDA, J., DZUBIELLA, J., CREMER, P. S. & JUNGWIRTH, P. 2017. Beyond the Hofmeister series: ion-specific effects on proteins and their biological functions. Journal of Physical Chemistry B, 121, 1997-2014. Copyright © 2017, American Chemical Society."

In this theory, ions on the left side of the Hofmeister series are Kosmotropes and those placed on the right side are Chaotropes as seen in Figure 1.2. According to this theory salts that withdraw water from the protein decrease solubility and are kosmotropes, and those that are weak in withdrawing water increase solubility and are called chaotropes. From Figure 1.2, kosmotropes are strongly hydrated, high charge density anions that steal water and salt out the proteins. Chaotropes are weakly hydrated, low charge density anions that cannot order water molecules causing salting in of proteins. Study of the hydration abilities of anions gives us an insight in to how these ions interact with solute and solvent. The size of hydrated ions is directly related to their hydration free energy. Also, ions with strong hydration compete with protein to interact with water. Kosmotropic ions are structure makers and increase hydrogen bonding in water whilst chaotropes decrease hydrogen bonding in water. This water withdrawing effect of salts can be related to their hydration strength (Jungwirth and Cremer, 2014, Jungwirth, 2015). These effects are observed at concentrations of Hofmeister anions from 100 to 2000 mM (Bye et al 2016). Sulphate and thiocyanate are good examples of kosmotropes and chaotropes respectively. Chloride has medium to neutral effects and is in

between stabilizers and destabilizers. This water structure maker/breaker theory dominated thinking on the Hofmeister effects until the 1980s, when a range of experimental and molecular dynamics studies appeared which suggested that the effects of solutes on water structure did not extend far enough into solution to lead to effects as large as those described by the Hofmeister series. Since then, there have been 3 main theories proposed on how Hofmeister ions affect protein stability and solubility.

The Preferential interaction theory says that kosmotropes are preferentially excluded from the protein surface, stabilize the proteins, and precipitate the protein whereas chaotropes preferentially interact with protein surfaces, destabilize the proteins, and increase solubility (Timasheff, 1993, Timasheff, 2002). On the other hand, preferential hydration and volume excluded effect theories explain that kosmotropes exert excluded volume effects by withdrawing free water (Bye et al 2016). In preferential hydration effect theory cosolutes are preferentially hydrated and do not make direct interactions with the protein which makes more water molecules available to interact with the protein surface thereby precipitating and stabilizing the protein (Timasheff, 2002). In volume excluded effect theory cosolutes in the bulk water increase the osmotic pressure surrounding the protein and cause the protein to favour the folded state as proteins have a smaller surface area when in folded state (Liu and Bolen, 1995, Santoro et al., 1992). It also assumes that a cosolute in the bulk water is excluded from the protein surface and this preferential exclusion leads to an increase in stability and decrease in solubility. All these theories (preferential interaction, preferential hydration and volume excluded effect) have good arguments to support them. It is not clear whether they are different, or just different ways of explaining the same thing, and it is clear that the exact mechanism behind these effects is not either properly understood or validated.

Raman spectroscopy studies find that ions do not have long range effects (Smith et al., 2007) and molecular dynamic simulation studies reveal that ions influence only those water molecules that are close to them, and that beyond 1 nm ion–water interactions are very minimal (Pluharova et al., 2017). Effects of salts on water molecules outside their immediate hydration layer are also minute. But experiments on water-salt interactions using pressure perturbation calorimetry contradict this (Bye and Falconer, 2015). Heat on pressurization (ΔQ) values at various salt concentrations indicate that the change in molar enthalpy relative to pure water is not linear even at infinite dilution. This suggests that salt-water interactions may still be significant outside the first hydration layer (Bye et al., 2014).

1.2 Role of free energy

Studying how salts affect the free energy of protein components helps to understand different mechanisms of salt-protein interactions (Robinson and Jencks, 1965). The free energy of the native state of proteins is a sum of the free energies of individual residue-residue and residue-solvent interactions (von Hippel and Schleich, 1969). Protein stability can be defined as the difference in the free energy of folded and unfolded state. The hydrogen bonding potential between amide and carboxyl groups is one of the factors that affect the configuration of the polypeptide (von Hippel and Schleich, 1969, Kauzmann, 1959). As denaturants are added, the spatial arrangement of the polypeptide is disordered leading to a loss of intra molecular hydrogen bonding inside the protein, and hydrogen bonding between protein and water will increase ultimately leading to protein denaturation. A decrease of a few joules per mole could alter a protein's three-dimensional structure. Thermodynamic balance affects protein stability and solubility. Solubility and thermodynamic quantities greatly influence hydrophobic collapse. The hydrophobicity of a protein is the sum of the hydrophobicities of all the amino acid residues in a protein molecule. Destabilizers alter the free energy between peptide group and solvent, and side chains and solvent (Nozaki and Tanford, 1963).

1.2.1 Role of free energy in salting in/salting out

Melander and Horvath (1977) studied the effect of salt on electrostatic and hydrophobic interactions and showed that its role in hydrophobic affinity chromatography explains the lyotropic properties of salts. This led to a salting out theory that explains protein solubility (Melander and Horvath, 1977). According to this theory, the salting out effects on protein are determined from the standard state chemical potentials on salt concentration, which can be approximated to the solvation free energy of the protein molecule. Calculating the product of surface free energy and solvent accessible surface area gives the solvation free energy, which determines salting out of proteins. Favourable protein-salt interactions decrease solvation free energy leading to salting-in and an increase in solubility, and reduced stability (Curtis et al., 2002).

Salt effects on proteins can be understood by studying protein-salt interactions at three different types of sites on the protein molecule: with exposed peptide groups, nonpolar groups, and charged groups (von Hippel and Schleich, 1969, Robinson and Jencks, 1965). At low ionic strength, a charged protein is a simple ion and the higher the concentration of salt, the smaller

the average distance between charged groups. Measuring molal surface tension increment of the salts (equal to the derivative of surface tension of solution with respect to salt molarity) gives us an idea of its hydrophobic interactions (Melander and Horvath, 1977). Salts increase the surface tension of solutions. Hence the solubility of non-polar substances also depends on surface tension of the solvent. Hydrophobic free energy change is related to non-polar areas of contact and surface tension of salt solutions. Unfavourable protein-salt interactions at non-polar groups are mostly observed in salting out effects compared to interactions with charged surface and peptide groups (Curtis et al., 2002). This salting out makes the protein stable.

1.3 Effect of temperature on protein denaturation

At high temperature, thermal energy breaks down hydrogen bonds, thereby denaturing proteins (Dill and Shortle, 1991, Dill, 1990), while low temperatures increase the enthalpically driven interactions between protein hydrophobic interior groups and water molecules (Privalov, 1990, Tsai et al., 2002). This cold denaturation is consistent with the effect of Hofmeister ions on poly(N-isopropylacrylamide) (PNIPAM): chaotropes decrease the lower critical solution temperature (LCST) in PNIPAM causing hydrophobic collapse (Zhang and Cremer, 2010).

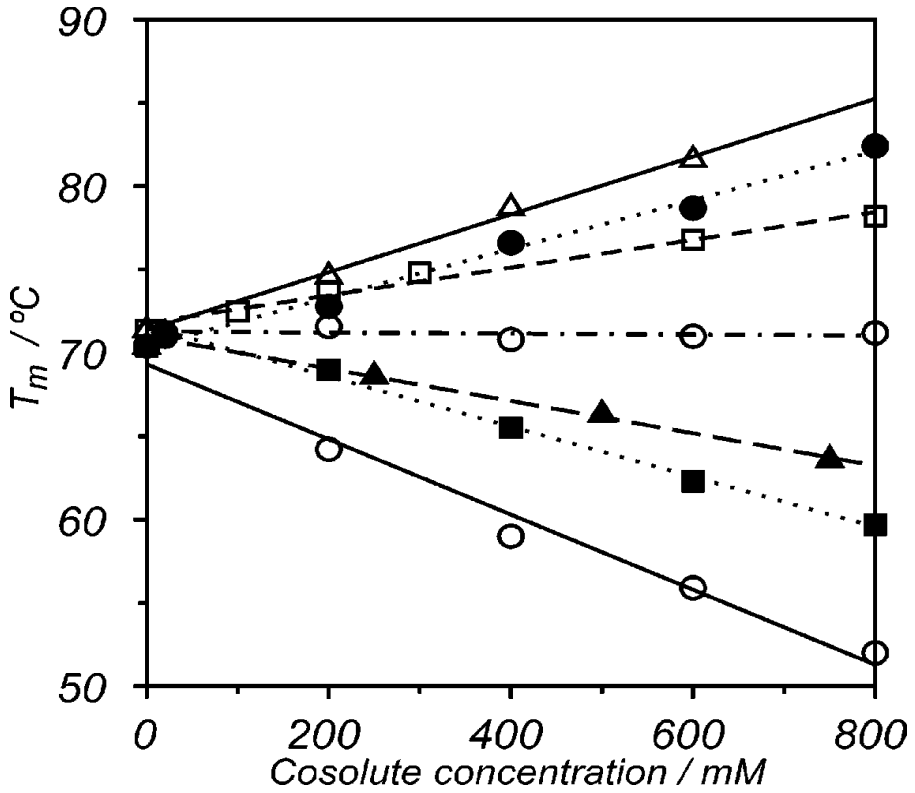

Figure 1.3. Dependence of T_m values on solute concentration from circular dichroism and fluorescence spectroscopy; only differential scanning calorimetry is used in the case of sodium nitrate. Sulphate (Δ, solid line), phosphate (●, dotted line), fluoride (O, dashed line), chloride (O, dashed-dotted line), nitrate (▲, dashed line), perchlorate (■ , dotted line), and thiocyanate (O, solid line. The linear effects observed indicate that stabilizing effects follow the Hofmeister series (Sulphate > phosphate > fluoride> chloride > nitrate > perchlorate > thiocyanate). "Reprinted (adapted) with permission from Tadeo, X., Pons, M. & Millet, O. 2007. Influence of the Hofmeister anions on protein stability as studied by thermal denaturation and chemical shift perturbation. Biochemistry, 46, 917-923. Copyright © 2007, American Chemical Society."

Tadeo et al., 2007 studied the effects of various lyotropic salts on the thermal stability of the IgG binding domain of B1 protein L (ProtL) by circular dichroism, fluorescence spectroscopy, and differential scanning calorimetry as seen in Figure 1.3. Their findings support volume exclusion and preferential solvation models.

1.4 Refinement of Structure maker/breaker theory

Jordan Bye and coworkers refined the structure maker/breaker theory and concluded that the effect of ions resulted from their water organizing ability rather than direct interactions with protein surfaces.

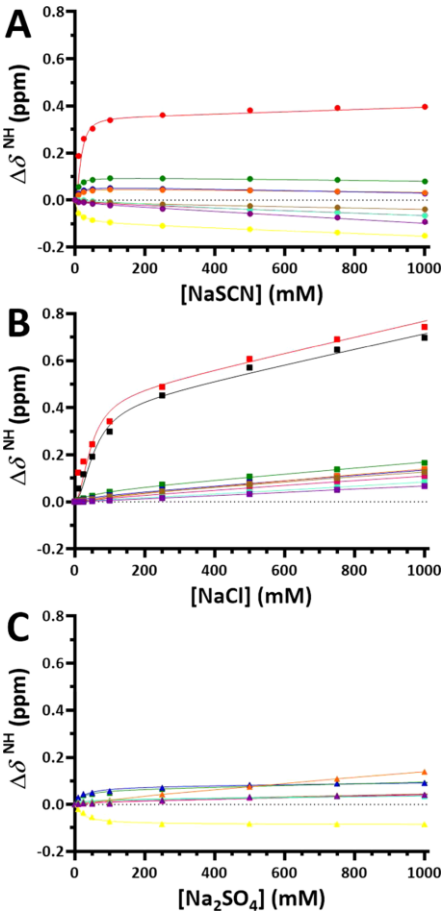

Figure 1.4. Linear chemical shift changes of amide group protons of different amino acids in the presence of various salts at concentrations above 250 mM is observed. A. Sodium thiocyanate. B. Sodium chloride. C. Sodium sulfate. "Reprinted (adapted) with permission from Bye et al., 2016 and any further permissions should be directed to the ACS."

Observation of chemical shift changes in NMR in barnase found two behaviours: Hofmeister ions bind to protein surfaces mostly at the peptide backbone and not with non-polar groups at concentrations less than 100 mM, with no further increase in interactions between protein surface and anions at higher concentrations up to 1000 mM. Linear chemical shift changes are observed from 100 – 1000 mM (Figure 1.4) (Bye et al., 2016).

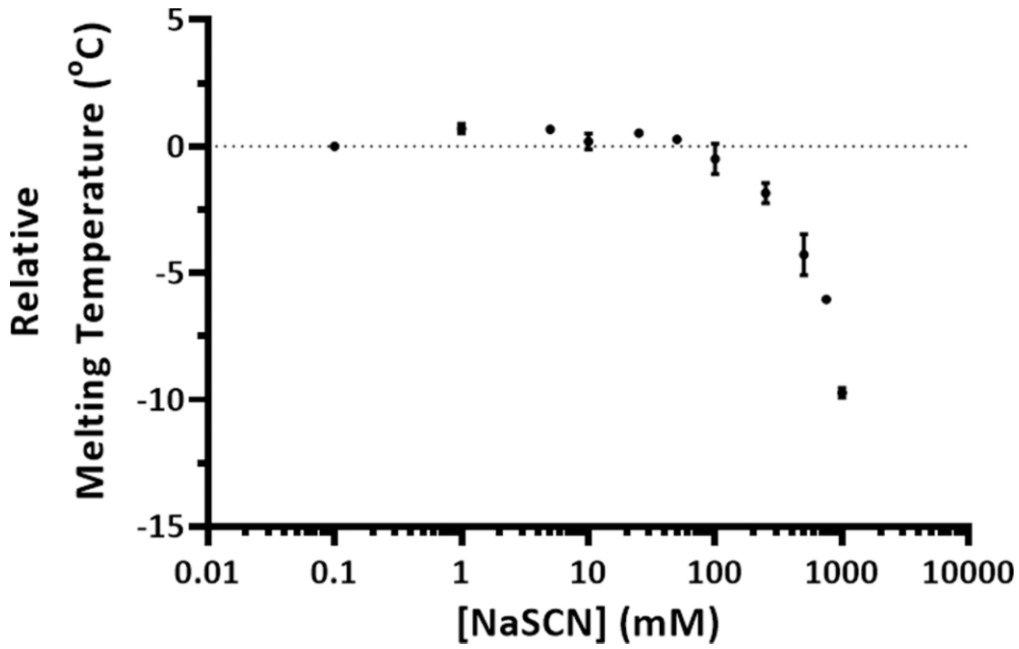

Figure 1.5. DSC studies showing change in T_m of barnase in the presence of increasing concentrations of sodium thiocyanate. "Reprinted (adapted) with permission from Bye et al., 2016 and any further permissions should be directed to the ACS."

Differential scanning calorimetry studies reveal that both sulphate and thiocyanate have two-stage effects. At concentrations less than 100 mM, the former does not affect T_m and the latter has a small stabilizing effect (Figure 1.5). As the concentration increases, binding patterns disappear, and sulphate is found to decrease T_m whilst thiocyanate increases Tm. Another anion, chloride, has smaller stabilizing effects at low concentrations but no significant effects are observed at concentrations 100 – 1000 mM. The study concluded that interaction between water molecules is strengthened in the presence of sulphate and chloride, whilst the presence of thiocyanate weakens water – water interactions and strengthens water – protein interactions (Bye et al., 2016).

Sulphate orders water molecules around itself seizing water molecules from the protein. This makes water dipoles less available; the protein is outcompeted and intramolecular interactions in the protein are strengthened. Also, the free energy of the unfolded protein is increased which preferentially stabilizes the folded protein, thus decreasing solubility and increasing stability. This implies that kosmotropes work by being stabilizers. Thiocyanate is less able to withdraw/order water, allowing more water molecules to hydrogen bond with protein, which loosely organizes water molecules: in fact they organize water more loosely than water itself. This poor organization of water molecules allows more water molecules to hydrogen bond with protein, increasing solubility and decreasing stability (Bye et al., 2016).

This proves that chaotropes are destabilizers. These findings show the limitations in the previously discussed preferential hydration, preferential interaction and volume excluded models and make them invalid.

1.5 Inverse Hofmeister series

The charge on protein molecules also determines their interactions with Hofmeister ions (Bostrom et al., 2005). Anions bind to nitrogen atoms because they carry a positive charge whilst cations bind to the oxygen atom in the carboxyl group which carry a partial negative charge (Melander and Horvath, 1977). This follows the inverse Hofmeister series, meaning that ions stabilize and solubilize proteins in the opposite order to the conventional Hofmeister series. Inverse Hofmeister effects are also observed for positively charged proteins while normal Hofmeister effects are observed for proteins like lysozyme at a pH above their isoelectric point. In liquid-liquid phase separation of lysozyme, it is observed that lysozyme follows inverse Hofmeister at lower concentrations and reverts to direct Hofmeister when concentration is increased (Zhang and Cremer, 2010, Bostrom et al., 2005). Inverse Hofmeister is observed for monovalent anion electroselectivities as well. Not just the interaction of water and solutes with protein but increase in protein-protein interactions also results in lower solubility and increased stability (Melander and Horvath, 1977).

1.6 Osmolytes

Protein structure and function are highly affected by various factors like pressure (both osmotic and hydrostatic), temperature, and chemical denaturants. Osmolytes are low molecular weight compounds that can counteract these effects and enable the organisms in high osmotic strength, high pressure, deserts, high temperature and icy land environments to carry out cellular functions without the need for protein modification (Yancey et al., 1982, Yayanos et al., 1979, Yancey and Somero, 1979, DeLong et al., 1997, Saladino et al., 2011, Kumar and Kishore, 2013). They also prevent proteins from unfolding and ligand binding under high hydrostatic pressure in oceans. Studying these osmolytes helps us to design cosolvents to make proteins more stable and soluble and increase the shelf life. These proteins have wide industrial applications from therapeutics like antibodies, recombinant proteins in bio-pharmaceutical companies to industrial enzymes in textiles, detergents, paper, and pulp processing industries.

There are many known solutes that are effective osmolytes, like trimethylamine-N-oxide (TMAO), glycine betaine, ectoine, polyols, urea, sarcosine and sugars (Venkatesu et al.,

2007, Yancey, 2005, Yancey et al., 2004, Yancey et al., 2002, Yancey and Somero, 1980, Venkatesu et al., 2009, Kumar and Kishore, 2013, Herzog et al., 2019). Mass spectroscopy and protein NMR studies on rat and rabbit kidney suggest that osmolytes help the cells to maintain osmotic balance under high stresses like in the presence of high amounts of sodium chloride (Bagnasco et al., 1986). Examples include glycerol which allows glucose-6-phosphate dehydrogenase and glycerol dehydrogenase to function under high salt concentrations (Borowitzka and Brown, 1974). It is clear that the exact mechanism behind these effects is not either properly understood or validated and highly debated. (Zou et al., 2002, Hu et al., 2010, Bennion and Daggett, 2004, Auton et al., 2008, Paul and Patey, 2008, Bolen, 2001, Street et al., 2006, Stumpe and Grubmuller, 2007, Bolen and Baskakov, 2001, Hua et al., 2008, Canchi et al., 2010, Wei et al., 2010, Bolen and Rose, 2008).

1.6.1 Urea

Urea is a known protein denaturant and the exact mechanism of protein denaturation by urea is yet to be fully understood (Caballero-Herrera et al., 2005, De Sancho et al., 2009, Daggett, 2006). Two possible explanations are direct binding to the peptide backbone of the protein molecule (Mountain and Thirumalai, 2003, Huang et al., 2012), and an indirect mechanism where urea reduces hydrophobic interactions by altering water structure (Bennion and Daggett, 2003).

Osmolytes other than urea are compatible solutes that allow the protein to retain its structure and function normally even at extreme conditions like high salt concentrations (Brown and Simpson, 1972, Borowitzka and Brown, 1974, Yancey et al., 1982, Somero, 1986).

1.6.2 TMAO

TMAO (trimethylamine N-oxide) is an organic compound with one positive and one negative charge hence overall neutral as seen in Figure 1.6. TMAO is one of the widespread osmolytes accumulated by many marine organisms like cartilaginous fishes, sting ray, dogfish shark, guitar fish, and thornback ray to counteract osmotic stress and destabilising effects of protein denaturants (Borowitzka and Brown, 1974, Yancey and Somero, 1980). TMAO belongs to the strong counteracting class of nitrogenous osmolytes (Yancey et al., 1982, Baskakov and Bolen, 1998).

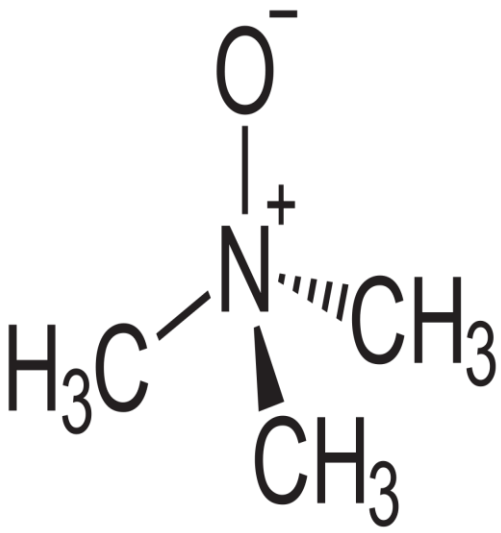

Figure 1.6. Structure of Trimethylamine-N oxide (TMAO)

Counteracting effects of urea-induced protein inhibition by osmolytes are well documented (Bennion and Daggett, 2004, Yancey and Somero, 1980, Yancey and Somero, 1979, Hu et al., 2009, Bolen, 2001, Baskakov et al., 1998, Baskakov and Bolen, 1998, Ratnaparkhi and Varadarajan, 2001, Meersman et al., 2011, Meersman et al., 2009, Withers and Guppy, 1996, Maeda et al., 1996, Singh et al., 2007, Holthauzen and Bolen, 2007, Zou et al., 2002, Venkatesu et al., 2009, Venkatesu et al., 2007, Kumar and Kishore, 2013).

Urea is uncharged, TMAO has one positive and one negative charge and hence overall is neutral. Urea is known to self-associate and the presence of osmolytes like TMAO further increases the self-association of urea thereby decreasing the denaturing effects of urea (Paul and Patey, 2007). The presence of TMAO leads to a marked reduction in the perturbation of functional activities of proteins in the presence of denaturants (Venkatesu et al., 2009, Daggett, 2006, Baskakov et al., 1998, Baskakov and Bolen, 1998, Mukherjee et al., 2005, Bennion and Daggett, 2004, Auton and Bolen, 2005).

Maintaining an appropriate balance of urea and TMAO concentration is very important, otherwise proteins tend to get too rigid at high concentrations of stabilizers which might raise Michaelis constant (K_m) values to alarmingly high levels. This will affect proteins' catalytic activity. Many marine organisms like cartilaginous fishes, sting ray, dogfish shark, guitar fish, and thornback ray maintain a 2:1 ratio of urea to TMAO (Borowitzka and Brown, 1974, Yancey and Somero, 1980). This suggests that half the amount of TMAO to urea concentration is sufficient to counteract protein inhibition and denaturation (Bennion and Daggett, 2004, Yancey et al., 2002). Preferential interaction and thermal transition studies on

protein folding/unfolding and free energies of urea and TMAO reveal their combined effects are thermodynamically additive (Lin and Timasheff, 1994). Kinetic studies on TMAO's ability to counteract protein denaturation caused by urea on lactate dehydrogenase (LDH) supports the argument that the counteraction hypothesis is independent of the source of the protein (Baskakov et al., 1998).

1.6.3 Protein stability and TMAO's counteracting inhibitory effects of urea

Some studies suggest that TMAO enhances water structure while urea distorts the water structure (Wei et al., 2010, Yang and Gao, 2010). TMAO enhances water structure and reduces entropy in water molecules leading to increase in protein stability (Zou et al., 2002). TMAO also offsets protein inhibitory effects of urea by different interactions with the amide unit of the peptide backbone. Involvement of the peptide backbone applies the stabilization principle of TMAO against urea-induced protein denaturation to all proteins regardless of their cell origin (Baskakov et al., 1998). Increase in solvent accessible surface area is thermodynamically favourable for denaturation compared to pure aqueous solutions (Auton and Bolen, 2004). From Figure 1.7, the population of tetrahedrally oriented waters increases when TMAO is added whilst water structure remains the same in the presence of urea.

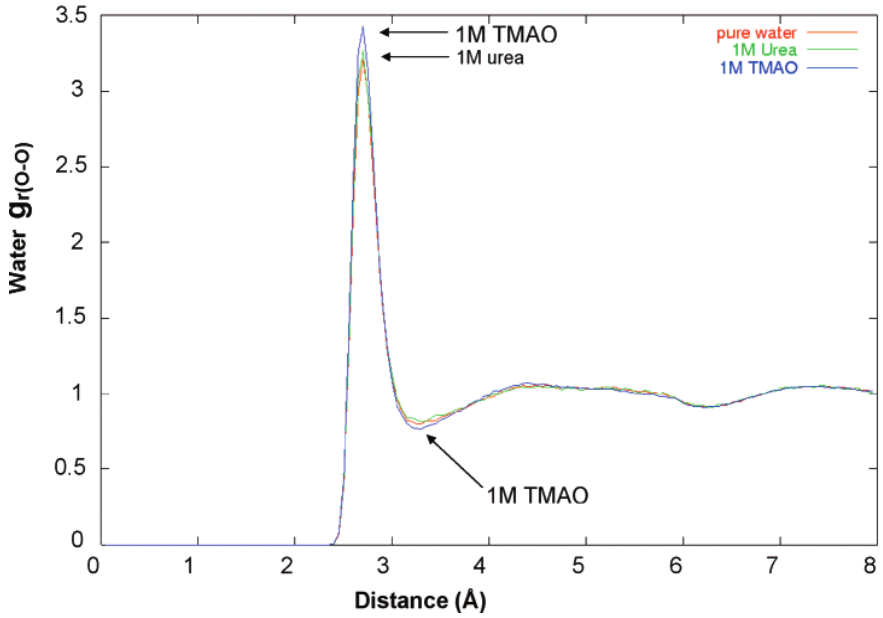

Figure 1.7. Water O-O radial distribution functions in solutions of pure water, 1 M urea and 1 M TMAO, calculated by molecular dyamics simulatons. Addition of urea has little effect on the water structure (green curve), whereas addition of TMAO causes an increase in the first peak, and a decrease in the minimum at 3.2 Å (blue curve), both of which indicate an increased ordering of water molecules. "Reprinted (adapted) with permission from Zou, Q., Bennion, B. J., Daggett, V. & Murphy, K. P. 2002. The molecular mechanism of stabilization of proteins by TMAO and its ability to counteract the effects of urea. Journal of the American Chemical Society, 124, 1192-1202. Copyright © 2002, American Chemical Society."

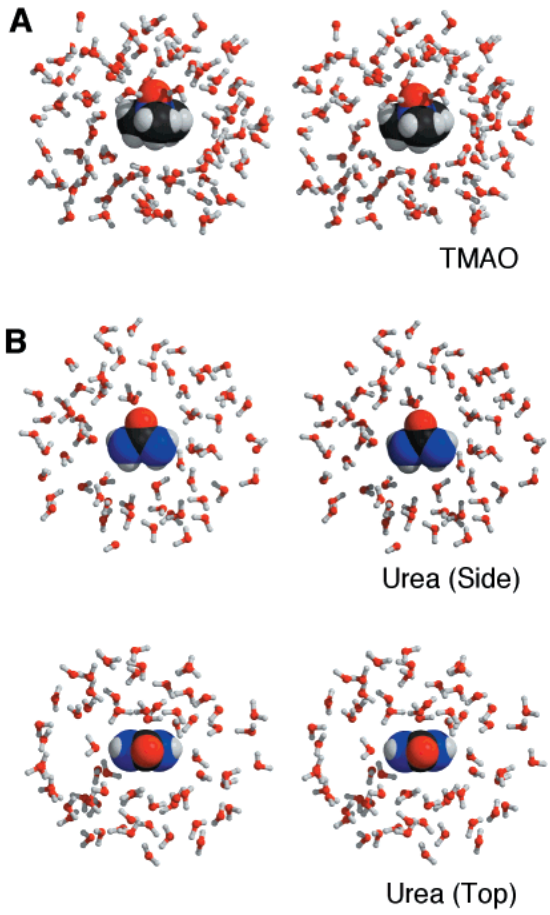

Figure 1.8. Stereoviews of MD simulations of TMAO (top) surrounded by solvating water molecules and urea (middle and bottom) surrounded by solvating water molecules. TMAO orders the surrounding water molecules by increasing hydrogen bonding in water whereas the number of hydrogen bonds decreases in presence of urea. Figures created using MOLSCRIPT and Raster3d. "Reprinted (adapted) with permission from Zou, Q., Bennion, B. J., Daggett, V. & Murphy, K. P. 2002. The molecular mechanism of stabilization of proteins by TMAO and its ability to counteract the effects of urea. Journal of the American Chemical Society, 124, 1192-1202. Copyright © 2002, American Chemical Society."

Molecular dynamics simulation images from Figure 1.8 indicate TMAO increases greater spatial and long-range ordering and better organizes water molecules around itself leading to increase of hydrogen bonding in water molecules compared to urea which poorly orders water molecules with decreased hydrogen bonding (Zou et al., 2002). MD simulation studies also reveal that TMAO makes a few direct interactions by means of hydrogen bonding with lysine and arginine side chains, which order water molecules and prevent water and urea from interacting with water resulting in increased interaction between water molecules. However, a major mode of action is indirect interactions through which TMAO stabilizes protein by ordering water molecules around itself and thereby preventing solvent hydrogen bonding leading to an increase in the strength of intra protein hydrogen bonds. This counteracts urea, which competes with water molecules for intra molecular hydrogen bonding with the

protein. By doing so TMAO keeps the protein fold intact and keeps the protein stable. The hydrogen bond lifetime in water is increased by 3 times when 1 M TMAO is added.

TMAO shortened and strengthened hydrogen bonds. Rosgen and Jackson-Atogi, 2012 used the Kirkwood-Buff approach and suggested that TMAO in a urea mixture behaves like a hard sphere gas and excludes itself from peptide groups.

1.6.3.1 Role in enzyme Catalysis

Kinetic studies on lactate dehydrogenase explain how enzyme activity is restored by TMAO. Urea shifts the equilibrium towards open structures and TMAO turns the equilibrium towards the compact structures which is the active form of enzymes (Baskakov et al., 1998). Urea and TMAO have different effects on K_m and k_{cat} values. Urea increases K_m value and decreases k_{cat} value whereas TMAO does the opposite in reducing K_m and increasing k_{cat} (Baskakov et al., 1998). In a study of urea-induced time dependant inactivation, LDH was inactivated by urea 300-fold compared to control sample and only 10 fold when TMAO is added to urea at 1:1 ratio (Baskakov and Bolen, 1998). TMAO helps the protein to retain its structure and greatly reduces the rate of protein dissociation (Baskakov and Bolen, 1998). Kinetic studies on 4 enzymes (creatine kinase, pyruvate kinase, lactate dehydrogenase, and glutamate dehydrogenase) extracted from elasmobranch fishes found that TMAO at a concentration ratio of 2:1 can reverse the urea-induced increase of K_m and decrease of V_{max} values (Yancey and Somero, 1980).

1.6.4 Ectoine

Ectoine is an uncharged organic compound with a chemical formula $C_6H_{10}N_2O_2$ as seen in Figure 1.09. Ectoine is a compatible solute (Brown, 1976) accumulated by some extremophilic and halophilic microorganisms to counteract high temperature, osmotic stress and high pressure without disturbing the metabolism of the cell (Yancey, 2005, Kempf and Bremer, 1998, Ventosa et al., 1998, Wittmar et al., 2020). Ectoine was first discovered in a halophilc microorganism, *Ectothiorhodospira halochloris* and has since been found in many microorganisms like *Halomonas elongata, Halorhodospira halophila, Halomonas titanicae* etc. Ectoine influences the stability of biomolecules and helps preserve the native structure of proteins and lipid bilayers (Hahn et al., 2015, Smiatek et al., 2012, Oprzeska-Zingrebe et al., 2018, Smiatek, 2014, Oprzeska-Zingrebe et al., 2019, Buenger and Driller, 2004, Hahn et al., 2016, Eiberweiser et al., 2015, Yu and Nagaoka, 2004, Roychoudhury et al., 2012). Ectoine

also has destabilising effects particularly on DNA (Oprzeska-Zingrebe et al., 2019, Oprzeska-Zingrebe et al., 2018, Wittmar et al., 2020, Meyer et al., 2017) .

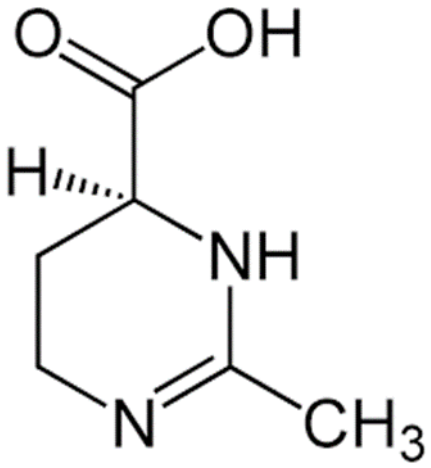

Figure 1.9. Structure of ectoine.

Ectoine interacts with water molecules. Neutron diffraction studies of aqueous solutions show that ectoine enhances hydrogen bonds in water (Zaccai et al., 2016). Hydration shells are formed around ectoine that change the dynamics of water molecules especially those water molecules present in the first hydration shell (Smiatek, 2014, Smiatek et al., 2012, Hahn et al., 2015).

X-ray photoelectron and polarization modulation infrared reflection absorption spectroscopy (PM IRRAS) studies on the interaction between DNA and ectoine suggested that ectoine affects hydrogen bonding in the DNA, and DNA interacts predominantly with water in the presence of lower concentrations of ectoine such as 0.1 M while at higher concentrations up to 2.5 M, almost all water molecules interact with ectoine, implying that ectoine has a direct role in DNA structure (Wittmar et al., 2020). This suggests that ectoine either interacts with water or its presence makes the other solutes like DNA in this case to interact with water.

1.6.5 Betaine

Betaine ($C_5H_{11}NO_2$) is a modified glycine with three methyl groups as seen in Figure 1.10. It is overall a neutral chemical compound with positive and negative charged functional groups. Betaine is accumulated by marine organisms like invertebrates, halophilic bacteria and some plant and mammalian species to counteract osmotic stress, high temperature, salinity, and protein denaturants (Yin et al., 2000, Yancey, 2001, Bedford et al., 2002, Bedford et al., 1998, Edmands et al., 1995). Glycine betaine is also commonly found in *Escherichia coli* for its

osmoprotectant activities (Record et al., 1998, Cayley and Record, 2003). Glycine betaine also improves the thermal stability of proteins (Yancey and Somero, 1979, Santoro et al., 1992, Anjum et al., 2000).

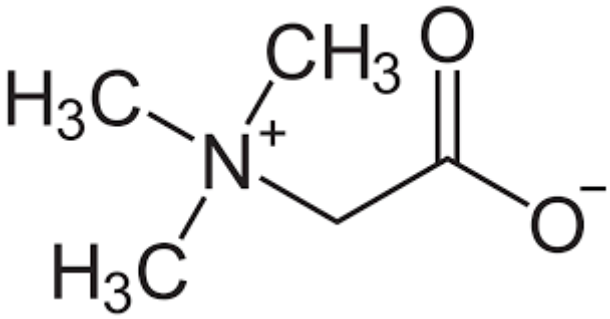

Figure 1.10. Structure of betaine.

Glycine betaine linearly increases the stability of protein with concentration while urea linearly decreases the same (Guinn et al., 2011, Myers et al., 1995, Felitsky and Record, 2003, Hong et al., 2004, Santoro et al., 1992, Felitsky et al., 2004). This can be compared to the Hofmeister series ions' effect on protein stability where sulphate increases while thiocyanate decreases protein stability (Vonhippe.Ph and Schleich, 1969, Guinn et al., 2011, Pegram et al., 2010, Baldwin, 1996).

Molecular dynamics simulations and spatial distribution function (SDF) studies by Kumar and Kishore (2013) on the effect of mixtures of betaine plus urea on the local water structure reveal that the hydrogen bonding network in water increases as compared to pure water when betaine and urea are in synergy. The strengthening of individual hydrogen bonding between water molecules is related to protein stability (Zou et al., 2002, Paul and Patey, 2007). The results of Kumar and Kishore (2013) also indicate that interaction of betaine increases with water in the urea plus betaine mixture and results in the exclusion of betaine from the protein surface. Felitsky et al., 2004 studied the interaction of glycine betaine with LacI HTH DNA binding domain and hen egg white lysozyme and bovine serum albumin using circular dichroism, and all-gravimetric vapour pressure osmometry (VPO) found that betaine is excluded from the surface of hen egg white lysozyme. Some other studies also suggest that betaine is preferentially excluded from lysozyme and folded bovine serum albumin (Arakawa and Timasheff, 1983, Timasheff, 1998, Courtenay et al., 2000).

Many previous researchers (Auton et al., 2001) have also proposed that betaine and other osmolytes exclude themselves from the protein surface and increase the stability of the

protein (Bennion and Daggett, 2004, Zhang et al., 2012, Shimizu and Smith, 2004, Kumar and Kishore, 2013, Timasheff, 2002, Wei et al., 2010, Liu and Bolen, 1995, Bolen and Baskakov, 2001).

1.7 Chemical shift mapping or Chemical shift perturbation (CSP) as a method to study protein-ligand interactions

Williamson, 2013 of our lab has extensively studied chemical shift mapping or chemical shift perturbation (CSP) as a technique to study protein binding and explained in detail in his paper about various types of fitting chemical shift changes. Some excerpts from his body of work are summarised in this section.

CSP is a technique to study the structural changes induced by a ligand on a protein molecule by measuring the chemical shift changes. In this technique a labelled protein (^{13}C or ^{15}N sometimes both when measuring HN, C shifts) and unlabelled ligand is used. A typical ^{1}H NMR takes 3 minutes and a ^{15}N HSQC takes 90 minutes (depending on the experimental settings like number of scans). Utilizing a highfield spectrometer (500 MHZ to 800 MHZ) with a cryocooled probe an NMR titration of 9 increasing sample concentrations should be completed in 15 – 18 hrs (spread across two working days). When a ligand is added to a complex/protein, the resulting chemical shift changes are mapped to measure the exact location of the binding site. If one measures the peaks at each titration point and then follows the movement of peaks (shift mapping/titration mapping), this gives information about how each peak moves with the titration (increased concentration of ligand). Information obtained from CSP can also be used to measure the binding affinity/dissociation constant K_d or to determine the structure of the complex (ligand-protein). Through-space interactions influence ^{1}H, ^{15}N and $^{13}C'$ shifts. ^{15}N and ^{13}C shifts are influenced by through-bond interactions in addition to through-space interactions. CSP is very sensitive to structural changes and and any actual binding interactions can be accurately measured. Peaks that move most are the ones where ligand is most likely to bind. The shape of the titration curve can be fitted to the titration curve (chemical shift vs. concentration of ligand) to measure the binding affinity i.e., to obtain values for K_d. If a ligand doess not bind no changes in chemical shift will be seen. It is crucial to maintain the same experimental conditions such as buffer and pH throughout the titration to get repeatability of spectra and rule out any interfering effects. For example, variations in pH upon the addition of ligand can give false peak movement, hence constant pH needs to be maintained all the way through. CSP can be used to measure K_d values even without the need

of triple resonance assignments. However, established assignments make CSP a more potent technique.

The most useful and pragmatic approach to calculate CSP are by summing chemical shifts as several separate effects and creating equations built on origin of chemical shifts or even geometrical factors like distances. The parameters are then fitted such that best fit is attained amongst observed and experimental shifts. There are certain limitations to this method as well like any inaccuracies in referencing or peak picking/mapping can cause errors in shift tables. Likewise, occasionally errors could be due to massive difference between fitted and observed values. These methods have done very well for the calculations of ^{1}H shifts and are handy for the calculations of $^{13}C\alpha$ and $^{13}C\beta$ shifts.

Primary chemical shifts and secondary chemical shifts are produced differently in ^{1}H nuclei due to distinct chemical conditions. Backbone amide HN groups generally resonate at 7-9 ppm whereas CH_3 groups resonate at 0-2.5 ppm. These shifts are produced by through-bond interactions owing to partial charges on heavy atoms. Primary shifts can be bypassed by considering just the secondary shifts which are described as the the difference between the observed shift and the random coil shifts (the combination of structures embraced by an unstructured peptide). Secondary shift can be described as a composition of sum of effects:

$$\sigma = \sigma^{p} + \sigma^{ani} + \sigma^{ring} + \sigma^{E} \qquad \text{eq 1.1}$$

where σ^{p} caused by paramagnetic effects, σ^{ani} caused by magnetic anisotropy, σ^{ring} arises from aromatic ring currents, σ^{E} arises from electric fields produced by charged atoms.

The largest amide backbone HN shifts are caused by hydrogen bonding interactions. Since these interactions are very short-range and extremely directional, they cause tiny random errors in the calculation and can result in inaccuracies of calculated chemical shift. Ring current effects control the secondary shifts in proteins whereas hydrogen bonding dominates the secondary shifts for amide protons and can be calculated reasonably accurately. Often, relating a shift change to a single structural change is difficult since observed shift changes are often a composition of sum of competing smaller effects.

$^{13}C\alpha$ and $^{13}C\beta$ shifts too arise from the shielding of electrons, however what makes carbon shifts different from proton shifts are the presence of electrons in both *s* and *p* orbitals implying carbon shifts are more dependent on local dihedral angles and geometry of bonds. The long-range effects affect the carbon like they do for proton. Carbon nuclei are mostly

buried and hence least affected by external forces, thus minimising the effects of through space effects. Since they are in the middle of the amino acid, neighbouring residues will have little overall effect on their secondary shifts. The effects of ligand binding on the carbon shifts are minimal because most of the effects are due to the backbone conformation of the amino acid itself (~4 ppm) and aided by the orientations of sidechains (~0.6 ppm) and amide bonds on either side.

^{15}N and $^{13}C'$ shifts are the most challenging to calculate because they can be affected by multiple factors like identity and sidechain conformation of the preceding amino acid (22 ppm), backbone dihedral angles (13 ppm), hydrogen bonding (8 ppm). Hydrogen bonding significantly affects the secondary shifts of nitrogen and the interesting part here is that hydrogen bonding is on its directly attached carbonyl group rather than the amide nitrogen itself. Carbonyl carbon like nitrogen shift too is affected by multiple factors and follows a similar pattern as nitrogen and are hard to calculate. The difference is effects on carbon are smaller and it is the following residue that is important and not the preceding residue.

Protein and ligand reversible binding at a single site are explained by the formula $[P][L]/[PL]$. Where $[P]$, $[L]$ are free protein and ligand concentrations while $[PL]$ is a complex. This binding interaction is typified by rate constants for forward reaction ($[P][L]k_{on}$) and backward reaction ($[PL]k_{off}$) and the dissociation constant K_d. K_d can be explained as concentration of $[P]$, $[L]$ required to saturate half the binding sites. Appearance of spectra during the titration (chemical shift mapping) can be distinguished into fast and slow exchange measured by the difference in exchange rates of free and bound complex called off-rate k_{off}. Exchange is fast if the k_{off} is greater than the difference in chemical shift between free and bound, (around K_d < µM). Using ^{15}N HSQC method K_d can be be determined by measuring peak positions i.e., by calculating the distance moved by the peak, weighting ^{15}N shifts by a factor of about 0.14 compared to ^{1}H shifts and select those residues for which the weighted shift change is larger than the standard deviation of the shift for all residues. In slow to intermediate exchange rates measuring K_d becomes difficult due to line broadening. Ligand binding at multiple sites can frequently be typified, by real-time fitting of many calculated shift changes, or just by adding up substoichiometric quantities of ligand.

Total concentrations (sum of free and bound forms) of of $[L]$ and $[P]$ during a titration can be written as

$$[L]_t = [L] + [PL] \text{ and } [P]_t = [P] + [PL]$$

Observed chemical shift change from the free state (δ_{obs}) in fast exchange is the weighted average of the shifts in free (δ_f f_f) and bound states (δ_b f_b)

$$\delta_{obs} = \delta_f f_f + \delta_b f_b$$

The final equation for fitting the K_d from measured values of the chemical shift at different concentrations of protein and ligand can be written as

$$\delta_{obs} = \Delta\delta_{max}\{([P]_t + [L]_t + K_d) - [([P]_t + [L]_t + K_d)^2 - 4[P]_t[L]_t]^{1/2}\}/2[P]_t$$

where δ_{obs} is the change in δ_{obs}, and $\Delta\delta_{max}$ is the maximum chemical shift change after saturation (calculated as part of the fitting procedure).

1.7.1 Choice of nuclei

^{15}N HSQC spectra is the easiest and common method to locate chemical shift changes and map ligand binding since it requires only single labelled protein (^{15}N); it is cost effective/cheap to express protein, spectra are the easiest to assign, sensitive, detects only one signal per amino acid residue from the backbone (except protein) and a few sidechains Gln, Trp, Asn, Arg. These sidechains are the functional groups that interact with ligand assuming ^{15}N shifts hydrogen bond with adjacent carbonyl residue. Since this causes large shift changes for the ^{15}N of residue i + 1, interaction of ligand with carbonyl will also be observed in the shift changes of adjacent amide nitrogen (i + 1 residue).

^{13}C HSQC is not as helpful as ^{15}N HSQC as signal changes are small and interference from water signal makes mapping of the spectra challenging especially near Hα region. Since carbon nuclei are buried and not solvent exposed, structural changes caused by the ligand will have little influence on them and hence they are obvious signs of direct binding induced effects.

2D ^{13}C HNCO also gives smaller signals like ^{13}C HSQC but are easier to map since there is not interference of water signal. However, they are more complicated to interpret for reasons given above.

1.8 Conclusion

Even after many decades of research on osmolytes their mode of action is still unclear: For example, whether they stabilize proteins by preferential exclusion (Bolen and Baskakov, 2001, Lin and Timasheff, 1994, Gallagher and Sharp, 2003, Jiao and Smith, 2011, Courtenay

et al., 2000, Athawale et al., 2005, Shimizu and Smith, 2004, Shimizu, 2004, Abui and Smith, 2004, Rosgen and Jackson-Atogi, 2012, Zhang et al., 2012, Kumar and Kishore, 2013, Timasheff, 2002) or by affecting water structure (Bennion and Daggett, 2004, Rezus and Bakker, 2009, Zou et al., 2002, Zaccai et al., 2016, Wittmar et al., 2020). There are some more arguments like osmolyte TMAO directly interacts with urea and counteracts its destabilising effects (Meersman et al., 2009, Paul and Patey, 2007). Also needing to be investigated is whether osmolytes directly interact with protein surface and backbone or whether they behave like Hofmeister kosmotropes in organizing water around themselves and stabilizing proteins by decreasing solubility (Bye et al., 2016).

1.9 Aim of work in this thesis

The aim of the thesis was to elucidate a possible mechanism by which the osmolytes affect protein structure and stability. We hypothesise that osmolytes work in a similar manner to Hofmeister series ions: that they interact strongly with water and compete with the protein for water binding, which is how they counteract the effect of urea. The experimental data from DSC and NMR techniques helps us understand the mechanism by which osmolytes affect protein structure and stability, whether they directly interact with the protein or act indirectly by affecting the water structure around the protein like Hofmeister series ions do.

In more detail: Differential scanning calorimetry was used to study how the osmolytes affect thermal stability of the proteins and counteract the destabilising effects of known protein denaturants like urea (Chapter 3). NMR spectroscopy was used to study the chemical shift changes caused by osmolytes on protein barnase thereby elucidating the effects of osmolytes on protein and water structure (Chapter 4). This was carried out by conducting a series of titrations with barnase as a protein model. NMR chemical shifts give detailed information on binding, affinity and solvation, and were therefore used extensively to test different models of protein stabilisation.

Separate NMR experiments were also conducted to study the interaction of osmolytes with protein denaturants like urea (Chapter 5).

All the experimental methods were described in detail in chapter 2 and results in chapters 3-5 with a separate conclusion chapter (Chapter 6).

2 CHAPTER 2: MATERIALS AND METHODS FOR BARNASE EXPRESSION AND PURIFICATION

2.1.1 Reagents

All the following solutions were prepared using distilled water (Milli-Q system from Millipore). All the solutions were either filter sterilized using 0.2 µM and 0.45 µM filter or filter sterilization under vacuum pressure or autoclaved wherever applicable.

Table 2.1. Table describing the preparation of different reagents used in protein expression and purification.

Reagent Name	**pH**	**Application**	**Preparation/Ingredients**
Thiamine 1mg/ml stock	NA	M9 media	filter sterilize and store in small aliquots at -20°
$^{13}C_6$-glucose 20% solution (0.2g/ml)	NA	M9 media	filter sterilize and store at 4°
$^{15}NH_4Cl$ 25% solution (0.25g/ml)	NA		filter sterilize and store at 4°
1 M MgSO4 (100 ml)	NA		autoclave
1 M $CaCl_2$ (100 ml)	NA		autoclave
LB agar (500 ml)	NA	To grow *E. coli* cells on Petri plate	5 g sodium chloride, 5 g tryptone, 2.5 g yeast extract, 7.5 g agar, Ampicillin and Kanamycin antibiotics are added to a final concentration of 100 µg/ml each
Trace elements (100 ml)	8.0		$CaCl_2.2H_2O$ 550 mg MnSO4.H2O 140 mg $CuSO_4.5H_2O$ 40 mg $ZnSO_4.7H_2O$ 220 mg

			$CoCl_2.6H_2O$ 45 mg $Na_2MO_4.2H_2O$ 26 mg H_3BO_4 40 mg KI 26 mg Once the above chemicals are added to 70 ml water and adjusted to pH 8.0, add EDTA 500mg and readjust pH to 8.0, add $FeSO_4.7H_2O$ 375 mg. Make up to 100 ml and autoclave.
M9 (1000 ml):	7.4	M9 Media	6.0 g Na_2HPO_4 3.0 g KH_2PO_4 0.5 g NaCl Adjust the pH to 7.4, autoclave. 650 µl Trace elements 1.0 ml thiamine 4.0 ml (25%) $^{15}NH_4Cl$ 15 ml $^{13}C_6$-glucose 1.0 ml 1M $MgSO_4$ 0.1 ml 1M $CaCl_2$
16% Resolving gel	NA	SDS PAGE	Lower Buffer (1.5 M Tris-HCl pH 8.8) 2.5 ml, 40% w/v Bis acrylamide 4 ml H_2O 3.5 ml, shake, 10% w/v APS 100 µl, shake and add TEMED 10 µl

Stacking gel	NA	SDS PAGE	Upper Buffer (0.5 M Tris-HCL pH 6.8) 2.5 ml, 40% w/v Bis acrylamide 1.125 ml H_2O 6.375 ml, shake, 10% w/v APS 110 µl, shake and add TEMED 11 µl
Lysis Buffer (500ml)	7.4	Cell Lysis	25 mM Tris HCl pH 7.4 + 5mM $MgCl_2$, filter sterilize
Tris Buffer	7.4	Q Sepharose column, dialysis	50 mM Tris HCl pH 7.4 + 0.02% NaN_3, filter sterilize
Tris Buffer-GuHCl	7.4	Q Sepharose column	50 mM Tris HCl pH 7.4 + 0.02% NaN_3 + 6 M GuHCl, filter sterilize
Acetate Buffer	5.0	SP Sepharose column, dialysis	50 mM Na Acetate pH 5.0 + 0.02% NaN_3, filter sterilize
Acetate Buffer - NaCl	5.0	SP Sepharose column	5 0mM Na Acetate pH 5.0 + 0.02% NaN_3 + 1 M NaCl, filter sterilize
Acetate Buffer - Urea	5.0	SP Sepharose column	50 mM Na Acetate pH 5.0 + 0.02% NaN_3 + 6 M Urea, filter sterilize
Running buffer		SDS PAGE	Tris-HCl 25 mM Glycine 200 mM SDS 0.1% (w/v)
2× Laemmli loading buffer		SDS PAGE	Bromophenol blue 0.004% 2-mercaptoethanol 10% Glycerol 20% SDS 4% Tris-HCL 1.125 M

2.1.2 Escherichia coli strain:

Barnase from catalytically inactive H102A of *Bacillus amyloliquefaciens* in *E coli* M15 cells was transformed with pQE-60 plasmid. The H012A mutant was used because expression of the active RNAse kills the *E. coli* cells and results in very low expression.

E. coli cells were taken out from -80^{o}C and streaked on a Luria-Bertani (LB) agar plate containing ampicillin and kanamycin and incubated at 37°C overnight. Cells from the LB agar plate were added to a M9 media starter culture of 50 ml and incubated at 37°C overnight.

2.1.3 Protein expression:

Protein was expressed in a total volume of 2 L broth. So, 10 ml of starter culture was added to the flasks each containing 500 ml M9 broth. All the flasks were incubated at 37°C till they reached a UV absorbance of 0.6-1.0 at 600nm. Every 45 mins the optical density was measured using a UV-Visible spectrophotometer (nanodrop). When the OD reached 0.69, flasks were removed from the incubator and 0.5ml IPTG (to produce a final concentration of 1 mM from 1 M stock) was added to each flask. This addition activates the lac operon for protein expression. Flasks were incubated at 25°C overnight. Flasks were taken out from the incubator and growth medium was transferred into centrifuge tubes and spun for 10 minutes at 8000 rpm at 4°C in a Beckman Avanti J-251 centrifuge. After centrifugation, the supernatant was discarded, and the pellet was collected. After cell harvesting, the pellet was taken, and cells were broken open by sonication to release intracellular proteins. 20 ml of lysis buffer (containing a half tablet of Roche complete protease inhibitor and a pinch of DNase to digest nucleic acids if any are present) was added to the pellet in a 50 ml falcon tube, placed in a beaker containing ice and sonicated for 4*30 seconds at 10 microns amplitude. Sonication was done with 30 seconds time interval between each round to prevent the tube from getting hot. The resulting suspension after sonication was centrifuged at 18000 rpm for 40 minutes at 4°C. Pellet was discarded and supernatant was dialyzed overnight in 2 L of Tris buffer. This supernatant was taken for the next step i.e., protein purification.

2.1.4 Dialysis method:

Preparing a protein sample of high purity is essential to avoid any artifacts in the experiments that they will be used for. A dialysis method was used for bringing the sample to equilibrium with the solvent and to minimize the presence of solutes. Dialysis helps to bring the sample in to a particular pH so that the protein sample and reference sample will have same pH composition (Ibarra-Molero et al., 2016). The kind of solvent, volume of solvent and duration of dialysis and redialysis varies from one stage to another in the purification process based on the requirement. Dialysis tubing (Spectrapor) of 5000 MWC was cut to the required length and enough space was left for expansion. The tube was placed in water for half an hour

to remove glycerol residues. The dialysis tube was clipped at the bottom and the sample from cell lysis was transferred into it with the help of a funnel, and the top of the tube was closed with a clip. The tube was placed in a beaker containing 2 litres of Tris buffer. The beaker was placed on a magnetic stirrer overnight at 4^{o}C to ensure the sample in the tube was mixed and all the contents are in equilibrium. Once the dialysis was completed, the sample was transferred to centrifuge tubes/vials.

2.1.5 Protein Purification:

Ion exchange chromatography separates different proteins based on their charge difference. Barnase was separated and purified from other cellular proteins and nucleic acids via a 2-step process using two different columns: Q-sepharose and SP-sepharose.

2.1.6 Q-sepharose

Barnase solution (from tris buffer dialysis) was passed through the anion exchange resin Q-sepharose, which binds negatively charged molecules like DNA whilst eluting the positively charged molecule barnase. Since barnase does not bind and elutes freely, a gradient was not required. In this separation, the AKTA instrument was given a thorough system wash followed by column wash with 50 mM Tris buffer. Pressure was set at default (usually 1 MPa), and the flow rate was 2.0 ml/min. Once the UV absorbance and conductivity reached baseline, the sample was loaded. Fractions were collected once the UV absorbance at 280 nm started to increase. The column was eluted with 50 mM tris buffer until UV absorbance reached baseline again. The column was then washed with Tris-GuHcl (50 mM Tris HCl plus 6 M GuHCl) to remove any bound protein. The column was washed with ethanol and returned to 20% ethanol to store. The pooled fractions absorbing at 280 nm were run on a 16% SDS-PAGE gel to confirm the presence of barnase. The sample was dialyzed in 4 litres of 50 mM sodium acetate buffer at 4^{o}C overnight to prepare it for the next step of purification i.e., SP sepharose.

2.1.7 SP sepharose

Barnase solution from acetate buffer dialysis was taken for cation exchange purification. Barnase is retained on the column and eluted only at high concentration of sodium chloride (eluting buffer). NaCl competes with the protein to bind with the column and disrupts interaction between the cation resin and barnase. Prior to loading sample, the column was thoroughly washed with 50 mM sodium acetate buffer (washing buffer). The pressure was set

to default (usually 1 MPa), flow rate was 2.0 ml/min. Once the UV absorbance and conductivity reached baseline, the sample was loaded. After the sample was completely loaded, the column was washed with washing buffer until UV absorbance again reached baseline. A linear salt gradient with buffer A=50 mM Na acetate, B= 50 mM Na acetate plus 1 M NaCl was applied. Barnase started to elute at a NaCl concentration of approximately 120 mM and fully eluted at approximately 260 mM. Fraction size was set to 5 ml and sample fractions were collected once the UV absorbance at 280 nm started increasing. Once the barnase peak had eluted, the column was washed with Na Acetate plus 6 M urea buffer to remove any bound protein. The column was washed with ethanol and returned to 20% ethanol to store. Collected pooled fractions were run on a 16% SDS-PAGE gel to confirm the presence of barnase.

2.1.8 Dialysis:

The sample was placed in a dialysis tube and dialyzed in 4 litres of water at 4^{o}C overnight, and redialysed next day again. Then the sample was concentrated to 0.5 ml and made up to 20 ml with 5 mM sodium acetate buffer pH 5.8 in a viva spin and centrifuged to 0.5 ml volume. This sample was made up to 20 ml again and concentrated back to 0.5ml. The sample was diluted to 3.91 ml with 5mM sodium acetate buffer pH 5.8 and the concentration of protein was found to be 785 µM (calculated using nanodrop reading with mol. weight and extinction coefficient values).

2.1.9 SDS-PAGE analysis:

Sodium dodecyl sulphate polyacrylamide gel electrophoresis (SDS-PAGE) was used to analyse the purity and molecular size of the protein. Plates were sealed with tape to prevent gel leakage and the assembled plates were fixed into the gel apparatus. 10 ml of resolving gel was prepared, poured into the gap between the plates and left for 10 minutes for polymerization. Isopropanol (3-4 drops) was added to remove any air bubbles and level the gel. Once the resolving gel had solidified, IPA was removed with tissue paper and 4ml of 4% stacking gel was added to the resolving gel in the plates. A comb was placed on the stacking gel immediately. All the samples were heated for 5 minutes at 95^{o} C to mix them.10 µl of protein marker (250-10 kDa Dual precision protein marker from BioRad) was used as a standard to compare and identify the various samples. The gel plate was placed in the gel tank and filled completely up to the top with SDS-loading buffer. Samples and protein marker were loaded in the well for electrophoresis. Initially voltage was applied at 80 volts for 5 minutes and then

increased to 180 volts for 1 hour. Once the electrophoresis was complete, the gel was carefully removed and placed in a box containing Instant Blue stain for 30 minutes. After 30 minutes the gel was observed, and a photograph was taken.

2.2 DIFFERENTIAL SCANNING CALORIMETRY

2.2.1 Materials

Barnase, sodium acetate and acetic acid for buffer, TMAO, ectoine, urea, HPLC grade water and ultra-pure water were sourced from Sigma Aldrich with >99 % purity.

2.2.2 Experimental settings for DSC

0.5 mg/ml protein of 300 µl volume and appropriate blank samples were run in sample and reference cells. Samples were degassed under vacuum for an hour before loading into the cells and were run in a temperature range of 20 ^{o}C to 90 ^{o}C with 1.5 ^{o}C heating rate per minute and equilibration phase of 600 seconds. Idling temperature was set at 20 ^{o}C. After every run, sample and water cells were washed with HPLC grade water. The DSC instrument used in this experiment for the stability studies is a capillary Nano-DSC supplied by TA Instrument, DE, US.

2.2.3 Sample preparation for DSC

0.5 mg/ml barnase prepared in 5 mM acetate buffer at pH 6.0 with combinations of different osmolytes was used. TMAO at 0 to 3 M concentrations, ectoine at 0 to 2 M, and urea at 0 to 3 M was used against barnase at different stages of experiments. All the salt preparations were made in 5 mM acetate buffer pH 6.0 to maintain the same concentration of buffer and pH as that of the protein. Blank (reference) samples were run with exactly the same concentrations of buffer and osmolytes except that they do not contain protein. All the experiments were run in duplicate and a few in triplicate. Sample concentrations and volumes were calculated using the formula $V_2=(N_1V_1)/N_2$ which is derived from $N_1V_1=N_2V_2$. Sample preparations are described in Tables 2.2 – 2.7.

Table 2.2. Calculation for 1 ml sample preparation with barnase (0.5 mg/ml), TMAO, acetate buffer. Amount of TMAO to be added is calculated using the formula $V_2=(N_1V_1)/N_2$ where N_1 is the required molarity, V_1 is the required volume, N_2 is the molarity of the stock solution. All the samples in 5 mM acetate buffer pH 6.0.

Preparation of TMAO solution in M	**N_1 in M**	**V_1 in ml**	**N_2 in M**	**V_2 in ml $=(N_1V_1)/N_2$**	**Barnase (0.5 mg/ml from 12.12 mg/ml stock)**	**Acetate buffer to make final DSC sample of 1 ml.**
0	0	1	5	0	0.04125	0.95875
0.01	0.01	1	5	0.002	0.04125	0.95675
0.1	0.1	1	5	0.02	0.04125	0.93875
1	1	1	5	0.2	0.04125	0.75875
3	3	1	5	0.6	0.04125	0.35875

Table 2.3. Calculation for 1 ml sample preparation with barnase (0.5 mg/ml), ectoine, acetate buffer. Amount of ectoine to be added is calculated using the formula $V_2=(N_1V_1)/N_2$ where N_1 is the required molarity, V_1 is the required volume, N_2 is the molarity of the stock solution. All the samples in 5 mM acetate buffer pH 6.0.

Preparation of ectoine solution in M	**N_1 in M**	**V_1 in ml**	**N_2 in M**	**V_2 in ml $=(N_1V_1)/N_2$**	**Barnase (0.5 mg/ml from 12.12 mg/ml stock)**	**Acetate buffer to make final DSC sample of 1 ml.**
0	0	1	3	0.0000	0.04125	0.95875
0.01	0.01	1	3	0.0033	0.04125	0.95542
0.1	0.1	1	3	0.0333	0.04125	0.92542
1	1	1	3	0.3333	0.04125	0.62542

Table 2.4. Calculation for 1 ml sample preparation with barnase (0.5 mg/ml), urea, acetate buffer. Amount of urea to be added is calculated using the formula $V_2=(N_1V_1)/N_2$ where N_1 is the required molarity, V_1 is the required volume, N_2 is the molarity of the stock solution. All the samples in 5 mM acetate buffer pH 6.0.

Preparation of urea solution in M	**N_1 in M**	**V_1 in ml**	**N_2 in M**	**V_2 in ml $=(N_1V_1)/N_2$**	**Barnase (0.5 mg/ml from 12.12 mg/ml stock)**	**Acetate buffer to make final DSC sample of 1 ml.**
0	0	1	6	0.0000	0.04125	0.95875
1	1	1	6	0.1667	0.04125	0.79208
2	2	1	6	0.3333	0.04125	0.62542
3	3	1	6	0.5000	0.04125	0.45875

Table 2.5. Calculation for 1 ml sample preparation with barnase (0.5 mg/ml), Varying urea, 1 M TMAO and acetate buffer. Amount of urea and TMAO to be added were calculated using the formula $V_2=(N_1V_1)/N_2$ in the previous tables. All the samples in 5 mM acetate buffer pH 6.0.

Preparation of varying urea in M + 1 M TMAO	**Amount of 5 M urea to be added to get required concentrations in ml**	**Barnase (0.5 mg/ml from 12.12 mg/ml stock)**	**Amount of 5 M TMAO to be added to get 1 M final concentration in ml**	**Acetate buffer to make final DSC sample of 1 ml.**
0	0	0.04125	0.2	0.75875
1	0.2	0.04125	0.2	0.55875
2	0.4	0.04125	0.2	0.35875
3	0.6	0.04125	0.2	0.15875

Table 2.6. Calculation for 1 ml sample preparation with barnase (0.5 mg/ml), Varying TMAO, 1 M urea and acetate buffer. Amount of urea and TMAO to be added were calculated using the formula $V_2=(N_1V_1)/N_2$ in the previous tables. All the samples in 5 mM acetate buffer pH 6.0.

Preparation of varying TMAO in M + 1 M urea	**Amount of 6 M urea to be added to get 1 M final concentration ml**	**Barnase (0.5 mg/ml from 12.12 mg/ml stock)**	**Amount of 5 M TMAO to be added to get required varied1 M final concentrations in ml**	**Acetate buffer to make final DSC sample of 1 ml.**
0.5	0.166	0.04125	0.1	0.69275
2	0.166	0.04125	0.4	0.39275
3	0.166	0.04125	0.6	0.19275

Table 2.7. Calculation for 1 ml sample preparation with barnase (0.5 mg/ml), Varying ectoine, 1 M urea and acetate buffer. Amount of urea and ectoine to be added were calculated using the formula $V_2=(N_1V_1)/N_2$ in the previous tables. All the samples in 5 mM acetate buffer pH 6.0.

Varying ectoine in M + 1 M urea	**Amount of 6 M urea to be added to get 1 M final concentration ml**	**Barnase (0.5 mg/ml from 12.12 mg/ml stock)**	**Amount of 3 M TMAO to be added to get required varied1 M final concentrations in ml**	**Acetate buffer to make final DSC sample of 1 ml.**
0.5	0.166	0.04125	0.166	0.62675
1	0.166	0.04125	0.333	0.45975
2	0.166	0.04125	0.666	0.12675

2.2.4 Data fitting

DSC experiments and data fitting were done using Nano-Analyze software. Once the sample and blank samples were run, the water reference must be blanked from the sample blank before subtracting the blank from the sample. Raw heat data needs to be converted to molar heat capacity, which is done by selecting the baseline range over the thermogram and adding the molecular weight, concentration of the protein and volume of the sample. A sigmoidal baseline consisting of both first and second order polynomials needs to be added to calculate thermodynamic quantities like Entropy (ΔS), Enthalpy (ΔH) and Melting Temperatures (T_m) values. The baseline was fitted by selecting the range of data for the integration. The grey lines/arcs on the thermogram need to be adjusted using 5 baseline nodes (as shown in Figure 3.3) such that the fitted baseline from the pre transition region is passing through the pre and post transition baselines, and the grey line from the post transition region is passing through the post transition baseline points and over the baseline (red color) in the transition region. Details of the data fitting for DSC are discussed in detail in chapter 3.

2.3 NMR Experiments and Data Processing

2.3.1 Sample preparation for NMR - Barnase-TMAO Titration protocol

2.3.1.1 A typical protocol for example barnase-TMAO titration as follows:

A stock solution of 3 M TMAO was prepared in 5 mM acetate buffer pH 5.8, and filter sterilized using a 0.45 µm filter. TMAO was adjusted to pH 6.2 with 0.1M HCl. 550 µl of 785 µM, pH 6.0 barnase was placed in an Eppendorf vial, 1 µl of 100 mM TSP stock solution in D_2O was added (to get 0.2 mM final conc) and 49 µl 10 % D_2O. TSP and D_2O was placed in a capillary tube inside the NMR tube to rule out any interaction of TSP with TMAO. The pH was measured, and the sample was transferred into a 5 mm NMR tube. Barnase sample was put into the NMR tube and titrated against TMAO by serially increasing the concentration of TMAO, starting from 0 M, and then serially increased to 0.01 M, 0.025, 0.05, 0.10, 0.25, 0.5, 0.75, and 1 molar. NMR was run and spectra were taken at each TMAO addition. By the end of the titrations, the barnase concentration got diluted due to the addition of TMAO and was calculated to be 523 µM.

At the end of the titrations, samples were removed from the NMR tube, transferred into an Eppendorf vial and their pH was measured. Amount of TMAO to be added was solved from the above formula as y =[v3(c1-c3)]/(c2-c1), where finding for c1 gives final concentration of

TMAO, c3 is previous concentration of TMAO present in the NMR tube, v3 is volume of sample in NMR tube, c2 is concentration of stock, y is the volume of TMAO added at each concentration. Sample preparations for all the osmolyte – barnase titrations are described in Tables 2.8 – 2.10.

Table 2.8. Amount of TMAO to be added was calculated with y =[v3(c1-c3)]/(c2-c1), where finding for c1 gives final concentration of TMAO, c3 is previous concentration of TMAO present in the NMR tube, v3 is volume of sample in NMR tube, c2 is concentration of stock.

Preparation of TMAO in mM	c1	c2	v3	c3	[v3(c1-c3)]	(c2-c1)	y =[v3(c1-c3)]/(c2-c1)	Barnase concentration in mM
10	10	3000	550	0	5500	2990	1.8	782
25	25	3000	551.8	10	8277.6	2975	2.8	778
50	50	3000	554.6	25	13865.5	2950	4.7	772
100	100	3000	559.3	50	27966.1	2900	9.6	759
250	250	3000	569.0	100	85344.8	2750	31.0	720
500	500	3000	600.0	250	150000.0	2500	60.0	654
750	750	3000	660.0	500	165000.0	2250	73.3	589
1000	1000	3000	733.3	750	183333.3	2000	91.7	523

2.3.2 Sample preparation for NMR - Barnase-ectoine Titration protocol

A protocol similar to that of Barnase – TMAO was followed for barnase-ectoine and barnase betaine titrations, except that stock solution concentrations were slightly different as mentioned in the below tables 2.9 and 2.10.

For barnase-betaine titrations, by the end of the titrations barnase concentration got diluted due to the addition of betaine and was calculated to be 518 µM.

For barnase-ectoine titrations barnase initial concentration was increased to 875 µM so that the final concentration was close to that of barnase-TMAO titrations and at the end of the titrations barnase concentration got diluted due to the addition of ectoine and was calculated to be 525 µM. Also, initial sample volume was 500 µl and unlike TMAO and betaine titrations for ectoine, TSP was not in a separate tube since the practice of adding TSP in a capillary tube was started only while repeating the TMAO titrations which will be discussed in the results chapter.

Table 2.9. Amount of ectoine to be added was calculated with y =[v3(c1-c3)]/(c2-c1), where finding for c1 gives final concentration of ectoine, c3 is previous concentration of ectoine present in the NMR tube, v3 is volume of sample in NMR tube, c2 is concentration of stock.

Preparation of ectoine in mM	c1	c2	v3	c3	[v3(c1-c3)]	(c2-c1)	y =[v3(c1-c3)]/(c2-c1)	Barnase concentration in mM
10	10	2500	500	0	5000	2490	2.0	872
25	25	2500	502	10	7530	2475	3.0	866
50	50	2500	505	25	12625	2450	5.2	858
100	100	2500	510.2	50	25510	2400	10.6	840
250	250	2500	520.8	100	78120	2250	34.7	788
500	500	2500	555.5	250	138875	2000	69.4	700
750	750	2500	624.9	500	156225	1750	89.3	613
1000	1000	2500	714.2	750	178550	1500	119.0	525

Table 2.10. Amount of betaine to be added was calculated with y =[v3(c1-c3)]/(c2-c1), where finding for c1 gives final concentration of betaine, c3 is previous concentration of betaine present in the NMR tube, v3 is volume of sample in NMR tube, c2 is concentration of stock.

Preparation of betaine in mM	c1	c2	v3	c3	[v3(c1-c3)]	(c2-c1)	y =[v3(c1-c3)]/(c2-c1)	Barnase concentration in mM
10	10	2940	550	0	5500	2930	1.9	782
25	25	2940	551.9	10	8278.2	2915	2.8	778
50	50	2940	554.7	25	13867.9	2890	4.8	772
100	100	2940	559.5	50	27975.8	2840	9.9	758
250	250	2940	569.4	100	85404.9	2690	31.7	718
500	500	2940	601.1	250	150278.8	2440	61.6	651
750	750	2940	662.7	500	165676.2	2190	75.7	585
1000	1000	2940	738.4	750	184589.0	1940	95.1	518

2.3.3 Data acquisition

NMR spectra from barnase-TMAO and barnase-ectoine titrations were acquired at 25 °C on an 800 MHz spectrometer (Avance I Bruker). A 5 mm tube was used for most of the titrations and shaped tube was used for the samples with salt concentrations above 0.75 M to avoid loss of signal and get better signal sensitivity. 3-trimethylsilyl-2,2,3,3-($^{2}H_4$) propionate (TSP) was used for referencing ^{1}H chemical shifts at 0.0 ppm, and ^{15}N and ^{13}C chemical shifts were calculated relative to TSP. Chemical shift reference values were obtained from barnase entry 4964 in the BiomagResBank. These values were used as a basis for backbone assignment

of barnase using ^{1}H, ^{15}N HSQC, ^{13}C HSQC, 3D-HNCO, 3D-HNCA, HNCACB, and HNCOCACB experiments. Chemical shifts were monitored at each salt addition on Topspin. Macros (home written scripts on Linux) were used to process spectra and assign the peaks using the FELIX software. The naccess programme was used to calculate the solvent-accessible surface area from the PDB file 1a2p.

2.4 Backbone assignment

Spectra were processed and peaks were assigned using the FELIX2007 software (Felix NMR, Inc., San Diego, CA). The assignment of peaks was done using home-written macros running under Linux. This involves the following steps.

The following 3D experiments were done for resonance assignment.

Table 2.11. Table describing correlation between different atoms in the peptide backbone studied in various experiments for backbone assignment. The superscript ^{i} is the same residue as HN and $^{i-1}$ is the preceding residue. HN to $C\alpha^{i-1}$ means the HN of a residue correlate to the Cα of the preceding residue.

Experiment	Correlates
^{15}N HSQC	HN to NH
HNCA	HN to $C\alpha^{i}$ and [$C\alpha^{i-1}$]
HN (CO)CA	HN to $C\alpha^{i-1}$
HNCACB	HN to $C\alpha^{i}$, C_{β}^{i}, [$C\alpha^{i-1}$] and [C_{β}^{i-1}]
HN(CO)CACB	HN to $C\alpha^{i-1}$and C_{β}^{i-1}
HN(CA)CO	HN to CO^{i} and [CO^{i-1}]
HNCO	HN to CO^{i-1}

2.4.1 Peak picking

Main chain assignments were obtained by correlating the chemical shifts of the amide groups of a spin system with nuclei in the same and preceding residue. The side chain or main chain atom is referred to as a matching atom. For example, an HNCA experiment correlates an amide group with the α-carbon chemical shift of its own residue and with the α-carbon chemical shift of the preceding residue. This α-carbon ($C\alpha^{i}$) is referred to as the matching atom. The chemical shifts of the matching atoms will be correlated to the adjacent residues to link the amide groups in a polypeptide sequence. The chemical shift of an inter residue matching atom

in amide group A is equivalent to that of an intra residue shift of the same matching atom in amide group B. The α-carbon atom of a preceding residue is called $C\alpha^{i-1}$. For convenience C^{i} is referred as Cα and $C\alpha^{i-1}$ as PCα. Similarly, β-Carbon atom will be referred here as C_{β} and PC_{β}, and carbonyl (CO) atoms as CO and PCO.

2.4.2 Checked table analysis and assignment output distribution

Converting spin systems to corresponding residue type in the protein sequence is accomplished by a programme called Asstools. This programme assigns Cα, PCα, Cβ, PCβ, CO, PCO to amino acid type (residue name and number) after comparing chemical shifts from a spin system to that of preceding spin systems (PCα with Cα, PCβ with Cβ, CO with PCO). This programme initially does 30 stochastic repeats and, in each run, assigns spin systems to residues in the protein sequence. Results from these repeats were calculated to match the chemical shifts of self and preceding residues. These runs were repeated till the scores were 30 out of 30 correct on assignment output distribution. If scores were less good, peak picking was checked to correctly select ppm values on peaks to correct any errors.

2.4.3 Titration Mapping.

All the experimental (1D and 2D) spectra were phase corrected and the centre point of the ^{1}H frequencies was noted. In Linux Konsole, the centre point of the spectrum, the SR value and F2 SFO values were typed in to reference the hydrogen, nitrogen, and carbon shifts. The resultant centre of heterospectrum value is noted in the processing macro.

After processing and referencing the peaks from the HSQC, CHSQC, and HNCO experiments in Felix using a processing macro, crosspeaks derived from the assignment were fit to the spectrum for the first experiment of the titration using the peak edit function in Felix. These cross-peak entities were copied for the subsequent titrations in the series by using a copy macro. The positions of the cross-peak items for each resonance at each step of the titration were adjusted using an edit macro. At the end of the titration mapping, an output macro was used to output the files from Felix to text files. Any residues which could not be assigned due to peak overlapping were excluded using nawk scripts. All the above steps were executed using appropriate macros in the command terminal of Felix software for all the 3 experiments i.e., HSQC, CHSQC, and HNCO. Data from the above was used to make box plots for each residue of the protein using nawk and python scripts. All the data from ^{15}NHSQC, ^{13}CHSQC, and HNCO was segregated, and chemical shift changes were fitted to straight line and binding

curve equations using home written Linux scripts which will be explained in detail in chapter 4.

Table 2.12. Different set of macros used for titration mapping in ^{15}NHSQC, ^{13}CHSQC, HNCO experiments.

Titration	Type of Exp	Process Macro	Titration (TTN) edit Macro
Barnase-TMAO	^{15}NHSQC	yk_baranse_tmao_2ndset_hsqc_process.mac	yk_baranse_tmao_2ndset_hsqc_ttn.mac
Barnase-TMAO	^{13}CHSQC	yk_baranse_tmao_2ndset_chsqcali_process.mac	yk_baranse_tmao_2ndset_chsqcali_ttn.mac
Barnase-TMAO	2D HNCO	yk_baranse_tmao_2ndset_hnco_process.mac	yk_baranse_tmao_2ndset_hnco_ttn.mac
Barnase-ectoine	^{15}NHSQC	yk_baranse_ectoine_hsqc_process.mac	yk_baranse_ectoine_hsqc_ttn.mac
Barnase-ectoine	^{13}CHSQC	yk_baranse_ectoine_chsqcali_process.mac	yk_baranse_ectoine_chsqcali_ttn.mac
Barnase-ectoine	2D HNCO	yk_baranse_ectoine_hnco_process.mac	yk_baranse_ectoine_hnco_ttn.mac
Barnase-betaine	^{15}NHSQC	yk_baranse_betaine_hsqc_process.mac	yk_baranse_betaine_hsqc_ttn.mac
Barnase-betaine	^{13}CHSQC	yk_baranse_betaine_chsqcali_process.mac	yk_baranse_betaine_chsqcali_ttn.mac
Barnase-betaine	2D HNCO	yk_baranse_betaine_hnco_process.mac	yk_baranse_betaine_hnco_ttn.mac

2.5 Urea – osmolytes ^{1}H NMR experiments

These experiments were primarily conducted to study the interaction between osmolytes (TMAO, ectoine, betaine) and urea, hence barnase will be absent in these experiments. Since the volume of titrant added at each step is small, pH changes are very small (<0.05), hence all the solutions (buffer, urea, osmolytes) were maintained at the same pH of 5.8 (unlike barnase titrations where TMAO and betaine had to be prepared at pH 0.2 more than barnase) after confirming with dummy experiments. Standard NMR spectra of osmolytes (without urea) were also run to differentiate the changes in chemical shift of osmolytes in the presence and absence of osmolytes.

2.5.1.1 A typical protocol: urea-TMAO titration.

Stock solutions of TMAO and urea were prepared in 5 mM acetate buffer pH 5.8. All the salt preparations were filter sterilized using a 0.45 µm filter. 550 µl of 20 mM urea was placed in a 5 mm NMR tube and referenced against 0.2 mM TSP in 10% D_2O (placed in a capillary tube to rule out any interaction of TSP with osmolytes). This will be 0 mM TMAO. A 1D NMR was obtained, and the spectrum was recorded. In the next step 5 mM TMAO was

added to the same tube to titrate against urea and NMR was again run and the spectrum was recorded. The TMAO concentration in the tube was gradually increased at various increments (0, 5, 10, 15, 20, 40, 60, 80, 100) till 100 mM and NMR was run and spectrum recorded at each addition of TMAO. All the calculations were done with the formula c1 =[(c3v3) + (c2+y)]/(v3+y), where c1 is the final concentration of TMAO, c3 is the previous concentration of TMAO present in the NMR tube, v3 is the volume of sample in the NMR tube, c2 is concentration of stock, and y is the volume of TMAO added at each concentration. A similar protocol was followed for barnase-ectoine and barnase-betaine titrations, except TMAO was replaced with ectoine and betaine in the titrations. Spectra were recorded and monitored on Topspin software at each addition of salt. Another experiment i.e., standard spectra of TMAO/ectoine/betaine was conducted with the same method except that it was without the addition of 20 mM urea. All the sample preparations are described in Tables 2.13 – 2.15.

Table 2.13. Amount of TMAO to be added was calculated with y =[v3(c1-c3)]/(c2-c1), where finding for c1 gives final concentration of TMAO, c3 is previous concentration of TMAO present in the NMR tube, v3 is volume of sample in NMR tube, c2 is concentration of stock.

Preparation of TMAO in mM	c1	c2	v3	c3	[v3(c1-c3)]	(c2-c1)	y =[v3(c1-c3)]/(c2-c1)
5	5	3000	550	0	2750	2995	0.9
10	10	3000	550.9	5	2755	2990	0.9
15	15	3000	551.8	10	2759	2985	0.9
20	20	3000	552.8	15	2764	2980	0.9
40	40	3000	553.7	20	11074	2960	3.7
60	60	3000	557.4	40	11149	2940	3.8
80	80	3000	561.2	60	11224	2920	3.8
100	100	3000	565.1	80	11301	2900	3.9

Table 2.14. Amount of ectoine to be added was calculated with y =[v3(c1-c3)]/(c2-c1), where finding for c1 gives final concentration of ectoine, c3 is previous concentration of ectoine present in the NMR tube, v3 is volume of sample in NMR tube, c2 is concentration of stock

Preparation of ectoine in mM	c1	c2	v3	c3	[v3(c1-c3)]	(c2-c1)	y =[v3(c1-c3)]/(c2-c1)
5	5	2500	550	0	2750	2495	1.10
10	10	2500	551.1	5	2756	2490	1.11
15	15	2500	552.2	10	2761	2485	1.11
20	20	2500	553.3	15	2767	2480	1.12
40	40	2500	554.4	20	11089	2460	4.5
60	60	2500	558.9	40	11179	2440	4.6
80	80	2500	563.5	60	11270	2420	4.7
100	100	2500	568.2	80	11364	2400	4.7

Table 2.15.Amount of betaine to be added was calculated with y =[v3(c1-c3)]/(c2-c1), where finding for c1 gives final concentration of betaine, c3 is previous concentration of betaine present in the NMR tube, v3 is volume of sample in NMR tube, c2 is concentration of stock.

Preparation of betaine in mM	c1	c2	v3	c3	[v3(c1-c3)]	(c2-c1)	y =[v3(c1-c3)]/(c2-c1)
5	5	2940	550	0	2750	2935	0.9
10	10	2940	550.9	5	2755	2930	0.9
15	15	2940	551.9	10	2759	2925	0.9
20	20	2940	552.8	15	2764	2920	0.9
40	40	2940	553.8	20	11075	2900	3.8
60	60	2940	557.6	40	11152	2880	3.9
80	80	2940	561.5	60	11229	2860	3.9
100	100	2940	565.4	80	11308	2840	4.0

2.6 Osmolytes ^{1}H NMR standard spectra

These experiments are like urea-osmolytes ^{1}H NMR titrations except that these are without urea and just pure osmolyte solutions i.e., TMAO, ectoine, and betaine. Chemical shift changes from this standard spectrum will be used as a reference while measuring the effects of urea on osmolytes in the urea-osmolyte titration discussed earlier.

A typical protocol for standard NMR spectra of osmolytes, for example TMAO is as follows.

Stock solutions of TMAO were prepared in 5 mM acetate buffer pH 5.8. Salt preparations were filter sterilized using a 0.45 µm filter. 550 µl of 5 mM acetate buffer was placed in a 5 mm NMR tube and referenced against 0.2 mM TSP in 10% D_2O (placed in a capillary tube to rule out any interaction of TSP with osmolytes). This will be 0 mM TMAO. The NMR was obtained, and spectrum was recorded. In the next step 5 mM TMAO was added to the same tube and NMR was again run and spectrum was recorded. TMAO concentration in the tube was gradually increased at various increments (0, 5, 10, 15, 20, 40, 60, 80, 100) till 100 mM and NMR was run and spectrum recorded at each addition of TMAO. All the calculations were done with the formula c1 =[(c3v3) + (c2+y)]/(v3+y), where c1 gives the final concentration of TMAO, c3 is the previous concentration of TMAO present in the NMR tube, v3 is the volume of sample in the NMR tube, c2 is the concentration of stock, and y is the volume of TMAO added at each concentration. A similar protocol was followed for ectoine

and betaine standard spectra titrations, except TMAO was replaced with ectoine and betaine in the titrations. All the sample preparations are described in Tables 2.16 – 2.18. Spectra were recorded and monitored on Topspin software at each addition of salt.

Table 2.16. Amount of TMAO to be added was calculated with y =[v3(c1-c3)]/(c2-c1), where finding for c1 gives final concentration of TMAO, c3 is previous concentration of TMAO present in the NMR tube, v3 is volume of sample in NMR tube, c2 is concentration of stock.

Preparation of TMAO in mM	c1	c2	v3	c3	[v3(c1-c3)]	(c2-c1)	y =[v3(c1-c3)]/(c2-c1)
5	5	3000	550	0	2750	2995	0.9
10	10	3000	550.9	5	2755	2990	0.9
15	15	3000	551.8	10	2759	2985	0.9
20	20	3000	552.8	15	2764	2980	0.9
40	40	3000	553.7	20	11074	2960	3.7
60	60	3000	557.4	40	11149	2940	3.8
80	80	3000	561.2	60	11224	2920	3.8
100	100	3000	565.1	80	11301	2900	3.9

Table 2.17. Amount of ectoine to be added was calculated with y =[v3(c1-c3)]/(c2-c1), where finding for c1 gives final concentration of ectoine, c3 is previous concentration of ectoine present in the NMR tube, v3 is volume of sample in NMR tube, c2 is concentration of stock

Preparation of ectoine in mM	c1	c2	v3	c3	[v3(c1-c3)]	(c2-c1)	y =[v3(c1-c3)]/(c2-c1)
5	5	2500	550	0	2750	2495	1.10
10	10	2500	551.1	5	2756	2490	1.11
15	15	2500	552.2	10	2761	2485	1.11
20	20	2500	553.3	15	2767	2480	1.12
40	40	2500	554.4	20	11089	2460	4.5
60	60	2500	558.9	40	11179	2440	4.6
80	80	2500	563.5	60	11270	2420	4.7
100	100	2500	568.2	80	11364	2400	4.7

Table 2.18. Amount of betaine to be added was calculated with y =[v3(c1-c3)]/(c2-c1), where finding for c1 gives final concentration of betaine, c3 is previous concentration of betaine present in the NMR tube, v3 is volume of sample in NMR tube, c2 is concentration of stock

Preparation of betaine in mM	**c1**	**c2**	**v3**	**c3**	**[v3(c1-c3)]**	**(c2-c1)**	**y =[v3(c1-c3)]/(c2-c1)**
5	5	2940	550	0	2750	2935	0.9
10	10	2940	550.9	5	2755	2930	0.9
15	15	2940	551.9	10	2759	2925	0.9
20	20	2940	552.8	15	2764	2920	0.9
40	40	2940	553.8	20	11075	2900	3.8
60	60	2940	557.6	40	11152	2880	3.9
80	80	2940	561.5	60	11229	2860	3.9
100	100	2940	565.4	80	11308	2840	4.0

3 CHAPTER 3: EFFECT OF OSMOLYTES ON THE STABILITY OF PROTEIN BARNASE

3.1 OBJECTIVE

The objective of the work described in this chapter was to study the effect of osmolytes on the stability of barnase by Differential scanning calorimetry (DSC). This was accomplished by a series of different titrations. The first three titrations are of pure osmolyte solutions i.e., TMAO, ectoine, and urea against barnase to see the effect of these osmolytes on the barnase stability. In addition, since urea is a known protein destabilizer, to know to what extent TMAO and ectoine can counteract the destabilising effects of urea, mixed osmolyte solutions of TMAO plus urea and ectoine plus urea were titrated against the barnase. The results of these titrations are discussed in the later sections.

3.2 DIFFERENTIAL SCANNING CALORIMETRY (DSC)

3.2.1 Principle

DSC is a calorimetric technique used to study a change in the state of proteins, primarily used for stability studies (thermal denaturation). It measures the change in heat released or absorbed when a protein is unfolded. It has two cells covered by cylindrical jackets: one is loaded with the sample and the other with the blank, which typically contains a solution identical to the sample except that there is no protein. The cells are usually made from alloys of gold or platinum. The calorimeter is set up so that heating is supplied to the reference cell at a constant rate. It tries to keep the temperature of the sample cell at the same temperature as the reference.

When energy is transferred to a sample cell containing protein and a reference cell containing blank buffer, and the same heating rate is applied, cells will reach different temperatures since they have different solution compositions and thus different heat capacities (Ibarra-Molero et al., 2016). The cell with the protein sample consumes a different amount of energy compared to the reference cell which is measured by the difference in power absorbed by the sample cell in order to heat it to the same temperature as the blank (Privalov and Potekhin, 1986). The difference in the heating energy between sample and reference cell is used to calculate the heat capacity of the protein. When heat capacity is plotted against temperature, the thermal peak shows the protein unfolding (Ibarra-Molero et al., 2016).

The water surrounding the hydrophobic groups on protein molecules is more ordered (Pace et al., 2009). This is because water does not form hydrogen bonds with non-polar groups. All this makes the cell with protein sample consume more heat, thereby increasing the heat capacity. The difference in heat capacity of the sample cell (partial C_p) and blank cell is the molar heat capacity that can be obtained by subtracting the scan of blank from the sample. This molar heat capacity C_p is used to calculate thermodynamic parameters like Entropy (ΔS) and Enthalpy (ΔH).

The thermodynamic definition of the protein stability is the difference in free energy (ΔG) between folded and unfolded state.

$$\text{Unfolded state} \Longleftrightarrow \text{Folded state}$$

The sign for change in free energy (ΔG) determines whether a reaction is thermodynamically favourable or unfavourable.

Under normal conditions, ΔG for folding must be negative as the folded state is thermodynamically favourable. Since protein folding is a two-state process for most proteins and is reversible, parameters like ΔG, ΔH and $T\Delta S$ can be determined experimentally using DSC. Folding thermodynamic parameters ΔG, ΔH and $T\Delta S$ play a huge role in stability of the protein. Proteins in the unfolded state exist in many conformations. When protein transforms to a folded state the degree of disorder decreases which results in a decrease in entropy called the conformational entropy $\Delta S_{conf.}$ Conformational entropy is unfavourable to the entropy of folding ΔS. Conformational entropy ΔS_{conf} is a major contributor to protein denaturation. For a protein to fold spontaneously, and thus where the change in free energy (ΔG) is negative, favorable ($\Delta H - T\Delta S$) is required. Non-covalent forces such as van der Waals forces and hydrogen bonding contribute to favourable ΔH, and the hydrophobic effect contributes to a favourable $T\Delta S$ (Pace et al., 2014b, Pace et al., 2014a, Myers and Pace, 1996). The contribution from these noncovalent forces helps to counteract the conformational entropy and the protein gets stabilised.

Heat capacity is an important parameter to study the thermodynamic equilibrium of protein denaturation. As the temperature of the protein increases, protein in folded state (native state) starts to unfold and an endothermic peak is formed. Once the thermal transition is completed the protein unfolding is considered to be complete (Privalov and Potekhin, 1986). The region of the DSC trace where the graph goes up and then comes back down is called the transition region. The baseline before unfolding starts is called pre transition baseline (low temperature), and a new baseline is formed (high temperature) when unfolding is complete. The area under this curve is integrated to calculate the enthalpy change (ΔH) for the transition. The excess heat associated with temperature is the enthalpy of unfolding ΔH (Johnson, 2013) which is measured as the integration of molar heat capacity against temperature (equation 3.1 and Figure 3.1).

$$\Delta H = \int_{T_1}^{T_2} C_p dT \qquad \textbf{(3.1)}$$

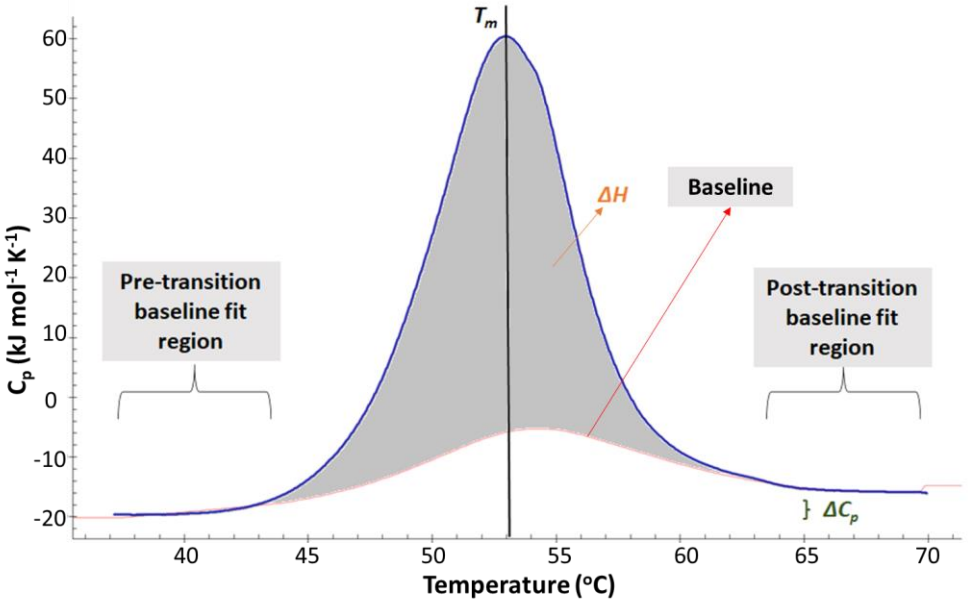

Figure 3.1. DSC thermogram for 0.5 mg/ml barnase in 5 mM acetate buffer at pH 6.0 describing various thermodynamic quantities.

Entropy (ΔS) is the integration

$$\Delta S = \int_{T_1}^{T_2} (C_p/T) dT \qquad \textbf{(3.2)}$$

Clearly, to be able to obtain values for enthalpy and entropy from the DSC curve, it is important to be able to fit the shape of the baseline accurately. It is not always simple to do this, and hence the values for enthalpy and entropy have considerable error associated with them.

Another important measurement that can be obtained from DSC is the melting temperature (T_m). T_m is the peak of the thermal transition curve at which half of the protein is in folded state and the other half is in unfolded state. This T_m is used as a measure of protein stability. The higher the value of T_m, the greater the stability of the protein, and the lower the value of T_m the lower the stability of the protein. Ions that are known as stabilisers increase the T_m while the destabilising ions decrease the T_m. T_m is affected by many parameters like pH, presence of co-solutes, protein concentration, heating rate, and pressure (Sanchezruiz, 1992, Arakawa and Timasheff, 1982, Santoro et al., 1992, Ibarra-Molero et al., 2016, Johnson, 2013). If the concentration of the protein is higher, protein aggregation is more likely to take place and there may be a greater exothermic heat change leading to a decrease in heat capacity. Fluctuations in pH can give artifacts in the baseline and can also make the T_m value leass accurate (Lopez and Makhatadze, 2002). The heating rate is normally between 0.1 ^{o}C/min to 4

^{o}C/min for heating the sample and reference cells. Any alteration in this can affect the T_m (Sanchezruiz et al., 1988). Thus, it is essential to maintain all the parameters at the suggested range to generate error free thermal scans. Nonetheless, it is usually possible to obtain reliable and accurate values for T_m.

3.3 Data Fitting

DSC experiments and data fitting were done using Nano-Analyze software. Once the sample and blank samples were run, the water reference must be blanked from the sample before subtracting the blank from the raw data (Figure 3.2). Raw heat data needs to be converted to molar heat capacity, which is done by providing the values of the molecular weight, concentration of the protein and volume of the sample.

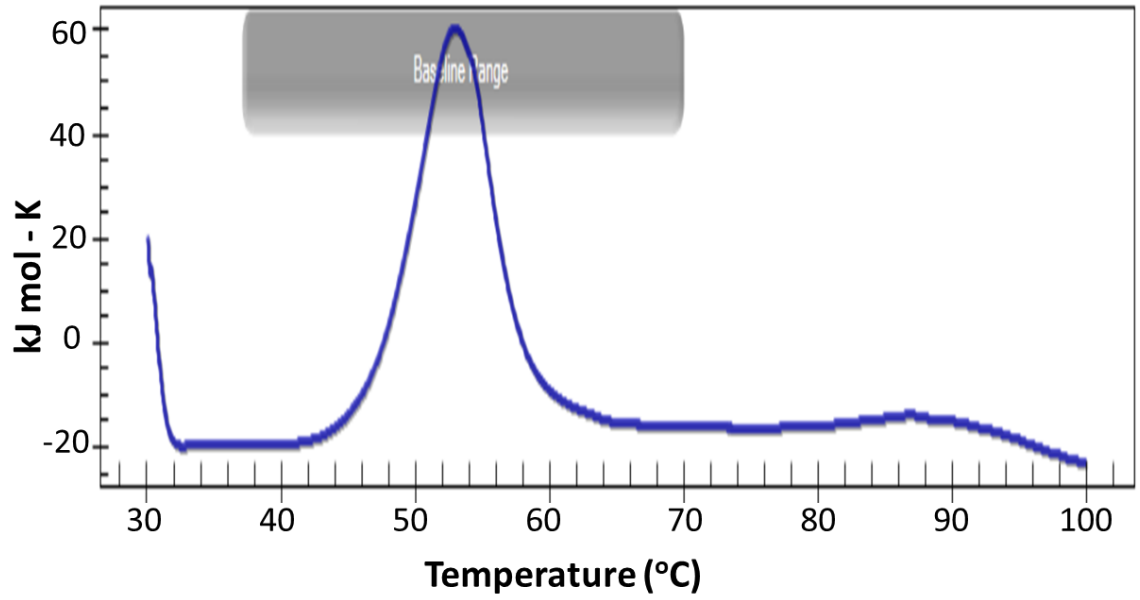

Figure 3.2. DSC raw data for 0.5 mg/ml barnase in 5 mM acetate buffer at pH 6.0

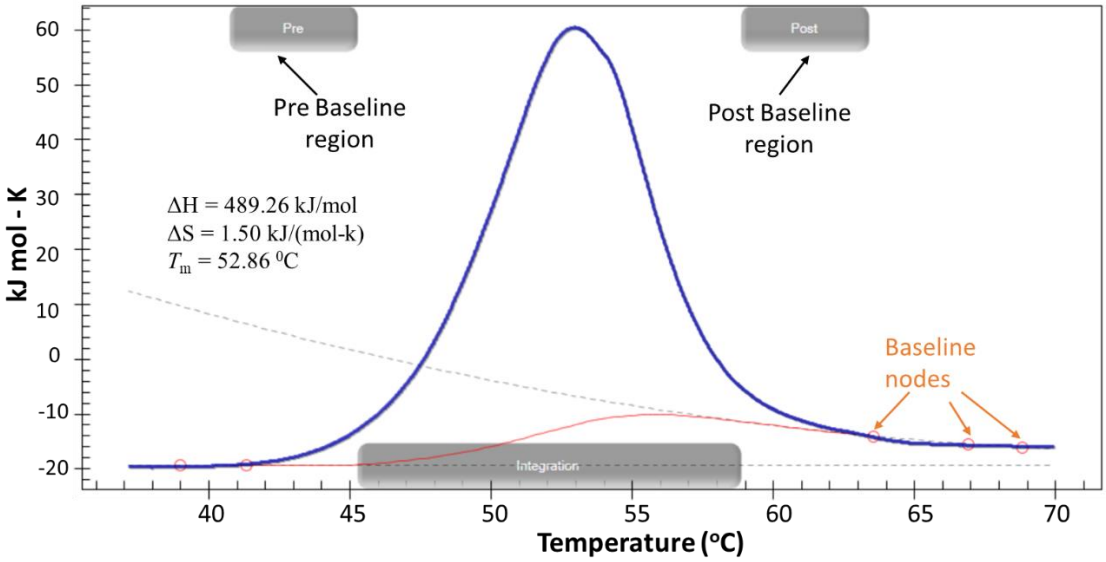

Figure 3.3. DSC thermogram (without baseline node adjustment) for 0.5 mg/ml barnase in 5 mM acetate buffer at pH 6.0 describing how the baseline was determined.

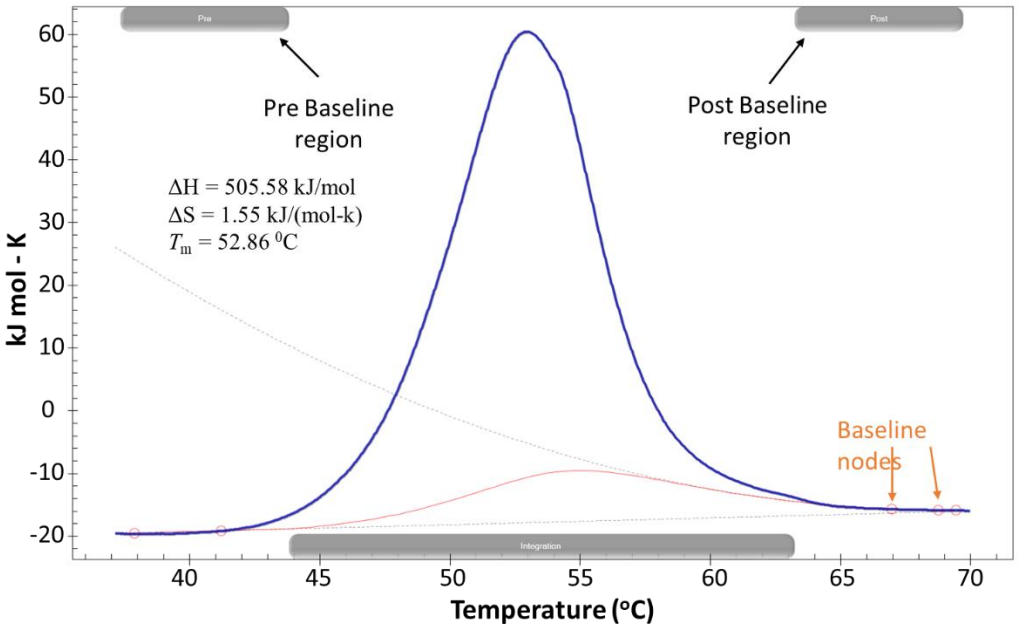

Figure 3.4. DSC thermogram for 0.5 mg/ml barnase in 5 mM acetate buffer at pH 6.0 describing how the baseline was determined. When temperature is plotted on X-axis and heat capacity on Y-axis, and a sigmoidal baseline was drawn, baseline nodes (on the right side) were adjusted to fit the baseline and calculate different thermodynamic parameters by using the software NanoAnalyze.

A sigmoidal baseline consisting of second order polynomials needs to be added to calculate thermodynamic quantities like Entropy (ΔS), Enthalpy (ΔH) and Melting Temperatures (T_m) values. The grey lines/arcs on the thermogram need to be adjusted using 5 baseline nodes (as shown in figure 3.3) such that the fitted baseline from the pre transition

region is passing through the pre and post transition baselines, and the grey line from the post transition region is passing through the post transition baseline points and over the baseline (red colour) in the transition region. The fitted baseline (red) should be a smooth curve (as shown in figure 3.4). Adjusting these grey lines is critical to get good values of Entropy (ΔS), Enthalpy (ΔH) and Melting Temperatures (T_m).

Any discrepancy in setting up these lines would give different values though T_m would still be largely the same as seen in figure 3.3 which has slightly different ΔS and ΔH before its nodes are adjusted and the graph with adjusted nodes is seen in figure 3.4. After baseline node adjustment ΔH has changed from 489.26 kJ/mol to 505.58 kJ/mol and ΔS has changed from 1.50 kJ $mol^{-1}K^{-1}$ to 1.55 kJ $mol^{-1}K^{-1}$ while T_m value remained the same (within two decimal places). But getting the right values of Entropy (ΔS) and Enthalpy (ΔH) is essential to calculate the change in free energy of unfolding at the melting temperature $\Delta\Delta G$ (T_m).

Finally, it should be added that thermodynamic parameters can only be fitted reliably if the protein unfolding is reversible: for example, if the protein refolds correctly when the temperature is lowered. This can in principle be detected by gradually reducing the temperature and looking to see if the curve on the way down is the same shape as the curve on the way up or is different (described as hysteresis). However, changes in baseline can make this difficult in practice. A simple check can be carried out. If the protein precipitates after unfolding, then usually the gradient on the high temperature side of the DSC curve is steeper than the gradient of the low temperature side, making the fitted DSC curve unsymmetrical. If this is the case, then the thermodynamic parameters need to be treated with caution, though the melting temperature is usually still fairly reliable. All the thermodynamic parameters were calculated by the Nano-Analyze software with the modified Gibbs-Helmholtz equation.

3.4 RESULTS AND DISCUSSION

3.4.1 The effect of TMAO on thermal stability of barnase

TMAO (trimethylamine oxide) is an organic compound with one positive and one negative charge hence overall neutral. It is known to have stabilizing effects on proteins and to have the ability to counteract denaturants when present at high concentrations. An overlay of thermograms for TMAO concentrations between 1-3000 mM is shown in figure 3.5. The initial T_m of barnase was 53.2 ± 0.4 ^oC. Addition of TMAO has a small stabilising effect by about 1.5 ^oC at 0.01 M. When the concentration of TMAO was increased by ten times i.e., 0.1 M, T_m

went up by just 0.21 °C more, so the effect is far from linear. A further increase in concentration to 1 M raised the T_m by only 0.3 °C. This is a 100-fold rise in concentration of TMAO from the first addition and T_m is not rising much. Addition of 3 M TMAO caused a slight dip in T_m by 0.32 °C. This could be due to the aggregation of barnase because of the high concentration of TMAO. When T_m values from all these additions were drawn to a smooth line, as shown in figure 3.5 and table 3.1 it suggests that T_m once raised by the small addition of TMAO i.e., at 10 mM protein would get saturated and any further additions will not make much difference to the overall T_m. Changes in enthalpy, entropy and free energy are discussed in section 3.4.7.

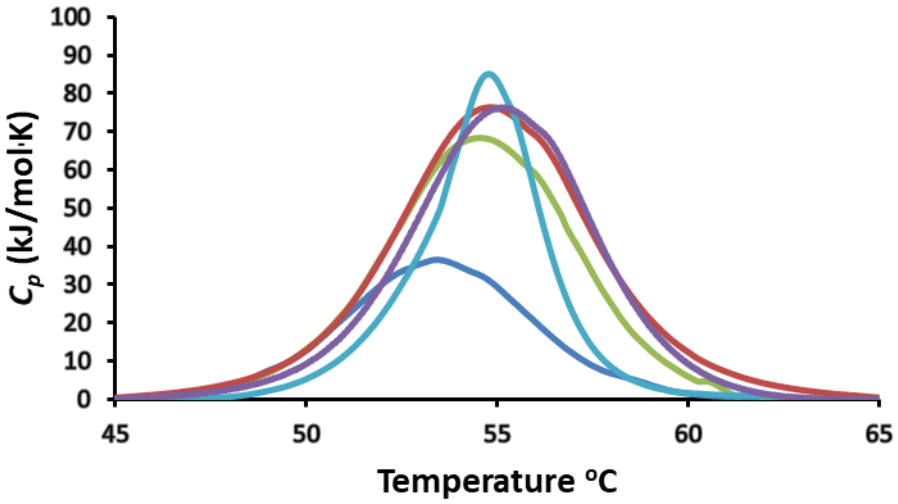

Figure 3.5. An overlay of DSC thermograms for 0.5 mg/ml barnase in 5 mM acetate buffer at pH 6.0 in the presence of 0 M (blue), 0.01 M (green), 0.1 M (red), 1 M (purple), 3 M (cyan) TMAO.

Table 3.1. Melting temperature (T_m), Enthalpy $\Delta H(T_m)$, Entropy $\Delta S(T_m)$ and change in free energy of unfolding $\Delta\Delta G$ (T_m) values for barnase in the presence of varied concentrations of TMAO between 0-3000 mM, all the samples in 5 mM acetate buffer pH 6.0.

TMAO (mM)	T_m(°C)	ΔT_m(°C)	$\Delta H(T_m)$(kJ/mol)	$\Delta S(T_m)$(kJ/mol^{-1}K^{-1})	$\Delta\Delta G(T_m)$ (kJ mol^{-1})
0	53.2 ± 0.4		505.6 ± 200.3	1.6 ± 0.6	0.0
10	54.6 ± 0.1	1.5	477.2 ± 84.0	1.5 ± 0.3	-2.2 ± 0.3
100	54.8 ± 0.0	1.7	469.9 ± 38.7	1.4 ± 0.1	-2.5 ± 0.3
1000	55.1 ± 0.0	2.0	414.2 ± 57.0	1.3 ± 0.2	-2.6 ± 0.4
3000	54.8	1.6	324.1 ± 60.2	1.0 ± 0.3	-1.7 ± 0.8

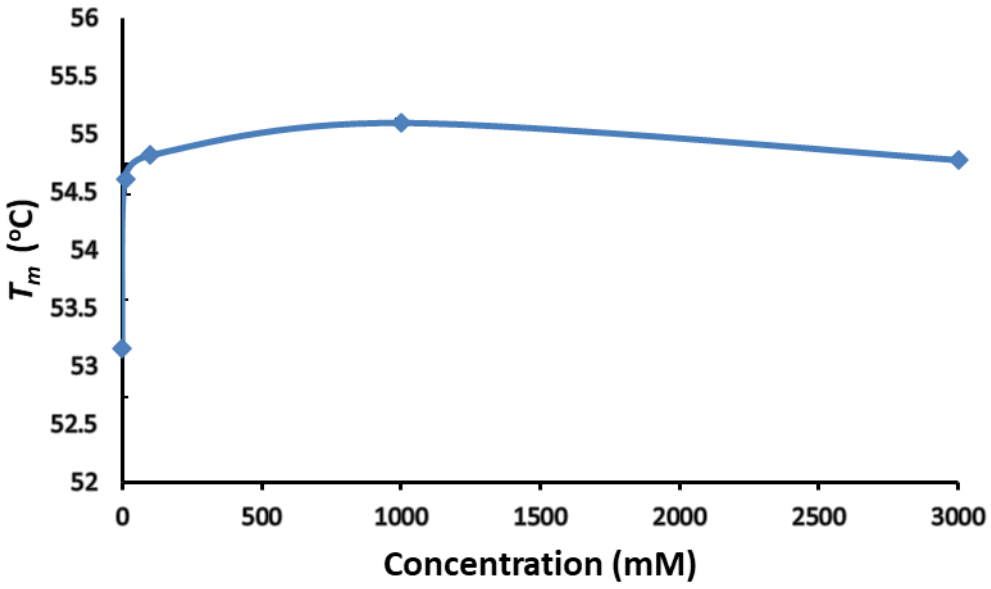

Figure 3.6. Melting temperature (Tm) values for barnase in the presence of varied concentrations of TMAO. All the samples are in 5 mM acetate buffer pH 6.0.

3.4.2 The effect of ectoine on thermal stability of barnase

Ectoine is a small natural organic compound known to have stabilizing effects on proteins and ability to counteract denaturants when present at high concentrations. An overlay of thermograms for ectoine concentrations between 1-1000 mM is shown in figure 3.7. Ectoine is normally stated to be a stabilising osmolyte. It is therefore surprising to see that it destabilises barnase by a small extent. The initial T_m of barnase was 53.2 ± 0.4 °C. Addition of ectoine has a small de-stabilising effect by about 0.9 °C at 0.01 M. When the concentration of ectoine was increased by ten times i.e., 0.1 M, T_m dropped by 0.5 °C. A further increase in ectoine concentration to 1 M dropped the T_m by 0.3 °C. This is a 100-fold raise in concentration of ectoine from the first addition and T_m is not dropping much but still it is a significant destabilising effect as shown in figure 3.8 and table 3.2. Overall, at 1 M Ectoine T_m dropped by 1.6 °C which is almost as much difference in T_m caused by TMAO, but the difference is that ectoine is exhibiting an opposite effect on barnase stability to that of TMAO. As for TMAO, the effect is not linear with concentration; rather, it behaves like a binding isotherm, with saturation behaviour.

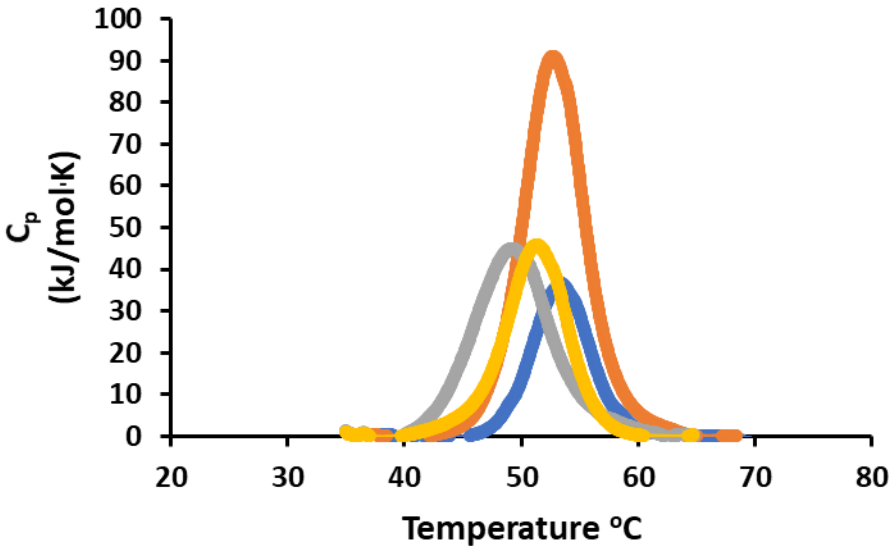

Figure 3.7. DSC thermograms for 0.5 mg/ml barnase in acetate buffer at pH 6.0 in the presence of 0 M (blue), 0.01 M (orange), 0.1 M (grey), 1 M (yellow) ectoine.

Table 3.2. Temperature of maximum unfolding (T_m), Enthalpy $\Delta H(T_m)$, Entropy $\Delta S(T_m)$ and change in free energy of unfolding $\Delta\Delta G$ (T_m) values for barnase in the presence of varied concentrations of ectoine between 0-1000 mM, all the samples in 5 mM acetate buffer pH 6.0.

Ectoine (mM)	T_m(°C)	ΔT_m(°C)	$\Delta H(T_m)$(kJ/mol)	$\Delta S(T_m)$(kJ/mol^{-1}K^{-1})	$\Delta\Delta G(T_m)$ (kJ mol^{-1})
0	53.2 ± 0.4		506 ± 200	1.6 ± 0.6	0.0
10	52.3 ± 0.5	-0.9	5967 ± 60	1.8 ± 0.2	1.6 ± 0.2
100	51.8 ± 0.1	-1.3	405 ± 46	1.2 ± 0.1	1.6 ± 0.3
1000	51.5 ± 0.0	-1.6	3767 ± 91	1.2 ± 0.3	1.8 ± 0.3

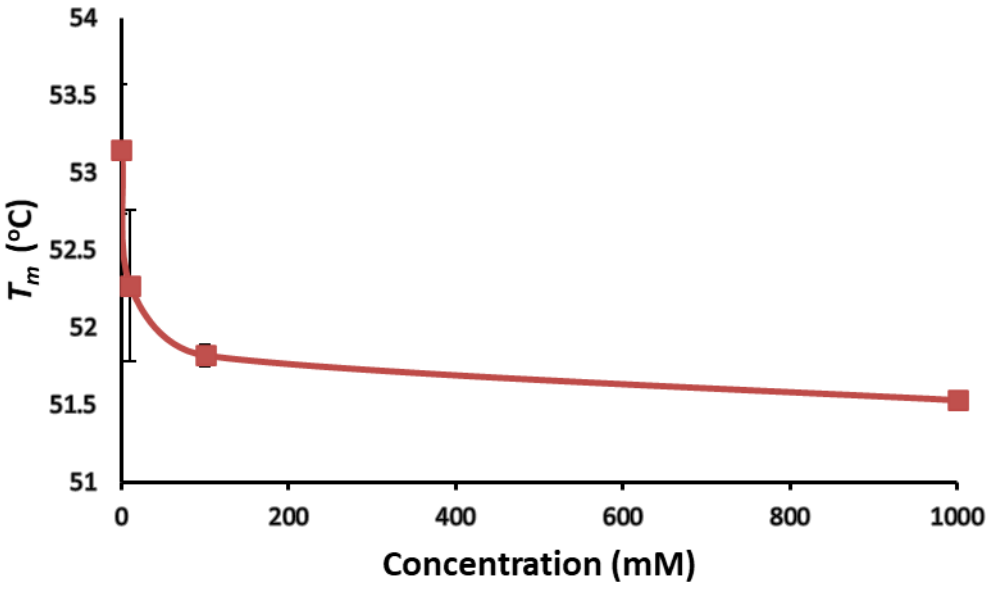

Figure 3.8. Melting temperature (T_m) values for barnase in the presence of varied concentrations of ectoine. All the samples are in 5 mM acetate buffer pH 6.0.

3.4.3 The effect of urea on thermal stability of barnase

Urea is an uncharged organic compound known to have destabilizing effects on proteins. An overlay of thermograms for urea concentrations between 1-1000 mM is shown in figure 3.9. The initial T_m of barnase was 53.2 ± 0.4 °C as shown in fig 3.9 which is an overlay of thermograms for barnase at varied concentrations of urea. Addition of urea has a large destabilising effect by about 4.5 °C at 1 M. When the concentration of urea was doubled, T_m dropped by 5.2 °C. A further increase in concentration to 3 M dropped the T_m by 6.7 °C. Overall, at 3 M, urea produced a total drop in T_m of 16.4 °C as shown in figure 3.10 and table 3.3. The drop in melting temperature is not a surprise, because urea is a known protein denaturant. However, it is interesting to note that urea behaves the way that a denaturant is expected to behave, in that the loss in stability is almost linear, in marked contrast to the effects of TMAO and ectoine. We note that the destabilising effect of urea (-4.5 °C at 1 M) is larger than the effects of TMAO (2.0 °C at 3 M) or ectoine (-1.6 °C at 3 M).

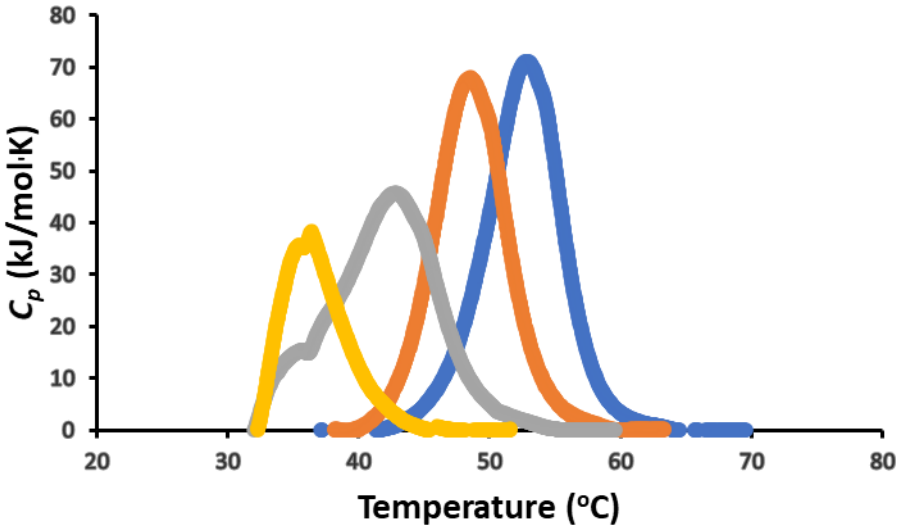

Figure 3.9. An overlay of DSC thermograms for 0.5 mg/ml barnase in 5 mM acetate buffer at pH 6.0 in the presence of 0 (blue), 1000 (orange), 2000 mM (grey), and 3000 mM (yellow) urea.

Table 3.3. Melting temperature (T_m), Enthalpy ΔH(T_m), Entropy ΔS(T_m) and change in free energy of unfolding ΔΔG (T_m) values for barnase in the presence of varied concentrations of urea between 0-3000 mM, all the samples in 5 mM acetate buffer pH 6.0. *no thermodynamic parameters are listed at 3 M urea because the unfolding is not reversible.

Urea (mM)	T_m(°C)	ΔT_m(°C)	$\Delta H(T_m)$(kJ/mol)	$\Delta S(T_m)$(kJ/mol^{-1}K^{-1})	$\Delta\Delta G(T_m)$ (kJ mol^{-1})
0	53.2 ± 0.4	0.0	506 ± 200	1.6 ± 0.6	0.0
1000	48.7 ± 0.1	-4.5	423 ± 59	1.3 ± 0.2	5.5 ± 0.4
2000	43.5 ± 1.0	-9.7	367 ± 7	1.2 ± 0.0	7.6 ± 0.7
3000	36.8 ± 0.1	16.4	*		

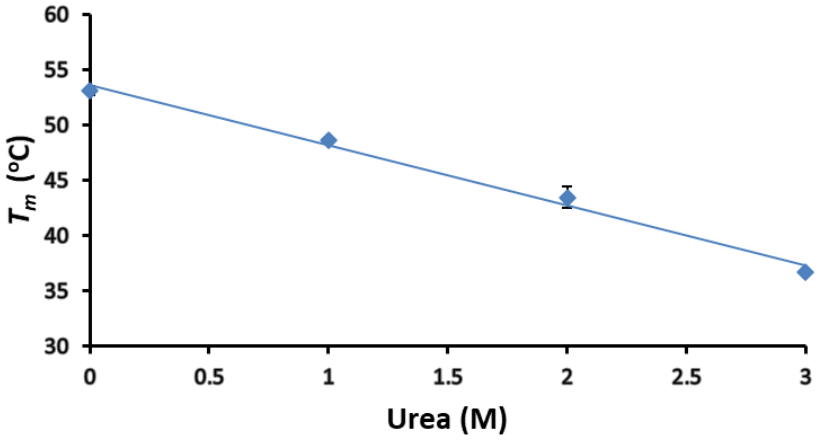

Figure 3.10. Melting temperature (Tm) values for barnase in the presence of varied concentrations of urea from 0 M to 3 M (all the samples in 5 mM acetate buffer pH 6.0).

3.4.4 The effect of TMAO on barnase in the presence of increasing concentrations of urea

Now that the effects of TMAO alone (stabilising) and urea (destabilising) have been presented, we present the effect of mixed osmolyte solutions of TMAO and urea that describes TMAO's counteraction of the destabilising effects of urea as shown in Figure 3.11 and Table 3.4. When 1 M TMAO was added to urea of varying concentrations from 1 M to 3 M, the T_m value which earlier dropped was restored by 2.3 ^{o}C at 1 M addition of as shown in table 3.5. Addition of 2 M TMAO to 2 M urea caused a raise in T_m by 4 ^{o}C compared to 2.5 ^{o}C raise caused by 1 M TMAO against the same amount of urea as shown in Figure 3.11 and Table 3.5. This experiment confirms that addition of TMAO restores the T_m value. This prompted us to plan the next experiment with higher proportions of TMAO against as shown in Table 3.6.

Table 3.4. Melting temperature (T_m), Enthalpy $\Delta H(T_m)$, Entropy $\Delta S(T_m)$ and change in free energy of unfolding $\Delta\Delta G$ (T_m) values for barnase in the presence of increasing concentrations of urea plus 1 M TMAO (all the samples in 5 mM acetate buffer pH 6.0).

Urea (M) against 1 M TMAO	T_m(°C)	ΔT_m(°C)	$\Delta H(T_m)$(kJ/mol)	$\Delta S(T_m)$(kJ/mol^{-1}K^{-1})	$\Delta\Delta G(T_m)$ (kJ mol^{-1})
0	55.1 ± 0.4	0	414 ± 57	1.3 ± 0.2	0.0
1	51 ± 0.0	-4.1	623 ± 182	1.9 ± 0.6	7.2 ± 0.3
2	46 ± 0.2	-9.1	372 ± 49	1.2 ± 0.2	7.5 ± 0.4
3	40.6 ± 0.1	-14.5	276 ± 120	0.9 ± 0.4	4.9 ± 1.0

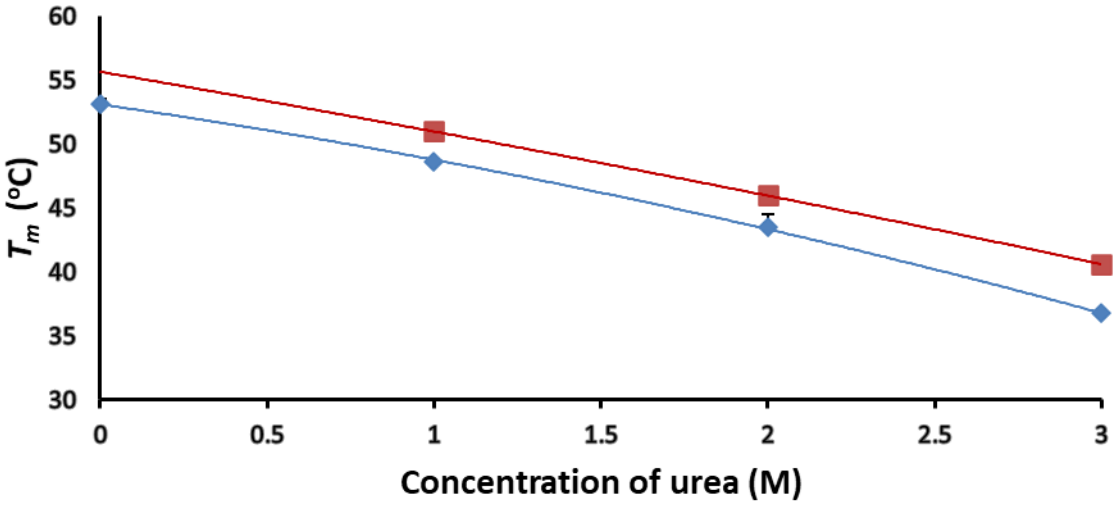

Figure 3.11. Melting temperature (T_m) values for barnase in the presence of varied concentrations of urea (blue) and mixed osmolyte solution (Concentration of urea varied from 0 M to 1 M and TMAO concentration maintained constant at 1 M) (Red), (all the samples in 5 mM acetate buffer pH 6.0).

Table 3.5. Table describing TMAO's counteraction of urea. Raise in melting temperature (T_m) values for barnase with the addition of TMAO to the increasing concentrations of urea (all the samples in 5 mM acetate buffer pH 6.0).

Concentrations of urea (M)	Urea without TMAO T_m(°C)	Urea (M) against 1 M TMAO T_m(°C)	Raise in T_m in the presence of 1 M TMAO (°C)
0	53.1 ± 0.4	55.1 ± 0.4	2.0
1	48.7 ± 0.1	51 ± 0.0	2.3
2	43.5 ± 1.0	46 ± 0.2	2.5
3	36.8 ± 0.1	40.6 ± 0.1	3.8

3.4.5 The effect of increasing concentrations of TMAO on Barnase in the presence of 1 M Urea

This experiment reveals the extent to which TMAO can counteract destabilising effects of urea. Addition of 0.5 M TMAO against 1 M urea restored the T_m by 1.1 °C. Addition of 1 M TMAO restored T_m by a further 1.3 °C. Addition of 2 M TMAO resulted in a slight drop in restored T_m value by 0.8 °C. Addition of 3 M TMAO raised the restored T_m value by a further 0.4 °C. Overall, at a TMAO to urea ratio of 3:1 T_m is restored by 1.9 °C.

The T_m value of barnase in the presence of 1 M urea was 48.7 °C and when TMAO was added the T_m was between 49.7 ± 0.1 °C and 50.6 ± 0.0 °C. So, T_m is clearly higher than the 48.7 °C which it was in the presence of 1 M urea. This experiment proves that TMAO can resist the destabilising effects of urea, as the T_m which was brought down by 1 M urea by 4.5 °C is restored by TMAO at all the concentrations from 0.5 to 3 M with the highest being at 3M additions as shown in Table 3.6 and Figure 3.12 and. Restoration of T_m value by TMAO is not complete though, as the original T_m of 0.5 mg/ml barnase was 53.2 °C and addition of TMAO could only cause a 1.9 °C rise when the original drop by urea is 4.5 °C.

Table 3.6. Melting temperature (T_m), Enthalpy $\Delta H(T_m)$, Entropy $\Delta S(T_m)$ and change in free energy of unfolding $\Delta\Delta G$ (T_m) values for barnase in the presence of increasing concentrations of TMAO plus 1 M urea (all the samples in 5 mM acetate buffer pH 6.0).

TMAO (M) against 1 M urea	T_m(°C)	ΔT_m(°C)	$\Delta H(T_m)$(kJ/mol)	$\Delta S(T_m)$(kJ/mol^{-1}K^{-1})	$\Delta\Delta G(T_m)$ (kJ mol^{-1})
0.0	48.7 ± 0.1	0.0	423 ± 59	1.3 ± 0.2	0.0
0.5	49.7 ± 0.1	1.1	442 ± 11	1.4 ± 0.0	-1.5 ± 0.3
1.0	51 ± 0.0	2.3	623 ± 182	1.9 ± 0.6	-4.7 ± 1.0
2.0	50.2 ± 0.0	1.5	462 ± 11	1.4 ± 0.0	-2.3 ± 0.2
3.0	50.6 ± 0.0	1.9	576.4 ± 198.3	1.8 ± 0.6	-3.6 ± 0.3

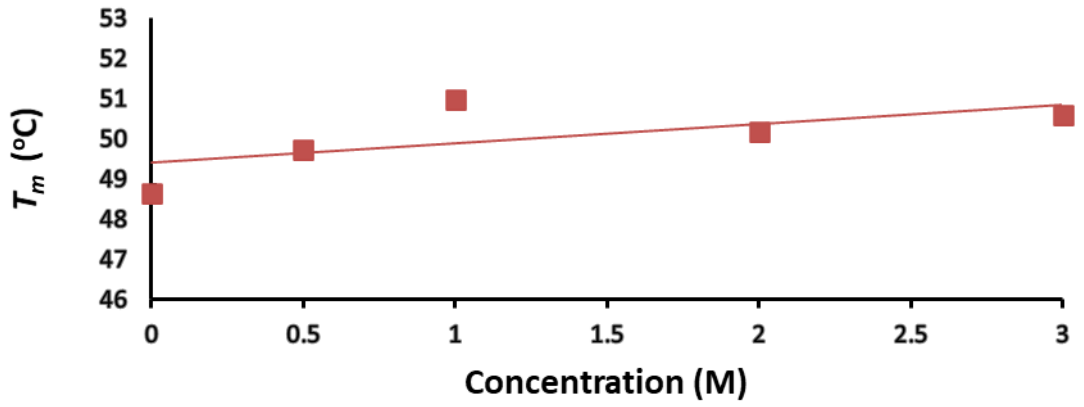

Figure 3.12. Melting temperature (T_m) values for barnase in the mixed osmolyte solutions of increasing concentrations of TMAO plus urea concentration maintained constant at 1 M (all the samples in 5 mM acetate buffer pH 6.0).

3.4.6 The effect of increasing concentrations of ectoine on barnase in the presence of 1 M Urea

Now that the effects of ectoine alone (destabilising) and urea (destabilising) have been presented, we present the effect of mixed osmolyte solutions of ectoine and urea that describes the additional effect of ectoine on top of the already destabilising effects of urea. This experiment reveals the extent to which ectoine can counteract the destabilising effects of urea. Addition of ectoine adds to the already destabilising effects of 1 M urea i.e., 4.5 °C from the original T_m of 0.5 mg/ml barnase. Addition of 0.5 M ectoine against 1M urea dropped the T_m by a further 0.9 °C. Addition of 1 M ectoine dropped the T_m by a further 0.4 °C. Addition of 2

M ectoine dropped the T_m value by a further 1.7 °C as shown in figure 3.13 and table 3.7. Overall, at an ectoine to urea ratio of 2:1, T_m is dropped by 3 °C. This shows ectoine has slightly opposite effects on barnase to that of TMAO. Ectoine does not appear to stabilise barnase against urea denaturation at all: rather, it slightly destabilises it.

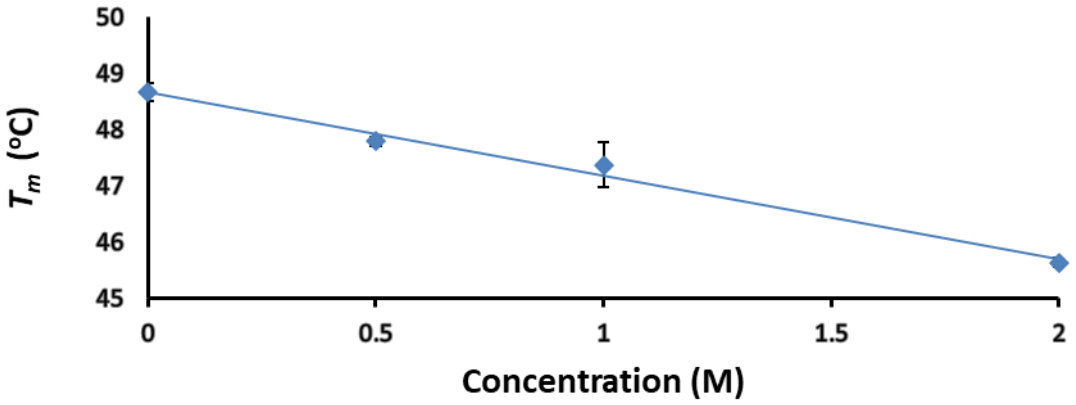

Figure 3.13. Melting temperature (T_m) values for barnase in the mixed osmolyte solutions of increasing concentrations of ectoine plus 1 M urea (all the samples in 5 mM acetate buffer pH 6.0).

Table 3.7. Melting temperature (T_m), Enthalpy ΔH(T_m), Entropy ΔS(T_m) and change in free energy of unfolding ΔΔG (T_m) values for barnase in the presence of increasing concentrations of ectoine plus 1 M urea (all the samples in 5 mM acetate buffer pH 6.0).

Ectoine (M) against 1 M urea	T_m(°C)	ΔT_m(°C)	$\Delta H(T_m)$(kJ/mol)	$\Delta S(T_m)$(kJ/mol^{-1}K^{-1})	$\Delta\Delta G(T_m)$ (kJ mol^{-1})
0	48.7 ± 0.1	0.0	423 ± 59	1.3 ± 0.2	0
0.5	47.8 ± 0.1	-0.9	373 ± 90	1.2 ± 0.3	1.0 ± 0.2
1	47.4 ± 0.4	-1.3	473 ± 6	1.5 ± 0.0	1.8 ± 0.3
2	45.6 ± 0.1	-3.0	384± 101	1.2 ± 0.3	3.3 ± 0.4

3.4.7 Analysis of Free energy, Heat capacity, Enthalpy, and Entropy values

Values for enthalpy $\Delta H(T_m)$ and entropy $\Delta S(T_m)$ were calculated directly by the Nano-Analyse software from the DSC experiments. These values were substituted to calculate molar heat capacity (ΔC_p) using the Kirchoff relation and the free energy $\Delta\Delta G$ using the modified Gibbs-Helmholtz equation (Santoro et al., 1992, Hu et al., 1992, Becktel and Schellman, 1987, Bye and Falconer, 2014). To determine ΔC_p under different salt and pH concentrations, the Kirchoff relation was used, which was calculated by the resultant gradient (slope m) value from a plot of ΔH against T_m (equation 3.3).

$$\Delta C_p = \left(\frac{\Delta H}{\Delta T_m}\right) \quad \textbf{(3.3)}$$

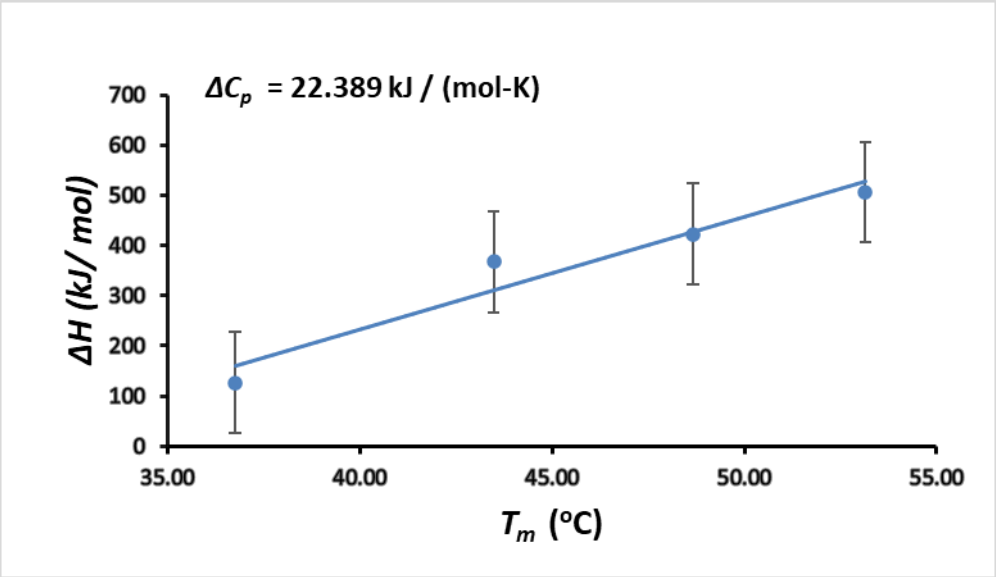

Figure 3.14. Change in heat capacity (ΔCp) values for urea calculated as a gradient from plotting ΔH on Y- axis against Tm on X- axis.

Gibbs free energy is the maximum amount of reversible work that can be performed at a constant pressure and volume given by equation 3.4 where H is enthalpy, T is absolute temperature and S is the entropy.

$$\boldsymbol{G = H - TS} \quad \textbf{(3.4)}$$

Helmholtz free energy is the work done in a closed thermodynamic system at constant temperature and volume and given by equation 3.5 where U is the internal energy, T is absolute temperature and S is the entropy.

$$\boldsymbol{F = U - TS} \quad \textbf{(3.5)}$$

For our analysis we have used the modified Gibbs-Helmholtz equation to calculate the change in free energy of unfolding $\Delta\Delta G$ (T_m) as in equation 3.6 (Bye and Falconer, 2014). In addition to T_m, $\Delta H(T_m)$, ΔC_p, and melting temperature without salt (T_{mr}) values were substituted in the modified Gibbs-Helmholtz equation to calculate the change in free energy of unfolding $\Delta\Delta G$ (T_m) as in equation 3.6.

$$\Delta\Delta G(T_m) = \Delta H(T_m)\left(1 - \frac{T_m}{T_{mr}}\right) + \Delta C_p\left[(T_m - T_{mr}) - T_m \ln\left(\frac{T_m}{T_{mr}}\right)\right] \quad \textbf{(3.6)}$$

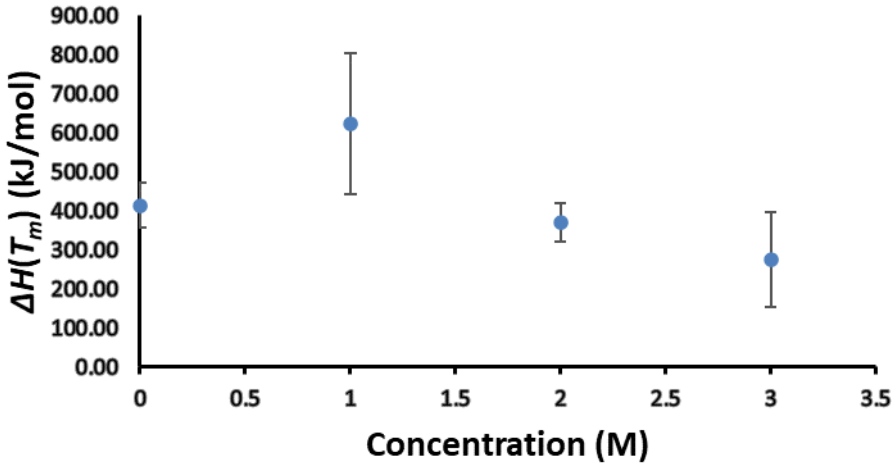

Figure 3.15. Enthalpy ΔH(T_m) values for barnase unfolding at increasing concentrations of urea plus 1 M TMAO against concentration on X- axis (all the samples in 5 mM acetate buffer pH 6.0).

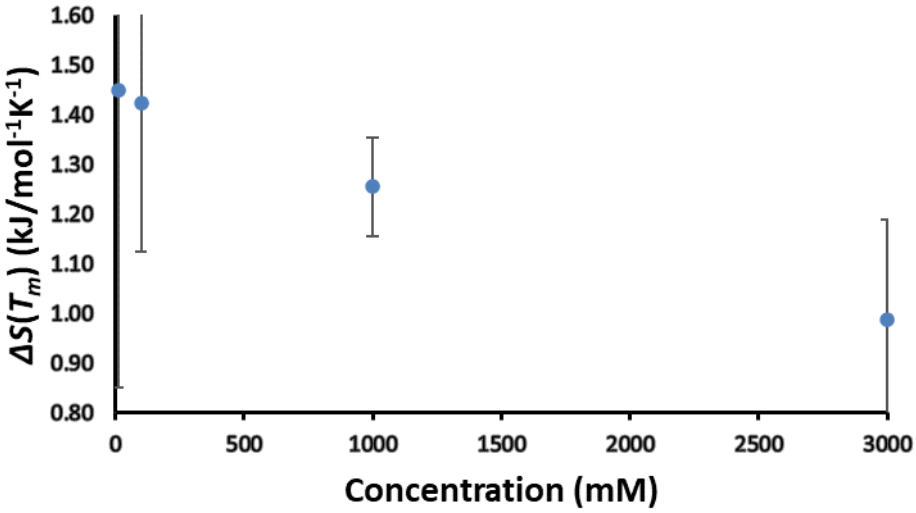

Figure 3.16. Entropy ΔS(T_m) values for barnase unfolding at various concentrations of TMAO between 0-3000 mM (all the samples in 5 mM acetate buffer pH 6.0).

$\Delta H(T_m)$ and $\Delta S(T_m)$ values changed significantly with the addition of osmolytes. As the concentration of osmolytes increased, the values decreased more and more in all the experiments as shown in figures 3.15 and 3.16. However, in the mixed osmolyte solution where TMAO was added to the urea, $\Delta H(T_m)$ and $\Delta S(T_m)$ values have increased. This increase in $\Delta H(T_m)$ and $\Delta S(T_m)$ values in mixed osmolyte solution is probably because of the presence of

two co-solutes. We suggest that the changes in $\Delta H(T_m)$ and $\Delta S(T_m)$ values are due to the changes in solvent structure. Some of the energy required to unfold the protein is also used to reorganize the solvent around the protein and this change in solvent structure affects the amount of heat absorbed by the system. TMAO and ectoine organize water molecules around themselves, thereby competing with the hydrophobic groups for water (Zou et al., 2002). The hydrophobic groups that are buried inside the protein are exposed when the protein is unfolded. The increase in the amount of energy absorbed during the unfolding of a protein is due to the large amount of water around these newly exposed apolar groups (Makhatadze and Privalov, 1990). This water has a higher heat capacity than the bulk water and when this water is disrupted due to the ions reorganizing it around themselves, it results in reduction in the heat absorbed by the system. TMAO enhances water structure and reduces entropy in water molecules leading to an increase in protein stability (Zou et al., 2002). Reduction in the values of enthalpy and heat capacity could be attributed to the competing nature of ions with the protein for bulk water (Bye et al ., 2016).

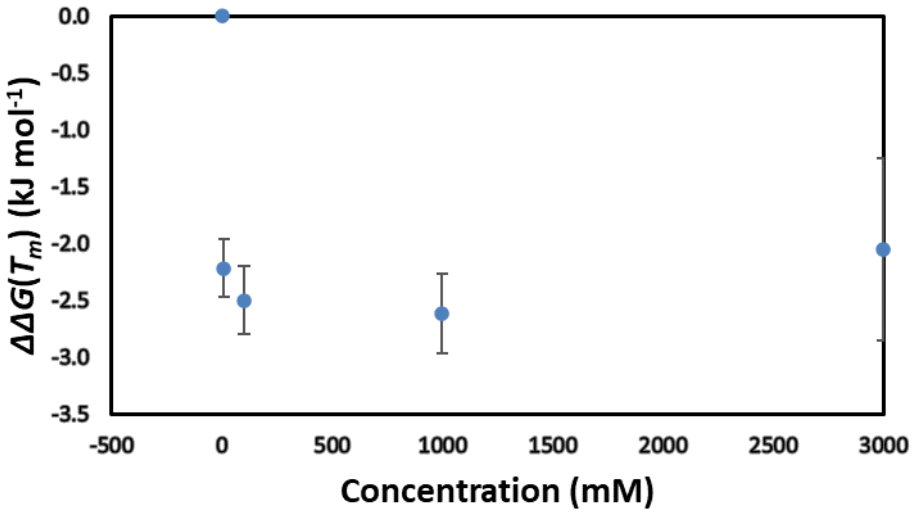

Figure 3.17. Change in free energy of unfolding $\Delta\Delta G(T_m)$ values for barnase in the presence of various concentrations of TMAO between 0-3000 mM (all the samples in 5 mM acetate buffer pH 6.0).

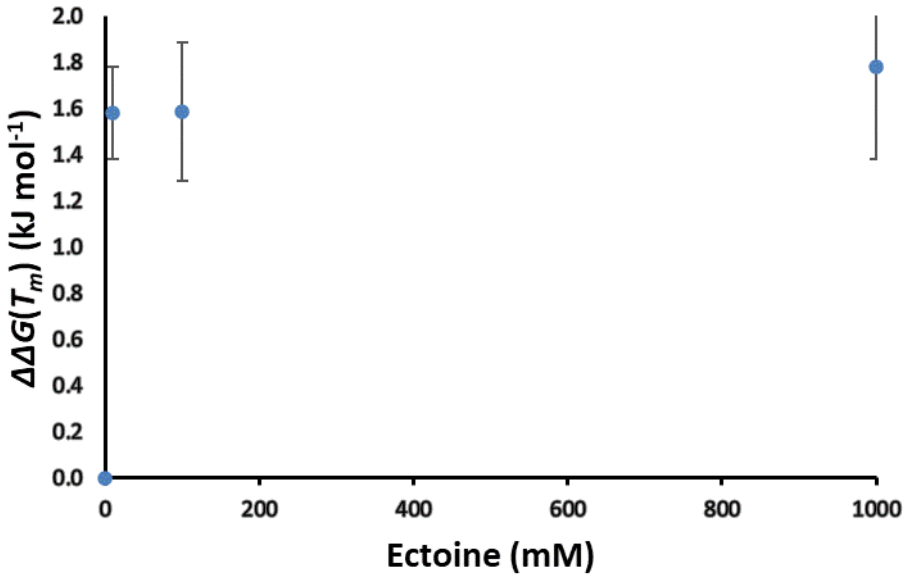

Figure 3.18. Change in free energy of unfolding ΔΔG(T_m) values for barnase in the presence of various concentrations of ectoine between 0-1000 mM (all the samples in 5 mM acetate buffer pH 6.0).

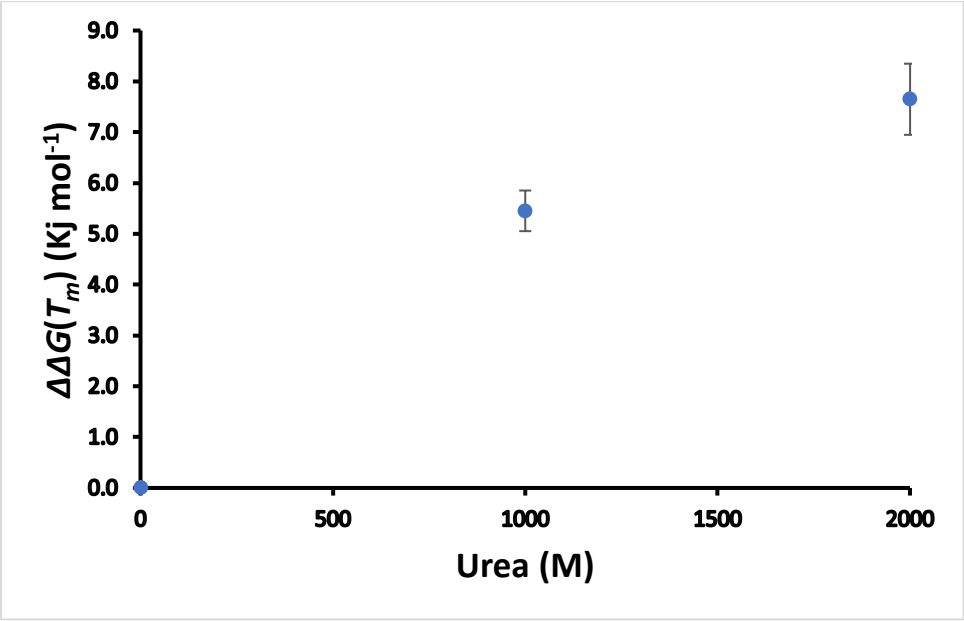

Figure 3.19. Change in free energy of unfolding ΔΔG(T_m) values for barnase in the presence of various concentrations of urea between 0-2000 M (all the samples in 5 mM acetate buffer pH 6.0).

Also, $\Delta\Delta G(T_m)$ decreases with the increase in the T_m in presence of TMAO. This is because the protein is getting stabilised. For urea and ectoine solutions $\Delta\Delta G(T_m)$ gets more positive with the increase in concentration as the T_m drops, confirming the destabilising of the protein as shown in figure 3.18 and 3.19.

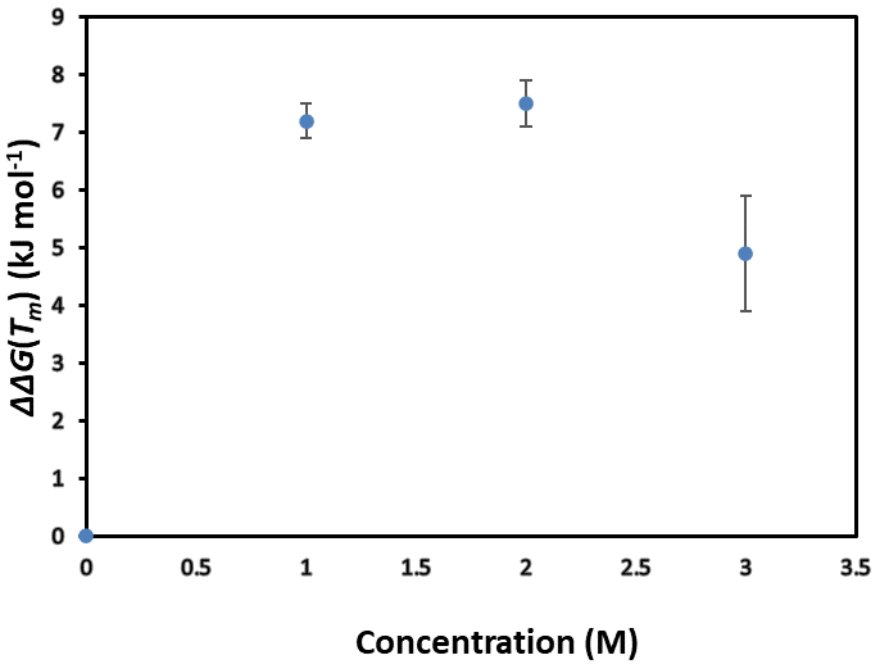

Figure 3.20. Change in free energy of unfolding ΔΔG(T_m) values for barnase in the presence of increasing concentrations of urea plus 1 M TMAO (all the samples in 5 mM acetate buffer pH 6.0).

In the mixed osmolyte solution where urea concentration was increased against TMAO, $\Delta\Delta G(T_m)$ gets positive and increases with the increase in concentration of urea as T_m keeps dropping: a sign of protein getting destabilised as shown in figure 3.20. However, in the mixed osmolyte solutions when TMAO concentration was increased $\Delta\Delta G(T_m)$ values were decreasing with a positive sign. This is because T_m is getting increased and at the same time still smaller than T_{mr} which means TMAO can partially counteract the destabilising effects of urea.

3.4.8 A summary of changes in T_m value and what it means for barnase stability in terms of urea counteracting stabilising ability of osmolytes

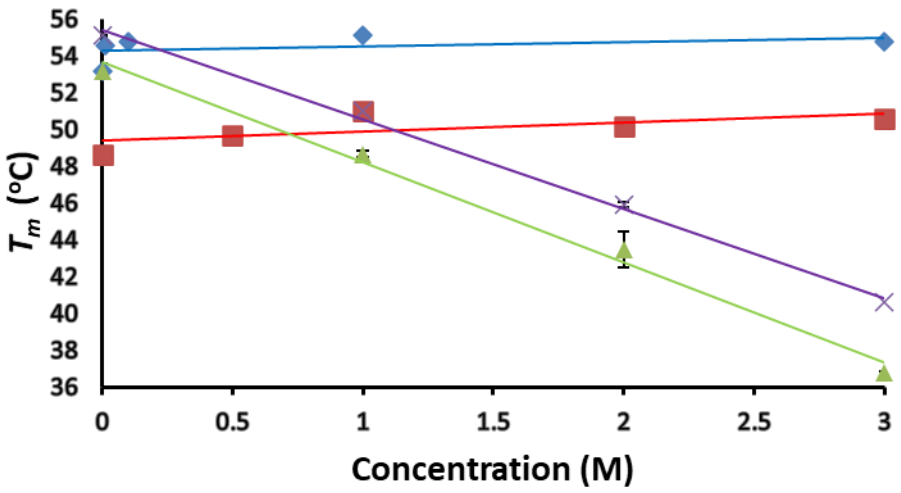

Figure 3.21. Melting temperature (T_m) values for barnase in the presence of varied concentrations of TMAO from 0 M to 3 M (blue), mixed osmolyte solution of increasing urea from 0 M to 1 M plus TMAO concentration maintained constant at 1 M (violet), varied concentrations of urea from 0 M to 3 M (green), mixed osmolyte solution of increasing TMAO from 0 M to 1 M plus urea concentration maintained constant at 1 M (red). (All the samples in 5 mM acetate buffer pH 6.0).

To study to what extent osmolytes can stabilise the protein and counteract the destabilising effects of urea, T_m values from pure osmolyte solutions and mixed osmolytes were plotted on a single graph as shown in figure 3.21. Urea destabilises barnase by about 4.5 ^{o}C at 1 M and the slope goes increasingly downward as the concentration of the denaturant is further increased, which is expected as it is a strong denaturant. TMAO has a small stabilising effect by about 1.5 ^{o}C at 0.01 M and further additions up to 1 M did not raise the T_m much making the graph almost a flat line. No aggregation of barnase is observed against TMAO. In contrast to TMAO, ectoine has surprisingly a small destabilising effect by about 0.9 ^{o}C at 0.01 M and the slope goes downward as we increase the concentration.

TMAO on its own can raise the T_m value by about 1.6 ^{o}C at 3M concentration and can counteract the destabilisation caused by urea.

Now we have studied mixed osmolyte solutions of TMAO and urea. When urea concentration was fixed at 1 M against varied concentrations of TMAO from 0.5 M to 3 M, T_m value which earlier dropped in the presence of urea is restored by at least 2 ^{o}C in the presence

of TMAO. And when TMAO concentration was fixed at 1 M and urea concentration is increased from 0 to 3 M, T_m values restored by 2.3 ^oC at 1 M addition of TMAO. This however is not the same in the presence of varied concentrations of ectoine from 0.5 M to 2 M against 1 M urea. Since ectoine is already bringing down the T_m by itself, presence of urea just brings the T_m further down by about 3 ^oC.

When compared with Hofmeister series ions like sulphate and thiocyanate, changes in melting temperatures caused by osmolytes are small (Bye et al., 2016). Sulphate massively raises the T_m while thiocyanate brings down the T_m. All this data suggests that although TMAO cannot stabilise proteins much by itself, it can counteract destabilising effects of denaturants like urea, whilst ectoine like thiocyanate destabilizes the protein barnase.

3.5 CONCLUSIONS

To make proteins more stable, addition of certain ions, or osmolytes with stabilising effects are needed. These can be Hofmeister ions like sulphate, or osmolytes like TMAO, ectoine etc. The general stabilising mechanisms are thought to be noncovalent forces like hydrophobic effect and hydrogen bonding to a larger extent and formation of ion pairs to some extent. The van der Waals interactions in the interior of a protein are much stronger in the folded state compared to the unfolded state and with non-polar groups being buried inside increases the stability of the folded proteins (Pace et al., 2009). For every -CH_2 group buried, -4 kJ mol^{-1} is added to the Gibbs free energy (ΔG) which increases the stability. That is -700 kJ mol^{-1} for a 100 amino acid residue protein added from non-covalent interactions for a 100 amino acid protein, which acts to counteract the conformational entropy that destabilises the protein.

Stabilizing ions (like sulphate in the Hofmeister series) are suggested to organise water molecules around themselves which makes water dipoles less available, outcompeting the protein, strengthening the intramolecular interactions in the protein (Bye et al., 2016). It is also suggested that the presence of TMAO increases the hydrogen bonding in the water molecules thus reducing the interaction of water with the protein (Zou et al., 2002). The heat capacity of the sample increases as more water is organised around the salt and the non-covalent interactions that TMAO has with water. This requires more heat to break the hydrogen bonding, increasing the stability and free energy. Stabilising ions competing with the protein for the water molecules increase the free energy for unfolding (ΔG) (Bye and Falconer, 2014).

Molecular dynamic simulation studies of TMAO and urea do suggest the water withdrawal ability of TMAO and weak ordering of water molecules by destabilisers like urea (Zou et al., 2002). However, there are other contrasting views like direct binding to the peptide backbone of the protein molecule (Mountain and Thirumalai, 2003, Huang et al., 2012), and an indirect mechanism where urea reduces hydrophobic interactions by altering water structure (Bennion and Daggett, 2003).

When compared with Hofmeister series anions like thiocyanate, changes in melting temperatures caused by osmolytes are small though similar to that of sulfate (Bye et al., 2016). Sulphate raises the T_m by 1.5 ^{o}C while thiocyanate massively brings down the T_m by 10 ^{o}C (Bye et al., 2016). All these data suggest that although TMAO only stabilises proteins weakly, it can counteract the destabilising effects of denaturants like urea, whilst ectoine like thiocyanate destabilizes the protein barnase.

Bye and Falconer (2014) proposed that solutes that exert stabilisation on proteins do so because they are strongly hydrated and compete with the protein for interactions with water. This competition increases the free energy of unfolding and therefore makes the protein more stable. We hypothesise that TMAO works in a similar manner: namely, that it interacts strongly with water and competes with the protein for water binding, which is how it counteracts the effect of urea.

4 CHAPTER 4: EFFECT OF OSMOLYTES ON BARNASE REVEALED BY NMR EXPERIMENTS

4.1 OBJECTIVE

In the previous chapter, the effect of osmolytes on the stability of the protein barnase was studied by DSC, and the results suggested that TMAO can counteract the denaturant urea whilst ectoine like thiocyanate destabilizes the protein barnase. If osmolytes can counteract the effect of denaturants, do they do this by direct interaction with the protein, or indirectly by interactions with water? Hence, we wanted to explore if osmolytes interact directly with the protein surface and thereby counteract the denaturants. So, we came up with the work in this chapter where interaction of osmolytes (TMAO, ectoine, betaine) with the barnase was studied using ^{15}N HSQC, ^{13}C HSQC, and 2D-HNCO experiments. Since these experiments were primarily conducted to study the effect of osmolytes on the peptide backbone using 2D NMR, double labelled barnase (^{13}C ^{15}N) was used. Since the volume of titrant added at each step had to be serially increased and the additions were at large volumes, trial experiments showed that the pH would drop by at least 0.2 if titrant and protein were buffered to the same pH. Hence to maintain the constant pH, TMAO and betaine had to be prepared at a pH 0.2 more than barnase after confirming with dummy experiments.

4.2 Protein expression and purification

The experimental details for the work described in this results chapter are described in Chapter 2. Barnase is a ribonuclease made up of 110 amino acid residues with a molecular weight of 12.3827 kDa, extinction coefficient of 26,930 M^{-1} cm^{-1} and isoelectric point (pI) 8.8. Its uniprot ID is (P00648). *E. coli* strain M15 (pRep4) has kanamycin resistance and expression vector pQE60 has ampicillin resistance and barnase gene is under control of the Lac operon. *E. coli* cells were cultured in M9 minimal media and IPTG was added to activate Lac operon, leading to protein expression. Cells were harvested to extract and purify barnase by centrifugation, lysis buffer treatment of pellet, dialysis and purification using ion exchange chraomatography on AKTA. Results from SDS PAGE and ion exchange chromatography are explained below.

Unlabelled barnase is shown in the lanes 1-7 in Figure 4.1. Lane 1, 2, 3, 4 from SDS-PAGE electrophoresis (Figure 4.1) confirm the presence of barnase at various stages of protein expression like cell lysis by lysis buffer treatment, dialysis with tris buffer, and anion exchange chromatography (figure 4.2, figure 4.3). In the supernatant from cell lysis, the sample eluted (lane 4 in Figure 4.1) from Q Sepharose column of anion exchange chromatography (Figure 4.2) has a protein band, whereas samples from the GuHCl wash in Q Sepharose did not show any band. Again, the sample collected from the linear gradient fraction (lane 7) from the SP Sepharose (Figure 4.3) column has a protein band whilst samples from urea wash did not show any protein band.

^{13}C ^{15}N labelled barnase is shown in the lanes 8-12 in Figure 4.1. Lane 9, 10, 12, and 8 from SDS-PAGE electrophoresis (Figure 4.1) confirm the presence of ^{13}C ^{15}N barnase at various stages of protein expression like cell lysis by lysis buffer treatment, dialysis with acetate buffer, and anion exchange chromatography (figure 4.2, figure 4.3). In the supernatant from cell lysis, the sample eluted (lane 10 in Figure 4.1) from Q Sepharose column of anion exchange chromatography (Figure 4.2) has a protein band. Again, the sample collected by applying linear gradient fraction (50 mM acetate plus 1 M Nacl) from the SP Sepharose as seen in lane 8, Figure 4.1 and black peak, Figure 4.3 column has a protein band. Samples from urea wash (lane 11) did not show any protein band.

Barnase H102A cells cultured in 2 litres of M9 media gave a total yield of 23.37 mg, calculated by UV absorbance.

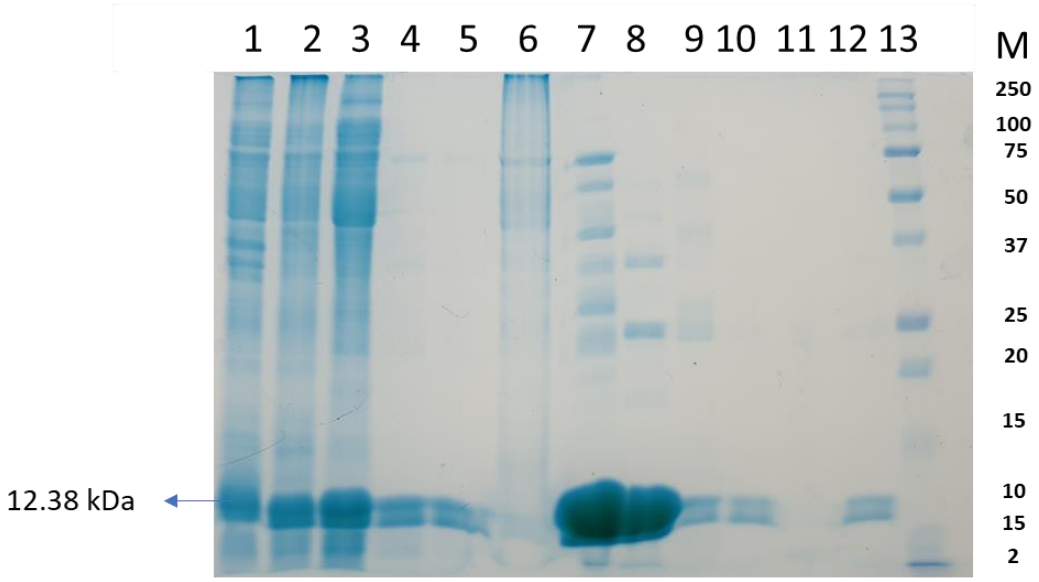

Figure 4.1. SDS-PAGE gel showing the presence of Barnase. Unlabelled barnase is shown from lanes 1-7. ^{13}C and ^{15}N labelled barnase shown from lanes 8-13. Lane 1: Barnase from H102A cells after lysis buffer treatment. Lane 2: Supernatant after cells were sonicated. Lane 3: Supernatent dialyzed in Tris Buffer. Lane 4: Barnase eluted from Q Sepharose column. Lane 5: Eluent sample from Q Sepharose dialysed in acetate buffer. Lane 6: GuHCl wash from Q Sepharose. Lane 7: Barnase eluted from SP Sepharose column. Lane 9: Supernatent from H102A cells after lysis buffer treatment and Tris buffer dialysis. Lane 10: Barnase eluted from Q Sepharose column. Lane 11: urea wash. Lane 12: sample from acetate dialysis. Lane 13: Protein marker. Lane 8: Final sample (Through elution from SP Sepharose column).

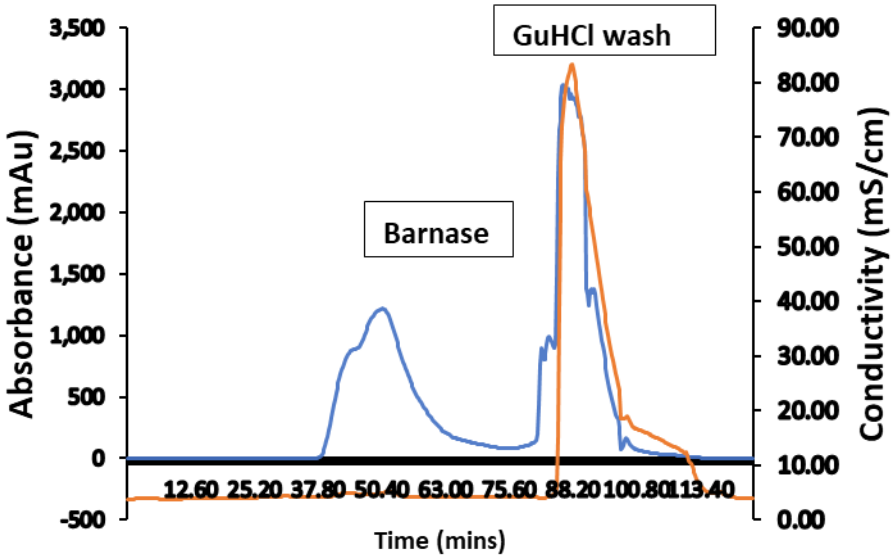

Figure 4.2. Chromatogram from Q-Sepharose column purification with barnase peak. Blue peak showing elution of barnase in supernatant of H102A cells (from cell lysis dialyzed in Lysis buffer). After barnase is eluted from Q Sepharose column, all the other cellular proteins and nucleotides bound to the column are washed away by GuHCl buffer as seen by changing conductivity (red peak) and a UV peak.

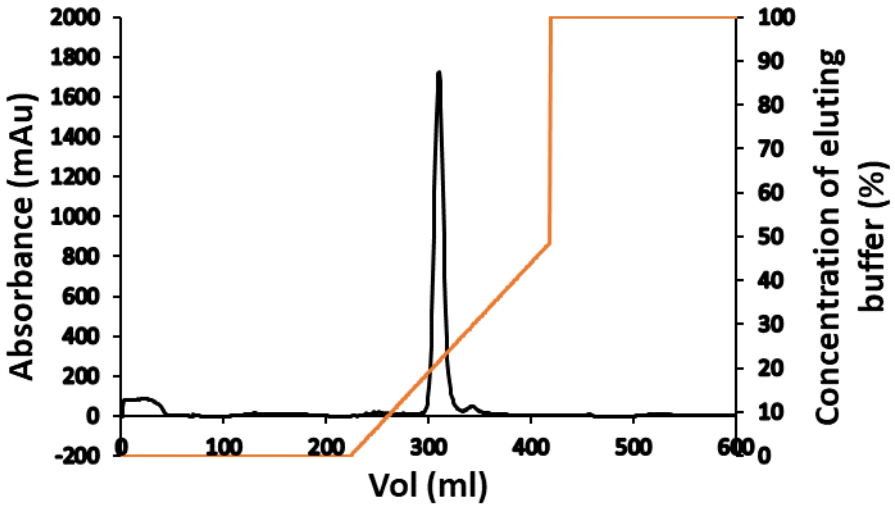

Figure 4.3. Chromatogram from SP Sepharose column purification showing barnase elution (black peak) through linear gradient fraction with the increasing concentration of eluting buffer (red peak).

4.3 Optimising the buffer and pH for barnase

Considerable time and effort were spent early on during this process to determine the optimum conditions for the titrations. Our intention was to measure the interactions between barnase and osmolyte, using as few other components in solution as possible. TSP was added to the solution in order to provide a chemical shift reference. We hoped not to need any pH buffer (since our hope was that the protein can buffer itself, because the osmolytes are electrically neutral and buffered to the same pH as the protein), in order to keep the system as simple as possible. Most previous titrations have been carried out at pH values around 6, because this is a good pH for NMR. Barnase has two histidine residues. One is a crucial active site ligand (H102) which was mutated to alanine in our protein in order to remove catalytic activity. The other is well away from the active site and is not thought to play any part in the function of barnase. Therefore, the binding of H102A barnase to ligands does not have any strong pH dependence, meaning that pH 6 is a sensible value to choose.

With Dr. Clare Trevitt, many tests were done to find the best way to prepare barnase as shown in Table 4.1. The protein was prepared and dialysed against HPLC grade water. We both prepared protein independently and made solutions, but there was a surprisingly large variation between the NMR spectra. Some of the peaks were not in the same place as reported by Jordan Bye when protein was in distilled water as seen in Figure 4.4. In particular, the

signals for L42 and R83 showed large and unpredictable changes in their positions. In addition, in the absence of any buffer, measurement of the pH of the solution using our standard narrow diameter pH probe proved to be very difficult, with wide variation in readings for no obvious reason.

Table 4.1. Various buffer and pH preparations for barnase

Solvent for dialysis	**pH and reagent used to adjust pH**
Distilled water	6.5 with HCl and KOH
HPLC grade water	6.1 with 5mM Tris
HPLC grade water	6.5 with 5mM Tris
5mM acetate buffer pH 5.8	6.0

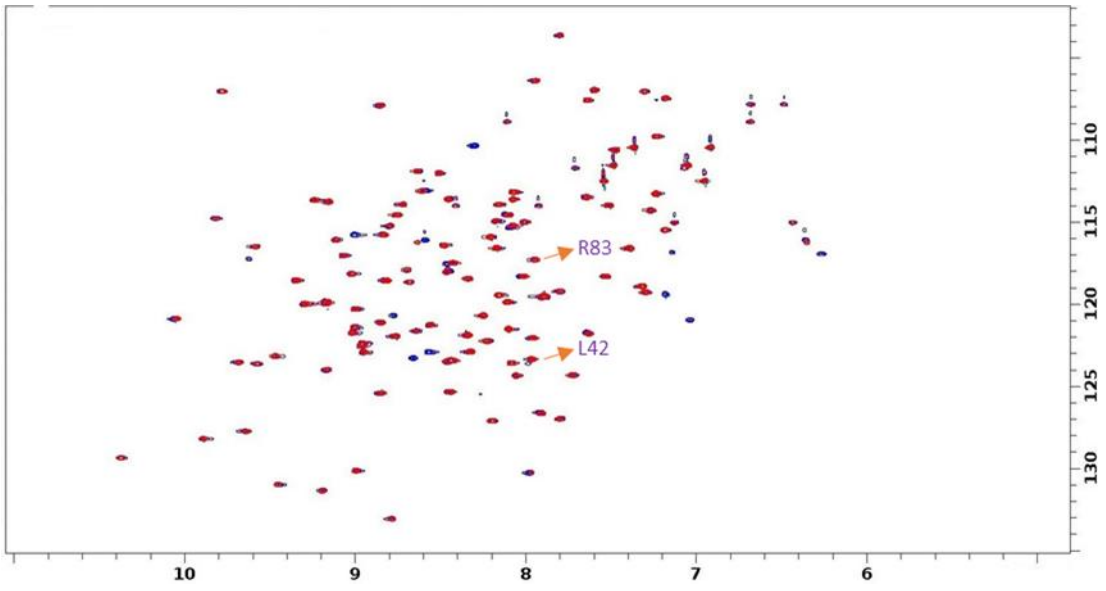

Figure 4.4. Barnase in water. $^{1}H^{15}N$ HSQC spectra of barnase (blue color) overlayed over Jordan Bye's spectra (red color)

After extensive discussions, it was finally agreed that we should include the presence of a minimal amount of buffer in the solutions. The obvious buffer to use is phosphate, because it has a pK_a close to 6, and does not have a ^{1}H signal. However, previous work in the lab (Pandya et al., 2018) had showed that phosphate causes changes in barnase dynamics, presumably because it binds to the active site close to the sites for binding RNA phosphate backbone. Therefore, we decided to use 5 mM acetate as a standard buffer. This gave stable pH measurements. The pK_a of acetate is 4.6, and thus it is not an ideal buffer at pH 6, but any

other buffer would have more protons. NMR spectra of barnase sample dialyzed in 5 mM sodium acetate buffer pH 5.8 were found to be satisfactory when compared to spectra from Clare Trevitt and Jordan Bye, because peaks were in the same place and reproducible as seen in Figure 4.5. So, we decided to continue the further experiments in this condition.

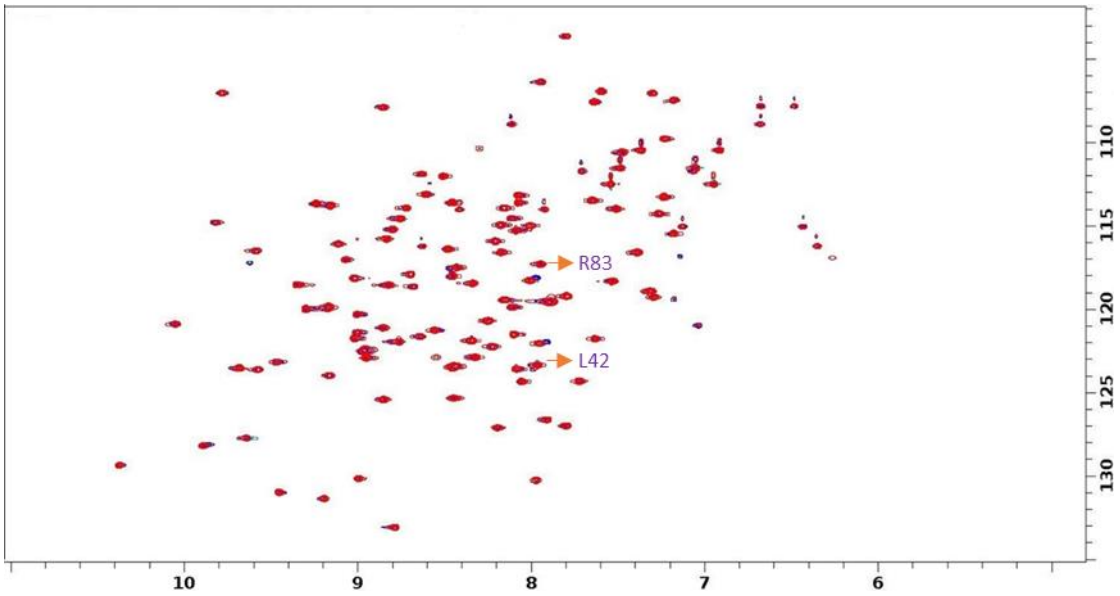

Figure 4.5. Barnase in 5 mM acetate buffer. $^{1}H^{15}N$ HSQC spectra of barnase (blue color) overlayed over Jordan Bye's spectra (red color)

4.4 Backbone assignment

The HSQC spectrum of barnase has been assigned previously [Bye et al., 2016 and Clare Trevitt personal information], but peaks can shift due to small changes in solution conditions, and there are some peaks very close together in the spectrum, so the assignments were checked using a set of 3D spectra on double labelled protein. Converting spin systems to corresponding residue type in the protein sequence is accomplished by a programme called Asstools. This programme initially does 30 stochastic repeats and, in each run, assigns spin systems to residues in the protein sequence. Results from these repeats were calculated to match the chemical shifts of self and preceding residues. These runs were repeated till the scores were 30 out of 30 correct on assignment output distribution (as seen in Table 4.2).

Table 4.2. Assignment output distribution list of the backbone assignment of barnase for each residue showing residue sequence number, amino acid type, spin system number and the number of assignments.

A

```
1 A 0 (30)
2 Q 0 (30)
3 V 103 (30)
4 I 118 (30)
5 N 110 (30)
6 T 7 (30)
7 F 85 (30)
8 D 35 (30)
9 G 2 (30)
10 V 104 (30)
11 A 97 (30)
12 D 52 (30)
13 Y 115 (30)
14 L 81 (30)
15 Q 48 (30)
16 T 29 (30)
17 Y 56 (30)
18 H 40 (30)
19 K 17 (30)
20 L 63 (30)
21 P 0 (30)
22 D 66 (30)
23 N 22 (30)
24 Y 73 (30)
25 I 67 (30)
26 T 26 (30)
27 K 88 (30)
28 S 33 (30)
29 E 114 (30)
30 A 98 (30)
31 Q 82 (30)
32 A 107 (30)
33 L 58 (30)
34 G 1 (30)
35 W 102 (30)
36 V 128 (30)
37 A 125 (30)
38 S 14 (30)
39 K 74 (30)
40 G 6 (30)
41 N 36 (30)
42 L 96 (30)
43 A 59 (30)
44 D 39 (30)
45 V 13 (30)
46 A 116 (30)
47 P 0 (30)
48 G 21 (30)
49 K 129 (30)
50 S 27 (30)
51 I 108 (30)
52 G 32 (30)
53 G 4 (30)
54 D 90 (30)
55 I 69 (30)
```

B

```
56 F 127 (30)
57 S 106 (30)
58 N 60 (30)
59 R 77 (30)
60 E 43 (30)
61 G 3 (30)
62 K 62 (30)
63 L 68 (30)
64 P 0 (30)
65 G 41 (30)
66 K 86 (30)
67 S 87 (30)
68 G 51 (30)
69 R 92 (30)
70 T 100 (30)
71 W 113 (30)
72 R 93 (30)
73 E 34 (30)
74 A 83 (30)
75 D 109 (30)
76 I 119 (30)
77 N 47 (30)
78 Y 94 (30)
79 T 80 (30)
80 S 28 (30)
81 G 10 (30)
82 F 101 (30)
83 R 64 (30)
84 N 130 (30)
85 S 31 (30)
86 D 95 (30)
87 R 111 (30)
88 I 105 (30)
89 L 126 (30)
90 Y 70 (30)
91 S 89 (30)
92 S 30 (30)
93 D 44 (30)
94 W 49 (30)
95 L 76 (30)
96 I 71 (30)
97 Y 123 (30)
98 K 57 (30)
99 T 50 (30)
100 T 61 (30)
101 D 131 (30)
102 A 72 (30)
103 Y 5 (30)
104 Q 75 (30)
105 T 42 (30)
106 F 65 (30)
107 T 53 (30)
108 K 124 (30)
109 I 91 (30)
110 R 120 (30)
```

4.5 Optimising the buffer conditions for osmolytes

This chapter describes NMR titrations of osmolytes into barnase, using as low a buffer concentration as possible (5 mM). It is important to keep the pH constant during the titration, so that any chemical sift changes seen are due only to the osmolyte. Preliminary experiments showed that if protein and osmolyte were separately adjusted to pH 5.8 in 5 mM acetate, then

addition of osmolyte produces a decrease in the pH of barnase to about 5.6. This could be explained by osmolyte binding leading to a displacement of protons from the protein surface. It is possible to remove the sample from the NMR tube at each titration point and adjust the pH using a pH meter, but this leads to an unacceptable loss of solution. We therefore tried dummy experiments (i.e., titrations of unlabelled protein just to measure the pH) to work out the best conditions and concluded that an acceptably stable pH over the titration course could be produced by using an osmolyte pH rather higher than the protein pH, as set out in the Tables below.

Table 4.3. Dummy experiments showing different end points of pH for barnase-TMAO titrations.

Dummy exp No	**Barnase pH**	**TMAO pH**	**Final pH at 1 M**	**Volume in µl (5M stock solution of TMAO)**
1	6	8.23	7.33	165
2	6	5.8	5.67	165
3	6	6	5.85	165
4	6	6.15	5.95	165

When TMAO and barnase pH were set to the same values, the final pH drops by 0.2. Hence TMAO pH was adjusted to 6.14 such that it was 0.15 pH more than barnase. In the final barnase-TMAO titration point, the pH dropped only slightly to 5.95 from 6.0 at 0 mM betaine.

Therefore, a TMAO pH of 6.15 against barnase pH of 6.0 was considered the best and the same conditions were replicated for actual experiments.

Ectoine stock solution was prepared at 2.5 M in acetate buffer and pH adjusted to 5.99. When titrated against pH 6.0 barnase, final pH of the titration was found to be 5.95 as seen in Table 4.4. Unlike TMAO in the presence of ectoine pH does not reduce with the increasing concentrations, so trials with different pH starting points were not needed.

Table 4.4. Dummy experiments showing different end points of pH for barnase-ectoine titrations.

Dummy exp No	Barnase pH	ectoine pH	Final pH at 1 M	Volume in µl (2.5 M stock solution of ectoine)
1	5.95	5.99	5.95	333

As was done for TMAO, various pH conditions for betaine were tried as shown in Table 4.5. The pH of double labelled barnase was found to be 5.95 after concentrating in a vivaspin to 752 µM. Unlabelled barnase was used for the dummy experiment, and the pH was adjusted to 5.94 to match the double labelled barnase pH. When the betaine pH was also 5.95, at the final barnase-betaine titration, the pH dropped to 5.72 from 5.94. In a second dummy experiment, the betaine pH was increased to 6.14 such that it was 0.2 pH more than the barnase pH of 5.94. In the final barnase-betaine titration, the pH dropped to 5.91 from 5.94 at 0 mM betaine.

Table 4.5. Dummy experiments showing different end points of pH for barnase-betaine titrations.

Dummy exp No	Barnase pH	betaine pH	Final pH at 1 M	Volume in µl (2.5 M stock solution of betaine)
1	5.95	5.95	5.72	283
2	5.95	6.14	5.91	283

Concentrations of unlabelled barnase were lower at 423 µM for dummy 1 and 558 µM for dummy 2 which should still work for actual experiments when the barnase will be at 750 µM. Therefore, a betaine pH of 6.14 against barnase pH of 5.94 is the best. In conclusion betaine pH must be kept higher than barnase like it was for TMAO.

4.6 Results

4.6.1 $^{1}H^{15}N$ HSQC experiments

All the titrations were carried out using a ^{13}C ^{15}N barnase concentration of 785 µM. The barnase sample was placed in the NMR tube and titrated against TMAO by serially increasing the concentration of TMAO, starting from 0 M, and then serially increased to 0.01 M, 0.025, 0.05, 0.10, 0.25, 0.5, 0.75, and 1 M. NMR was run, and spectra were taken at each TMAO addition. A similar method was followed for titrations of barnase with ectoine and betaine. As

described above, the pH of the osmolytes was adjusted such that the final pH of the titration was not too different from the starting pH of barnase as shown earlier in Tables 4.3 – 4.5. The final sample pH at the end of titrations for TMAO was found to be 5.95, which is slightly lower than the starting pH value of 6.0. For betaine the final sample pH at the end of titrations was found to be 5.91 which is slightly lower than the starting pH value of 5.95.

A first titration series was carried out using 5 M TMAO stock solution. The high concentration of TMAO was chosen in order to minimise volume changes during the addition of osmolyte. However, the solution was difficult to dissolve and to titrate, so the data in the titration series were felt to be unreliable. The titration was therefore repeated using a final stock solution concentration of 3 M. The repeat titration was much better and is reported here. For ectoine-barnase titrations, TSP (which is used as reference) was directly adding to the solution while for titrations with TMAO and betaine, it was taken in a capillary tube instead of directly adding to the solution and this capillary tube was carefully inserted in the NMR tube. This is done to rule out any interaction of TSP (which is used as reference) with osmolytes.

Spectra from ^{15}N HSQC experiments were recorded in the presence of increasing concentrations of TMAO, ectoine, and betaine as shown in Figures 4.6 – 4.8. Each ligand concentration is assigned a rainbow colour and printed as a separate file and merged as a single file to show the titration and all this is accomplished by using a Linux script provided by Dr. Nicola Baxter (Baxter et al., 2017).

.

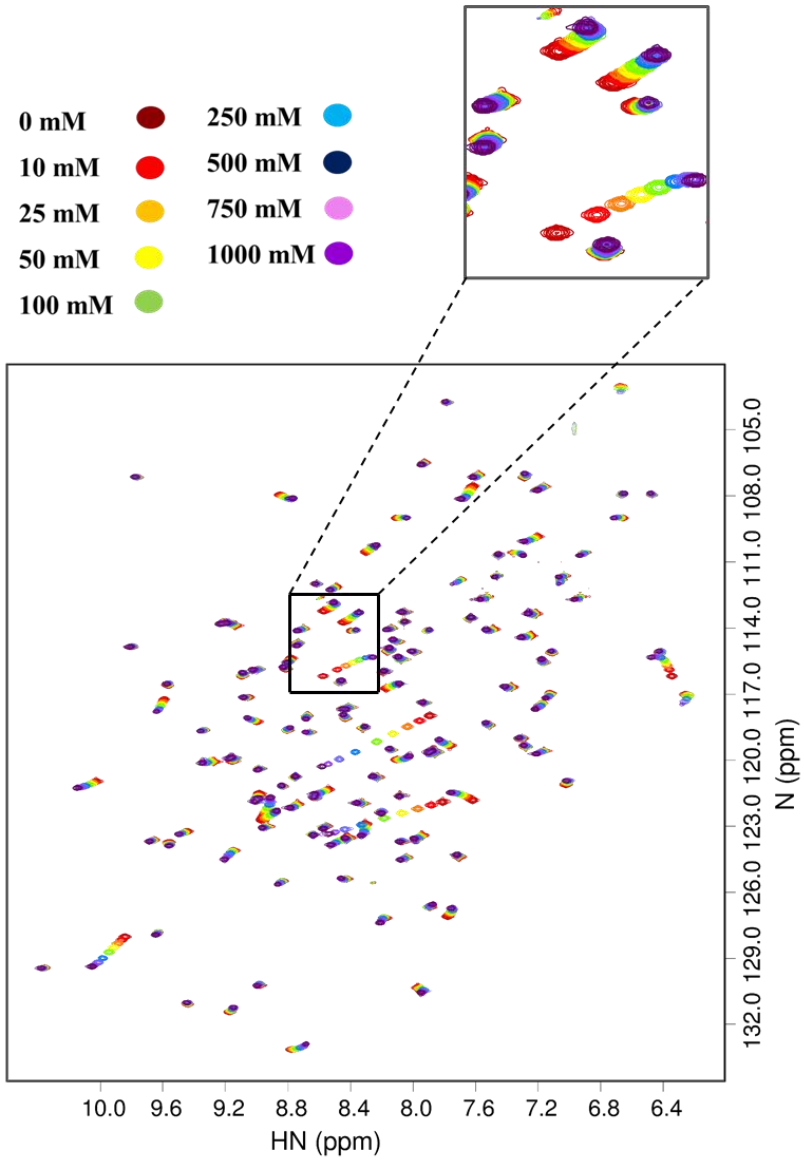

Figure 4.6. Spectra from $^{1}H^{15}N$ HSQC titration of barnase with TMAO, with each peak representing a H-N pair and the two coordinates showing proton (X axis) and N (Y axis) chemical shifts in the presence of varied concentrations of TMAO from 0 mM to 1000 mM. Each ligand concentration is assigned a rainbow colour. An enlarged region is also shown.

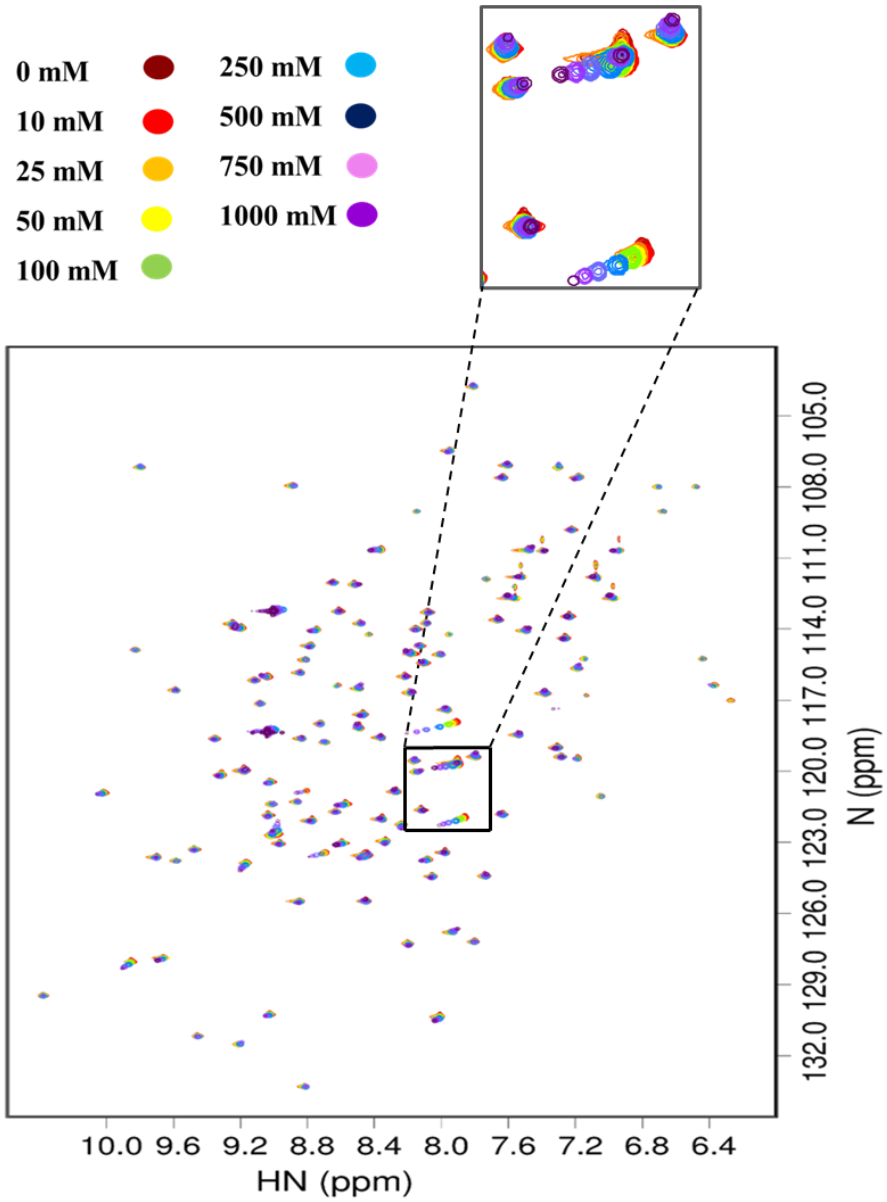

Figure 4.7. Spectra from $^{1}H^{15}$NHSQC experiments of barnase with each peak representing H-N pair and two coordinates showing proton (X axis) and N (Y axis) in the presence of varied concentrations of ectoine from 0 mM to 1000 mM. Each ligand concentration is assigned a rainbow colour. An enlarged region is also shown.

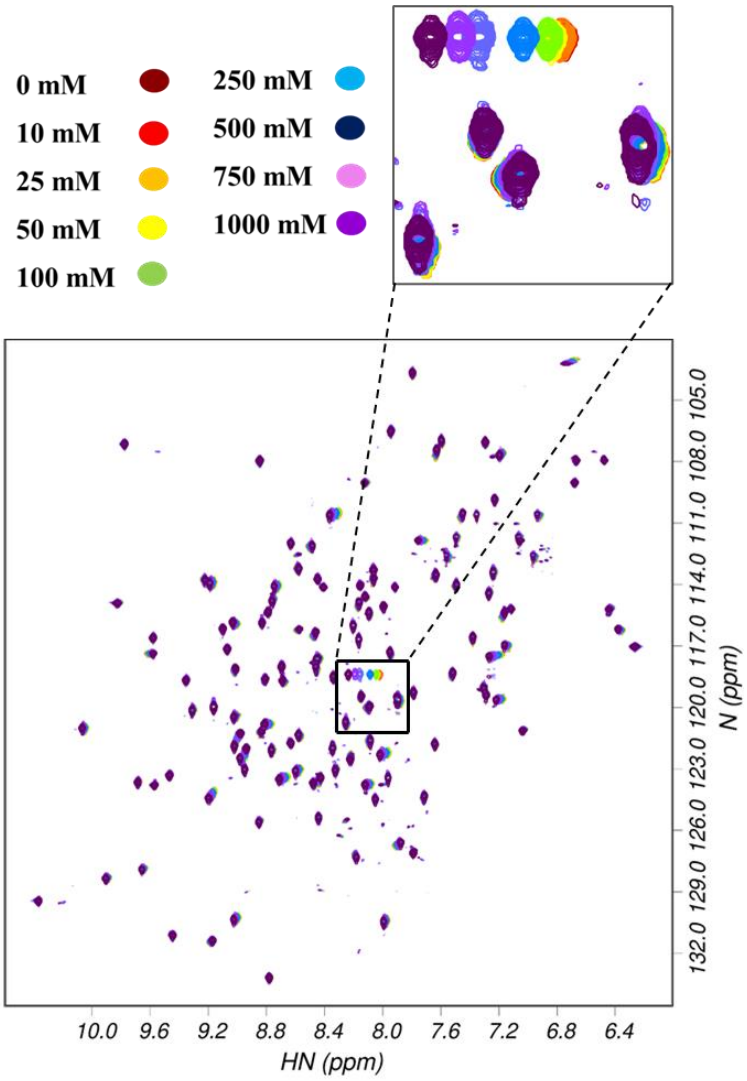

Figure 4.8. Spectra from $^{1}H^{15}$NHSQC experiments of barnase with each peak representing H-N pair and two coordinates showing proton (X axis) and N (Y axis) in the presence of varied concentrations of betaine from 0 mM to 1000 mM. Each ligand concentration is assigned a rainbow colour. An enlarged region is also shown.

4.6.1.1 Data Fitting

At each addition of osmolyte, the cross peaks were picked using a macro in Felix. Most peaks could be followed throughout the titrations. These were then outputted to text files, which were sorted and reorganised using a set of Linux scripts. After peak picking and checking of the data, the results were analysed by organising the data using a further set of linux scripts. For an initial view of the peak picking, the raw data for TMAO i.e., chemical shifts of each peak were plotted as box plots as seen in Figure 4.9, plotting change in chemical shift against osmolyte concentration. These plots were used to identify errors in the peak picking. Some of the residues, in particular L42 and R83, will be not fully visible in the plots, which is due to

them being too large in shift changes compared to others. Zooming out the plots will make these residues visible in the plot, but plot scales are adjusted such that majority of the residues are visible even if it means missing out a few. All peaks are included in the analysis.

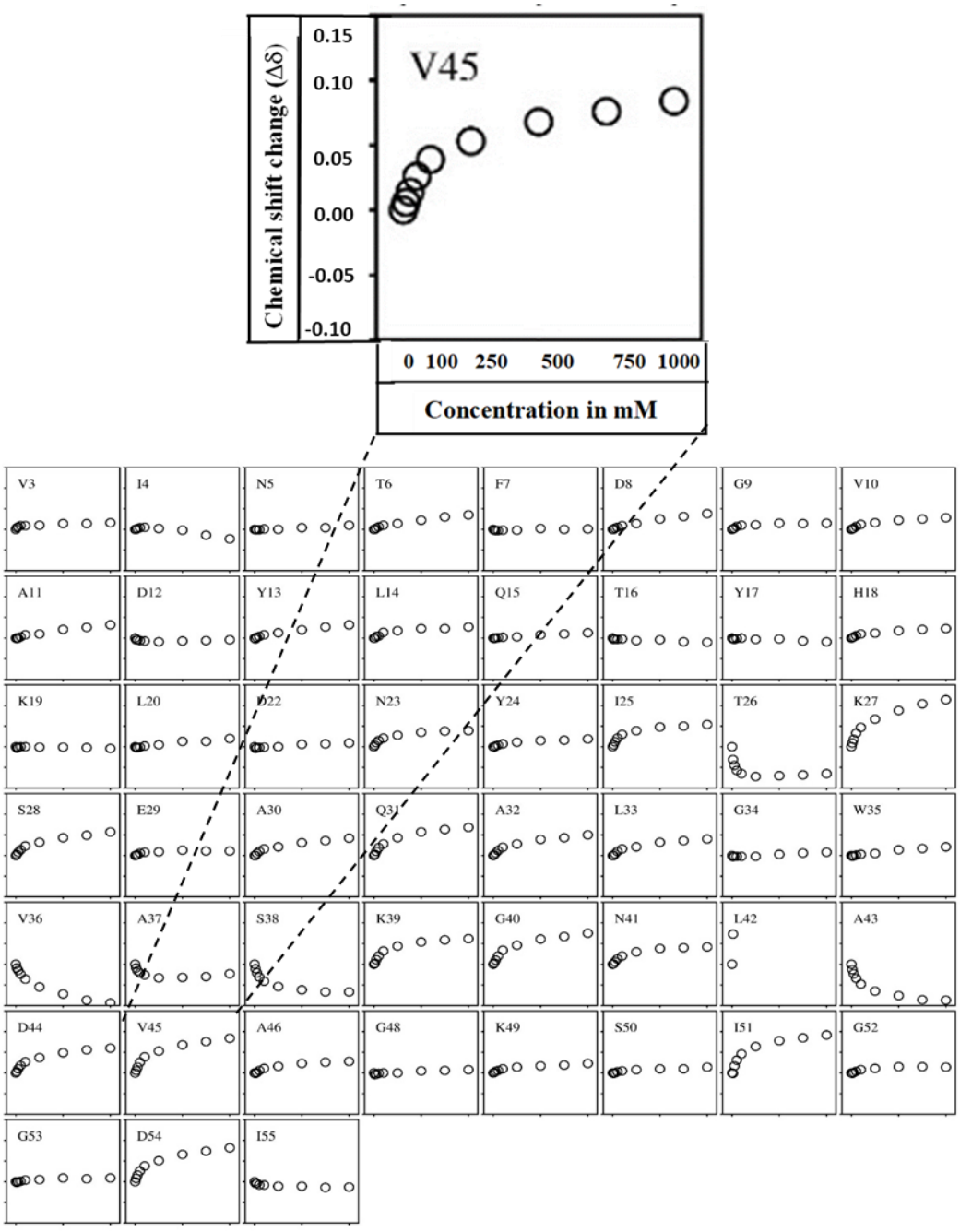

Figure 4.9. Data from ^{1}H ^{15}N HSQC showing hydrogen chemical shift changes (Y axis) of residues 1-55 of barnase. Each box in the graph represents data for an individual amino acid residue with proton chemical shift change on Y axis plotted against various concentrations of TMAO from 0 mM to 1000 mM (X-axis). The chemical shift changes are on a scale going from -0.1 to +0.15 ppm, as shown in the expansion of the V45 box.

We expected that peaks would fit to a sum of binding plus a linear shift change (Equation 4.2), as was found previously for the titrations of barnase with Hofmeister ions (Bye

et al., 2016; C Trevitt, personal communication). For the Hofmeister ions, the titration data fitted to dissociation constants K_d of around 20 mM (C Trevitt, personal communication), implying that the curved part of the data was complete by about 100 mM. The osmolyte titrations were therefore designed to allow accurate fitting of any such binding, by having more data points at the start of the titration, with wider spaced data later to measure the linear dependence.

The chemical shift changes for ^{1}H and ^{15}N nuclei of backbone amide groups of barnase against TMAO, betaine and ectoine for each residue were then fitted using a linear least squares routine. Fits to the simple linear shift change of Equation 4.1 are shown in Figure 4.10, which demonstrates that for many residues it is necessary to fit to a binding curve, because the data clearly do not fit well to a straight line (Equation 4.1). We developed a set of criteria for choosing which signals would be fitted using the simple linefit (Equation 4.1) and which required the full K_d linefit binding equation (Equation 4.2), based on the fitted K_d and $\Delta\delta_{max}$, as described below. Fits to K_d linefit are shown in Figure 4.11. All the data fitted well to this equation, giving us confidence that this was an appropriate equation for fitting the data.

Some residues have very small chemical shift changes for the binding curve component. On fitting these residues to the complete equation, the binding component tends to give poor results. Sometimes there is a small jump from the first point (with no osmolyte present) which then remains almost unchanged thereafter. This dataset fits to a very strong binding affinity, generally stronger than 5 mM, but a very small $\Delta\delta_{max}$. Such a fit is clearly meaningless. Some other residues had an almost linear chemical shift change, but with a small curvature to it. Such residues fitted to a very weak affinity (typically either greater than 900 mM or negative) and also a large $\Delta\delta_{max}$. This is also meaningless. In order to avoid meaningless fits, any nuclei fitting to affinities less than 5 mM or greater than 900 mM were considered to have meaningless fitted values. (They were checked visually in order to confirm lack of genuine binding.) Similarly, any residues that fitted to very small $\Delta\delta_{max}$ were considered to have meaningless fits, because the fitted value could have very large errors. Such nuclei were then fitted simply to a linear chemical shift change vs concentration (Equation 4.1) which will be referred to as linefits. All other nuclei were fitted to the full Equation 4.2. The cutoff value for $\Delta\delta_{max}$ was determined by looking at the data and deciding at what point the fitting to a K_d should be considered untrustworthy. Anything with a ^{1}H $\Delta\delta_{max}$ of between -0.03 and +0.03 ppm, or ^{15}N or ^{13}C $\Delta\delta_{max}$ of between -0.06 and +0.06 ppm were fit using linefit and for the rest of the nuclei if K_d is between 5 – 900 mM and $\Delta\delta_{max}$ values were larger than the above specified values, then

they were fit using K_d linefit. To do this selection, the nuclei must be sorted into the appropriate group, which was accomplished by Nawk scripts that were written to select nuclei based on the combination of K_d and $\Delta\delta_{max}$. Examples for the nuclei that fit for simple linear equation are N5, F7, K19, L20, D22 (fig 4.10) and for binding curve are N23, I25, G40, V45, D54 (fig 4.10).

The simple linear equation is Equation 4.1

$$\Delta\boldsymbol{\delta} = \boldsymbol{m}[\boldsymbol{L}]_{\boldsymbol{i}} + \mathbf{c} \qquad \textbf{(eq 4.1)}$$

where the chemical shift change is $\Delta\delta$, the gradient is m, osmolyte concentration is $[L]_i$ and the intercept is c. The intercept value c was always very close to zero. The full equation including binding is Equation 4.2 which will be referred to as K_d linefits.

$$\Delta\boldsymbol{\delta} = \left(\frac{\Delta\boldsymbol{\delta_{max}} \times [\boldsymbol{L}]_{\boldsymbol{i}}}{\boldsymbol{K_d} + [\boldsymbol{L}]_{\boldsymbol{i}}}\right) + \boldsymbol{m}[\boldsymbol{L}]_{\boldsymbol{i}} \qquad \textbf{(eq 4.2)(Bye et al., 2016)}$$

where $\Delta\delta$ is the change in chemical shift, $\Delta\delta_{max}$ is the maximum change in chemical shift on saturation, K_d is the dissociation constant, $[L]_i$ is the total concentration of ligand at titration point *i*, and m is the gradient. This equation is a sum of linear chemical shift change plus anion binding. It is worth adding that the form of the binding equation used here approximates the full equation and is only appropriate when the affinity is weak. Here the affinity is weak: the fitted dissociation constant is at least 5 mM, and the protein concentration is less than 1 mM. This is therefore a good approximation and is unlikely to give spurious results during the fitting calculation. Protein does dilute with the increasing concentrations of ligand, however the effect of protein concentration on chemical shifts in barnase has been studied and no shift changes are seen (M Williamson, personal communication).

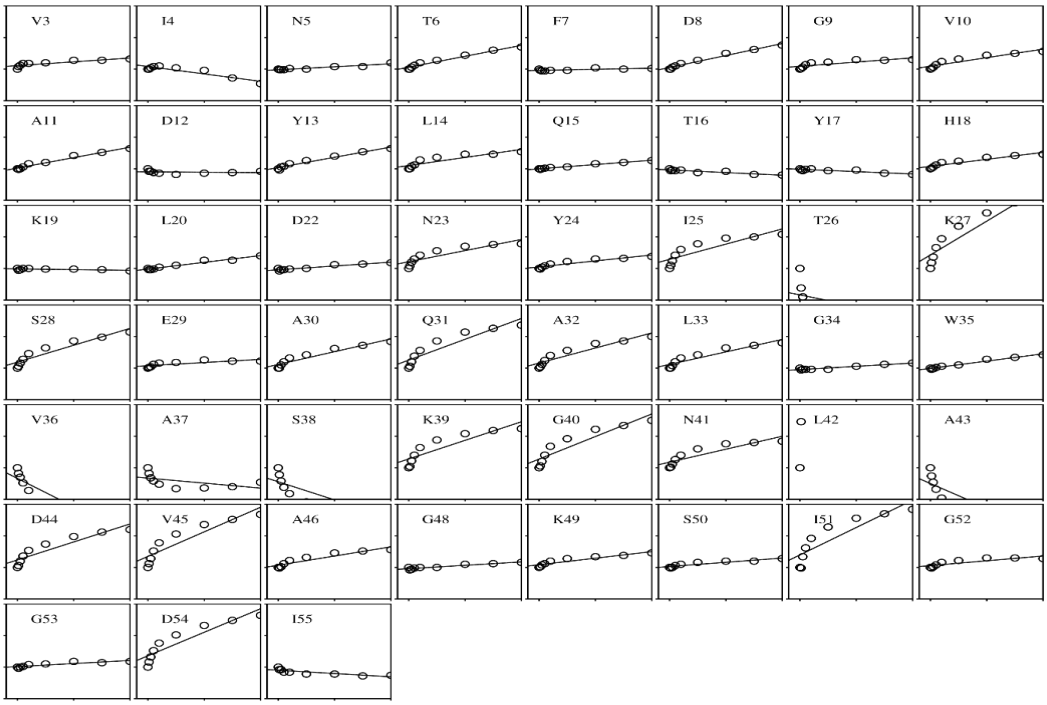

Figure 4.10. Data for individual residues from $^{1}H^{15}N$ HSQC showing proton chemical shift changes (Y axis) of barnase plotted against various concentrations of TMAO from 0 mM to 1000 mM (X-axis). The chemical shift changes are on a scale going from -0.05 to +0.10 ppm. The fitted line is the simple linear fit (Equation 4.1) which fits well for some residues but is clearly inadequate for many.

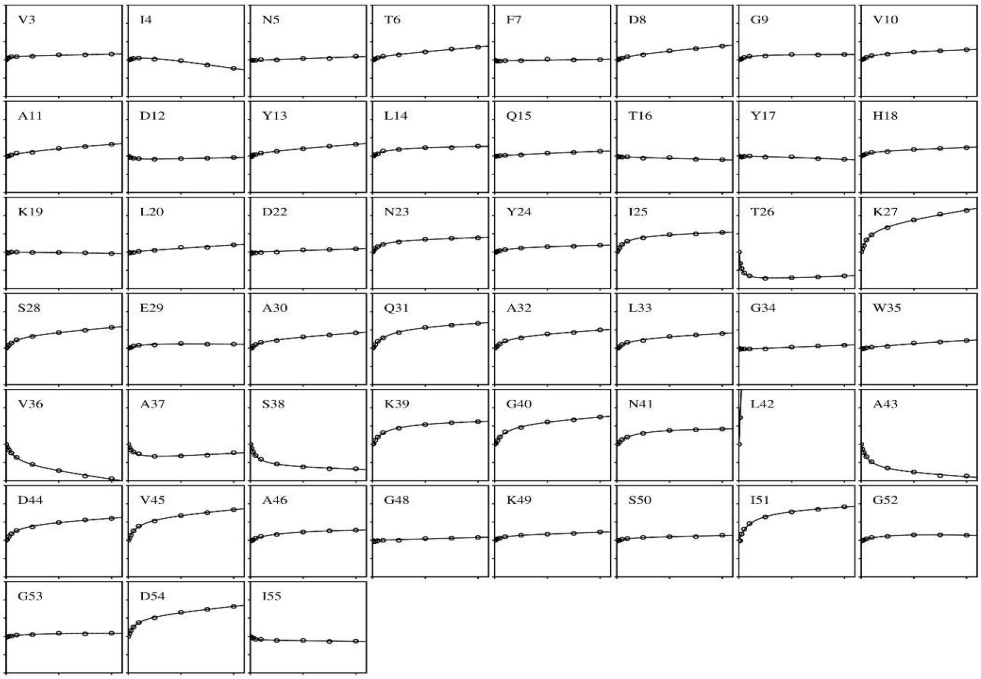

Figure 4.11. Data from K_d linefit of $^{1}H^{15}N$ HSQC showing proton chemical shift changes (Y axis) of residues 1-55 of barnase plotted against various concentrations of TMAO from 0 mM to 1000 mM (X-axis). The chemical shift changes are on a scale going from -0.1 to +0.15 ppm.

4.6.2 Analysis of $^{1}H^{15}N$ HSQC chemical shift changes

In the presence of TMAO, K27, Q31, K39, G40, V45, I51, D86 among protons (fig 4.11, 4.12) and I25, T26, K27, A37, S38, W35, G40, N58 among nitrogens (fig 4.13) were some of the residues that exhibited curved chemical shifts and therefore evidenced binding and chemical shift perturbation (CSP). The curved parts of the chemical shift profiles were previously attributed to anion binding (Bye et al., 2016). Ectoine and betaine have zero net charge, and TMAO has only partial charges on N and O. It was therefore not obvious whether the binding would be stronger or weaker than the Hofmeister ions studied by Bye et al (2016) and by C Trevitt. Among protons, F82, S85, T26 are the residues with biggest downfield shift movement and D86, R83, L42 with biggest upfield shift movement (Fig 4.11, 4.12). Among nitrogens, N84, S85, F82 are the residues with biggest downfield shift movement and N58, L42, R83 with biggest upfield shift movement (Fig 4.13, 4.14).

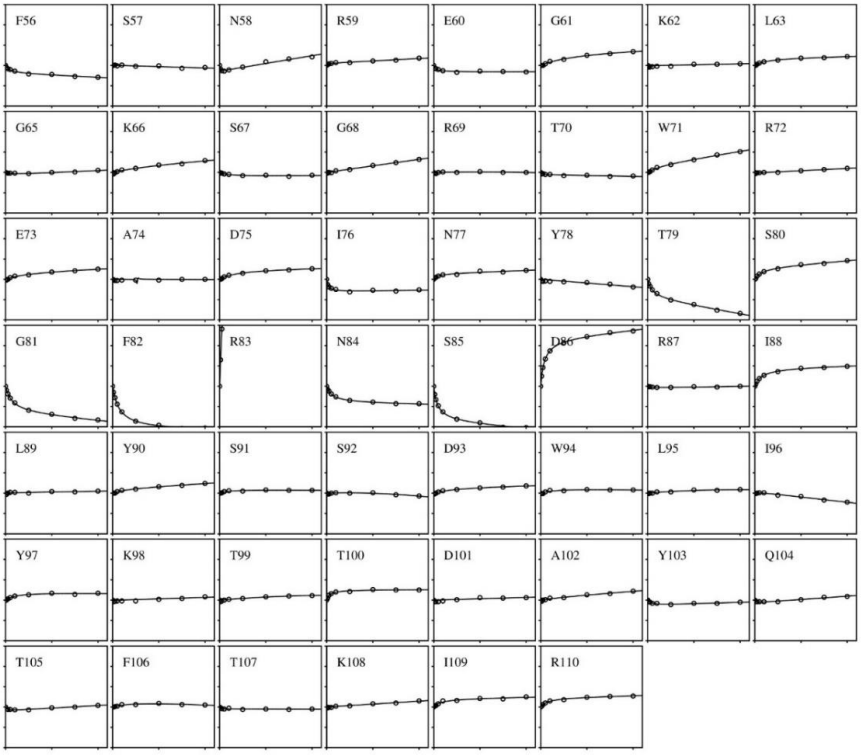

Figure 4.12. Data from K_d linefit of $^{1}H^{15}N$ HSQC showing hydrogen chemical shift changes (Y axis) of residues 56-110 of barnase plotted against various concentrations of TMAO from 0 mM to 1000 mM (X-axis). The chemical shift changes are on a scale going from -0.1 to +0.15 ppm.

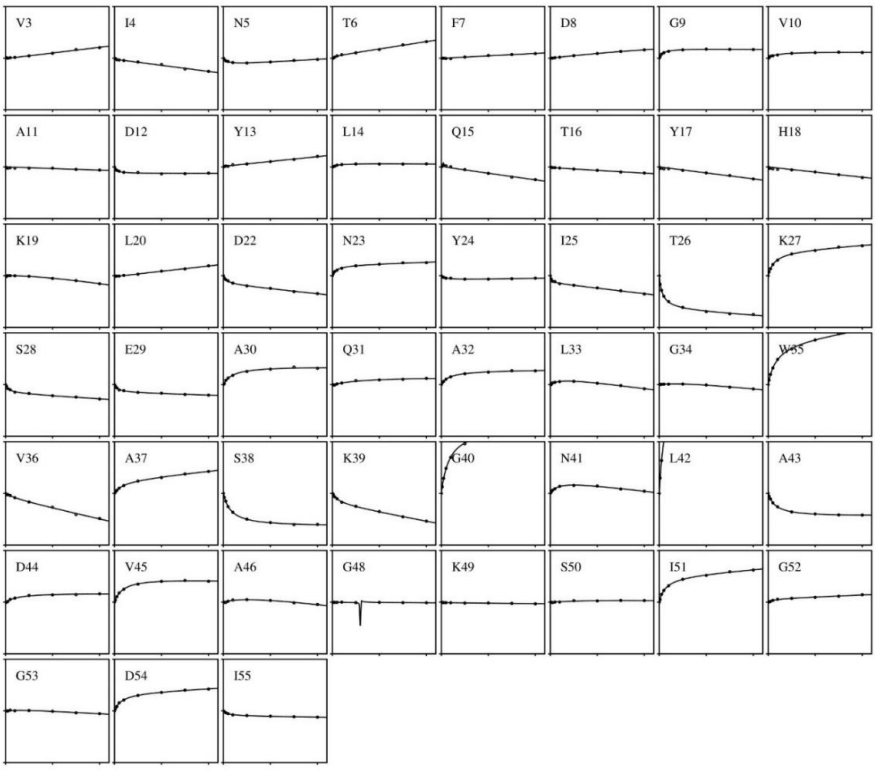

Figure 4.13. Data from K_d linefit of $^{1}H^{15}N$ HSQC showing nitrogen chemical shift changes (Y axis) of residues 1-55 of barnase plotted against various concentrations of TMAO from 0 mM to 1000 mM (X-axis). The chemical shift changes are on a scale going from -0.5 to +0.5 ppm.

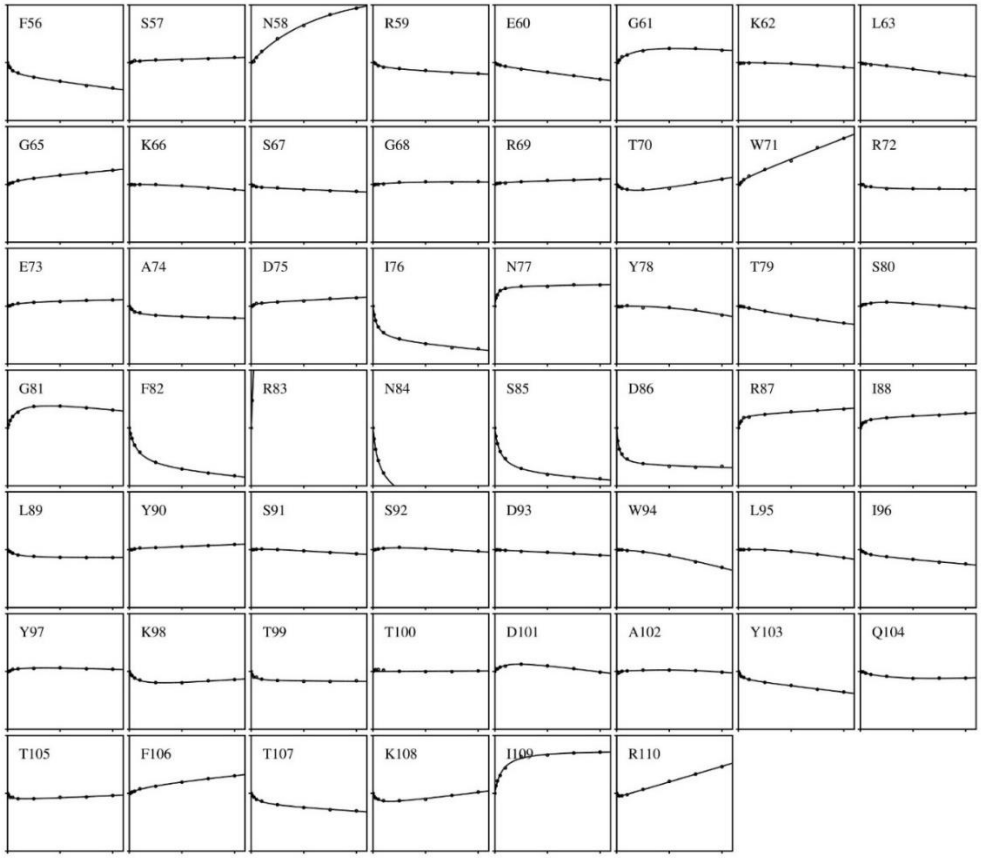

Figure 4.14. Data from K_d linefit of $^{1}H^{15}N$ HSQC showing nitrogen chemical shift changes (Y axis) of residues 56-110 of barnase plotted against various concentrations of TMAO from 0 mM to 1000 mM (X-axis). The chemical shift changes are on a scale going from -0.5 to +0.5 ppm.

The chemical shift changes are enormously big for L42 and R83 compared to other residues, sometimes as high as 2 to 4 times larger than the next biggest residue in terms of shift change. As commented above, these two residues also showed a big variation in solutions of apparently the same pH, in the absence of buffer. The sidechain of W35 also showed big variation. These three NH are close together and are connected by a conserved water-mediated hydrogen bonding network (Figure 4.15), which bridges across the interface between two different parts of the protein. L42 and R83 are also important for the catalytic activity of the protein (Buckle and Fersht, 1994). We therefore suggest that this hydrogen bonding network is sensitive and easily perturbed. It is not clear whether it plays any part in the catalytic activity of barnase, but the role played by L42 and R83 in catalysis suggests that it may be relevant in some way. In the subsequent analysis, we have not included an analysis of these two residues, because their chemical shift changes are anomalous and are clearly not simply due to binding events or protein solvation.

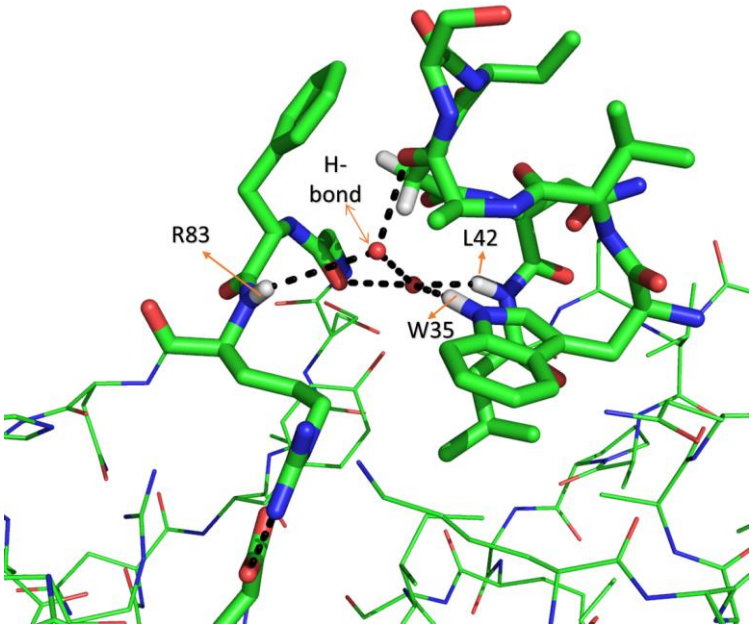

Figure 4.15. The NH of L42, R83 and W35 are connected by H-bonding (black dotted line).

Most residues were fitted to the full binding curve (Equation 4.2), as most residues show a binding effect and did not fit well to the simple linear equation (as seen in Fig 4.10). In general, stronger CSP were observed in nitrogen shifts than proton shifts. Nuclei that showed curved chemical shift changes were mostly at concentrations less than 0.1 M; beyond that, till 1 M, mostly linear chemical shift changes were observed. This provides the first indication that a reasonably strong binding affinity can be expected. Mostly upfield chemical shift changes were observed and a few residues exhibited downfield chemical shift changes which could be due to stronger hydrogen bonding (Bye et al., 2016). Some of the residues that have exhibited nonlinear chemical shift changes like V3, F7, G9, G48, and I55 in Fig 4.11 are solvent exposed and get saturated at concentrations of 0.1 M to 0.2 M TMAO. This could be due to TMAO binding to the protein surface leading to the saturation and therefore no further change in chemical shift.

Like TMAO, ectoine too causes chemical shift changes in many residues. However, most residues fit to the simple linear equation (Figs 4.16 and 4.17) rather than the binding saturation curve equation. This fitting of residues to Eq 4.1 means ectoine is binding very weakly to barnase compared to TMAO. Among protons I25, F82, G52 are the residues with biggest downfield shift movement and A32, L42, R83, with biggest upfield shift movement (Fig 4.16). Among nitrogens, I25, S38, N84 are the residues with biggest downfield shift

movement and L42, R59, R83 with biggest upfield shift movement (Fig 4.17). A big CSP was observed for residues L42 and R83 in the presence of ectoine like it was in the case of TMAO.

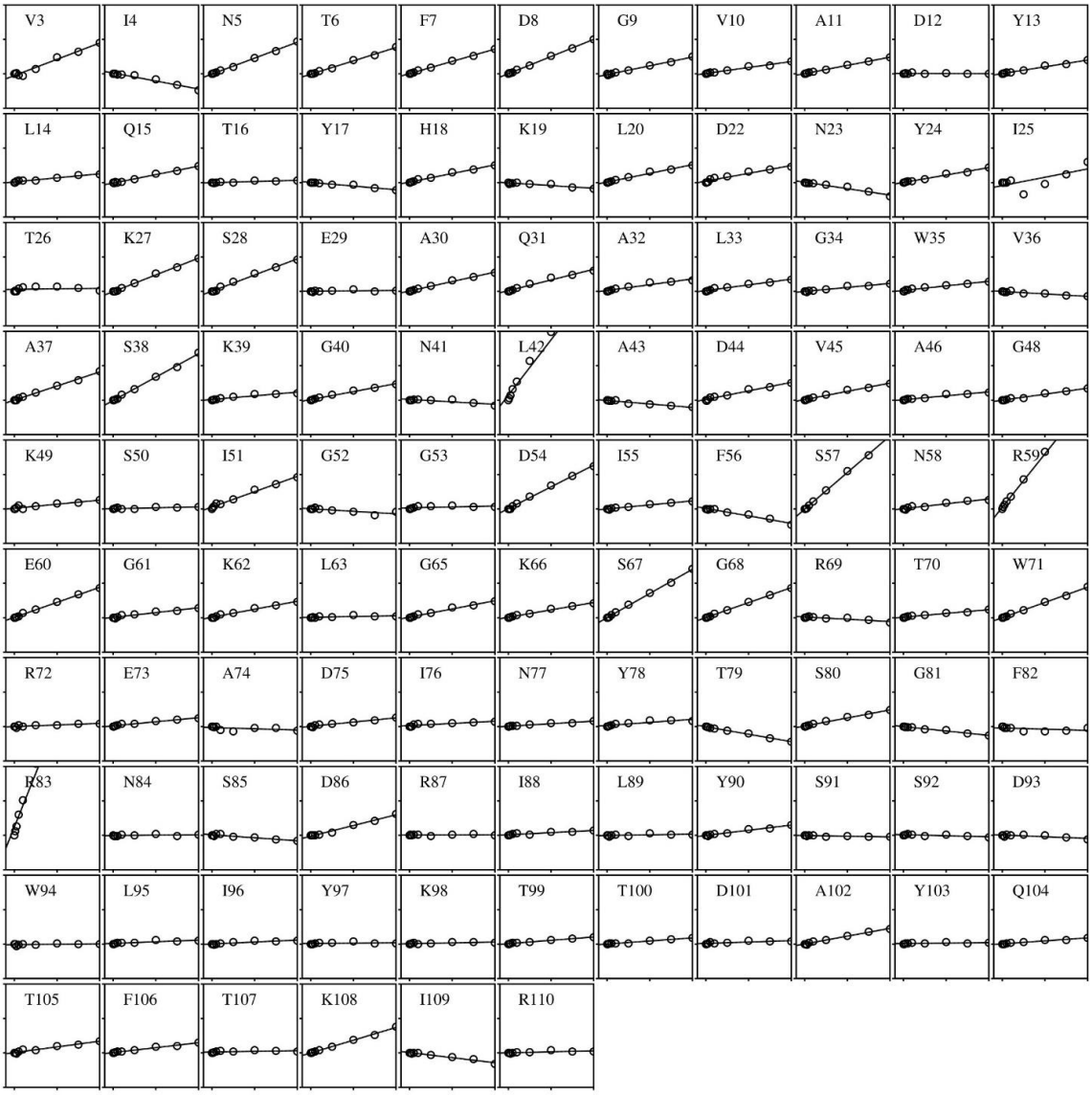

Figure 4.16. Data for linefit of individual residues from $^{1}H^{15}N$ HSQC showing proton chemical shift changes (Y axis) of barnase plotted against various concentrations of ectoine from 0 mM to 1000 mM (X-axis). The chemical shift changes are on a scale going from -0.05 to +0.10 ppm

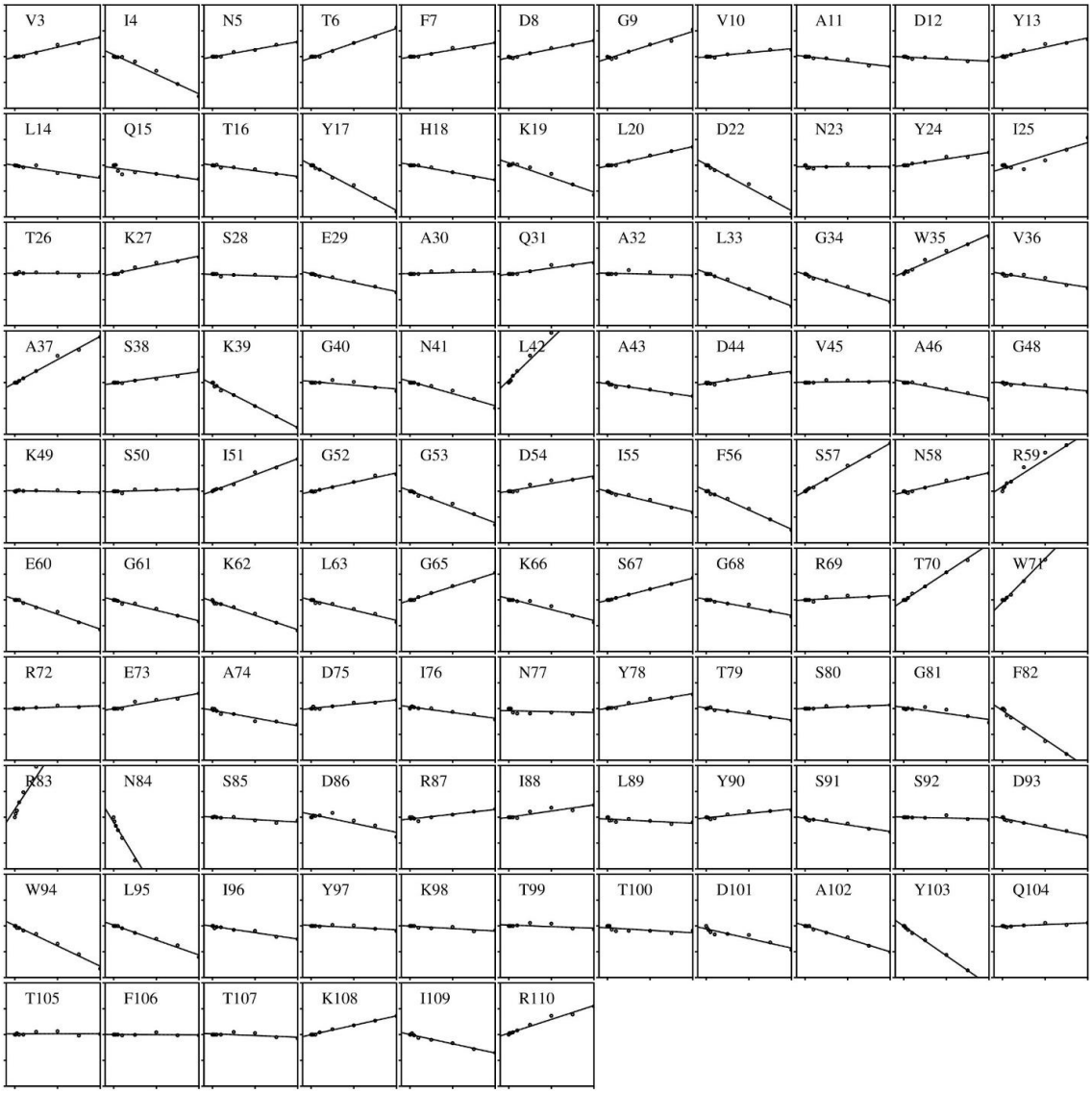

Figure 4.17. Data for linefit of individual residues from $^{1}H^{15}N$ HSQC showing proton chemical shift changes (Y axis) of barnase plotted against various concentrations of ectoine from 0 mM to 1000 mM (X-axis). The chemical shift changes are on a scale going from -0.2 to +0.2 ppm.

The general pattern of chemical shift changes for both TMAO and ectoine is in two stages. Curved chemical shift changes are observed till 0.1 M and linear chemical shift changes predominate from 0.1 M till 1 M. In the previous analysis of Hofmeister ions (Bye et al, 2016), curved changes were found to be due to direct binding of the ion, and linear changes were found to be indirect effects, due to effects of Hofmeister ions on the solvent, which then affected hydration of the protein. We assume that something similar is happening here, and in particular that the linear shift changes beyond 0.1 M are Hofmeister effects. Site-specific changes in the presence of ectoine are different from that of TMAO, which will be discussed in later sections.

Like TMAO and ectoine, betaine too causes chemical shift changes in many residues. However, most residues fit to the simple linear equation (Figs 4.18 and 4.19) rather than the binding saturation curve equation. This fitting of residues to Eq 4.1 means betaine is binding very weakly to barnase compared to TMAO and it is in fact weaker even than ectoine. Among protons N84 and N41 are the residues with biggest downfield shift movement and S38, R83 are the residues with biggest upfield shift movement (Fig 4.18). Among nitrogens, N84, G40 are the residues with biggest downfield shift movement and S38, W35 with biggest upfield shift movement (Fig 4.19). A big CSP was observed for residues L42 and R83 in the presence of betaine like it was in the case of TMAO and ectoine. Chemical shift changes for betaine are just linear changes from 0 M till 1 M. Unlike TMAO and ectoine, no curvature at smaller concentrations till 0.1 M was observed in the presence of betaine.

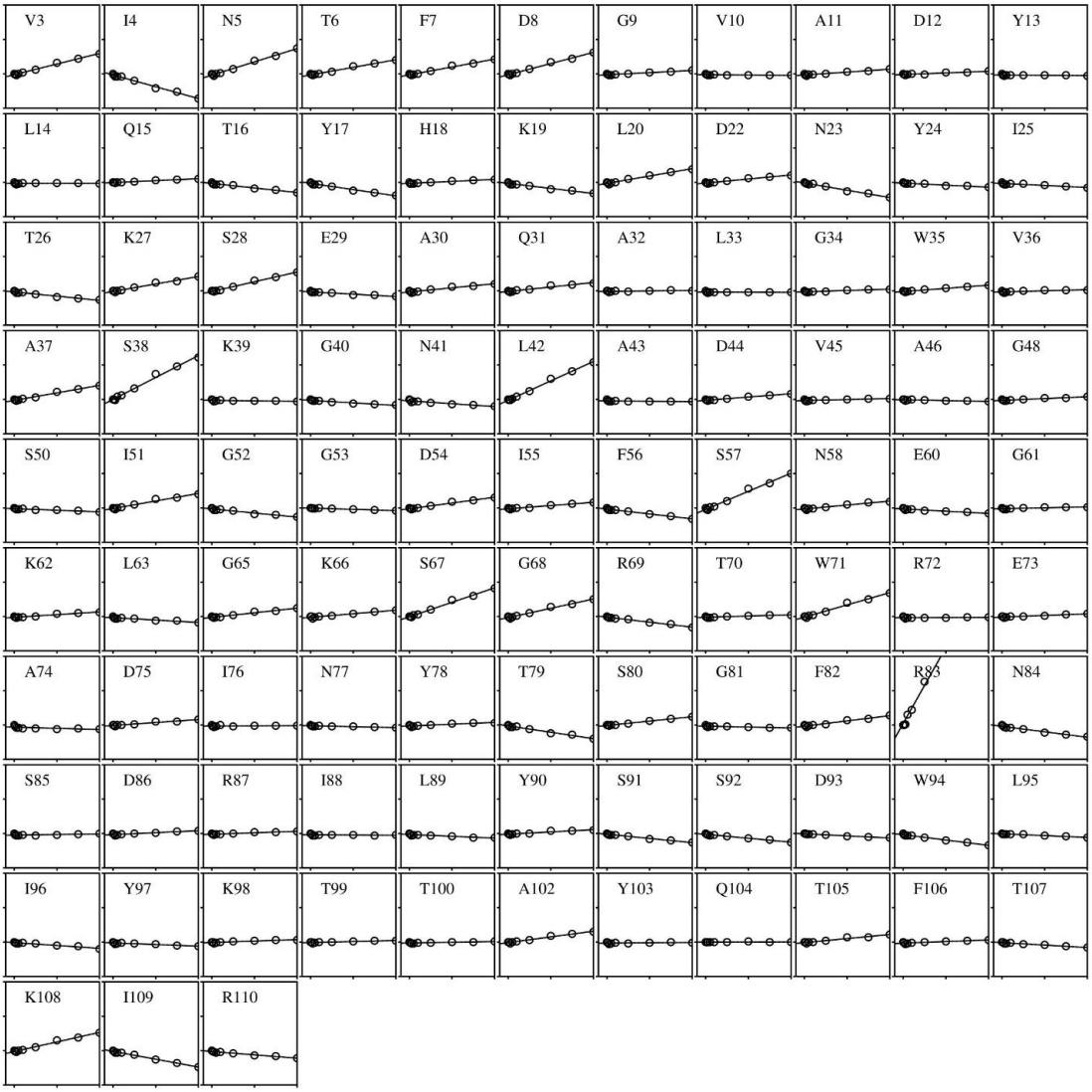

Figure 4.18. Data for linefit of individual residues from $^{1}H^{15}N$ HSQC showing proton chemical shift changes (Y axis) of barnase plotted against various concentrations of betaine from 0 mM to 1000 mM (X-axis). The chemical shift changes are on a scale going from -0.05 to +0.10 ppm.

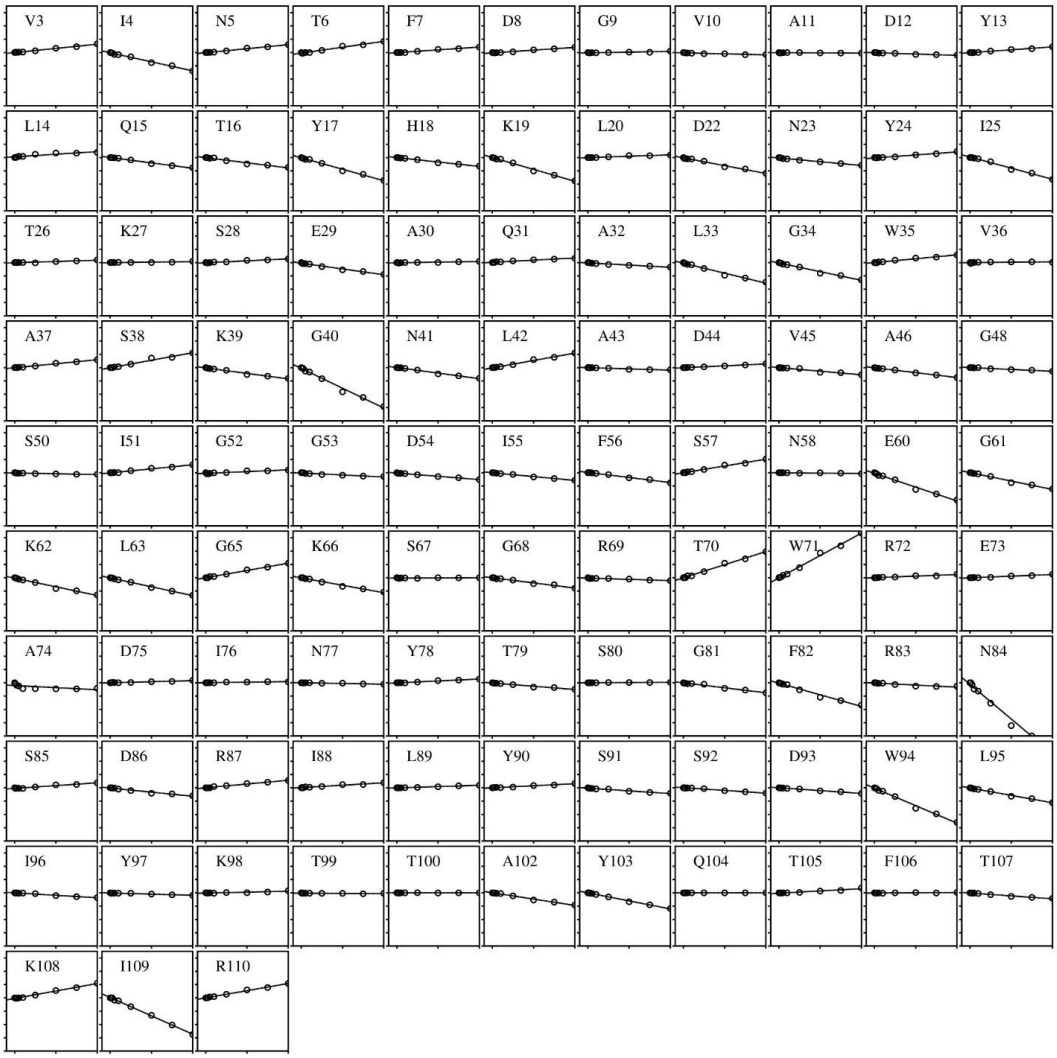

Figure 4.19. Data for linefit of individual residues from $^{1}H^{15}N$ HSQC showing nitrogen chemical shift changes (Y axis) of barnase plotted against various concentrations of betaine from 0 mM to 1000 mM (X-axis). The chemical shift changes are on a scale going from -0.4 to +0.35 ppm.

4.6.3 HNCO experiments

2D HNCO experiments were run, and spectra recorded in the presence of varied concentrations of TMAO, ectoine, and betaine as shown in Figures 4.20 – 4.22. Like in the ^{1}H ^{15}N HSQC experiments, peaks in HNCO experiments are sensitive towards increasing concentrations of TMAO, ectoine and betaine. Some carbonyl groups have big changes in chemical shift in the presence of TMAO, but the changes with ectoine and betaine are smaller.

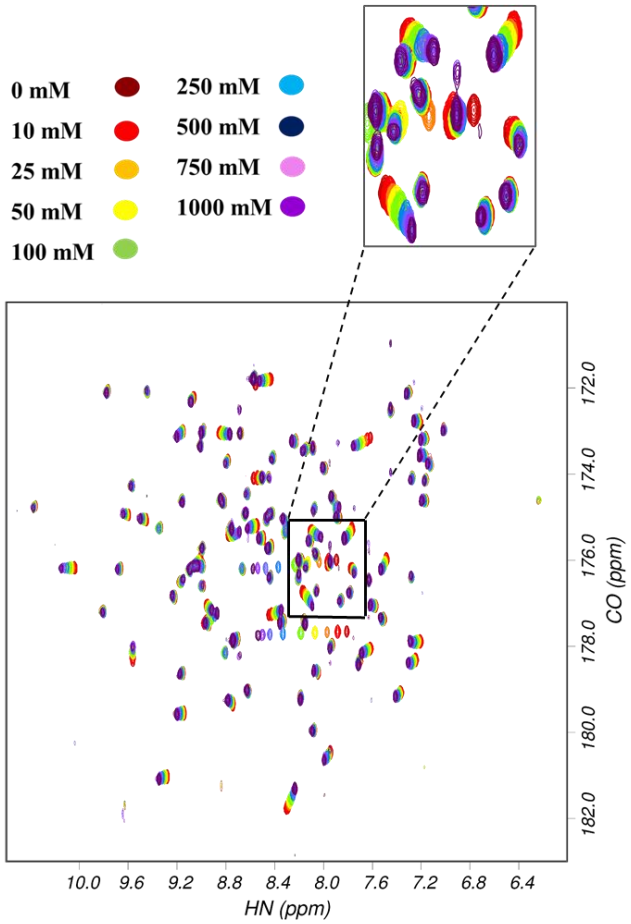

Figure 4.20. Spectra from HNCO experiments of barnase with two coordinates showing H (X axis) and CO^{i-1} (Y axis) in the presence of varied concentrations of TMAO from 0 mM to 1000 mM. Each ligand concentration is assigned a rainbow colour. An enlarged region is also shown.

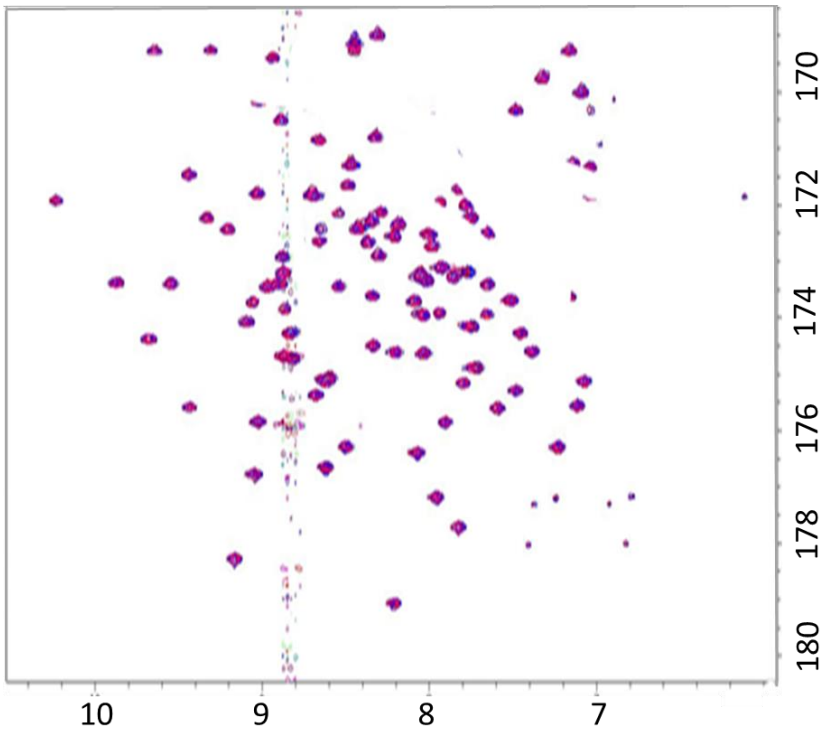

Figure 4.21. Spectra from HNCO experiments of barnase with two coordinate showing proton H (X axis) and CO^{i-1} (Y axis) in the presence of varied concentrations of ectoine from 0 mM to 1000 mM. Almost all signals shift so little that no change is visible at this scale.

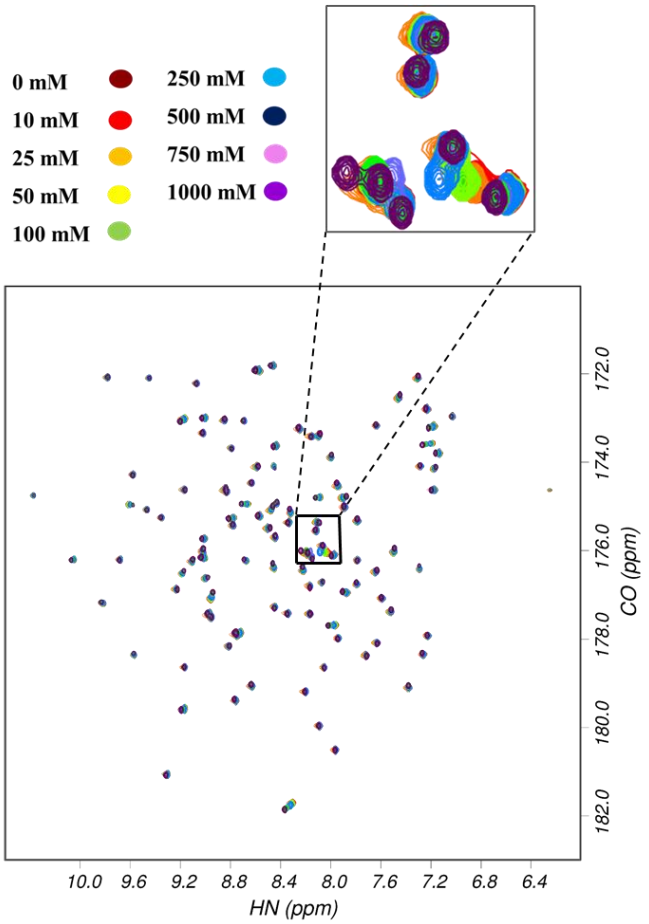

Figure 4.22. Spectra from HNCO experiments of barnase with two coordinate showing H (X axis) and CO^{i-1} (Y axis) in the presence of varied concentrations of betaine from 0 mM to 1000 mM. Each ligand concentration is assigned a rainbow colour. An enlarged region is also shown.

In the presence of TMAO, A37, D86, and G81 are the carbonyl residues with biggest downfield shift movement and S38, L42, and G40 with biggest upfield shift movement (Fig 4.23, 4.24). (Note that HNCO peaks are derived from the corresponding HSQC signal, so that for example A37 refers to the carbonyl group bonded to the amide nitrogen of A37, ie V36 CO.) Nuclei like N5, T6, F7, Y17 exhibit non-linear changes in chemical shift. L42 has a very large change in chemical shift which is similar to what was seen in $^{1}H\,^{15}N$ HSQC experiments. R83 too has large a chemical shift change which is similar to what was seen in $^{1}H\,^{15}N$ HSQC experiments.

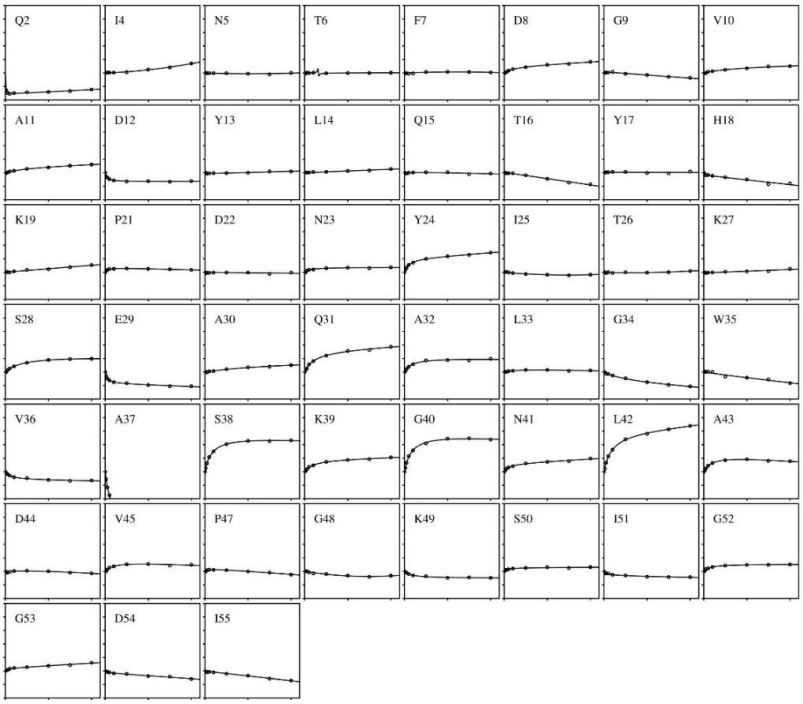

Figure 4.23. Data for k_d linefit of individual residues from HNCO fitted to Equation 4.2 showing carbonyl chemical shift changes (Y axis) of residues 1-55 of barnase plotted against various concentrations of TMAO from 0 mM to 1000 mM (X-axis). The chemical shift changes are on a scale going from -0.2 to +0.5 ppm.

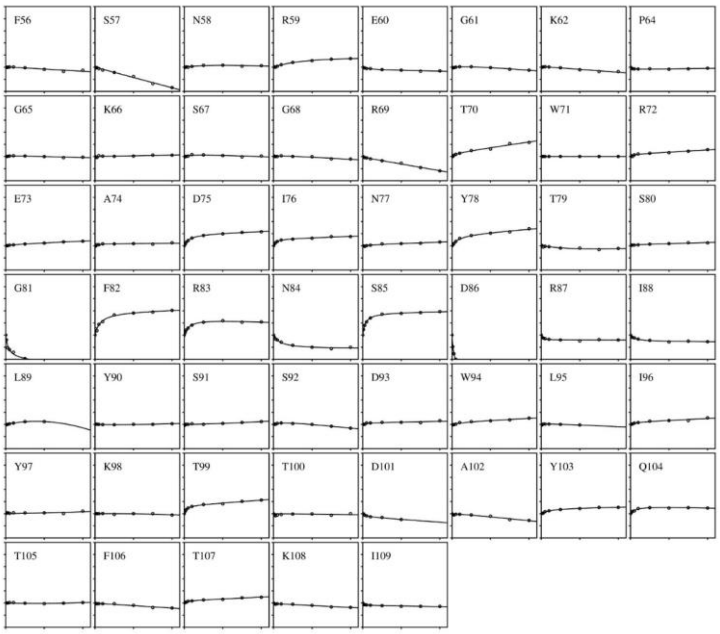

Figure 4.24. Data for k_d linefit of individual residues from HNCO showing carbonyl chemical shift changes (Y axis) of residues 56-110 of barnase plotted against various concentrations of TMAO from 0 mM to 1000 mM (X-axis). The chemical shift changes are on a scale going from -0.2 to +0.5 ppm.

In the presence of ectoine, Y24, T6, and A102 are the carbonyl residues with biggest downfield shift movement and N77, T99, K108 with biggest upfield shift movement (Fig 4.25, 4.26). Shift changes caused by ectoine are not as big as those in the presence of TMAO. Unlike in N HSQC experiments, the data for HNCO had to be fit to the binding curve equation since many residues are not fitting to the simple linear equation. This doesn't mean there is huge binding, however, it is just enough not to fit well to the simple linear equation. Like in $^{1}H^{15}N$ HSQC experiments, the general pattern of chemical shift changes for both TMAO and ectoine is in two stages. There are curved chemical shift changes till 0.1 M and linear chemical shift changes from 0.1 M till 1 M which looks like a Hofmeister effect. Site changes in the presence of ectoine are different from that of TMAO and will be discussed in later sections.

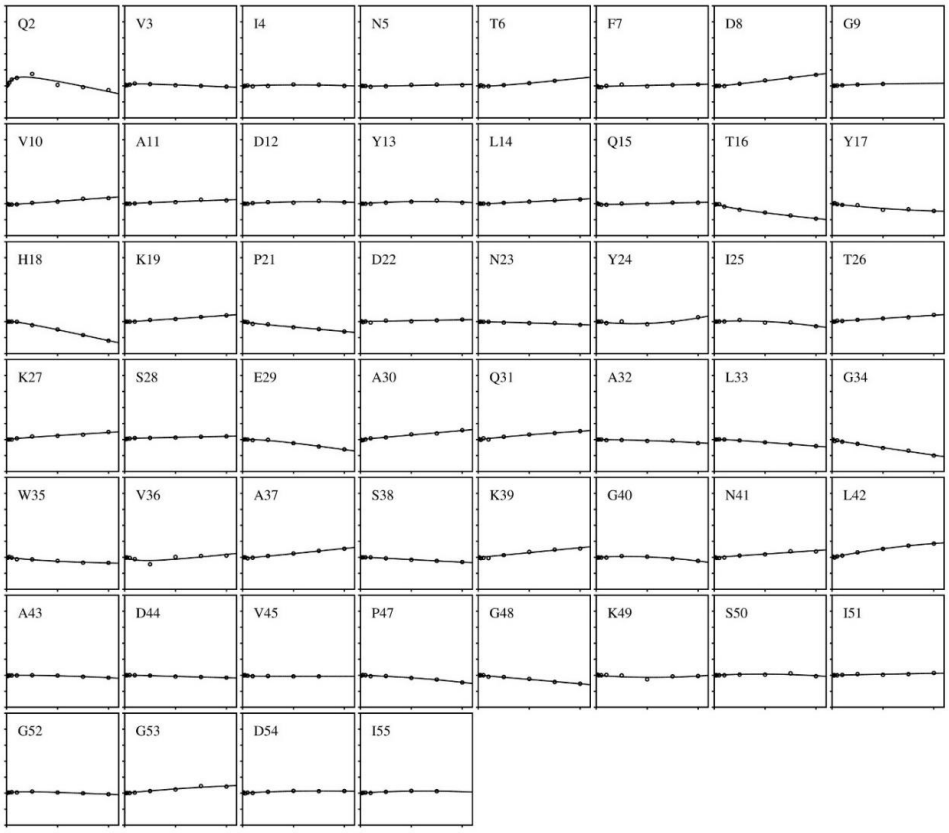

Figure 4.25. Data for K_d linefit of individual residues from HNCO showing carbonyl chemical shift changes (Y axis) of residues 1-55 of barnase plotted against various concentrations of ectoine from 0 mM to 1000 mM (X-axis). The chemical shift changes are on a scale going from -0.2 to +0.5 ppm.

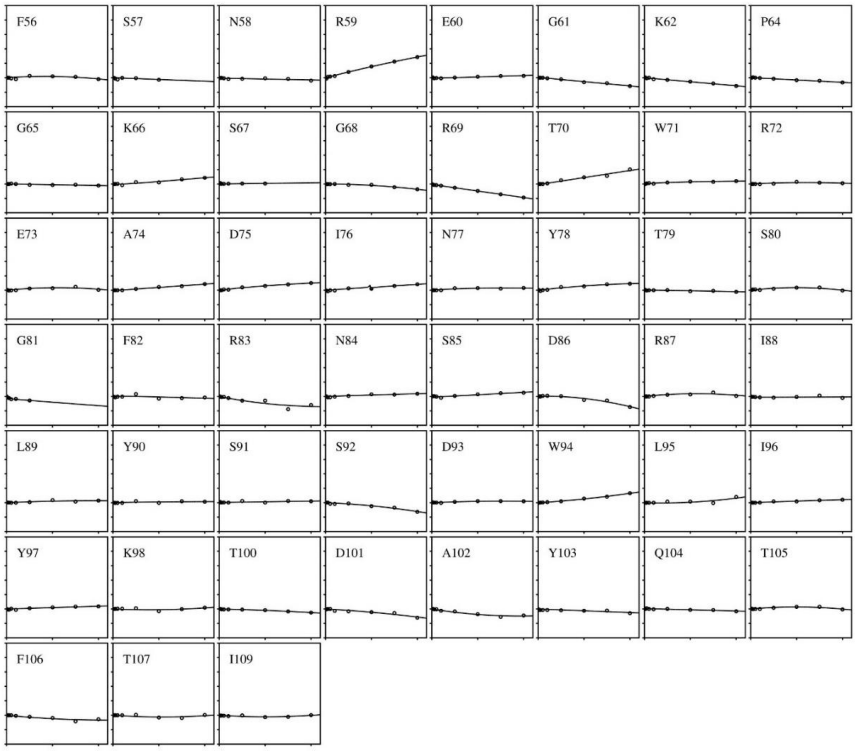

Figure 4.26. Data for K_d linefit of individual residues from HNCO showing carbonyl chemical shift changes (Y axis) of residues 56-110 of barnase plotted against various concentrations of ectoine from 0 mM to 1000 mM (X-axis). The chemical shift changes are on a scale going from -0.2 to +0.5 ppm.

In the presence of betaine, F82 is the carbonyl residue with biggest downfield shift movement and A37 with biggest upfield shift movement (Fig 4.27). Shift changes caused by betaine are similar to ectoine and are not as big as those in the presence of TMAO. Like in N HSQC experiments, the data for HNCO had to be fit to the simple linear equation since there is no binding. Like in $^{1}H^{15}N$ HSQC experiments, the general pattern of chemical shift changes for betaine are just linear changes from 0 M till 1 M. Unlike TMAO and ectoine, no curvature at smaller concentrations till 0.1 M was observed in presence of betaine.

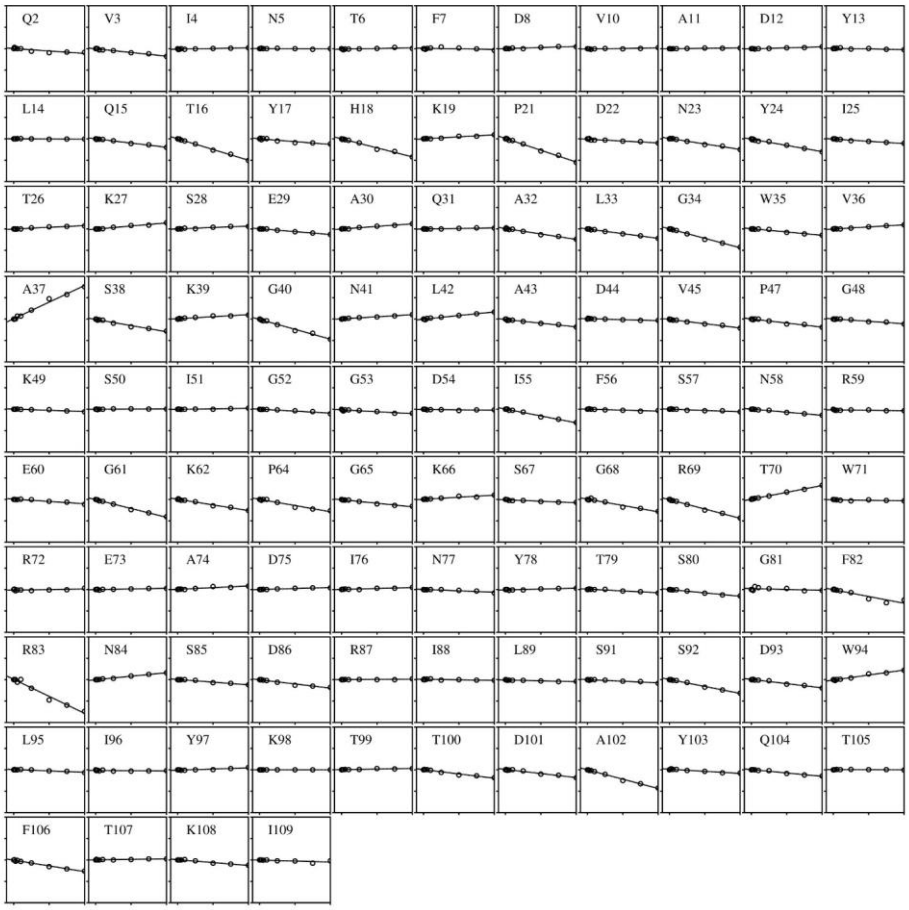

Figure 4.27. Data for linefit of individual residues from HNCO showing carbonyl chemical shift changes (Y axis) of barnase plotted against various concentrations of betaine from 0 mM to 1000 mM (X-axis). The chemical shift changes are on a scale going from -0.2 to +0.2 ppm.

4.6.3.1 $^{1}H^{13}C$ HSQC experiments

$^{1}H^{13}C$ HSQC experiments were run and spectra recorded in the presence of varied concentrations of TMAO and ectoine as shown in Figures 4.28 and 4.29. Chemical shift changes on Hα (Hydrogen alpha atom), H (other than alpha atom) and methyl groups (methyl groups were further split into methyl carbon and methyl hydrogen) were analysed and fit into the binding curve equation. Like in the $^{1}H^{15}N$ HSQC and HNCO experiments, peaks in $^{1}H^{13}C$ HSQC experiments are sensitive towards the increasing concentrations of TMAO and ectoine but changes in chemical shift were small and some of the residues were difficult to exactly map due to overlapping nuclei, interference from water signal, and loss of signal intensity (especially in case of ectoine), and hence had to be excluded.

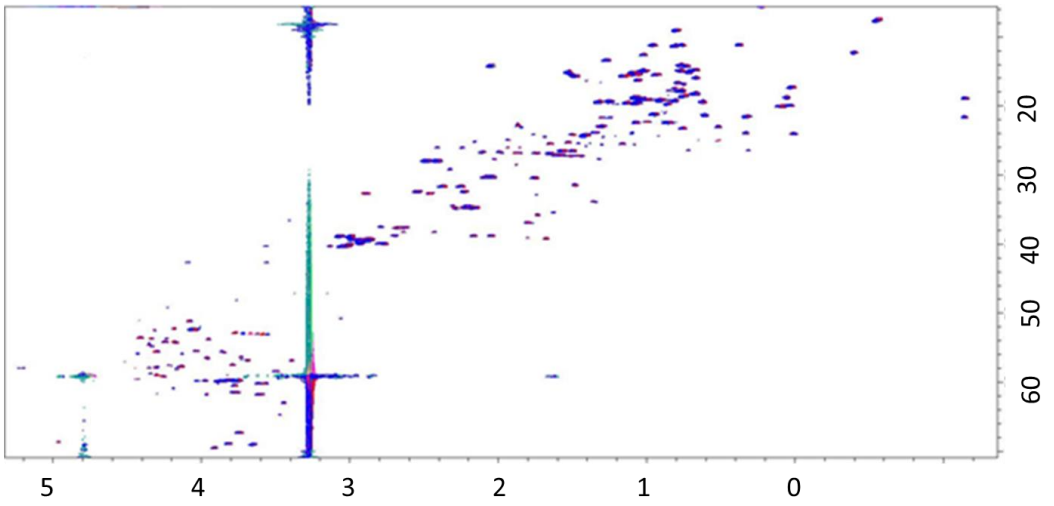

Figure 4.28. Spectra from $^{1}H^{13}C$ HSQC experiments of barnase with each peak representing C-H pair and two coordinates showing proton (X axis) and carbon (Y axis) in the presence of varied concentrations of TMAO from 0 mM to 1000 mM.

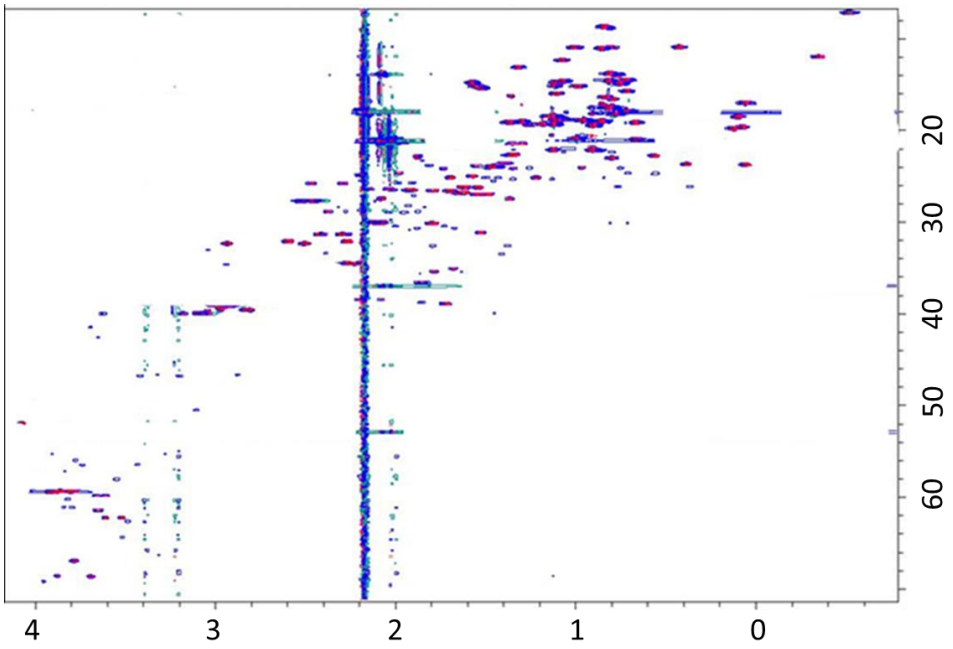

Figure 4.29. Spectra from $^{1}H^{13}C$ HSQC experiments of barnase with each peak representing C-H pair and two coordinate showing proton (X axis) and carbon (Y axis) in the presence of varied concentrations of ectoine from 0 mM to 1000 mM.

In the presence of TMAO, changes on methyl protons are mostly small with some exceptions like A37 and L42 (Fig 4.30). Bigger changes were observed for most of the methyl carbons (Fig 4.31). Hα (Hydrogen alpha) groups have significant changes in chemical shift (Fig 4.32). H (other than alpha) groups have not shown as big changes in chemical shift as Hα except for residues like L42, I51, R83, and D86 (Fig 4.33 and 4.34).

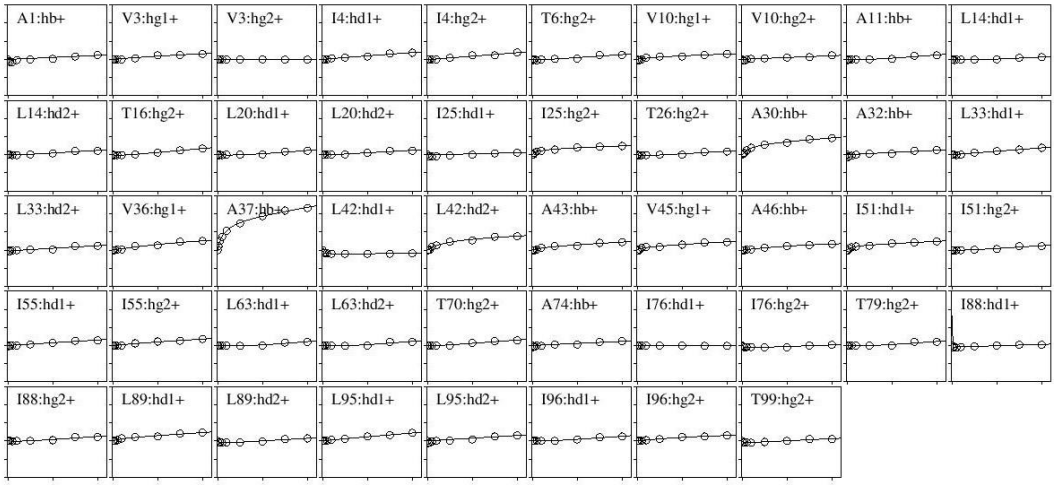

Figure 4.30. Data for k_d linefit of individual residues from $^{1}H^{13}C$ HSQC showing methyl hydrogen chemical shift changes (Y axis) of barnase plotted against various concentrations of TMAO from 0 mM to 1000 mM (X-axis). The chemical shift changes are on a scale going from -0.1 to + +0.15 ppm.

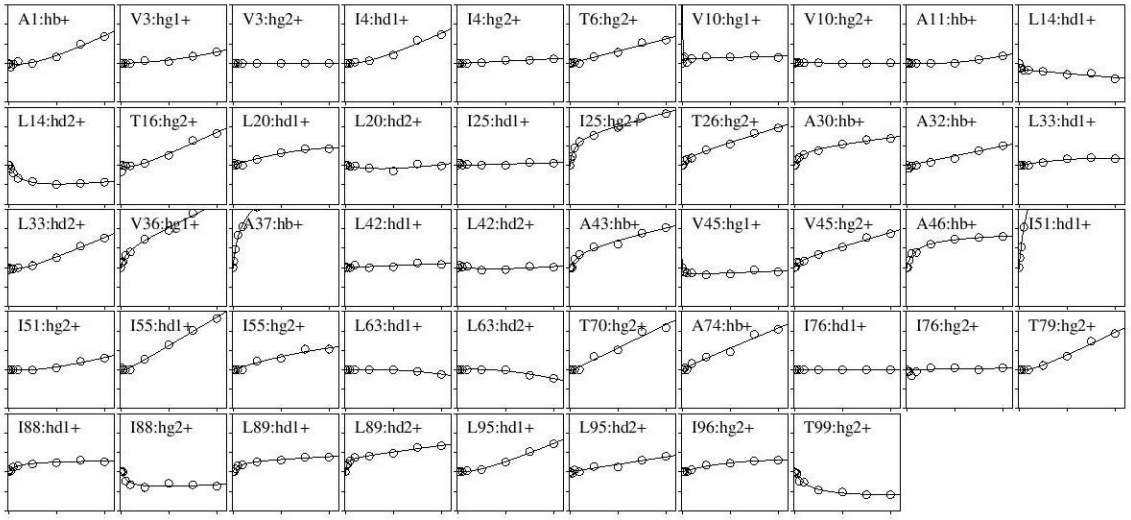

Figure 4.31. Data for K_d linefit of individual residues from $^{1}H^{13}C$ HSQC showing methyl carbon chemical shift changes (Y axis) of barnase plotted against various concentrations of TMAO from 0 mM to 1000 mM (X-axis). The chemical shift changes are on a scale going from -0.1 to +0.15 ppm.

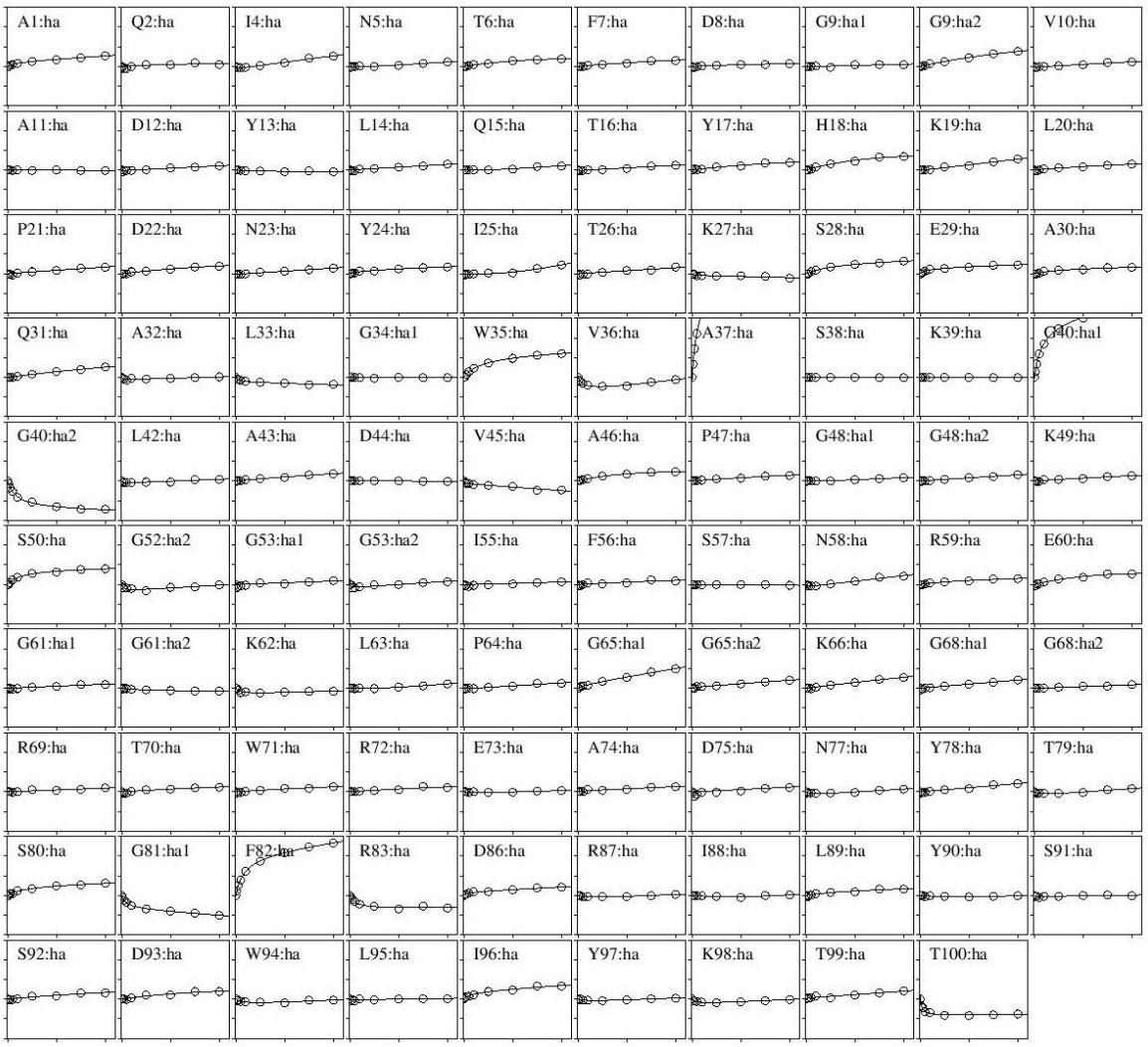

Figure 4.32. Data forKk_d linefit of individual residues from $^1H^{13}C$ HSQC showing alpha (α) hydrogen chemical shift changes (Y axis) of barnase plotted against various concentrations of TMAO from 0 mM to 1000 mM (X-axis). The chemical shift changes are on a scale going from -0.1 to +0.15 ppm.

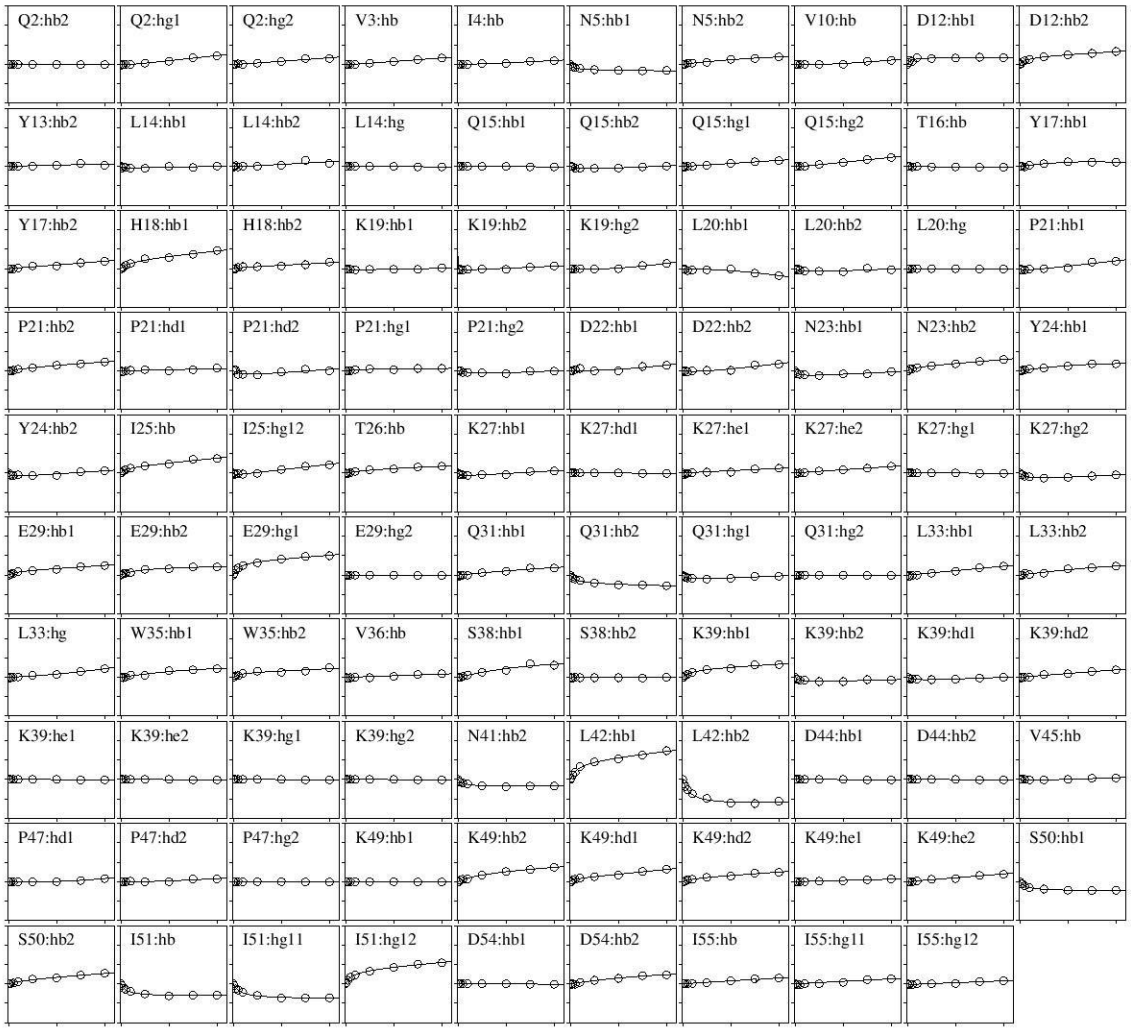

Figure 4.33. Data for K_d linefit of individual residues from $^{1}H^{13}C$ HSQC showing hydrogen (other than α) chemical shift changes (Y axis) of 1-55 residues of barnase plotted against various concentrations of TMAO from 0 mM to 1000 mM (X-axis). The chemical shift changes are on a scale going from -0.1 to +0.15 ppm.

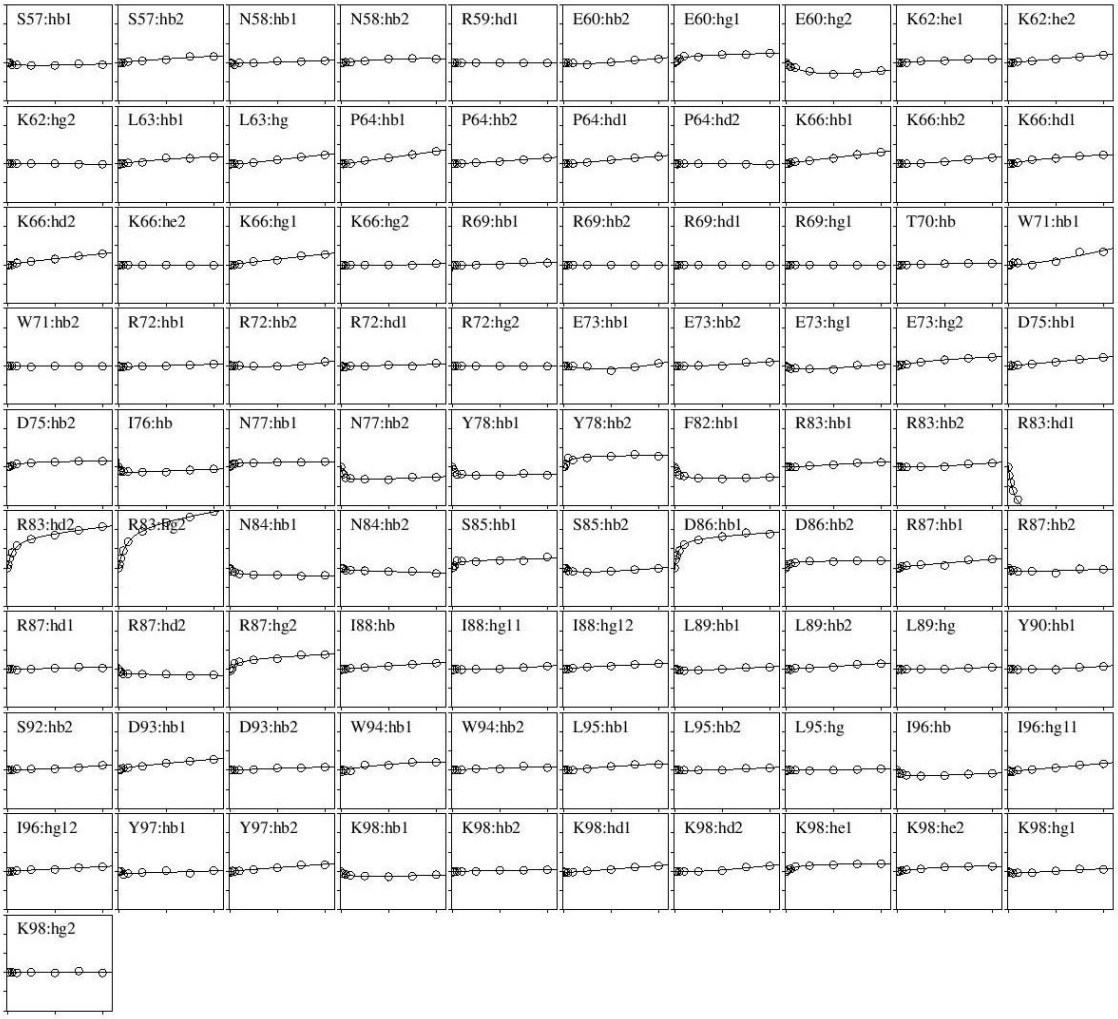

Figure 4.34. Data for K_d linefit of individual residues from $^1H^{13}C$ HSQC showing hydrogen (other than α) chemical shift changes (Y axis) of 57-110 residues of barnase plotted against various concentrations of TMAO from 0 mM to 1000 mM (X-axis). The chemical shift changes are on a scale going from -0.1 to +0.15 ppm.

In the presence of ectoine, changes in chemical shift are small and display mostly no big binding curve and nonlinear changes were observed. Because of overlapping, loss in signal intensity, and water interference many residues must be excluded which made analysis of CHSQC data difficult. No big changes were observed for methyl H groups (Fig 4.35). Hα (Hydrogen alpha) groups too have not shown significant changes in chemical shift except A37 (Fig 4.37). H (other than α) groups too have not shown significant changes in chemical shift (Fig 4.38). However, big changes were observed for most of the nuclei in methyl C groups (Fig 4.36). Unlike in $^1H^{15}N$ HSQC experiments, the data for $^1H^{13}C$ HSQC had to be fit to the binding curve equation since many residues are not fitting to the simple linear equation. Like in $^1H^{15}N$ HSQC experiments, the general pattern of chemical shift changes for both TMAO and ectoine

is in two stages: curved chemical shift changes till 0.1 M and linear chemical shift changes from 0.1 M till 1 M which looks like Hofmeister effect.

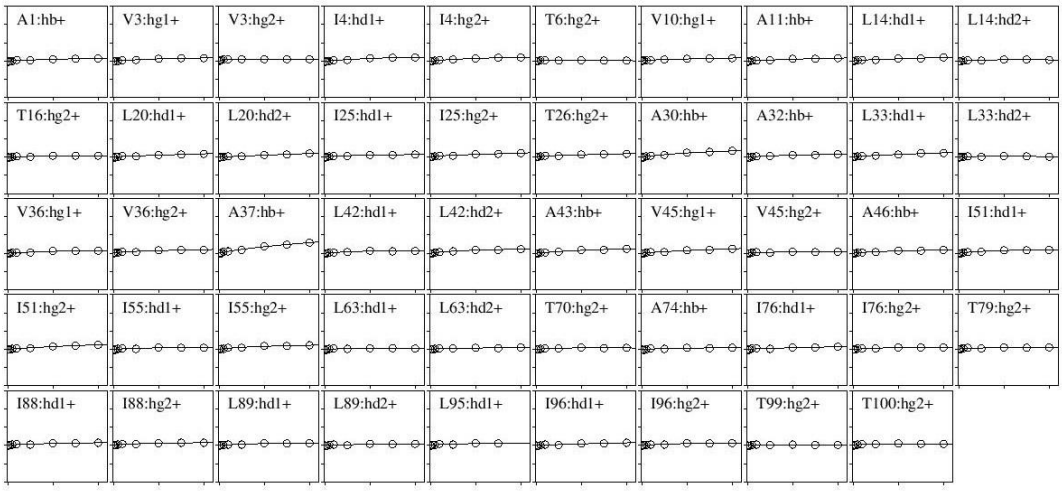

Figure 4.35. Data for K_d linefit of individual residues from $^{1}H^{13}C$ HSQC showing methyl hydrogen chemical shift changes (Y axis) of barnase plotted against various concentrations of ectoine from 0 mM to 1000 mM (X-axis). The chemical shift changes are on a scale going from -0.1 to +0.15 ppm.

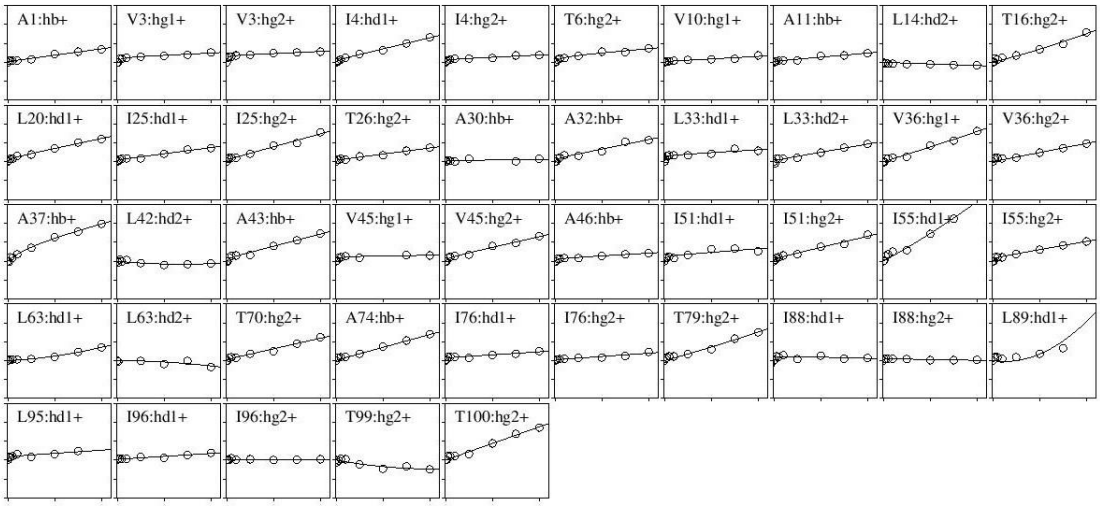

Figure 4.36. Data for K_d linefit of individual residues from $^{1}H^{13}C$ HSQC showing methyl carbon chemical shift changes (Y axis) of barnase plotted against various concentrations of ectoine from 0 mM to 1000 mM (X-axis). The chemical shift changes are on a scale going from -0.1 to +0.15 ppm.

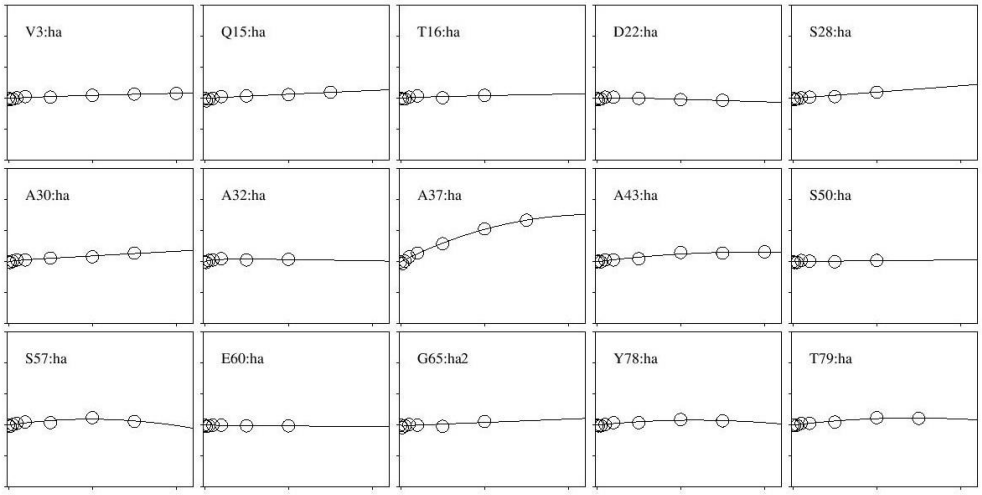

Figure 4.37. Data for K_d linefit of individual residues from $^{1}H^{13}C$ HSQC showing alpha (α) hydrogen chemical shift changes (Y axis) of barnase plotted against various concentrations of ectoine from 0 mM to 1000 mM (X-axis). The chemical shift changes are on a scale going from -0.0 to +0.15 ppm.

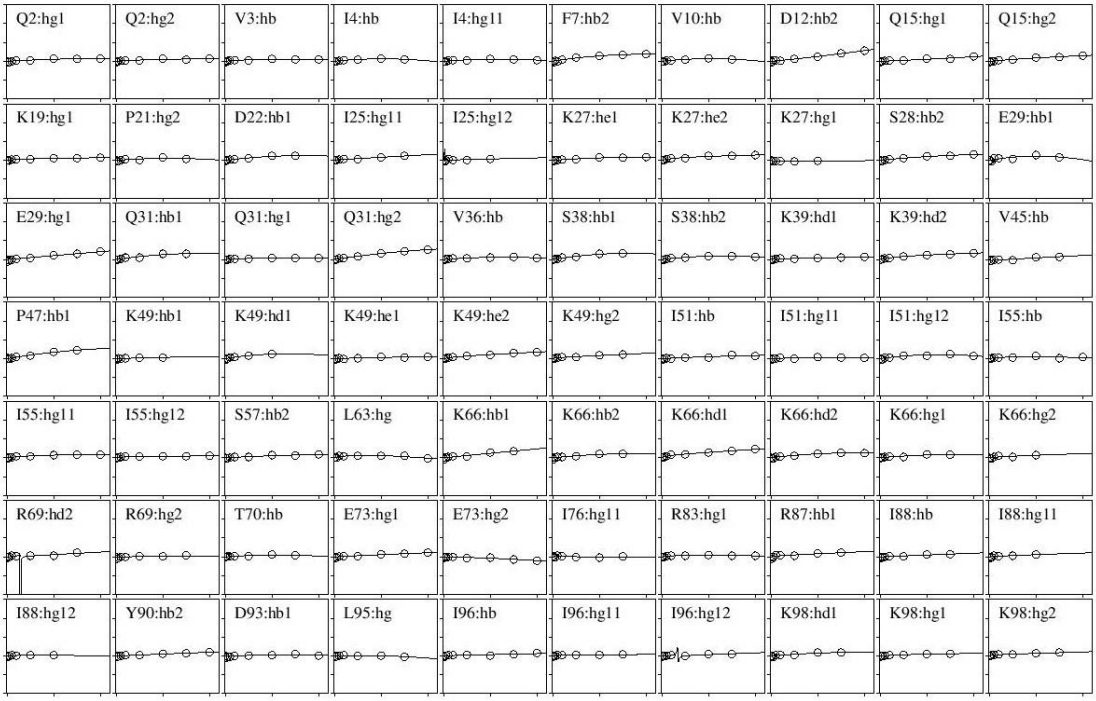

Figure 4.38. Data for K_d linefit of individual residues from $^{1}H^{13}C$ HSQC showing hydrogen (other than α) chemical shift changes (Y axis) of barnase plotted against various concentrations of ectoine from 0 mM to 1000 mM (X-axis). The chemical shift changes are on a scale going from -0.1 to +0.15 ppm.

4.6.4 Comparison of K_a values of different osmolytes

In this section the fitted binding affinities are discussed. A wide range of K_a values were observed.

Fitted affinities are meaningless if the shift change is very small, or if the fitted curve is almost linear. Therefore, we did not attempt to fit an affinity for a ^{1}H $\Delta\delta_{max}$ of between -0.03 and +0.03 ppm, or a ^{15}N or ^{13}C $\Delta\delta_{max}$ of between -0.06 and +0.06 ppm, or if K_d is between 5 – 900 mM. Any signals in this category were fit only to the straight-line Equation 4.1. Other signals were fitted using K_d linefit (Equation 4.2) to obtain m, K_d and $\Delta\delta_{max}$. For most purposes, it is convenient to treat binding affinities using the dissociation constant K_d, because it has units of concentration and therefore has an obvious interpretation as the concentration of ligand that leads to half of the binding sites being occupied. However, it is a confusing way of describing affinity because strong affinities have small values of K_d. Therefore, for example if one displays graphs of K_d for different residues, the most obvious data points are the largest K_d, which are the weakest and thus least important data. We therefore in this section describe the binding affinity in terms of the association constant K_a, which is the reciprocal of the dissociation constant. In this section K_a, are given in units of M^{-1}, which is actually 1000/ K_d when K_d is in mM. The big advantage of this is that a large K_a represents strong binding.

In the presence of TMAO, only 32 nuclei for H, 58 for N and 26 for C met the criteria for binding (Fig 4.39 and Table 4.6). There are a higher number of fitting nitrogen shifts than H or C, across osmolytes and Hofmeister series (Clare Trevitt's personal information). When the means of K_a values from individual shifts were compared it was found that nitrogen (mean K_a =19.0 M^{-1}) chemical shifts have slightly stronger K_a values than carbon (mean K_a =17.9 M^{-1}) and hydrogen shifts (mean K_a =15.5 M^{-1}), though these differences are not significant.

Table 4.6. Data showing mean K_a of various solutes.

Solute	Mean H K_a (M^{-1})	Number of nuclei that show binding affinity for H	Mean N K_a (M^{-1})	Number of nuclei that show binding affinity for N	Mean CO K_a (M^{-1})	Number of nuclei that show binding affinity for CO
TMAO	15.5 ± 13.1	32	19 ± 15.8	58	17.9 ± 13.8	26
Ectoine	3.2 ± 0.7	2	2.9 ± 3.3	11	11.3 ± 13.5	3
Betaine	-[a]	0	9.5 ± 10	2	-[a]	0
Sulfate	32.4 ± 29.2	27	29.8 ± 25.3	50	22.9 ± 23.2	41
Thiocyanate	30.7 ± 24	39	27.5 ± 25.1	63	24.2 ± 21.7	49
Chloride	8.6 ± 3.1	24	6.9 ± 5.7	53	7.8 ± 5.4	21

[a]No value is shown because no residues required fitting to a binding curve.

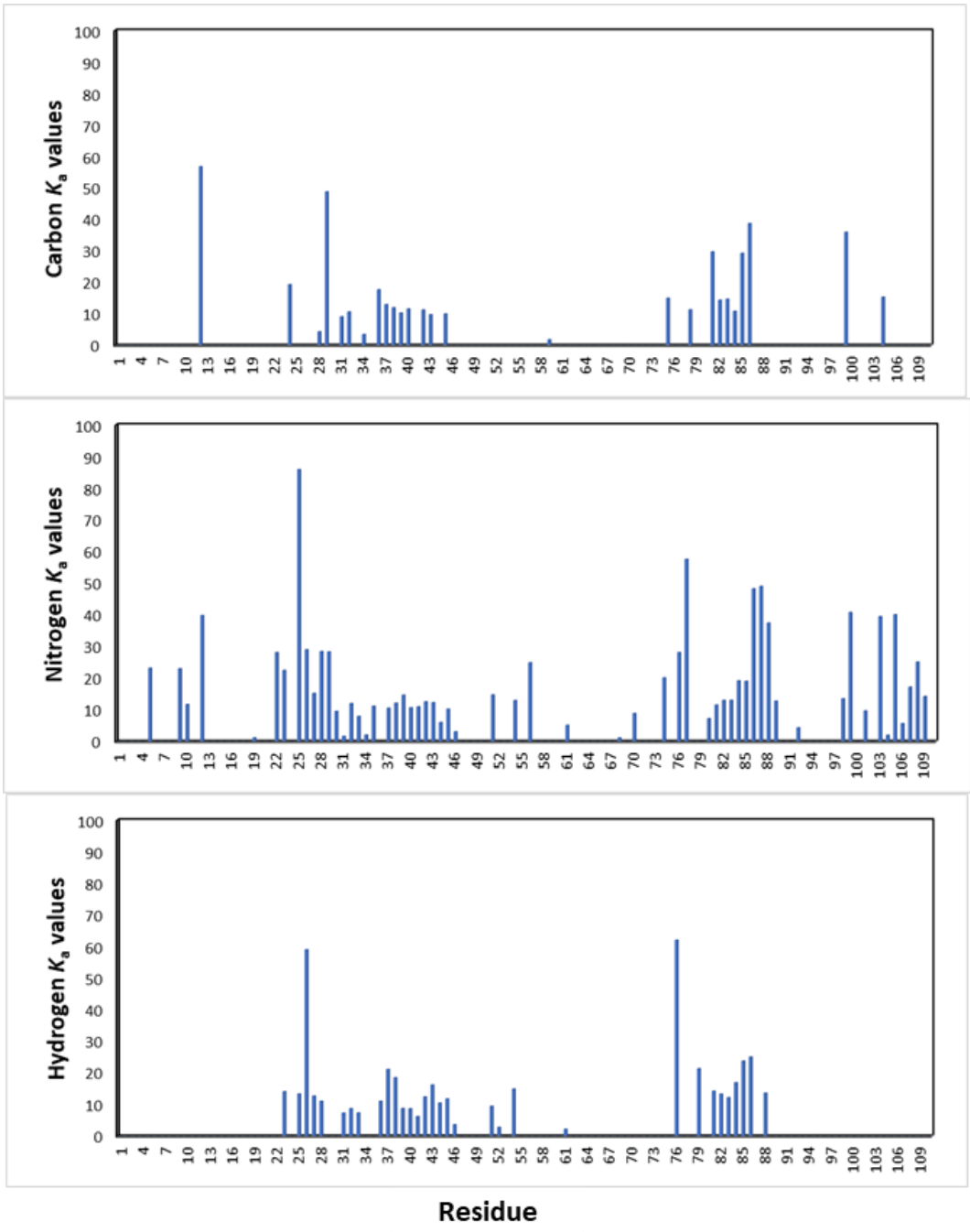

Figure 4.39. Comparison of K_a values from carbon, nitrogen, and hydrogen shifts for TMAO.

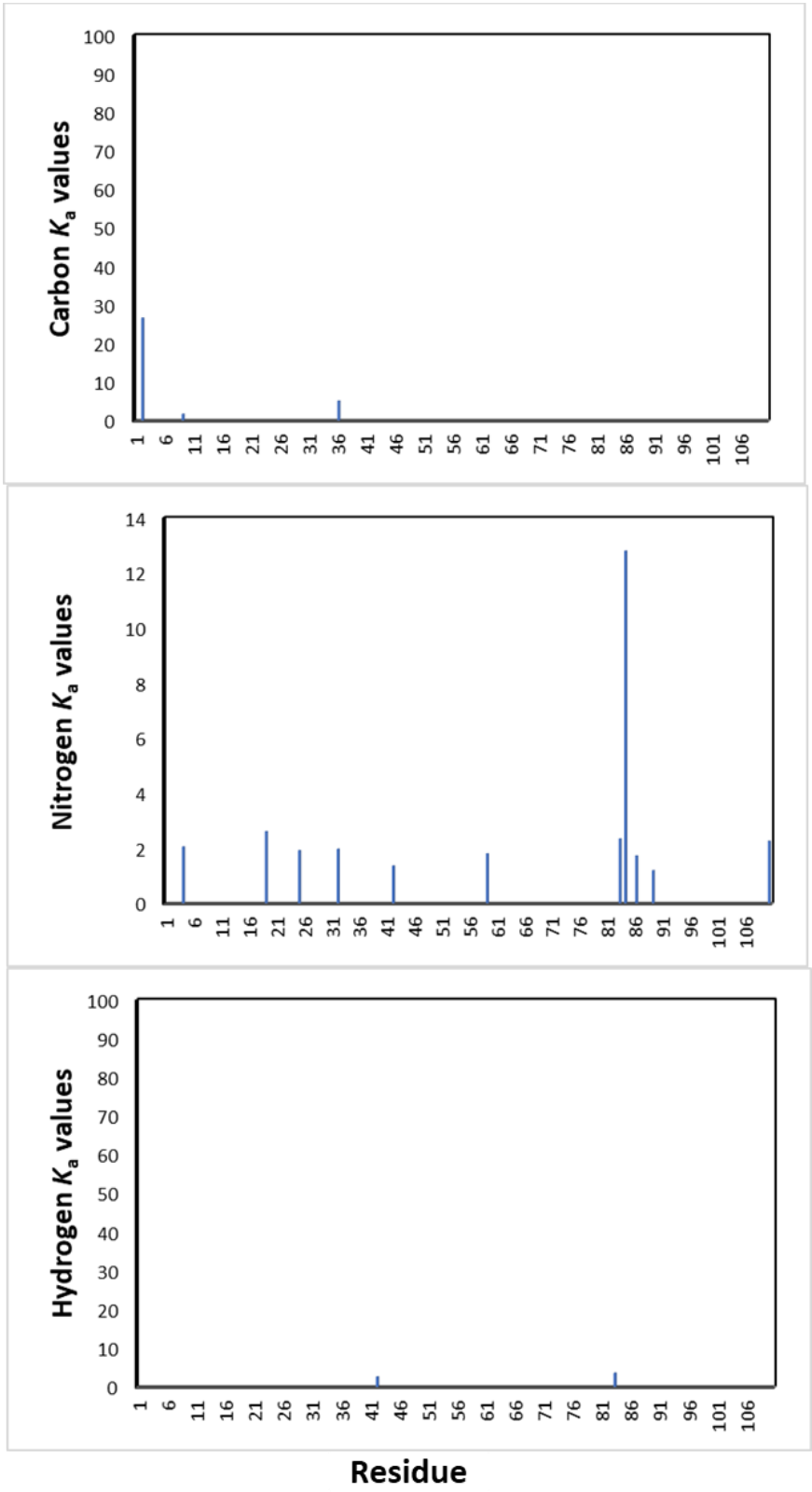

Figure 4.40. Comparison of K_a values from carbon, nitrogen, and hydrogen shifts for ectoine.

In the presence of ectoine only 2 nuclei for H, 11 for N and 3 for C show binding (Fig 4.40). Though there are a higher number of fitting nitrogen shifts than H or C, when the means of K_a values from individual shifts were compared it was found that carbon (mean K_a =11.3 M^{-1}) chemical shifts have stronger K_a values than nitrogen (mean K_a =2.9 M^{-1}) and hydrogen shift (mean K_a =3.2 M^{-1}). Again, the differences are not significant. These affinities are very weak, and about 3 times weaker than those for TMAO for hydrogen and nitogen. However, considering that many nuclei have not shown binding effects in hydrogen and carbon shifts it is better to conclude that ectoine binds very weakly than analysing which individual shift have better binding. In the presence of betaine only 2 nuclei for N show binding (Table 4.4). Considering that many nuclei have not shown binding effects in nitrogen shifts and not a single nucleus hydrogen and carbon shifts it is better to conclude that betaine does not bind.

When compared with Hofmeister series anions TMAO (H mean K_a =15.5 M^{-1}) binds stronger than chloride (H mean K_a =8.6 M^{-1}) but weaker than sulphate (H mean K_a =32.4 M^{-1}) and thiocyanate (H mean K_a =30.7 M^{-1}) as seen in Table 4.6. The number of nuclei that have shown binding effects in presence of TMAO (32 for H nuclei) are roughly the same as for Hofmeister anion sulphate (27 for H nuclei), thiocyanate (39 for H nucleie), and chloride (24 for H nuclei). This binding effect pattern is similar across the shifts. There is thus no clear difference in binding pattern between TMAO and the Hofmeister anions.

When we do a comparative analysis of K_a among different osmolytes and Hofmeister anions, ectoine does not have many residues to compare with other osmolytes and Hofmeister anions and betaine has almost no residues that bind. Hence, we can conclude that ectoine binds very weakly and betaine does not bind. In summary TMAO binds stronger than other osmolytes and chloride but weaker than sulphate and thiocyanate. Osmolytes have a clear influence on protein stability, but they clearly can do this without significant protein binding. This exclusion of residues after sorting them based on $\Delta\delta_{max}$ and further exclusion when selected based on their matching with other ions suggest that binding may not be necessary to cause chemical shift changes and effects of ions on protein is independent of their ability to bind.

4.6.5 Analysis of gradient values

There are two kinds of nuclei: ones that fit to the simple linear equation and those that do not fit the simple linear equation but fit the binding saturation curve. For those nuclei that do not have curved chemical shift changes, gradient values were selected from linefits, and for

those nuclei that have shown curved chemical shift changes, gradient values must be selected from K_d linefit graphs. Residues that are apparently fitting to linefit have either no binding or very strong or very weak binding. And those fitting to K_d linefit, fall in the K_d range 1 to 1000 mM. K_d values below 5 are ignored because they are due to fitting to a change in shift on the first addition of ligand and are probably not a genuine binding event. Large K_d are indistinguishable from a linear change, and ignoring these is better because shift changes like these should be treated as linear changes (ie using the m part). So only those nuclei that have K_d between 5 and 900 were considered. However, there are nuclei that have K_d between 5 and 900 but were difficult to believe to have a real K_d because their $\Delta\delta_{max}$ can be very small typically in the range of 0.01 – 0.015 across different residues. Hence these nuclei were sorted based on a combination of K_d and $\Delta\delta_{max}$ values. Anything with a ^{1}H $\Delta\delta_{max}$ of between -0.03 and +0.03, or ^{15}N and ^{13}C $\Delta\delta_{max}$ of between -0.06 and +0.06 were fit using linefit and for the rest of the nuclei, if K_d is between 5 – 900 and $\Delta\delta_{max}$ values were larger than the above specified values, then they were fit using K_d linefit. To do this selection nuclei must be sorted, and this is accomplished by Nawk scripts that were written to select the gradients on the combination of K_d and $\Delta\delta_{max}$.

These gradient values were used to view in *B*-factor putty mode in the barnase pdb file (1a2p_a) using python scripts. Gradients from individual nuclei (h, n, c) on the protein surface were analysed using pymol software. When analysed in this way as seen in Fig 4.28 both ectoine and TMAO have caused noticeable changes on the protein surface with gradients colored from blue (small) to red (biggest) depending on their size (Fig 4.41).

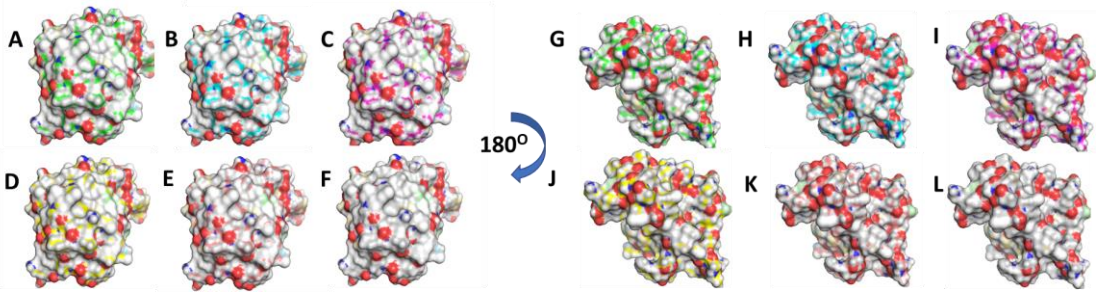

Figure 4.41. Gradients on protein surface observed using pymol: (A) TMAO proton. (B) TMAO nitrogen. (C) TMAO carbonyl. (D) Ectoine proton. (E) Ectoine nitrogen (F) Ectoine carbonyl. Gradients colored from blue (small) to red (biggest) depending on their size. Figures G-L are the 90° rotation of the corresponding figures of A-F.

The gradients have a wide spread of values, and little can be gained from looking at individual values, as shown above. Histograms of the gradients from all the three H, N, CO shifts of osmolytes and Hofmeister ions like sulphate, chloride and thiocyanate ectoine (Clare Trevitt's personal information) were made to study the similarities with respect to effects on chemical shift change on barnase as seen in Table 4.7 and Figure 4.42. Gradients were divided into bin size of 10 and the frequency of each bin was plotted. Gradient data for L42 and R83 is removed for all the osmolytes and Hofmeister anions while making histograms and calculating mean gradient values since they give enormously big gradient values compared to other nuclei and it also means extending bin sizes with many empty bins in between. Gradient data for Hofmeister series anions is collected from Bye et al., 2016 and Clare Trevitt's personal information.

Table 4.7. Mean values of amide proton gradients for various solutes in ppb/M

TMAO	Ectoine	Betaine	SCN	Sulphate	Chloride
9.7 ± 16.9	16.5 ± 21.3	4.3 ± 15.9	-50.7 ± 51.4	7 ± 21.8	-15.6 ± 25.8

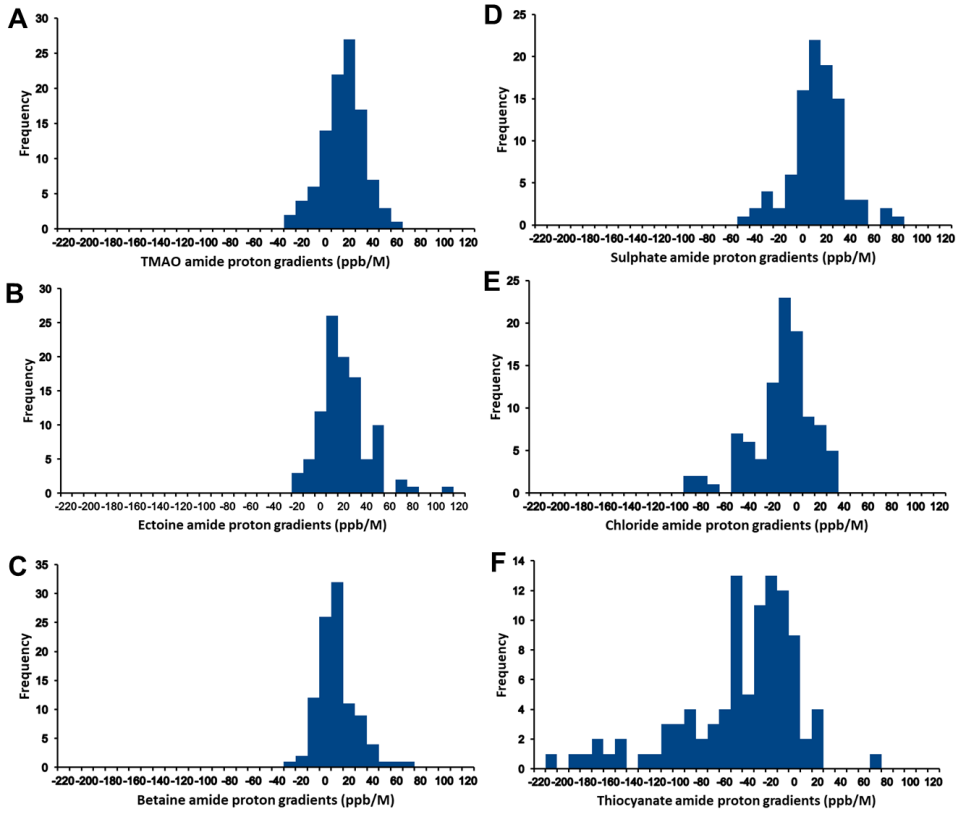

Figure 4.42. Histogram of gradients of amide protons of various solutes: (A) TMAO. (B) Ectoine. (C) Betaine. (D) Sulphate. (E) Chloride. (F) Thiocyanate

Gradients of residues are mostly between -40 to 80 ppb/M for all the three osmolytes. The highest frequency of gradients (i.e., the modal gradient) for betaine and ectoine are at gradient bin of 0 – 10 and for TMAO 10 – 20. Mean amide proton gradients of all the three osmolytes are in the range of 4 to 17 ppb/M and are not significantly different from each other with betaine having the smallest and ectoine largest mean gradient values. In contrast, the mean amide proton gradients of Hofmeister series are in the range of -50 to 7 ppb/M and are significantly different from each other with thiocyanate having the smallest and sulphate the largest mean gradient values. The average magnitude of the gradients gives information on how they order water molecules (chaotrope and kosmotrope). The mean gradient values of osmolytes are similar to sulphate (mean = 7 ppb/M), with TMAO (9.7 ppb/M) being very similar to sulphate.

Gradients from all the three H, N, CO shifts of osmolytes TMAO, ectoine and betaine were plotted on scatter plots to study the correlation against each other and to that of Hofmeister ions like sulphate, chloride and thiocyanate (Clare Trevitt's personal information) to study the similarities with respect to effects on chemical shift change on barnase as seen in Figure 4.43 and Tables 4.8 – 4.10. For correlation plots only those residues that are in common between ions that were being compared to are selected using nawk programming scripts. A slightly better correlation was found for proton and nitrogen shifts and poor for carbonyl chemical shifts.

Table 4.8. R^2 values from comparison of amide proton gradients of various solutes. NA- Not applicable.

	TMAO	Ectoine	Betaine	SCN	Sulphate	Chloride
TMAO	NA	0.4	0.42	0.12	0.13	0.55
Ectoine	0.4	NA	0.86	0.02	0.14	0.22
Betaine	0.42	0.86	NA	0.01	0.14	0.15

Table 4.9. R^2 values from comparison of amide nitrogen gradients of various solutes. NA- Not applicable.

	TMAO	Ectoine	SCN	Sulphate	Chloride
TMAO	NA	0.5	0.07	0.11	0.13
Ectoine	0.5	NA	0.01	0.04	0.07

Table 4.10. R^2 values from comparison of amide carbon gradients of various solutes. NA- Not applicable.

	TMAO	Ectoine	SCN	Sulphate	Chloride
TMAO	NA	0.22	0.11	0.16	0.25
Ectoine	0.22	NA	0.11	0.11	0.08

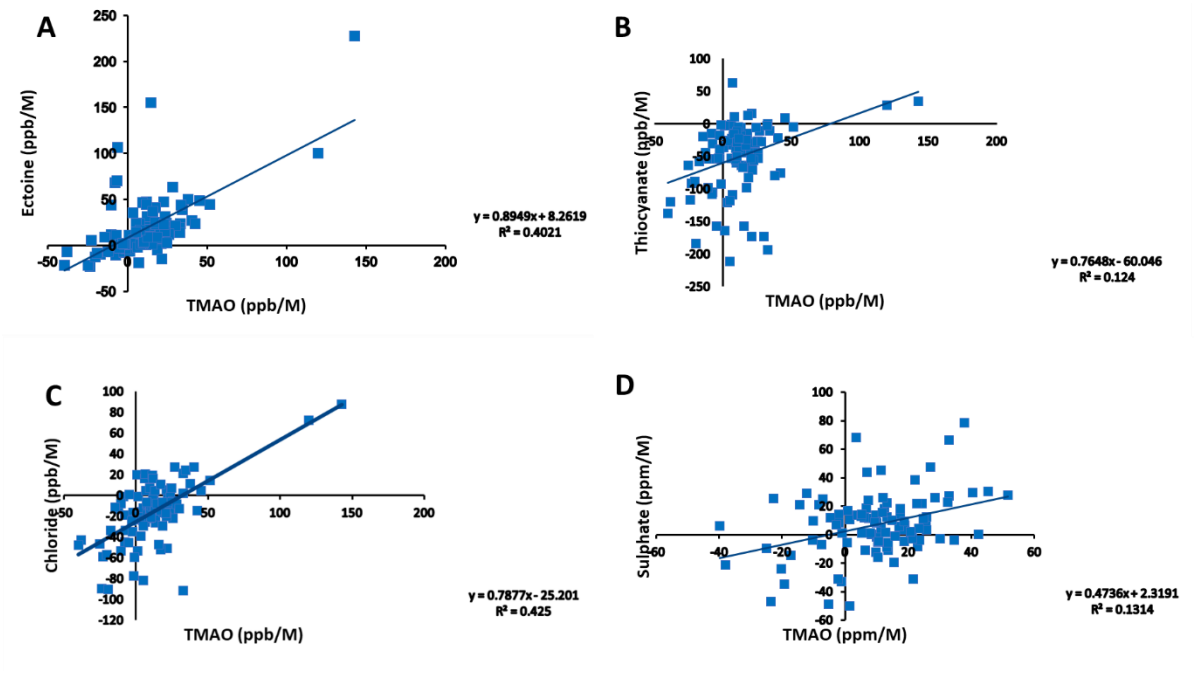

Figure 4.43. Comparison of gradients of amide protons for different solutes: (A) ectoine vs TMAO. (B) thiocyanate vs TMAO, used as an example of a Hofmeister ion. (C) chloride vs TMAO, used as an example of a Hofmeister ion. (D) sulphate vs TMAO, used as an example of a Hofmeister ion.

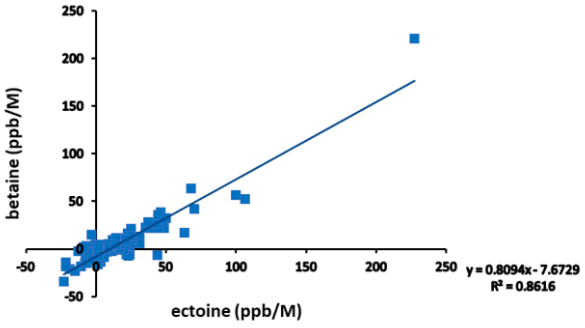

Figure 4.44. Comparison of gradients of amide protons for betaine vs ectoine.

Gradients for osmolytes when compared against Hofmeister ions generally gave very poor correlation values except for proton gradients for TMAO and chloride, while it is much

poorer in the case of nitrogen and carbon. This analysis has already removed any effects from direct solute/protein binding on the shifts, so all the effects seen here must arise from perturbation of water by the solutes. If the only effect that osmolytes cause on the protein chemical shift is via an effect on bulk solvent – ie, if all the solute does is to act as a chaotrope or a kosmotrope and make bulk water either less or more ordered - then the correlation coefficients would be close to 1. So presumably the reason they are not is that the solute does have an indirect (water-mediated) effect – complicated interactions such as second hydration sphere effects etc, in which a solvated solute interacts with a solvated protein. N and C shift changes have a stronger geometrical dependence than H shifts which might be the reason why correlations are worse for N and C (Williamson, 2013). The highest correlation of gradient values observed for an osmolyte against a Hofmeister series ion is for TMAO against chloride ($R^2 = 0.55$) as shown in Table 4.8 and Figure 4.43. This might also mean TMAO, and chloride have the smallest second hydration sphere effects, ie have least effect on the long range ordering of water molecules. It is also probably significant that of the three Hofmeister ions, chloride is the one that binds least well to the protein, implying that protein binding acts to obscure Hofmeister effects. This is also evidenced by the fact that the best correlation is between ectoine and betaine ($R^2 = 0.86$), the two cosolutes that bind most weakly to barnase as shown in Table 4.8 and Figure 4.44. The work carried out by Clare Trevitt suggests that sulphate and thiocyanate bind in an extended binding site spread out across the surface of the protein, and therefore that there is not a single well-defined binding site but rather that the bound ion diffuses around on the surface. It would therefore be reasonable to suppose that the more tightly binding ions (sulphate and thiocyanate) may also have more indirect interactions via a solvated ion, explaining why chloride has a better correlation of gradients with the osmolytes, because theh solvated chloride ion associates with the protein less than do sulphate and thiocyanate.

4.6.6 Analysis of buried and exposed residues

Gradient data from osmolytes were segregated into buried and exposed residues to study the similarities with respect to effects on chemical shift change on barnase and were analysed for H shifts through a histogram. As discussed above, shifts of N and C are too noisy to make such an analysis useful.

Proton surface area was calculated on pymol to identify the residues as buried and exposed. Proton surface area values were plotted on a scatter plot against their attached nitrogen

surface area (previously calculated using naccess by Bye et al., 2016 and Clare Trevitt's personal information). When calculated the average proton area for exposed nitrogens was7.3 ± 1.4 Å, and for buried nitrogens it was 4.6 ± 1.0 Å. The halfway value between was 6. So, all protons with solvent exposed surface area of less than 6 were considered as buried, and the others as surface exposed. Gradients from buried and exposed residues were separately analysed for H shifts of each osmolyte as a histogram as seen in Figure 4.45. In the preparation of Figure 4.45, gradients were divided into bin sizes of 10 ppb/M and the frequency of each bin is plotted.

To study if there is any similarity in pattern of the buried and exposed residues, gradients from buried residues of all the three osmolytes were also grouped and plotted as a histogram. A similar thing is done for exposed residues as seen in Figure 4.46. Gradients of buried residues are mostly between -40 to 60 ppb/M for all the three osmolytes. The highest frequency of gradients for betaine and ectoine are at a gradient bin of 0 – 10 and for TMAO 10 – 20 which is similar to data before segregation. Gradients of exposed residues are mostly between -40 to 80 ppb/M for all the three osmolytes. There is some difference in the distributions of buried and exposed protons, with the exposed protons having a wider distribution and slightly more positive gradients, but the differences are not great and do not look to be significant.

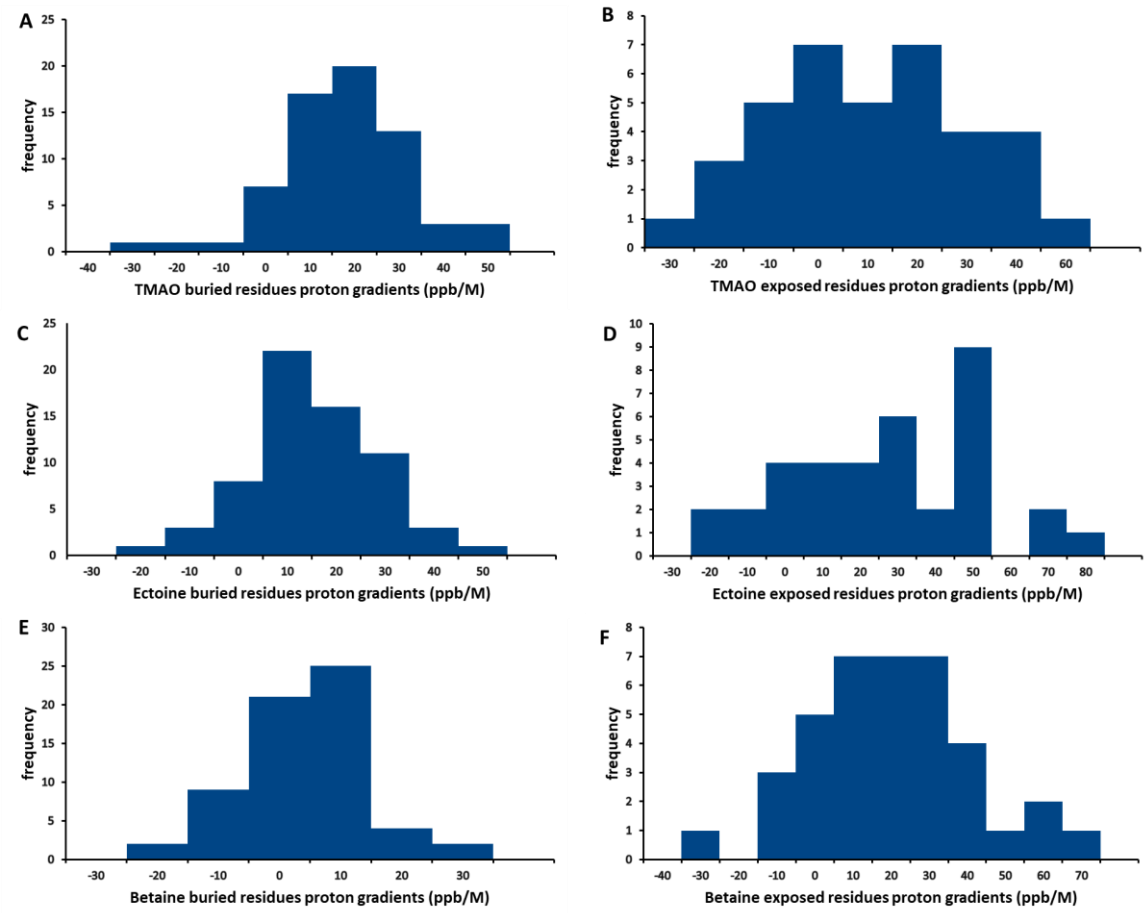

Figure 4.45. Histogram of buried and exposed residues - amide proton gradients for various osmolytes. (A) TMAO buried. (B) TMAO exposed. (C) Ectoine buried. (D) Ectoine exposed. (E) Betaine buried. (F) Betaine exposed.

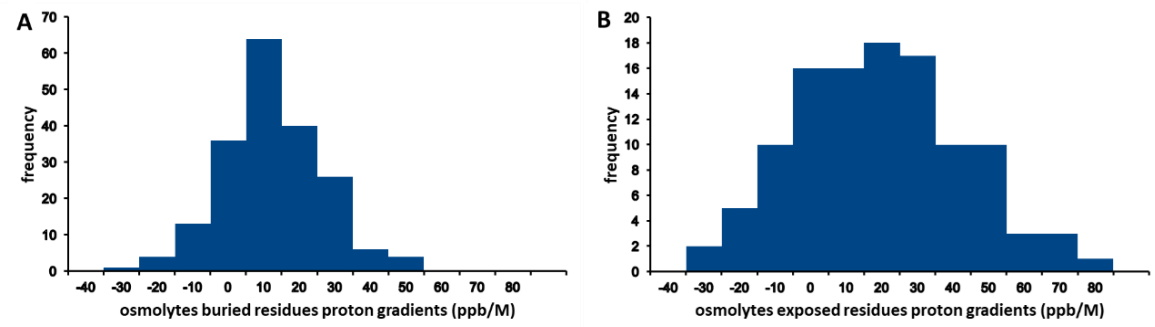

Figure 4.46. Histogram of amide proton gradients of osmolytes (combined data of TMAO, ectoine and betaine). (A). buried residues. (B). exposed residues.

To study if the buried residues were affected similarly across all the osmolytes, scatter plots for buried residue gradients were plotted and R^2 values were calculated to get exact correlation between osmolytes. The same was also done for the exposed residues. Amongst

buried residues no correlation was found for TMAO against ectoine or betaine, but good correlation was found between betaine and ectoine. Amongst exposed residues good correlation (R^2 =0.5 – 0.86) was found between exposed residues of one osmolyte with another.

However, no osmolyte has any correlation with any of the Hofmeister anions except for exposed residues of TMAO with chloride.

In summary, analysis of histograms and scatter plots suggests that exposed residues of osmolytes behave similarly. However, buried residues behave differently across osmolytes which is a surprise as there is no strong binding effect on protein by osmolytes.

4.6.7 Two-stage effect of osmolytes on barnase stability

TMAO has a two-stage effect on barnase. In the first stage TMAO binds to protein at smaller concentrations, typically less than 100 mM, and at higher concentrations no further binding is observed. TMAO interacts with the amide unit of the peptide backbone as seen in N HSQC results which gives the impression that in the mixed osmolyte solutions of TMAO plus urea, TMAO may offset protein inhibitory effects of urea by interactions with peptide backbone.

In the second stage, no further binding of osmolytes with protein is observed. At higher concentrations above 100 mM and up to 1000 mM, osmolytes could be affecting the bulk water. We hypothesise that TMAO, like sulphate, organises water molecules around itself, thereby depriving the protein of water (Bye et al., 2016). This water withdrawing effect of osmolytes can be related to their hydration strength (Jungwirth and Cremer, 2014). As the salt concentration increases, more and more water are organised around the ion and protein has to compete with the osmolyte for the water. This competition between protein and stabilising ions is explained in Franz Hofmeister's experiments on water absorbing ability of the ions (Kunz et al., 2004). This deprivation of bulk water decreases the ability of protein to interact with the water in the presence of kosmotropes.

Ectoine surprisingly did not interact much with the protein except for a few residues, and betaine shows no evidence at all of binding. From the DSC studies we have established that ectoine has slight destabilising effects on barnase. Destabilising ions are known to poorly organise the water molecules (Bye et al., 2016). Destabilising ions decrease the hydrogen bonding in the bulk water which allows the water to interact more with the protein surface.

From the DSC studies as discussed in the earlier chapter, destabilising ions reduce the $\Delta\Delta G(T_m)$ thereby destabilising the protein. This increased interaction of bulk water with the protein surface in presence of ectoine and the decrease of $\Delta\Delta G(T_m)$ increases the solubility and decreases the stability like chaotrope thiocyanate.

4.7 Discussion

Study of the chemical shift change data from $^{1}H^{15}N$ HSQC, $^{1}H^{13}C$ HSQC, and 2D-HNCO experiments clearly shows that TMAO and (to some extent) ectoine have two different effects which we call a two-stage effect: a direct binding interaction (i.e., a saturation curve), and a linear change in shift proportional to the concentration of osmolyte, characterised by the gradient. In the case of ectoine, binding to the protein backbone is negligible at concentrations less than 0.1 M and for most residues there is only a linear change in shift characterised by the gradient up to 1 M. Betaine doesn't have a two-stage effect but just a linear change in shift proportional to the concentration from 0 M to 1 M.

Importantly, the gradients induced by TMAO, ectoine and betaine are like sulphate of Hofmeister series as seen in Table 4.6. Analysis of buried and exposed residues suggests exposed residues behave similarly across osmolytes, but buried residues behave differently which is a surprise as there is no strong binding effect on protein by osmolytes.

Analysis of K_a values indicates that TMAO binds more strongly to the protein surface than ectoine. Missing K_a values in many residues of ectoine compared to TMAO further strengthens the argument that ectoine binds weaker than TMAO on protein surface. Analysis of K_a values indicates that only TMAO amongst the three studied osmolytes in this study binds to protein, ectoine binds very weakly and betaine does not bind. TMAO binds more strongly to the protein surface than ectoine and chloride but not as strong as ions at the extremes of the Hofmeister series. The observation that two out of the three osmolytes do not bind significantly suggests that osmolyte function does not require binding to the protein surface. Because the osmolytes produce similar gradients to sulphate but have different effects on stability between themselves and also in comparison to sulphate, this raises the possibility that binding to the protein does have an effect on stability, even though the binding is weak.

Betaine did not interact much with the protein except for a few N shift nuclei and this was probably due to its inability to organise the water molecules around itself at the higher concentrations like thiocyanate of Hofmeister series. Mean gradient values and mean K_a of betaine are the smallest amongst osmolytes.

Analysis of scatter plots of gradients and data from K_a values gives an interesting observation that correlation between one solute and another is dependent on how strongly they bind to the protein surface (Figures 4.43, 4.44 and Table 4.6). Our data segregates osmolytes and Hofmeister anions into three categories based on their binding affinities, those that bind strongly (sulphate, thiocyanate), those that bind moderately (TMAO, chloride) and those that bind weakly/no binding (ectoine, betaine). TMAO and chloride bind moderately to protein surface hence they both have good correlation between them. TMAO and weakly binding ectoine also have correlation between them. Ectoine and betaine do not bind, so they too have good correlation between them (in fact the best correlation of any pair of solutes, by some considerable margin). Whereas no correlation was found between any of the osmolytes (TMAO, ectoine, betaine) and sulphate or thiocyanate because unlike osmolytes, thiocyanate and sulphate bind strongly to protein surface at lower concentrations. In summary good correlation is found between those osmolytes and Hofmeister anions that have similar binding affinities. This further suggests that binding may be an important factor in the effect of solutes on proteins.

Stabilizing ions (like sulphate in the Hofmeister series) are widely agreed to organise water molecules around themselves, which makes water dipoles less available, outcompeting the protein, and strengthening the intramolecular interactions in the protein. It is also suggested that the presence of TMAO increases the hydrogen bonding in the water molecules thus reducing the interaction of water with the protein (Zou et al., 2002). Molecular dynamic simulation studies on the effect of TMAO and urea on neopentane molecules also reveal that water-water hydrogen bond lifetime increases in the presence of TMAO (Sarma and Paul, 2011). Thus, we conclude that TMAO probably is one such solute with strong hydration that competes with protein to interact with water. TMAO enhances water structure and reduces entropy in water molecules leading to increase in protein stability (Zou et al., 2002).

Since no increased direct binding of TMAO with protein is observed at the higher concentrations, and TMAO interacts with the protein surface and backbone only at concentrations less than 100 mM, it must be organising the water molecules around itself as suggested from the linear change in chemical shift of barnase from the NMR experiments. Molecular dynamics simulation studies indicate TMAO increases greater spatial and long-range ordering and better organizes water molecules around itself leading to an increase of hydrogen bonding in water molecules compared to urea which poorly orders water molecules with decreased hydrogen bonding (Zou et al., 2002). MD simulations studies also revealed

that TMAO makes a few direct interactions by means of hydrogen bonding with lysine and arginine side chains which order water molecules and prevent water and urea from interacting with water. However, a major mode of action is indirect interactions through which it stabilizes protein by ordering water molecules around itself and thereby preventing solvent hydrogen bonding leading to an increase in the strength of intra protein hydrogen bonds. This counteracts denaturants like urea which compete with water molecules for intra molecular hydrogen bonding with the protein. By doing so, TMAO keeps the protein fold intact and the protein stable.

The results of Kumar and Kishore, 2013 also indicate that interaction of betaine with water increases in the urea plus betaine mixture and results in the exclusion of betaine from the protein surface. The strengthening of individual hydrogen bonding between water molecules is related to the protein stability (Paul and Patey, 2007; Zou et al., 2002). There is an argument that the exclusion of osmolytes from the protein surface increases the stability of the protein (Bennion and Daggett, 2004; Kumar and Kishore, 2013; Shimizu and Smith, 2004; Timasheff, 2002; Wei et al., 2010; Zhang et al., 2012). The preferential interaction model and volume excluded model of protein stability have been disproved and a refined structure maker/breaker theory was proposed earlier by (Bye et al., 2016; Bye et al., 2014) that explains the effects of solutes based on the water withdrawal ability of stabilizing ions.

Gradient analysis suggests that osmolytes behave similarly to that of Hofmeister series anion sulphate but without strongly interacting with protein as indicated by the analysis of K_a values. At this stage it looks like osmolytes affect the protein structure by modulating water potential without directly interacting with the protein, which also suggests that perhaps direct binding between excipients and protein is not mandatory to affect the structure and stability. This conclusion agrees with (Zalar et al., 2020), who note that binding of excipients to protein is not a good predictor of stability and solubility. The hypothesis presented here is in line with the refined structure maker/breaker theory and further strengthens it. Since no strong direct binding is found between osmolytes and protein, and with osmolytes still able to affect the protein stability as the DSC data suggests, it leaves us only one more question - whether osmolytes directly interact with denaturant and stabilise the protein? To solve this, we need to study the osmolyte interaction with urea which will be discussed in the next chapter. If osmolytes do not interact with denaturant (urea) also then it only strengthens the argument that osmolytes like Hofmeister anion sulphate modulates the water structure and affects the protein stability.

5 CHAPTER 5: OSMOLYTE INTERACTIONS WITH UREA

5.1 OBJECTIVE

In the previous chapter, the effect of osmolytes on the protein barnase was studied by NMR, and the results suggested that TMAO binds weakly to the protein surface at concentrations less than 0.1 M, and ectoine and betaine mostly do not bind to the protein surface at all. This result implies that ectoine and betaine (and thus presumably all osmoytes) do not work primarily by binding directly to the protein surface. In which case, if osmolytes can counteract the effect of denaturants, do they do this by direct interaction with the denaturant, or indirectly by interactions with water? Hence, we wanted to explore if osmolytes interact directly with the protein denaturant instead of protein surface and thereby counteract the denaturants. So, we came up with the work in this chapter where interaction of osmolytes with the denaturant urea was studied. Since these experiments were primarily conducted to study the interaction between osmolytes (TMAO, ectoine, betaine) and urea, barnase was absent in these experiments. Since the volume of titrant added at each step is small, pH changes are very small (<0.05), hence all the solutions (buffer, urea, osmolytes) were maintained at the same pH of 5.8 (unlike barnase titrations where TMAO and betaine had to be prepared at a pH 0.2 more than barnase) after confirming with dummy experiments. Standard NMR spectra of osmolytes (without urea) were also run to differentiate the changes in chemical shift of osmolytes in the presence and absence of osmolytes.

5.1.1 Data fitting

TMAO-urea chemical shift data was fitted to a binding saturation curve to measure binding affinity between urea and TMAO.

$$\Delta\boldsymbol{\delta} = \left(\frac{\Delta\boldsymbol{\delta_{max}}\times[\boldsymbol{L}]_{\boldsymbol{i}}}{\boldsymbol{K_d}+[\boldsymbol{L}]_{\boldsymbol{i}}}\right) + \boldsymbol{m}[\boldsymbol{L}]_{\boldsymbol{i}} \qquad \textbf{(eq 5.1)(Bye et al., 2016)}$$

Where $\Delta\delta$ is change in chemical shift, m is the gradient for linear chemical shift change, $\Delta\delta_{max}$ is the maximum change in chemical shift after saturation, K_d is the dissociation constant, and $[L]_i$ is the total concentration of ligand at titration point *i*, and m is the gradient. This equation is a sum of linear chemical shift change plus anion binding.

K_d values fall in the range between 5 and 1000 mM for TMAO-urea titration, their $\Delta\delta_{max}$ values are -0.1 to 0.005 ppm for TMAO and urea in TMAO-urea titrations. However, error on $\Delta\delta_{max}$ values are two times bigger than the $\Delta\delta_{max}$ value itself. Hence, they are difficult to consider real and K_d values are difficult to believe for TMAO.

Ectoine and betaine data do not fit to the binding curve equation because changes are too small and cannot be fitted with any reliability. However, they could be fitted to a simple linear equation.

5.2 RESULTS

5.2.1 TMAO – Urea interactions

^{1}H NMR experiments were carried out to study urea-TMAO interactions. 1D proton spectra of 20 mM urea were recorded in the presence of increasing concentrations of TMAO from 0 to 100 mM as shown in Figure 5.1. Separate ^{1}H NMR standard spectra of TMAO were also recorded to compare the changes in chemical shift of TMAO in the absence of urea as well. To rule out any interaction of TSP (which is used as reference) with osmolytes, it was taken in a capillary tube instead of directly adding to the solution and this capillary tube was carefully inserted in the NMR tube.

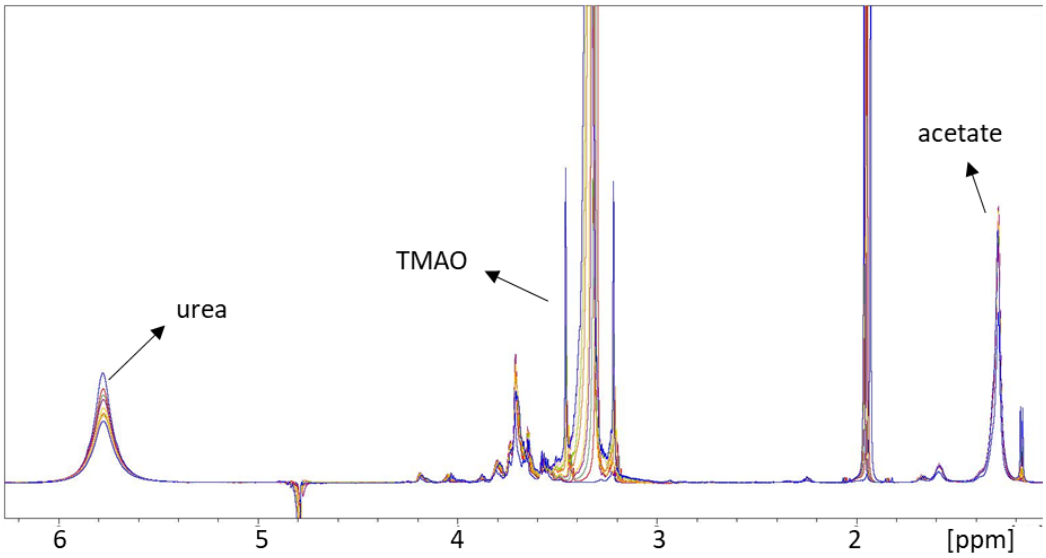

Figure 5.1. Spectra from ^{1}H NMR experiments showing proton peaks of 20 mM urea in the presence of varied concentrations of TMAO from 0 mM to 100 mM.

Table 5.1. Data from ^{1}H NMR showing change in chemical shift ($\Delta\delta$) values of various solutes.

TMAO conc (mM)	20 mM urea in presence of varying TMAO	Varying TMAO in presence of 20 mM urea	Varying TMAO without urea	5 mM actate
0	0	0	0	0
5	0.0017	0	0	-0.0145
10	0.0031	-0.0106	-0.0118	-0.0208
15	0.0029	-0.0183	-0.0172	-0.0251
20	0.0039	-0.0232	-0.0216	-0.0277
40	0.0032	-0.0323	-0.029	-0.0317
60	0.0037	-0.0356	-0.0328	-0.0322
80	0.0036	-0.0375	-0.0341	-0.0322
100	0.0028	-0.0385	-0.0353	-0.0317

Table 5.2. Data from 1H NMR showing gradients (m), dissociation constant (K_d), error values on m and K_d, and their associated chi-squared values of various solutes.

Solute	m (ppb/M)	m error	$\Delta\delta_{max}$	$\Delta\delta_{max}$ error	K_d (mM)	K_d error	χ^2
20 mM urea in presence of varying TMAO	-21.4	309.4	0.01	0.0	8.6	109.9	0.0
Varying TMAO in presence of 20 mM urea	461.3	1981.9	-0.15	0.6	82.3	248.9	0.6
Varying TMAO without urea	298.8	1408.4	-0.10	0.3	62.0	180.5	0.5
5 mM acetate	74.9	325.7	-0.04	0.0	9.5	16.2	0.0

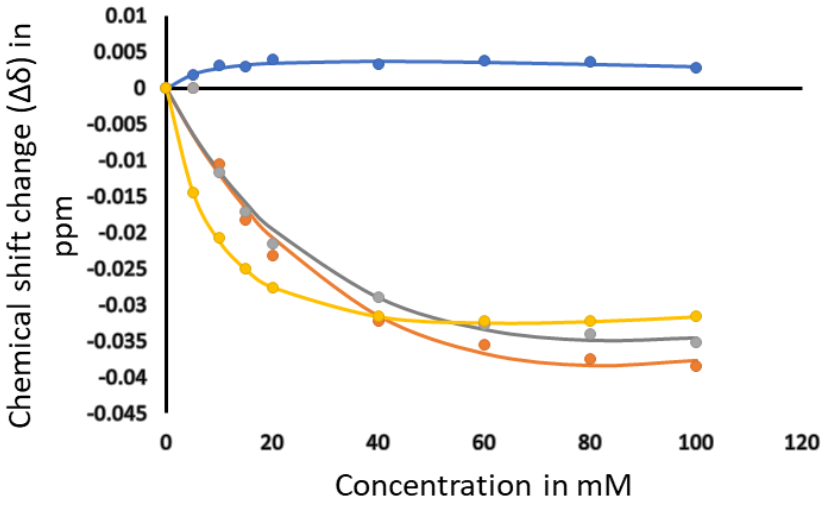

Figure 5.2. Data from ^{1}H NMR showing proton chemical shift changes (Y axis) of various solutes. A. Proton chemical shift of urea (urea concentration maintained constant at 20 mM in the presence of varying concentrations of TMAO from 0 mM to 100 mM) (blue). B. Proton chemical shift of TMAO (TMAO concentration varied from 0 mM to 100 mM in the presence of 20 mM urea (orange). C. Proton chemical shift of varied concentrations of TMAO from 0 mM to 100 mM without urea (grey). D. Proton chemical shift of 5 mM acetate (yellow). For all curves, round symbols are actual data and smooth curve is the fitted data.

As the concentration of TMAO was increased, in solutions containing just TMAO and 5 mM acetate, the chemical shift of TMAO changed by up to -0.035 ppm (Figure 5.2, grey symbols and table 5.1). In the solution containing TMAO and 20 mM urea, as the concentration of TMAO was increased from 0 mM to 100 mM, the chemical shift changes of TMAO changed by up to -0.039 ppm which is not much different from chemical shift change of TMAO from the solution containing just TMAO (without urea) i.e., -0.0353 ppm as seen in Table 5.1 and

Figure 5.2, yellow symbols. The similarity in chemical shift titration of TMAO in the presence and absence of urea indicates that the presence of urea is not making any difference to the chemical shift of TMAO: in other words, the spectra indicate that there is no interaction between TMAO and urea at 20 mM. Urea was used at concentration of 20 mM only and not at higher concentrations because the aim of the experiment was to study the effects of increasing concentrations of TMAO against urea and hence urea at 20 mM and TMAO at increasing concentrations of 0 to 100 mM was still 5 times the concentration of urea. Also, to be noted here is the chemical shift change of acetate (-0.0317 ppm) from acetate buffer used in the sample preparations which is not too different either from that of TMAO (fig 5.2). Urea peaks also did not move much in the presence of TMAO, showing only a small chemical shift change of 0.0028 ppm.

All the data was fit to equation 5.1 and the fitted line passes reasonably well through the symbols (Fig. 5.2). The chemical shift changes are all small, but real. The NMR data show a chemical shift change for TMAO alone, which can be fitted to a binding curve, with a fitted K_d of 82.3 mM, as seen in Table 5.2.

The chemical shift of TMAO is a chemical shift change of the TMAO signal relative to the TSP. TSP was placed in a capillary tube inside the NMR tube to rule out any interaction of TSP with TMAO.

Why does the TMAO signal move as its concentration increases? The obvious explanation is that there is self-association of TMAO, implying that the fitted K_d of 82.3 mM is actually a self-association constant, or dimerization constant. This seems reasonable. TMAO has zero net charge, but a fairly strong electric dipole, and has three hydrophobic methyl groups, so both hydrophobic interactions and dipole-dipole interactions could be involved. This is a reasonably strong dimerization constant, but very small chemical shift changes. If the dimer had a fixed structure (for example, with the two N^+-O^- dipoles aligned) then one would expect much larger chemical shift changes. It is therefore likely that the dimer has very variable geometry, giving rise to extensive chemical shift averaging and thus small chemical shift changes overall.

If this explanation is correct, and the chemical shift changes for TMAO are due to self-association, then why does the chemical shift of acetate change? Again, there is more than one

explanation but the most reasonable is that there is some interaction between acetate and TMAO. The fitted K_d is 82.3 mM (Table 5.1). This is of the same order of strength as the interactions between protein and ions such as sulphate, chloride, or thiocyanate (C. Trevitt, personal communication), so this seems reasonable.

The reason for carrying out this study was to look for interactions between TMAO and urea. Here the evidence is clear – there is no effect of TMAO on urea, and no interaction, because there are no chemical shift changes to urea on adding TMAO, and the chemical shift changes of TMAO in the presence of urea are identical to those without urea present (Figure 5.2, grey line).

Therefore, from this study we can conclude that there is a self-association of TMAO in water, with a dimerization constant of about 82.3 mM, and an interaction between TMAO and acetate with a K_d of about 62 mM, but that there is no detectable interaction between TMAO and urea.

5.2.2 Ectoine-urea interactions

A similar set of experiments was carried out to investigate interactions between ectoine and urea. ^{1}H NMR experiments were carried out to study the urea-ectoine interactions, and 1D proton spectra of urea were recorded in the presence of increasing concentrations of ectoine from 0 mM to 100 mM as seen in Figure 5.3. Separate ^{1}H NMR standard spectra of ectoine were also recorded to compare the changes in chemical shift of ectoine in the absence of urea as well.

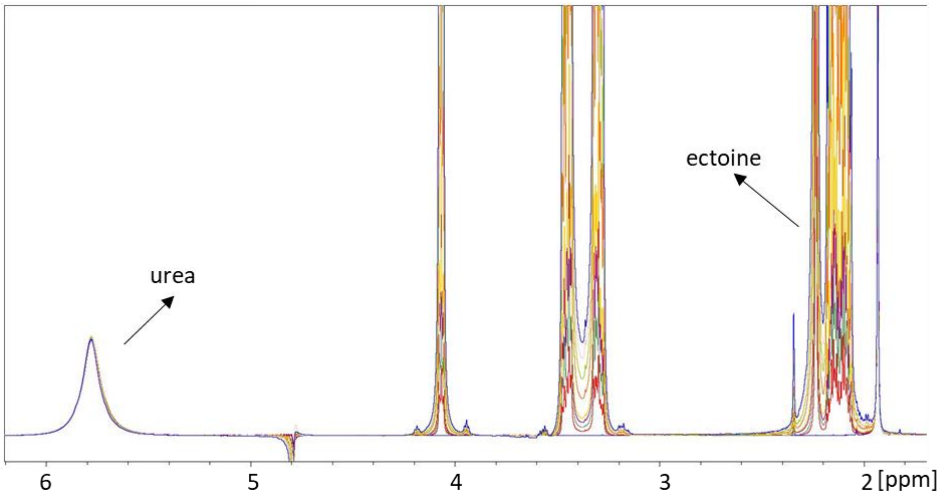

Figure 5.3. Spectra from 1H NMR experiments showing proton spectra of 20 mM urea in the presence of varied concentrations of ectoine from 0 mM to 100 mM.

Table 5.3. Data from 1H NMR showing change in chemical shift (Δδ) values of various solutes.

Ectoine con in mM	20 mM urea in presence of varying ectoine	Varying ectoine in presence of 20 mM urea	Varying ectoine without urea	5 mM actate
0	0	0	0	0
5	0.0005	0	0.0000	0.0006
10	0	-0.0001	-0.0006	0.0008
15	-0.0001	0	0.0003	0.0012
20	-0.0004	-0.0001	0.0004	0.0012
40	-0.0011	-0.0003	0.0013	0.0009
60	-0.0019	-0.0003	0.0018	0.0008
80	-0.0028	-0.0004	0.0021	0.0005
100	-0.0034	-0.0005	0.0024	0.0002

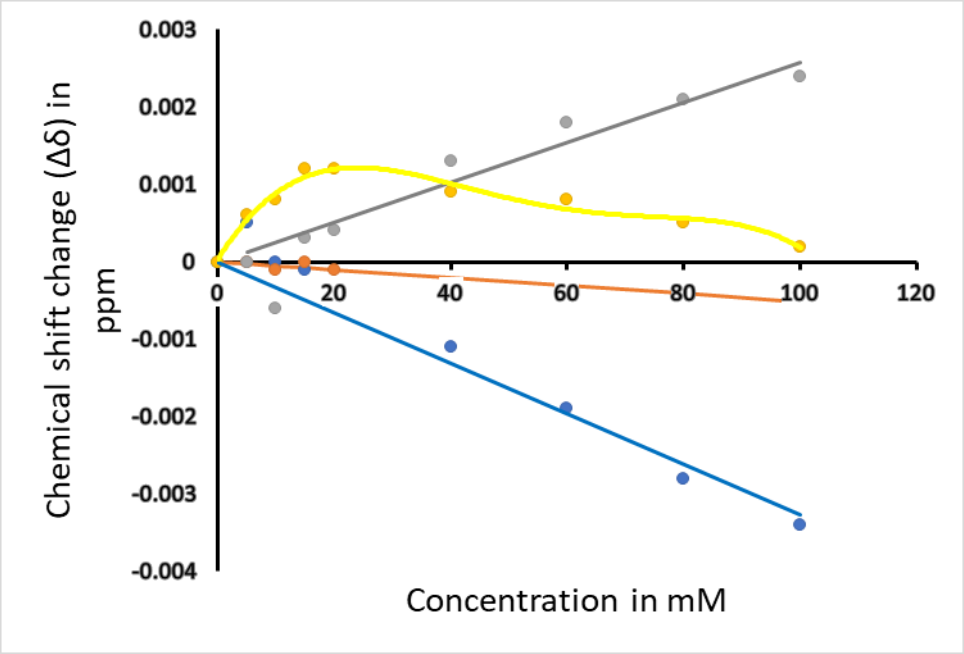

Figure 5.4. Data from ^{1}H NMR showing proton chemical shift changes (Y axis) of various ions. A. Proton chemical shift of urea (urea concentration maintained constant at 20 mM in the presence of varied concentrations of ectoine from 0 mM to 100 mM (Blue). B. Proton chemical shift of ectoine (ectoine concentration varied from 0 mM to 100 mM in the presence of 20 mM urea (orange). C. Proton chemical shift of varied concentrations of ectoine from 0 mM to 100 mM without urea (grey). D. Proton chemical shift of 5 mM acetate (yellow). Round symbols are actual data and straight lines are the fitted data.

In the solution containing ectoine and 20 mM urea, as the concentration of ectoine was increased from 0 mM to 100 mM, the chemical shift changes of ectoine changed by only -0.0005 ppm (as seen in Table 5.3 and Figure 5.4, orange symbols and Table 5.3), which is an order of magnitude smaller than any shift changes seen for TMAO and comes within the margins of error of measuring chemical shift values. The chemical shift changes throughout the spectra are very small. The analysis of these spectra is therefore simpler than for TMAO, because there are clearly no significant interactions of any kind, for any of the components in solution.

An attempt was made to fit the data to Equation 5.1, but the changes in shift are so small that no binding curves can be fitted with any reliability, hence data is fitted to a simple linear equation, mainly to make the data in the graph easier to follow.

5.2.3 Betaine-urea interactions

A similar set of experiments was carried out to investigate interactions between betaine and urea. ^{1}H NMR experiments were carried out to study the urea- betaine interactions, and 1D

proton spectra of urea were recorded in the presence of increasing concentrations of betaine from 0 mM to 100 mM as seen in Figure 5.5. Separate ^{1}H NMR standard spectra of betaine were also recorded to compare the changes in chemical shift of betaine in the absence of urea as well.

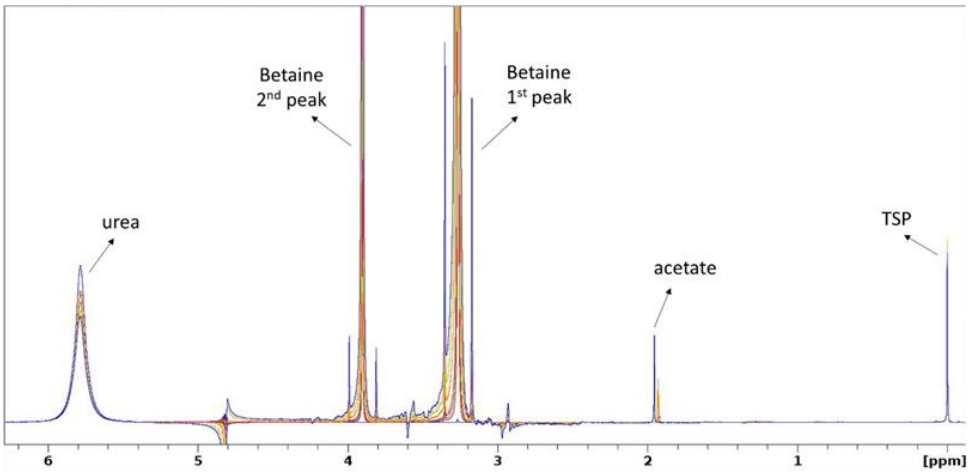

Figure 5.5. Spectra from ^{1}H NMR experiments showing proton spectra of 20 mM urea in the presence of varied concentrations of betaine from 0 mM to 100 mM.

Table 5.4. Data from 1H NMR showing change in chemical shift (Δδ) values of various solutes.

Betaine con in mM	20 mM urea in presence of varying betaine	Varying betaine 2nd peak in presence of 20 mM urea	Varying betaine 1st peak in presence of 20 mM urea	Varying betaine 2nd peak without urea	Varying betaine 1st peak without urea
0	0.0000	0.0000	0.0000	0.0000	0
5	0.0001	0.0000	0.0000	0.0000	0
10	-0.0002	-0.0001	-0.0001	0.0001	0.0001
15	-0.0004	-0.0001	-0.0002	0.0002	0.0002
20	-0.0005	-0.0002	-0.0002	0.0001	0.0001
40	-0.0005	0.0000	-0.0001	0.0003	0.0002
60	-0.0019	-0.0001	-0.0003	0.0000	-0.0001
80	-0.0022	-0.0001	-0.0003	0.0004	0.0001
100	-0.0024	-0.0001	-0.0005	0.0005	0.0001

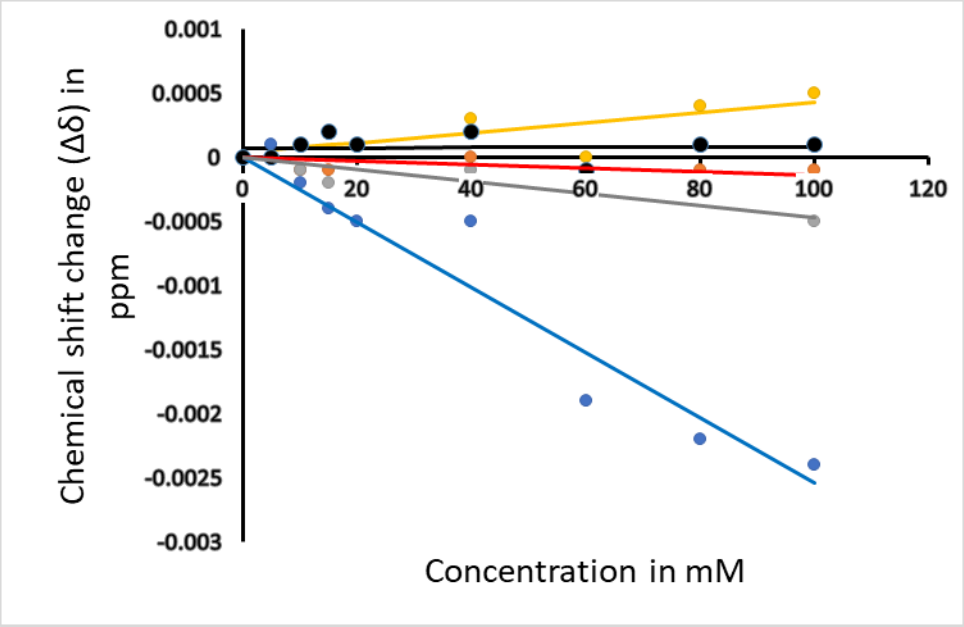

Figure 5.6. Data from ^{1}H NMR showing proton chemical shift changes (Y axis) of various solutes. A. Proton chemical shift of urea (urea concentration maintained constant at 20 mM in the presence of varying concentrations of betaine from 0 mM to 100 mM (blue). B. Proton chemical shift of betaine 1st peak (concentration of betaine varied from 0 mM to 100 mM in the presence of 20 mM urea (grey). C. Proton chemical shift of betaine 2nd peak (concentration of betaine varied from 0 mM to 100 mM in the presence of 20 mM urea (orange). D. Proton chemical shift of varied concentrations of betaine 1st peak from 0 mM to 100 mM without urea (black). E. Proton chemical shift of varied concentrations of betaine 2nd peak from 0 mM to 100 mM without urea (yellow). Round symbols are actual data and straight lines are the fitted data.

In the solution containing betaine and 20 mM urea, as the concentration of betaine was increased from 0 mM to 100 mM, the chemical shift changes of betaine changed by only -0.0005 ppm for 1st peak and -0.0001 for second peak as seen in Table 5.4 and Figure 5.6. Chemical shift changes of betaine in the absence of urea were not very different but with a difference that the 2nd peak (0.0005 ppm) moved more than the 1st peak (0.0001 ppm) and peak movement is upfield as indicated by positive values for shift changes compared to negative changes in shift values in the presence of urea. However, this is an order of magnitude smaller than any shift changes seen for TMAO, roughly similar to ectoine and comes within the margins of error of measuring chemical shift values. The chemical shift changes throughout the spectra are very small. Like in the case of ectoine the analysis of these spectra is therefore simpler than for TMAO, because there are clearly no significant interactions of any kind, for any of the components in solution.

An attempt was made to fit the data to Equation 5.1, but the changes in shift are so small that no binding curves can be fitted with any reliability, hence data is fitted to a simple linear equation to connect the dots and to make the data easier to follow.

5.3 Discussion

Understanding of interactions of stabilising osmolytes with denaturants like urea is very important to overall understanding of protein stability. From the previously discussed NMR experiments and DSC experiments of barnase/osmolyte titrations, we have learnt that there is no direct interaction happening between protein and osmolytes, and yet TMAO and ectoine are able to affect the protein structure and stability. This is especially clear for TMAO, which is shown by the DSC data to counteract the destabilising effects of urea, even though the NMR results show that it does not bind directly to the protein. The results presented in this chapter demonstrate clearly that it also does not bind directly to urea.

Small changes of chemical shifts of urea, TMAO and ectoine were observed with a binding curve seen for TMAO, indicating self-association of TMAO but no interaction with urea. For ectoine, there are no interactions of any kind. Hence it can be concluded that the osmolytes do not directly interact with urea.

We note that there are earlier research findings that have reported an interaction between osmolyte and urea. A study using Raman spectroscopy on mixed osmolyte solutions (Zetterholm et al., 2018) reported that TMAO directly interacts with urea. We suggest that some caution should be used in interpreting this result, which used saturated urea and TMAO solutions. The saturating concentration of urea in water is around 20 M and the saturating concentration of TMAO in water is greater than 10 M. It is not surprising that there should be an interaction between the two at these extremely high concentrations, which together are about half the concentration of water itself (55 M). This result leaves open the question of whether there are interactions at more physiological concentrations. Neutron scattering experiments by Meersman et al have also shown that TMAO forms hydrogen bonds with urea at a 2:1 concentration ratio (Meersman et al., 2009). These experiments were carried out at a mole fraction of TMAO of 0.05, in other words at a concentration of 2.5 M TMAO plus 2.5 M urea, at pH 9.2 (Meersman et al., 2009, Table 1). These concentrations are not as extreme as those used in Zetterholm et al. (2018), but are still sufficiently high that the two results (ie our result showing no interaction at 100 mM TMAO, 20 mM urea, and their result showing binding at 2.5 M TMAO, 2.5 M urea) could both be correct. The DSC results clearly show protein stabilisation at a concentration of 1 M, where one would expect little direct interaction. It is

worth noting that Meersman et al. (2009) suggests no direct interaction between TMAO and protein.

Urea is known to self-associate and the presence of osmolytes like TMAO further increases the self-association of urea thereby decreasing the denaturing effects of urea (Paul and Patey, 2007).

Ectoine interacts with water molecules. Neutron diffraction studies of solutions show ectoine enhances hydrogen bonds in water (Zaccai et al., 2016). Hydration shells are formed around ectoine that changes the dynamics of water molecules especially those water molecules present in the first hydration shell (Smiatek et al., 2012, Hahn et al., 2015, Smiatek, 2014).

Ectoine and hydroxyectoine both have distinct hygroscopic properties from urea and accumulate 7 and 9 water molecules around them in length scales smaller than 0.6 nm and bind more water molecules than urea.

X-ray photoelectron and PM IRRAS studies on the interaction between DNA and ectoine suggested that ectoine affects hydrogen bonding in the DNA, and DNA interacts with water in the presence of lower concentrations of ectoine like 0.1 M while at higher concentrations up to 2.5 M, interaction was mostly between ectoine and water (Wittmar et al., 2020). This suggests that ectoine either interacts with water or its presence makes the other solutes like DNA in this case to interact with water.

Molecular dynamic simulation and spatial distribution function (SDF) studies by Kumar and Kishore (2013) on the effect of mixtures of betaine plus urea on the local water structure reveal that the hydrogen bonding network in water increases as compared to pure water when betaine and urea are in synergy. The strengthening of individual hydrogen bonding between water molecules is related to the protein stability (Zou et al., 2002, Paul and Patey, 2007). Results reporte by (Kumar and Kishore, 2013) also indicate that the interaction of betaine with water becomes stronger in the urea plus betaine mixture and results in the exclusion of betaine from the protein surface.

In summary, some previous literature on TMAO/urea interactions have presented evidence for direct interactions between TMAO and urea, but these positive observations were

conducted at extremely high solute concentrations. Experiments carried out at more physiological concentrations have concluded that there are no direct interactions between the two solutes, but that the combination of the two solutes has a greater effect on water structure and dynamics than either solute alone.

Therefore, we propose that osmolytes do not directly interact with the urea, at the concentrations used in our experiments or found in biological systems. Our previous NMR results suggest that they also do not bind directly to barnase. We therefore conclude that the ability of TMAO to counteract the destabilising effects of urea is not by directly binding to urea but by its ability to modulate the water structure, while ectoine in a mixed osmolyte solution is slightly adding to the destabilising effects of urea by poorly organising water like to some extent thiocyanate in Hofmeister series does (Bennion and Daggett, 2004).

6 Chapter 6: Conclusion

The results presented in chapters 3-5 allow us to reach some tentative conclusions on how solutes are able to stabilise proteins.

Chapter 3 presents DSC data. These results reveal that when compared with Hofmeister series anions like thiocyanate (Bye et al., 2016), changes in melting temperatures caused by osmolytes are small but similar to that of sulfate. Sulphate raises the T_m while thiocyanate massively brings down the T_m. DSC data suggests that although TMAO stabilise proteins weakly, it can still counteract destabilising effects of denaturants like urea, whilst ectoine slightly destabilizes the protein barnase. The other interesting result from this chapter is that the effects of TMAO and ectoine on protein stability are saturable, i.e., they are large at low concentration but slow down at high concentration. This is unlike the effects of urea which are linear with concentration. In subsequent chapters, we develop the idea that saturable effects are due to direct binding, whereas linear effects are due to indirect effects from solvent. This observation raises the possibility that the effects of osmolytes (specifically, TMAO and ectoine) on protein stability may be due (in whole or in part) to protein binding.

Study of the chemical shift change data from $^{1}H^{15}N$ HSQC, $^{1}H^{13}C$ HSQC, and 2D-HNCO experiments in Chapter 4 clearly shows that TMAO and (to some extent) ectoine have two different effects which we call a two-stage effect: a direct binding interaction (i.e., a saturation curve), and a linear change in shift proportional to the concentration of osmolyte, characterised by the gradient. In the case of ectoine, binding to the protein backbone is negligible at concentrations less than 0.1 M and for most residues there is only a linear change in shift characterised by the gradient up to 1 M. Betaine has no two-stage effect but just a linear change in shift proportional to the concentration from 0 M to 1 M. This forms an interesting contrast to the results just discussed from Chapter 3. From Chapter 3 we conclude that at least some of the effects of TMAO and ectoine on protein stability may be due to binding. On the other hand, in Chapter 4 we conclude that the major effects of the three osmolytes are not due to binding but due to solvent-mediated effects. How can these two conclusions be reconciled? There are a number of points that should be made. (1) The results of Chapter 3 are mostly made in the presence of urea. Urea felt like a logical co-solute at the time, but in hindsight it may not be typical, because the osmolytes do not normally encounter urea, and their roles are typically to stabilise proteins against high salt, high temperature, or extremes of pH or pressure. (2) Although TMAO binds, and ectoine binds weakly, betaine (a very common osmolyte) does not

bind at all. (2) There is general agreement that osmolytes are “excluded” from the protein surface, implying that most of their activity does not arise from direct interaction. We can therefore minimally conclude that osmolytes do not need to bind in order to function (eg betaine).

Chapter 4 analyses the gradients produced by the osmolytes and by Hofmeister ions. It is of interest to note that thiocyanate, at the chaotrope end of the Hofmeister series, produces gradients of around -50 ppb/M; chloride (in the middle of the series) of -20 ppb/M, and sulphate (at the kosmotrope end) of +10 ppb/M. Thus, the gradients of the Hofmeister ions match well the idea that Hofmeister effects are mainly related to solvent-mediated effects. The three osmolytes studied here all have gradients of around +10 ppb/M; in other words, their gradient values resemble those of sulphate. We have argued that the gradients are a measure of the effects of solutes on water ordering. The logical conclusion is that the osmolytes have a similar effect on the solvent as does sulphate; they cause a local ordering of the solvent, which stabilises the protein.

It is however clear that it cannot be as simple as this. Despite having very similar gradients, the osmolytes and sulphate do not have the same effect on protein stability and solubility. There must therefore be other factors operating besides simply effect on bulk water structure.

Chapter 4 also presents an analysis of scatter plots of gradients and data from K_a values. It produces the interesting observation that correlation between one salt to another is dependent on how strongly they bind to the protein surface (Figures 4.43, 4.44 and Table 4.6). Our data segregates osmolytes and Hofmeister anions into three categories based on their binding affinities, those that bind strongly (sulphate, thiocyanate), those that bind moderately (TMAO, chloride) and those that bind weakly/no binding (ectoine, betaine). TMAO and chloride bind moderately to protein surface hence they have a good correlation between them. TMAO and weakly binding ectoine also have a correlation between them. Ectoine and betaine do not bind, so they too have good correlation between them. Whereas no correlation was found between any of the osmolytes (TMAO, ectoine, betaine) with sulphate or thiocyanate because unlike osmolytes, thiocyanate and sulphate bind to the protein surface at lower concentrations. In summary good correlation is found between those osmolytes and Hofmeister anions that have similar binding affinities. We speculate in Chapter 4 that second sphere binding may play a role, ie the interaction of a hydrated solute with the protein surface. This would mean that the

effect of solutes is not simply the effect on bulk solvent, and not a direct binding interaction, but a more general second sphere effect.

Finally, Chapter 5 shows that there is no direct interaction between osmolytes and urea. Small changes of chemical shifts of urea, TMAO and ectoine were observed with a binding curve seen for TMAO, indicating self-association of TMAO but no interaction with urea. For ectoine and betaine, there are no interactions of any kind. Hence it can be concluded that the osmolytes do not directly interact with urea.

The Hofmeister series describes effects on protein solubility and on protein stability (ie, whether it unfolds). Throughout most of this thesis, we have assumed that the two effects are closely related and arise from the same physical origin. This is an important question. If solubility and stability are two sides of the same coin, then different Hofmeister ions can improve stability but worsen solubility, or *vice versa*, but they can never improve both. On the other hand, if there is a different origin for the two effects, then it may be possible to find ways to improve both. In particular, if Hofmeister effects derive from effects of solutes on the bulk solvent, then there can be no way to separate the two effects. On the other hand, if there is a role of binding, then potentially the two effects could be separated.

The arguments above point to some role of binding, which would seem to be mainly on solubility. This would not be so unusual: the binding of a solute to the protein surface changes its charge distribution and its hydrophobicity, which could make the protein more or less stable. There is a well-studied phenomenon called the reverse Hofmeister effect, in which for proteins below their isoelectric point, the effect of solute ions is reversed at low concentration, and then changes over to the normal Hofmeister effect at higher concentrations of the solute (Bostroem et al., 2011). A recent study has suggested that binding of anions to specific sites on the protein surface may be responsible for the reverse Hofmeister effect (Yao et al., 2021).

Our previous studies (Bye et al., 2016 and Clare Trevitt unpublished) show that the Hofmeister anions sulphate and thiocyanate bind to the surface of barnase with similar affinities, although in different locations. They have very different gradients, and different effects on protein solubility and stability, which we have ascribed mainly to effects on the solvent. The osmolytes betaine, TMAO and ectoine studied here bind more weakly if at all and have less marked effects on protein solubility and stability compared to thiocyanate, but have the same gradients and same effect on solubility and stability (ie the same effect on bulk water) as sulphate. From this and the arguments raised above, we propose that some of the effects of

sulphate and thiocyanate are due to binding to the protein surface, making the surface either more hydrophilic (sulphate) or more hydrophobic (thiocyanate). This affects the solubility, though not necessarily the stability.

We therefore propose a further extension of the modified water breaker/maker theory. Highly solvated ions (sulphate, and also the three osmolytes studied here) structure water molecules around themselves. This makes the water less available to interact correctly with the protein surface, and so makes the protein less soluble but more stable. The osmolytes do not interact strongly with the protein surface. By contrast, sulphate does bind to the protein surface, which affects the protein charge and hydrophobicity. Similarly, thiocyanate disorders water around itself, and thus makes the protein more soluble but less stable. It also binds to the protein surface. This modified theory seems to fit the observed data (ie, the data presented here as well as result in the literature) and provides a useful platform for understanding the effects of co-solutes in general. Many previous researchers have also proposed that osmolytes affect water structure (Bennion and Daggett, 2004, Rezus and Bakker, 2009, Zou et al., 2002, Zaccai et al., 2016, Wittmar et al., 2020). For example, Zalar et al (2020) showed that excipient binding to the protein is not mandatory to affect protein solubility and stability.

We have also tentatively proposed that co-solutes interact with proteins not just by direct binding (ie, by desolvation followed by a direct interaction between solute and protein) but also by a solvent-mediated interaction, in which there is a single layer of structured water molecules between the protein and the solute. This needs further investigation.

This may provide some explanation for why there is such a wide range of chemical structures for osmolytes: they need to be soluble and well solvated, and not bind to the protein surface (specifically, they need to bind more strongly to water than they do to the protein, which is why they are “excluded” from the surface). Other than that, the only other requirement is that they should be cheap and easy to biosynthesise.

6.1 Future work

Using DSC, I have studied the effect of osmolyte on protein stability in the presence of denaturant like urea, i.e., in a mixture containing barnase plus osmolyte plus urea. And I have studied the effect of osmolyte on barnase and urea in separate titrations ie, osmolyte plus barnase and osmolyte plus urea but not a mixture of osmolyte plus barnase plus protein denaturant like urea/guanidine. But this does not give information about what osmolyte does

to protein structure in the presence of urea/guanidine. Hence, I would like to do more NMR titrations involving a mixture of barnase, osmolyte, and urea to study the structural changes induced by osmolytes like TMAO/ectoine/betaine on barnase in the presence of denaturants like urea/guanidine. I would also like to do fluorescence spectroscopy experiments to study the effect of osmolytes on protein stability at room temperature because DSC gave information about only thermal stability.

Finally, it is worth noting that all the experiments done at Sheffield have used a single protein, barnase. Barnase has an unusually high pI of 9.2, so may be an atypical protein. It would be useful to repeat all these studies on a protein with a lower isoelectric point.

7 Appendix

7.1 Nawk and Python scripts used for NMR data analysis

7.1.1 Compare Gradients

Objective: To compare Gradients intra osmolytes and Osmolyte versus Hofmeister to understand how similar/different one another with respect to their effects on protein structure and stability are.

.....
.....

TMAO VS Ectoine:

```
nawk '{if ($2=="tmao" && $3=="h") {print $0}}' alldata_line_kd_revised.txt | nawk '{if ($8<900 && $8>5 && sqrt($6^2)>0.03) {print $1,$4} else {print $1,$14}}' | sort_resNum > gradient_mixed_tmao_h
nawk '{if ($2=="ect" && $3=="h") {print $0}}' alldata_line_kd_revised.txt | nawk '{if ($8<900 && $8>5 && sqrt($6^2)>0.03) {print $1,$4} else {print $1,$14}}' | sort_resNum > gradient_mixed_ect_h
nawk '{if ($2=="tmao" && $3=="n") {print $0}}' alldata_line_kd_revised.txt | nawk '{if ($8<900 && $8>5 && sqrt($6^2)>0.06) {print $1,$4} else {print $1,$14}}' | sort_resNum > gradient_mixed_tmao_n
nawk '{if ($2=="ect" && $3=="n") {print $0}}' alldata_line_kd_revised.txt | nawk '{if ($8<900 && $8>5 && sqrt($6^2)>0.06) {print $1,$4} else {print $1,$14}}' | sort_resNum > gradient_mixed_ect_n
nawk '{if ($2=="tmao" && $3=="c") {print $0}}' alldata_line_kd_revised.txt | nawk '{if ($8<900 && $8>5 && sqrt($6^2)>0.06) {print $1,$4} else {print $1,$14}}' | sort_resNum > gradient_mixed_tmao_c
nawk '{if ($2=="ect" && $3=="c") {print $0}}' alldata_line_kd_revised.txt | nawk '{if ($8<900 && $8>5 && sqrt($6^2)>0.06) {print $1,$4} else {print $1,$14}}' | sort_resNum > gradient_mixed_ect_c

matchingResidues_From2Files gradient_mixed_tmao_h gradient_mixed_ect_h | sort_resNum_column3 > compare_gradient_mix_tmao_ect_h
matchingResidues_From2Files gradient_mixed_tmao_n gradient_mixed_ect_n | sort_resNum_column3 > compare_gradient_mix_tmao_ect_n
matchingResidues_From2Files gradient_mixed_tmao_c gradient_mixed_ect_c | sort_resNum_column3 > compare_gradient_mix_tmao_ect_c
```

.....
.....

Osmolytes vs Hofmeister:

```
nawk '{if ($2=="so4" && $3=="h") {print $0}}' alldata_line_kd_revised.txt | nawk '{if ($8<900 && $8>5 && sqrt($6^2)>0.03) {print $1,$4} else {print $1,$14}}' | sort_resNum > gradient_mixed_so4_h
nawk '{if ($2=="so4" && $3=="n") {print $0}}' alldata_line_kd_revised.txt | nawk '{if ($8<900 && $8>5 && sqrt($6^2)>0.06) {print $1,$4} else {print $1,$14}}' | sort_resNum > gradient_mixed_so4_n
```

```
nawk '{if ($2=="so4" && $3=="c") {print $0}}' alldata_line_kd_revised.txt | nawk '{if
($8<900 && $8>5 && sqrt($6^2)>0.06) {print $1,$4} else {print $1,$14}}' | sort_resNum >
gradient_mixed_so4_c

nawk '{if ($2=="scn" && $3=="h") {print $0}}' alldata_line_kd_revised.txt | nawk '{if
($8<900 && $8>5 && sqrt($6^2)>0.03) {print $1,$4} else {print $1,$14}}' | sort_resNum >
gradient_mixed_scn_h
nawk '{if ($2=="scn" && $3=="n") {print $0}}' alldata_line_kd_revised.txt | nawk '{if
($8<900 && $8>5 && sqrt($6^2)>0.06) {print $1,$4} else {print $1,$14}}' | sort_resNum >
gradient_mixed_scn_n
nawk '{if ($2=="scn" && $3=="c") {print $0}}' alldata_line_kd_revised.txt | nawk '{if
($8<900 && $8>5 && sqrt($6^2)>0.06) {print $1,$4} else {print $1,$14}}' | sort_resNum >
gradient_mixed_scn_c

nawk '{if ($2=="cl" && $3=="h") {print $0}}' alldata_line_kd_revised.txt | nawk '{if
($8<900 && $8>5 && sqrt($6^2)>0.03) {print $1,$4} else {print $1,$14}}' | sort_resNum >
gradient_mixed_cl_h
nawk '{if ($2=="cl" && $3=="n") {print $0}}' alldata_line_kd_revised.txt | nawk '{if
($8<900 && $8>5 && sqrt($6^2)>0.06) {print $1,$4} else {print $1,$14}}' | sort_resNum >
gradient_mixed_cl_n
nawk '{if ($2=="cl" && $3=="c") {print $0}}' alldata_line_kd_revised.txt | nawk '{if
($8<900 && $8>5 && sqrt($6^2)>0.06) {print $1,$4} else {print $1,$14}}' | sort_resNum >
gradient_mixed_cl_c
```

H:

```
matchingResidues_From2Files gradient_mixed_tmao_h gradient_mixed_so4_h |
sort_resNum_column3 > compare_gradient_mix_tmao_so4_h
matchingResidues_From2Files gradient_mixed_tmao_h gradient_mixed_scn_h |
sort_resNum_column3 > compare_gradient_mix_tmao_scn_h
matchingResidues_From2Files gradient_mixed_ect_h gradient_mixed_so4_h |
sort_resNum_column3 > compare_gradient_mix_ect_so4_h
matchingResidues_From2Files gradient_mixed_ect_h gradient_mixed_scn_h |
sort_resNum_column3 > compare_gradient_mix_ect_scn_h
matchingResidues_From2Files gradient_mixed_tmao_h gradient_mixed_cl_h |
sort_resNum_column3 > compare_gradient_mix_tmao_cl_h
matchingResidues_From2Files gradient_mixed_ect_h gradient_mixed_cl_h |
sort_resNum_column3 > compare_gradient_mix_ect_cl_h
```

N:

```
matchingResidues_From2Files gradient_mixed_tmao_n gradient_mixed_so4_n |
sort_resNum_column3 > compare_gradient_mix_tmao_so4_n
matchingResidues_From2Files gradient_mixed_tmao_n gradient_mixed_scn_n |
sort_resNum_column3 > compare_gradient_mix_tmao_scn_n
matchingResidues_From2Files gradient_mixed_ect_n gradient_mixed_so4_n |
sort_resNum_column3 > compare_gradient_mix_ect_so4_n
matchingResidues_From2Files gradient_mixed_ect_n gradient_mixed_scn_n |
sort_resNum_column3 > compare_gradient_mix_ect_scn_n
matchingResidues_From2Files gradient_mixed_tmao_n gradient_mixed_cl_n |
sort_resNum_column3 > compare_gradient_mix_tmao_cl_n
```

```
matchingResidues_From2Files gradient_mixed_ect_n gradient_mixed_cl_n |
sort_resNum_column3 > compare_gradient_mix_ect_cl_n
```

C:

```
matchingResidues_From2Files gradient_mixed_tmao_c gradient_mixed_so4_c |
sort_resNum_column3 > compare_gradient_mix_tmao_so4_c
matchingResidues_From2Files gradient_mixed_tmao_c gradient_mixed_scn_c |
sort_resNum_column3 > compare_gradient_mix_tmao_scn_c
matchingResidues_From2Files gradient_mixed_ect_c gradient_mixed_so4_c |
sort_resNum_column3 > compare_gradient_mix_ect_so4_c
matchingResidues_From2Files gradient_mixed_ect_c gradient_mixed_scn_c |
sort_resNum_column3 > compare_gradient_mix_ect_scn_c
matchingResidues_From2Files gradient_mixed_tmao_c gradient_mixed_cl_c |
sort_resNum_column3 > compare_gradient_mix_tmao_cl_c
matchingResidues_From2Files gradient_mixed_ect_c gradient_mixed_cl_c |
sort_resNum_column3 > compare_gradient_mix_ect_cl_c
.....
```

Copy all the output files to excel (gradient_correlation.ods) and plot the graph.

7.1.2 sort_ResNum

```
nawk ' {
   str = $1
   subs = substr(str, 2, 5)

   print subs, $1,  $2
}' $1 | sort -nk1 | nawk ' {print $2,$3} '
```

7.1.3 sort_resNum_column3

```
nawk ' {
   str = $3
   subs = substr(str, 2, 5)

   print subs, $1,  $2,  $3
}' $1 | sort -nk1 | nawk '{print $2,$3,$4}'
```

7.1.4 matchingResidues_From2Files

```
nawk '
FILENAME==file_1 {
  NR>1
```

```
  file1_m[$1]=$2
}
FILENAME==file_2 {
  NR>1
  file2_m[$1]=$2
}
END {
  for (id in file1_m) {
    if ((id in file1_m) && (id in file2_m)) {

     print file1_m[id], file2_m[id], id
    }
  }
}' file_1=$1 file_2=$2 $1 $2
```

7.1.5 Compare Gradients

Objective: To compare kD intra osmolytes and Osmolyte versus hofmeister to understand how similar/different one another with respect to their effects on protein structure and stability are. Selection of kD values based on kd 5-900 and $\Delta\delta_{max}$ -0.03 to +0.03 for H and -0.06 to +0.06

.....

TMAO VS Ectoine:

```
nawk '{if ($2=="tmao" && $3=="h") {print $0}}' alldata_line_kd_revised.txt | nawk '{if ($8<900 && $8>5 && sqrt($6^2)>0.03) {print $1,$8}}' > kD_tmao_h
nawk '{if ($2=="ect" && $3=="h") {print $0}}' alldata_line_kd_revised.txt | nawk '{if ($8<900 && $8>5 && sqrt($6^2)>0.03) {print $1,$8}}' > kD_ect_h
nawk '{if ($2=="tmao" && $3=="n") {print $0}}' alldata_line_kd_revised.txt | nawk '{if ($8<900 && $8>5 && sqrt($6^2)>0.06) {print $1,$8}}' > kD_tmao_n
nawk '{if ($2=="ect" && $3=="n") {print $0}}' alldata_line_kd_revised.txt | nawk '{if ($8<900 && $8>5 && sqrt($6^2)>0.06) {print $1,$8}}' > kD_ect_n
nawk '{if ($2=="tmao" && $3=="c") {print $0}}' alldata_line_kd_revised.txt | nawk '{if ($8<900 && $8>5 && sqrt($6^2)>0.06) {print $1,$8}}' > kD_tmao_c
nawk '{if ($2=="ect" && $3=="c") {print $0}}' alldata_line_kd_revised.txt | nawk '{if ($8<900 && $8>5 && sqrt($6^2)>0.06) {print $1,$8}}' > kD_ect_c

matchingResidues_From2Files kD_tmao_h kD_ect_h | sort_resNum_column3 > compare_kD_tmao_ect_h
matchingResidues_From2Files kD_tmao_n kD_ect_n | sort_resNum_column3 > compare_kD_tmao_ect_n
matchingResidues_From2Files kD_tmao_c kD_ect_c | sort_resNum_column3 > compare_kD_tmao_ect_c
```

.....

Osmolytes vs Hofmeister:

```
nawk '{if ($2=="so4" && $3=="h") {print $0}}' alldata_line_kd_revised.txt | nawk '{if
($8<900 && $8>5 && sqrt($6^2)>0.03) {print $1,$8}}' > kD_so4_h
nawk '{if ($2=="so4" && $3=="n") {print $0}}' alldata_line_kd_revised.txt | nawk '{if
($8<900 && $8>5 && sqrt($6^2)>0.06) {print $1,$8}}' > kD_so4_n
nawk '{if ($2=="so4" && $3=="c") {print $0}}' alldata_line_kd_revised.txt | nawk '{if
($8<900 && $8>5 && sqrt($6^2)>0.06) {print $1,$8}}' > kD_so4_c

nawk '{if ($2=="scn" && $3=="h") {print $0}}' alldata_line_kd_revised.txt | nawk '{if
($8<900 && $8>5 && sqrt($6^2)>0.03) {print $1,$8}}' > kD_scn_h
nawk '{if ($2=="scn" && $3=="n") {print $0}}' alldata_line_kd_revised.txt | nawk '{if
($8<900 && $8>5 && sqrt($6^2)>0.06) {print $1,$8}}' > kD_scn_n
nawk '{if ($2=="scn" && $3=="c") {print $0}}' alldata_line_kd_revised.txt | nawk '{if
($8<900 && $8>5 && sqrt($6^2)>0.06) {print $1,$8}}' > kD_scn_c

nawk '{if ($2=="cl" && $3=="h") {print $0}}' alldata_line_kd_revised.txt | nawk '{if
($8<900 && $8>5 && sqrt($6^2)>0.03) {print $1,$8}}' > kD_cl_h
nawk '{if ($2=="cl" && $3=="n") {print $0}}' alldata_line_kd_revised.txt | nawk '{if
($8<900 && $8>5 && sqrt($6^2)>0.06) {print $1,$8}}' > kD_cl_n
nawk '{if ($2=="cl" && $3=="c") {print $0}}' alldata_line_kd_revised.txt | nawk '{if
($8<900 && $8>5 && sqrt($6^2)>0.06) {print $1,$8}}' > kD_cl_c

H:
matchingResidues_From2Files kD_tmao_h kD_so4_h | sort_resNum_column3 >
compare_kD_tmao_so4_h
matchingResidues_From2Files kD_tmao_h kD_scn_h | sort_resNum_column3 >
compare_kD_tmao_scn_h
matchingResidues_From2Files kD_ect_h kD_so4_h | sort_resNum_column3 >
compare_kD_ect_so4_h
matchingResidues_From2Files kD_ect_h kD_scn_h | sort_resNum_column3 >
compare_kD_ect_scn_h
matchingResidues_From2Files kD_tmao_h kD_cl_h | sort_resNum_column3 >
compare_kD_tmao_cl_h
matchingResidues_From2Files kD_ect_h kD_cl_h | sort_resNum_column3 >
compare_kD_ect_cl_h

N:
matchingResidues_From2Files kD_tmao_n kD_so4_n | sort_resNum_column3 >
compare_kD_tmao_so4_n
matchingResidues_From2Files kD_tmao_n kD_scn_n | sort_resNum_column3 >
compare_kD_tmao_scn_n
matchingResidues_From2Files kD_ect_n kD_so4_n | sort_resNum_column3 >
compare_kD_ect_so4_n
matchingResidues_From2Files kD_ect_n kD_scn_n | sort_resNum_column3 >
compare_kD_ect_scn_n
matchingResidues_From2Files kD_tmao_n kD_cl_n | sort_resNum_column3 >
compare_kD_tmao_cl_n
matchingResidues_From2Files kD_ect_n kD_cl_n | sort_resNum_column3 >
compare_kD_ect_cl_n
```

C:
matchingResidues_From2Files kD_tmao_c kD_so4_c | sort_resNum_column3 > compare_kD_tmao_so4_c
matchingResidues_From2Files kD_tmao_c kD_scn_c | sort_resNum_column3 > compare_kD_tmao_scn_c
matchingResidues_From2Files kD_ect_c kD_so4_c | sort_resNum_column3 > compare_kD_ect_so4_c
matchingResidues_From2Files kD_ect_c kD_scn_c | sort_resNum_column3 > compare_kD_ect_scn_c
matchingResidues_From2Files kD_tmao_c kD_cl_c | sort_resNum_column3 > compare_kD_tmao_cl_c
matchingResidues_From2Files kD_ect_c kD_cl_c | sort_resNum_column3 > compare_kD_ect_cl_c
.....

Copy all the output files to excel (kD_Correlation.ods) and plot the graph.

7.1.6 Gradient input file for pymol (gradient_mixed_line_kdline_all_ions_pymol)

Objective: To select gradients for different ions from line and kd line based on $\Delta\delta_{max}$ and k_d and cat all of them into single file for using in pymol analysis.
.....
.....
TMAO VS Ectoine:

nawk '{if ($2=="tmao" && $3=="h") {print $0}}' alldata_line_kd_revised.txt | nawk '{if ($8<900 && $8>5 && sqrt($6^2)>0.03) {print $1,$2,$3,$4} else {print $1,$2,$3,$14}}' | sort_resNum_new > gradient_mixed_tmao_h ....sqrt($6^2)>0.03 absolute values. It applies greater than 0.03 and lower than -0.03 for $6
nawk '{if ($2=="ect" && $3=="h") {print $0}}' alldata_line_kd_revised.txt | nawk '{if ($8<900 && $8>5 && sqrt($6^2)>0.03) {print $1,$2,$3,$4} else {print $1,$2,$3,$14}}' | sort_resNum_new > gradient_mixed_ect_h
nawk '{if ($2=="tmao" && $3=="n") {print $0}}' alldata_line_kd_revised.txt | nawk '{if ($8<900 && $8>5 && sqrt($6^2)>0.06) {print $1,$2,$3,$4} else {print $1,$2,$3,$14}}' | sort_resNum_new > gradient_mixed_tmao_n
nawk '{if ($2=="ect" && $3=="n") {print $0}}' alldata_line_kd_revised.txt | nawk '{if ($8<900 && $8>5 && sqrt($6^2)>0.06) {print $1,$2,$3,$4} else {print $1,$2,$3,$14}}' | sort_resNum_new > gradient_mixed_ect_n
nawk '{if ($2=="tmao" && $3=="c") {print $0}}' alldata_line_kd_revised.txt | nawk '{if ($8<900 && $8>5 && sqrt($6^2)>0.06) {print $1,$2,$3,$4} else {print $1,$2,$3,$14}}' | sort_resNum_new > gradient_mixed_tmao_c
nawk '{if ($2=="ect" && $3=="c") {print $0}}' alldata_line_kd_revised.txt | nawk '{if ($8<900 && $8>5 && sqrt($6^2)>0.06) {print $1,$2,$3,$4} else {print $1,$2,$3,$14}}' | sort_resNum_new > gradient_mixed_ect_c

.....
.....
Hofmeister:

```
nawk '{if ($2=="so4" && $3=="h") {print $0}}' alldata_line_kd_revised.txt | nawk '{if
($8<900 && $8>5 && sqrt($6^2)>0.03) {print $1,$2,$3,$4} else {print $1,$2,$3,$14}}' |
sort_resNum_new > gradient_mixed_so4_h
nawk '{if ($2=="so4" && $3=="n") {print $0}}' alldata_line_kd_revised.txt | nawk '{if
($8<900 && $8>5 && sqrt($6^2)>0.06) {print $1,$2,$3,$4} else {print $1,$2,$3,$14}}' |
sort_resNum_new > gradient_mixed_so4_n
nawk '{if ($2=="so4" && $3=="c") {print $0}}' alldata_line_kd_revised.txt | nawk '{if
($8<900 && $8>5 && sqrt($6^2)>0.06) {print $1,$2,$3,$4} else {print $1,$2,$3,$14}}' |
sort_resNum_new > gradient_mixed_so4_c

nawk '{if ($2=="scn" && $3=="h") {print $0}}' alldata_line_kd_revised.txt | nawk '{if
($8<900 && $8>5 && sqrt($6^2)>0.03) {print $1,$2,$3,$4} else {print $1,$2,$3,$14}}' |
sort_resNum_new > gradient_mixed_scn_h
nawk '{if ($2=="scn" && $3=="n") {print $0}}' alldata_line_kd_revised.txt | nawk '{if
($8<900 && $8>5 && sqrt($6^2)>0.06) {print $1,$2,$3,$4} else {print $1,$2,$3,$14}}' |
sort_resNum_new > gradient_mixed_scn_n
nawk '{if ($2=="scn" && $3=="c") {print $0}}' alldata_line_kd_revised.txt | nawk '{if
($8<900 && $8>5 && sqrt($6^2)>0.06) {print $1,$2,$3,$4} else {print $1,$2,$3,$14}}' |
sort_resNum_new > gradient_mixed_scn_c

nawk '{if ($2=="cl" && $3=="h") {print $0}}' alldata_line_kd_revised.txt | nawk '{if
($8<900 && $8>5 && sqrt($6^2)>0.03) {print $1,$2,$3,$4} else {print $1,$2,$3,$14}}' |
sort_resNum_new > gradient_mixed_cl_h
nawk '{if ($2=="cl" && $3=="n") {print $0}}' alldata_line_kd_revised.txt | nawk '{if
($8<900 && $8>5 && sqrt($6^2)>0.06) {print $1,$2,$3,$4} else {print $1,$2,$3,$14}}' |
sort_resNum_new > gradient_mixed_cl_n
nawk '{if ($2=="cl" && $3=="c") {print $0}}' alldata_line_kd_revised.txt | nawk '{if
($8<900 && $8>5 && sqrt($6^2)>0.06) {print $1,$2,$3,$4} else {print $1,$2,$3,$14}}' |
sort_resNum_new > gradient_mixed_cl_c

.....
.....
cat gradient_mixed* > gradient_mixed_line_kdline_all_ions_pymol

gradient_mixed_line_kdline_all_ions_pymol | sort -dk1 -dk2 -dk3 >
gradient_mixed_line_kdline_all_ions_pymol_2

mv gradient_mixed_line_kdline_all_ions_pymol_2
gradient_mixed_line_kdline_all_ions_pymol

add title (res ion shift m) to gradient_mixed_line_kdline_all_ions_pymol


Copy gradient_mixed_line_kdline_all_ions_pymol to /barnase/osmolytes/pymol
```

7.1.7 Mapping of gradients on protein surface using Pymol

Objectuve: add_gradient_as_beta_to_pdb_v2.py ..... python script that takes res_number and m_values from osmolytes (input file) and writes them to protein structure file (for which B-factor is zeroed) and gives an output .pdb file to be viewed on pymol. edit this file as ect_ tmao_ scn_ as required.

Original script:

add_gradient_as_beta_to_pdb_v2.py ..... This will be modified as below depending on the experiment type. Also removed ddmax, kd, kd er, chi^2 from script and input file.

1a2p_a_with_h_zero_beta.pdb ..... protein file from pdb

gradient_mixed_line_kdline_all_ions_pymol ..... input file with gradients selected from line and kd line based on ddmax and kd for all ions

m_val_ect_c_alpha_1a2p_a.pdb ..... output .pdb file to be viewed on pymol with m_values that have replaced B Factor values.

.....

tmao_h_add_gradient_as_beta_to_pdb_v2_copy.py 1a2p_a_with_h_zero_beta.pdb gradient_mixed_line_kdline_all_ions_pymol > tmao_h_mval_1a2p.pdb .....script is for tmao_h

tmao_n_add_gradient_as_beta_to_pdb_v2_copy.py 1a2p_a_with_h_zero_beta.pdb gradient_mixed_line_kdline_all_ions_pymol > tmao_n_mval_1a2p.pdb .....edited for tmao_n

tmao_c_add_gradient_as_beta_to_pdb_v2_copy.py 1a2p_a_with_h_zero_beta.pdb gradient_mixed_line_kdline_all_ions_pymol > tmao_c_mval_1a2p.pdb

ectoine_h_add_gradient_as_beta_to_pdb_v2_copy.py 1a2p_a_with_h_zero_beta.pdb gradient_mixed_line_kdline_all_ions_pymol > ectoine_h_mval_1a2p.pdb

ectoine_n_add_gradient_as_beta_to_pdb_v2_copy.py 1a2p_a_with_h_zero_beta.pdb gradient_mixed_line_kdline_all_ions_pymol > ectoine_n_mval_1a2p.pdb

ectoine_c_add_gradient_as_beta_to_pdb_v2_copy.py 1a2p_a_with_h_zero_beta.pdb gradient_mixed_line_kdline_all_ions_pymol > ectoine_c_mval_1a2p.pdb

scn_h_add_gradient_as_beta_to_pdb_v2_copy.py 1a2p_a_with_h_zero_beta.pdb gradient_mixed_line_kdline_all_ions_pymol > scn_h_mval_1a2p.pdb

scn_n_add_gradient_as_beta_to_pdb_v2_copy.py 1a2p_a_with_h_zero_beta.pdb gradient_mixed_line_kdline_all_ions_pymol > scn_n_mval_1a2p.pdb

scn_c_add_gradient_as_beta_to_pdb_v2_copy.py 1a2p_a_with_h_zero_beta.pdb gradient_mixed_line_kdline_all_ions_pymol > scn_c_mval_1a2p.pdb

cl_h_add_gradient_as_beta_to_pdb_v2_copy.py 1a2p_a_with_h_zero_beta.pdb gradient_mixed_line_kdline_all_ions_pymol > cl_h_mval_1a2p.pdb

cl_n_add_gradient_as_beta_to_pdb_v2_copy.py 1a2p_a_with_h_zero_beta.pdb gradient_mixed_line_kdline_all_ions_pymol > cl_n_mval_1a2p.pdb

cl_c_add_gradient_as_beta_to_pdb_v2_copy.py 1a2p_a_with_h_zero_beta.pdb gradient_mixed_line_kdline_all_ions_pymol > cl_c_mval_1a2p.pdb

7.1.8 add_gradient_as_beta_to_pdb_v2.py

```
#!/usr/bin/env python

import cjcpdb
import sys
import math

pdb_file=sys.argv[1]
fit_output_file=sys.argv[2]

#make dicts
cl_h={}
cl_n={}
cl_c={}

scn_h={}
scn_n={}
scn_c={}

so4_h={}
so4_n={}
so4_c={}

scncl_h={}
scncl_n={}
scncl_c={}

scnso4_h={}
scnso4_n={}
scnso4_c={}

ect_h={}
ect_n={}
ect_c={}

tmao_h ={}
tmao_n ={}
tmao_c ={}

#readfile and specify columns
fh=open(fit_output_file)
data=fh.readlines()[1:]                    #read from second line
#data=fh.readlines()
for line in data:
  f=line.split()
  resnum=str(f[0][1:])
  ion   = f[1]
  shift = f[2]
  m     = float(f[3])
```

```
  m_er  = float(f[4])
  ddmax = float(f[5])
  dd_er = float(f[6])
  kd    = float(f[7])
  kd_er = float(f[8])
  chi2  = float(f[9])

  if m==0:
    ms=0
  else:
    ms=(m/((m**2)**0.25))/3   # ms is m_scaled!

  #populate dicts for tmao
  if ion=='tmao' and shift=='h':
    tmao_h[resnum]=ms
  if ion=='tmao' and shift=='n':
    tmao_n[resnum]=ms
  if ion=='tmao' and shift=='c':
    tmao_c[resnum]=ms


'''
#use this to add for each atom
fh=open(pdb_file)
data=fh.readlines()
for line in data:
  try:
    pl=cjcpdb.PDBLine(line)
    if pl.isAtom:
      if (pl.atname=="H02") and (pl.resid in cl_h.keys()):
        pl.b=cl_h[pl.resid]
      if (pl.atname=="N") and (pl.resid in cl_n.keys()):
        pl.b=cl_n[pl.resid]
      if (pl.atname=="C") and (pl.resid in cl_c.keys()):
        pl.b=cl_c[pl.resid]
      print pl
  except:
    print("resi absent")
'''


#use this to add sum h + n + c to CA fr putty type depiction
fh=open(pdb_file)
data=fh.readlines()
for line in data:
  try:
    pl=cjcpdb.PDBLine(line)
    if pl.isAtom:
     if pl.resid in tmao_h.keys():
        pl.b=tmao_h[pl.resid]
```

```
   print pl
except:
  print("resi absent")
```

8 REFERENCES

ABUI, M. & SMITH, P. E. 2004. A combined simulation and Kirkwood-Buff approach to quantify cosolvent effects on the conformational preferences of peptides in solution. *Journal of Physical Chemistry B,* 108**,** 7382-7388.

ANJUM, F., RISHI, V. & AHMAD, F. 2000. Compatibility of osmolytes with Gibbs energy of stabilization of proteins. *Biochimica Et Biophysica Acta-Protein Structure and Molecular Enzymology,* 1476**,** 75-84.

ARAKAWA, T. & TIMASHEFF, S. N. 1983. Preferential interactions of proteins with solvent components in aqueous amino acid solutions. *Archives of Biochemistry and Biophysics,* 224**,** 169-177.

ATHAWALE, M. V., DORDICK, J. S. & GARDE, S. 2005. Osmolyte trimethylamine-N-oxide does not affect the strength of hydrophobic interactions: Origin of osmolyte compatibility. *Biophysical Journal,* 89**,** 858-866.

AUTON, M., BASKAKOV, I., BOLEN, C. L. & BOLEN, D. W. 2001. On identifying the fundamental forces of osmolyte-induced protein stability. *Biophysical Journal,* 80**,** 558A-558A.

AUTON, M. & BOLEN, D. W. 2004. Additive transfer free energies of the peptide backbone unit that are independent of the model compound and the choice of concentration scale. *Biochemistry,* 43**,** 1329-1342.

AUTON, M. & BOLEN, D. W. 2005. Predicting the energetics of osmolyte induced protein folding/unfolding. *Proceedings of the National Academy of Sciences of the United States of America,* 102**,** 15065-15068.

AUTON, M., BOLEN, D. W. & ROSGEN, J. 2008. Structural thermodynamics of protein preferential solvation: Osmolyte solvation of proteins, aminoacids, and peptides. *Proteins-Structure Function and Bioinformatics,* 73**,** 802-813.

BAGNASCO, S., BALABAN, R., FALES, H. M., YANG, Y. M. & BURG, M. 1986. Predominant osmotically active organic solutes in rat and rabbit renal medullas. *Journal of Biological Chemistry,* 261**,** 5872-5877.

BALDWIN, R. L. 1996. How Hofmeister ion interactions affect protein stability. *Biophysical Journal,* 71**,** 2056-2063.

BASKAKOV, I. & BOLEN, D. W. 1998. Time-dependent effects of trimethylamine-N-oxide/urea on lactate dehydrogenase activity: An unexplored dimension of the adaptation paradigm. *Biophysical Journal,* 74**,** 2658-2665.

BASKAKOV, I., WANG, A. J. & BOLEN, D. W. 1998. Trimethylamine-N-oxide counteracts urea effects on rabbit muscle lactate dehydrogenase function: A test of the counteraction hypothesis. *Biophysical Journal,* 74**,** 2666-2673.

BAXTER, N. J., ZACHARCHENKO, T., BARSUKOV, I. L. & WILLIAMSON, M. P. 2017. Pressure-dependent chemical shifts in the R3 domain of talin show that it is thermodynamically poised for binding to either vinculin or RIAM. *Structure,* 25**,** 1856-1866.

BECK, D. A. C., BENNION, B. J., ALONSO, D. O. V. & DAGGETT, V. 2007. Simulations of macromolecules in protective and denaturing osmolytes: Properties of mixed solvent systems and their effects on water and protein structure and dynamics. *In:* HAUSSINGER, D. & SIES, H. (eds.) *Osmosensing and Osmosignaling,* 428, 373-96.

BECKTEL, W. J. & SCHELLMAN, J. A. 1987. Protein stability curves. *Biopolymers,* 26**,** 1859-1877.

BEDFORD, J. J., HARPER, J. L., LEADER, J. P., YANCEY, P. H. & SMITH, R. A. J. 1998. Betaine is the principal counteracting osmolyte in tissues of the elephant fish,

Callorhincus millii (Elasmobranchii, Holocephali). *Comparative Biochemistry and Physiology B-Biochemistry & Molecular Biology,* 119**,** 521-526.
BEDFORD, J. J., SCHOFIELD, J., YANCEY, P. H. & LEADER, J. P. 2002. The effects of hypoosmotic infusion on the composition of renal tissue of the Australian brush tailed possum *Trichosurus vulpecula*. *Comparative Biochemistry and Physiology B-Biochemistry & Molecular Biology,* 132**,** 645-652.
BENNION, B. J. & DAGGETT, V. 2003. The molecular basis for the chemical denaturation of proteins by urea. *Proceedings of the National Academy of Sciences of the United States of America,* 100**,** 5142-5147.
BENNION, B. J. & DAGGETT, V. 2004. Counteraction of urea-induced protein denaturation by trimethylamine N-oxide: A chemical chaperone at atomic resolution. *Proceedings of the National Academy of Sciences of the United States of America,* 101**,** 6433-6438.
BOLEN, D. W. 2001. Protein stabilization by naturally occurring osmolytes. *Methods in molecular biology (Clifton, N.J.),* 168**,** 17-36.
BOLEN, D. W. & BASKAKOV, I. V. 2001. The osmophobic effect: Natural selection of a thermodynamic force in protein folding. *Journal of Molecular Biology,* 310**,** 955-963.
BOLEN, D. W. & ROSE, G. D. 2008. Structure and energetics of the hydrogen-bonded backbone in protein folding. *Annual Review of Biochemistry,* 77**,** 339-362.
BOROWITZKA, L. J. & BROWN, A. D. 1974. Salt relations of marine and halophilic species of unicellular green-alga, dunaliella - role of glycerol as a compatible solute. *Archives of Microbiology,* 96**,** 37-52.
BOSTROEM, M., PARSONS, D. F., SALIS, A., NINHAM, B. W. & MONDUZZI, M. 2011. Possible origin of the inverse and direct Hofmeister series for lysozyme at low and high salt concentrations. *Langmuir,* 27**,** 9504-9511.
BOSTROM, M., TAVARES, F. W., FINET, S., SKOURI-PANET, F., TARDIEU, A. & NINHAM, B. W. 2005. Why forces between proteins follow different Hofmeister series for pH above and below pI. *Biophysical Chemistry,* 117**,** 217-224.
BROWN, A. D. 1976. Microbial water stress. *Bacteriological Reviews,* 40**,** 803-846.
BROWN, A. D. & SIMPSON, J. R. 1972. Water relations of sugar tolerant yeasts - role of intracellular polyols. *Journal of General Microbiology,* 72**,** 589-591.
BUCKLE, A. M. & FERSHT, A. R. 1994. Subsite binding in an RNase - structure of a barnase tetranucleotide complex at 1.76- Å resolution. *Biochemistry,* 33**,** 1644-1653.
BUENGER, J. & DRILLER, H. 2004. Ectoine: An effective natural substance to prevent UVA-induced premature photoaging. *Skin Pharmacology & Physiology,* 17**,** 232-237.
BYE, J. W., BAXTER, N. J., HOUNSLOW, A. M., FALCONER, R. J. & WILLIAMSON, M. P. 2016. Molecular mechanism for the Hofmeister effect derived from NMR and DSC measurements on barnase. *ACS Omega,* 1**,** 669-679.
BYE, J. W. & FALCONER, R. J. 2015. A study of the relationship between water and anions of the Hofmeister series using pressure perturbation calorimetry. *Physical Chemistry Chemical Physics,* 17**,** 14130-14137.
BYE, J. W., MELIGA, S., FERACHOU, D., CINQUE, G., ZEITLER, J. A. & FALCONER, R. J. 2014. Analysis of the hydration water around bovine serum albumin using terahertz coherent synchrotron radiation. *Journal of Physical Chemistry A,* 118**,** 83-88.
CABALLERO-HERRERA, A., NORDSTRAND, K., BERNDT, K. D. & NILSSON, L. 2005. Effect of urea on peptide conformation in water: Molecular dynamics and experimental characterization. *Biophysical Journal,* 89**,** 842-857.
CANCHI, D. R., PASCHEK, D. & GARCIA, A. E. 2010. Equilibrium study of protein denaturation by urea. *Journal of the American Chemical Society,* 132**,** 2338-2344.

CAYLEY, S. & RECORD, M. T. 2003. Roles of cytoplasmic osmolytes, water, and crowding in the response of *Escherichia coli* to osmotic stress: Biophysical basis of osmoprotection by glycine betaine. *Biochemistry,* 42**,** 12596-12609.

COOPER, A., JOHNSON, C. M., LAKEY, J. H. & NOLLMANN, M. 2001. Heat does not come in different colours: entropy-enthalpy compensation, free energy windows, quantum confinement, pressure perturbation calorimetry, solvation and the multiple causes of heat capacity effects in biomolecular interactions. *Biophysical Chemistry,* 93**,** 215-230.

COURTENAY, E. S., CAPP, M. W., ANDERSON, C. F. & RECORD, M. T. 2000. Vapor pressure osmometry studies of osmolyte-protein interactions: Implications for the action of osmoprotectants in vivo and for the interpretation of "osmotic stress" experiments in vitro. *Biochemistry,* 39**,** 4455-4471.

CURTIS, R. A., ULRICH, J., MONTASER, A., PRAUSNITZ, J. M. & BLANCH, H. W. 2002. Protein-protein interactions in concentrated electrolyte solutions - Hofmeister series effects. *Biotechnology and Bioengineering,* 79**,** 367-380.

DAGGETT, V. 2006. Protein folding-simulation. *Chemical Reviews,* 106**,** 1898-1916.

DE SANCHO, D., DOSHI, U. & MUNOZ, V. 2009. Protein folding rates and stability: How much is there beyond size? *Journal of the American Chemical Society,* 131**,** 2074-2075.

DELONG, E. F., FRANKS, D. G. & YAYANOS, A. A. 1997. Evolutionary relationships of cultivated psychrophilic and barophilic deep-sea bacteria. *Applied and Environmental Microbiology,* 63**,** 2105-2108.

DILL, K. A. 1990. Dominant forces in protein folding. *Biochemistry,* 29**,** 7133-7155.

DILL, K. A. & SHORTLE, D. 1991. Denatured states of proteins. *Annual Review of Biochemistry,* 60**,** 795-825.

EDMANDS, S. D., HUGHS, K. S., LEE, S. Y., MEYER, S. D., SAARI, E. & YANCEY, P. H. 1995. Time dependent aspects of osmolyte changes in rat kidney, urine, blood and lens with sorbinil and galactose feeding. *Kidney International,* 48**,** 344-353.

EIBERWEISER, A., NAZET, A., KRUCHININ, S. E., FEDOTOVA, M. V. & BUCHNER, R. 2015. Hydration and ion binding of the osmolyte ectoine. *Journal of Physical Chemistry B,* 119**,** 15203-15211.

FELITSKY, D. J., CANNON, J. G., CAPP, M. W., HONG, J., VAN WYNSBERGHE, A. W., ANDERSON, C. F. & RECORD, M. T. 2004. The exclusion of glycine betaine from anionic biopolymer surface: Why glycine betaine is an effective osmoprotectant but also a compatible solute. *Biochemistry,* 43**,** 14732-14743.

FELITSKY, D. J. & RECORD, M. T. 2003. Thermal and urea induced unfolding of the marginally stable lac repressor DNA binding domain: A model system for analysis of solute effects on protein processes. *Biochemistry,* 42**,** 2202-2217.

GALLAGHER, K. R. & SHARP, K. A. 2003. A new angle on heat capacity changes in hydrophobic solvation. *Journal of the American Chemical Society,* 125**,** 9853-9860.

GUINN, E. J., PEGRAM, L. M., CAPP, M. W., POLLOCK, M. N. & RECORD, M. T. 2011. Quantifying why urea is a protein denaturant, whereas glycine betaine is a protein stabilizer. *Proceedings of the National Academy of Sciences of the United States of America,* 108**,** 16932-16937.

HAHN, M. B., SOLOMUN, T., WELLHAUSEN, R., HERMANN, S., SEITZ, H., MEYER, S., KUNTE, H. J., ZEMAN, J., UHLIG, F., SMIATEK, J. & STURM, H. 2015. Influence of the compatible solute ectoine on the local water structure: implications for the binding of the protein G5P to DNA. *Journal of Physical Chemistry B,* 119**,** 15212-15220.

HAHN, M. B., UHLIG, F., SOLOMUN, T., SMIATEK, J. & STURM, H. 2016. Combined influence of ectoine and salt: spectroscopic and numerical evidence for compensating effects on aqueous solutions. *Physical Chemistry Chemical Physics,* 18**,** 28398-28402.

HERZOG, M., DWIVEDI, M., KUMAR HARISHCHANDRA, R., BILSTEIN, A., GALLA, H.-J. & WINTER, R. 2019. Effect of ectoine, hydroxyectoine and beta-hydroxybutyrate on the temperature and pressure stability of phospholipid bilayer membranes of different complexity. *Colloids and surfaces. B, Biointerfaces,* 178**,** 404-411.

HIPPEL, V. & SCHLEICH, T. 1969. Ion effects on solution structure of biological macromolecules. *Accounts of Chemical Research,* 2**,** 257-265.

HOFMEISTER, F. 1888. *Arch Exp Pathol Pharmakol,* 25**,** 1-30.

HOLTHAUZEN, L. M. F. & BOLEN, D. W. 2007. Mixed osmolytes: The degree to which one osmolyte affects the protein stabilizing ability of another. *Protein Science,* 16**,** 293-298.

HONG, J., CAPP, M. W., ANDERSON, C. F., SAECKER, R. M., FELITSKY, D. J., ANDERSON, M. W. & RECORD, M. T. 2004. Preferential interactions of glycine betaine and of urea with DNA: Implications for DNA hydration and for effects of these solutes on DNA stability. *Biochemistry,* 43**,** 14744-14758.

HU, C. Q., STURTEVANT, J. M., THOMSON, J. A., ERICKSON, R. E. & PACE, C. N. 1992. Thermodynamics of ribonuclease-t1 denaturation. *Biochemistry,* 31**,** 4876-4882.

HU, C. Y., KOKUBO, H., LYNCH, G. C., BOLEN, D. W. & PETTITT, B. M. 2010. Backbone additivity in the transfer model of protein solvation. *Protein Science,* 19**,** 1011-1022.

HU, C. Y., PETTITT, B. M. & ROESGEN, J. 2009. Osmolyte solutions and protein folding. *F1000 biology reports,* 1**,** 41.

HUA, L., ZHOU, R. H., THIRUMALAI, D. & BERNE, B. J. 2008. Urea denaturation by stronger dispersion interactions with proteins than water implies a 2-stage unfolding. *Proceedings of the National Academy of Sciences of the United States of America,* 105**,** 16928-16933.

HUANG, J. R., GABEL, F., JENSEN, M. R., GRZESIEK, S. & BLACKLEDGE, M. 2012. Sequence-specific mapping of the interaction between urea and unfolded ubiquitin from ensemble analysis of NMR and small angle scattering data. *Journal of the American Chemical Society,* 134**,** 4429-4436.

JIAO, Y. F. & SMITH, P. E. 2011. Fluctuation theory of molecular association and conformational equilibria. *Journal of Chemical Physics,* 135.

JUNGWIRTH, P. 2015. Beyond Hofmeister: Interactions between ions and proteins in water. *Abstracts of Papers of the American Chemical Society,* 249.

JUNGWIRTH, P. & CREMER, P. S. 2014. Beyond Hofmeister. *Nature Chemistry,* 6**,** 261-263.

KAUZMANN, W. 1959. Some factors in the interpretation of protein denaturation. *Advances in Protein Chemistry,* 14**,** 1-63.

KEMPF, B. & BREMER, E. 1998. Uptake and synthesis of compatible solutes as microbial stress responses to high-osmolality environments. *Archives of Microbiology,* 170**,** 319-330.

KUMAR, N. & KISHORE, N. 2013. Synergistic behavior of glycine betaine-urea mixture: A molecular dynamics study. *Journal of Chemical Physics,* 139**,** 115104.

LIN, T. Y. & TIMASHEFF, S. N. 1994. Why do some organisms use a urea-methylamine mixture as osmolyte - thermodynamic compensation of urea and trimethylamine n-oxide interactions with protein. *Biochemistry,* 33**,** 12695-12701.

LIU, Y. F. & BOLEN, D. W. 1995. The peptide backbone plays a dominant role in protein stabilization by naturally-occurring osmolytes. *Biochemistry,* 34**,** 12884-12891.

MAEDA, Y., YAMADA, H., UEDA, T. & IMOTO, T. 1996. Effect of additives on the renaturation of reduced lysozyme in the presence of 4 M urea. *Protein Engineering,* 9**,** 461-465.

MEERSMAN, F., BOWRON, D., SOPER, A. K. & KOCH, M. H. J. 2009. Counteraction of urea by trimethylamine N-oxide is due to direct interaction. *Biophysical Journal,* 97**,** 2559-2566.

MEERSMAN, F., BOWRON, D., SOPER, A. K. & KOCH, M. H. J. 2011. An X-ray and neutron scattering study of the equilibrium between trimethylamine N-oxide and urea in aqueous solution. *Physical Chemistry Chemical Physics,* 13**,** 13765-13771.

MELANDER, W. & HORVATH, C. 1977. Salt effects on hydrophobic interactions in precipitation and chromatography of proteins - interpretation of lyotropic series. *Archives of Biochemistry and Biophysics,* 183**,** 200-215.

MEYER, S., SCHROETER, M. A., HAHN, M. B., SOLOMUN, T., STURM, H. & KUNTE, H. J. 2017. Ectoine can enhance structural changes in DNA in vitro. *Scientific Reports,* 7, 15272.

MOUNTAIN, R. D. & THIRUMALAI, D. 2003. Molecular dynamics simulations of end-to-end contact formation in hydrocarbon chains in water and aqueous urea solution. *Journal of the American Chemical Society,* 125**,** 1950-1957.

MUKHERJEE, A., SANTRA, M. K., BEURIA, T. K. & PANDA, D. 2005. A natural osmolyte trimethylamine N-oxide promotes assembly and bundling of the bacterial cell division protein, FtsZ and counteracts the denaturing effects of urea. *Febs Journal,* 272**,** 2760-2772.

MYERS, J. K., PACE, C. N. & SCHOLTZ, J. M. 1995. Denaturant m-values and heat-capacity changes - relation to changes in accessible surface-areas of protein unfolding. *Protein Science,* 4**,** 2138-2148.

NOZAKI, Y. & TANFORD, C. 1963. Solubility of amino acids and related compounds in aqueous urea solutions. *Journal of Biological Chemistry,* 238**,** 4074-81.

OKUR, H. I., HLADILKOVA, J., REMBERT, K. B., CHO, Y., HEYDA, J., DZUBIELLA, J., CREMER, P. S. & JUNGWIRTH, P. 2017. Beyond the Hofmeister series: ion-specific effects on proteins and their biological functions. *Journal of Physical Chemistry B,* 121**,** 1997-2014.

OPRZESKA-ZINGREBE, E. A., KOHAGEN, M., KASTNER, J. & SMIATEK, J. 2019. Unfolding of DNA by co-solutes: insights from Kirkwood-Buff integrals and transfer free energies. *European Physical Journal-Special Topics,* 227**,** 1665-1679.

OPRZESKA-ZINGREBE, E. A., MEYER, S., ROLOFF, A., KUNTE, H.-J. & SMIATEK, J. 2018. Influence of compatible solute ectoine on distinct DNA structures: thermodynamic insights into molecular binding mechanisms and destabilization effects. *Physical Chemistry Chemical Physics,* 20**,** 25861-25874.

PACE, C. N., FU, H. L., FRYAR, K. L., LANDUA, J., TREVINO, S. R., SCHELL, D., THURLKILL, R. L., IMURA, S., SCHOLTZ, J. M., GAJIWALA, K., SEVCIK, J., URBANIKOVA, L., MYERS, J. K., TAKANO, K., HEBERT, E. J., SHIRLEY, B. A. & GRIMSLEY, G. R. 2014a. Contribution of hydrogen bonds to protein stability. *Protein Science,* 23**,** 652-661.

PACE, C. N., SCHOLTZ, J. M. & GRIMSLEY, G. R. 2014b. Forces stabilizing proteins. *Febs Letters,* 588**,** 2177-2184.

PANDYA, M. J., SCHIFFERS, S., HOUNSLOW, A. M., BAXTER, N. J. & WILLIAMSON, M. P. 2018. Why the energy landscape of barnase is hierarchical. *Frontiers in Molecular Biosciences,* 5, 115.

PAUL, S. & PATEY, G. N. 2007a. Structure and interaction in aqueous urea-trimethylamine-N-oxide solutions. *Journal of the American Chemical Society,* 129**,** 4476-4482.

PAUL, S. & PATEY, G. N. 2007b. The influence of urea and trimethylamine-N-oxide on hydrophobic interactions. *Journal of Physical Chemistry B,* 111**,** 7932-7933.
PAUL, S. & PATEY, G. N. 2008. Hydrophobic interactions in urea - Trimethylamine-N-oxide solutions. *Journal of Physical Chemistry B,* 112**,** 11106-11111.
PEGRAM, L. M., WENDORFF, T., ERDMANN, R., SHKEL, I., BELLISSIMO, D., FELITSKY, D. J. & RECORD, M. T. 2010. Why Hofmeister effects of many salts favor protein folding but not DNA helix formation. *Proceedings of the National Academy of Sciences of the United States of America,* 107**,** 7716-7721.
PLUHAROVA, E., LAAGE, D. & JUNGWIRTH, P. 2017. Size and origins of long-range orientational water correlations in dilute aqueous salt solutions. *Journal of Physical Chemistry Letters,* 8**,** 2031-2035.
PRIVALOV, P. L. 1990. Cold denaturation of proteins. *Critical Reviews in Biochemistry and Molecular Biology,* 25**,** 281-305.
RATNAPARKHI, G. S. & VARADARAJAN, R. 2001. Osmolytes stabilize ribonuclease S by stabilizing its fragments S protein and S peptide to compact folding-competent states. *Journal of Biological Chemistry,* 276**,** 28789-28798.
RECORD, M. T., COURTENAY, E. S., CAYLEY, D. S. & GUTTMAN, H. J. 1998. Responses of *E. coli* to osmotic stress: Large changes in amounts of cytoplasmic solutes and water. *Trends in Biochemical Sciences,* 23**,** 143-148.
REZUS, Y. L. A. & BAKKER, H. J. 2009. Destabilization of the hydrogen-bond structure of water by the osmolyte trimethylamine N-oxide. *Journal of Physical Chemistry B,* 113**,** 4038-4044.
ROBINSON, D. R. & JENCKS, W. P. 1965. Effect of concentrated salt solutions on activity coefficient of acetyltetraglycine ethyl ester. *Journal of the American Chemical Society,* 87**,** 2470-2479.
ROSGEN, J. & JACKSON-ATOGI, R. 2012. Volume exclusion and H-bonding dominate the thermodynamics and solvation of trimethylamine-N-oxide in aqueous urea. *Journal of the American Chemical Society,* 134**,** 3590-3597.
ROYCHOUDHURY, A., HAUSSINGER, D. & OESTERHELT, F. 2012. Effect of the compatible solute ectoine on the stability of the membrane proteins. *Protein and Peptide Letters,* 19**,** 791-794.
SALADINO, G., PIERACCINI, S., RENDINE, S., RECCA, T., FRANCESCATO, P., SPERANZA, G. & SIRONI, M. 2011. Metadynamics study of a beta-hairpin stability in mixed solvents. *Journal of the American Chemical Society,* 133**,** 2897-2903.
SANTORO, M. M., LIU, Y. F., KHAN, S. M. A., HOU, L. X. & BOLEN, D. W. 1992. Increased thermal stability of proteins in the presence of naturally occurring osmolytes. *Biochemistry,* 31**,** 5278-5283.
SARMA, R. & PAUL, S. 2011. Hydrophobic interactions in presence of osmolytes urea and trimethylamine-N-oxide. *Journal of Chemical Physics,* 135**,** 174501.
SARMA, R. & PAUL, S. 2013. Exploring the molecular mechanism of trimethylamine-N-oxide's ability to counteract the protein denaturing effects of urea. *Journal of Physical Chemistry B,* 117**,** 5691-5704.
SHIMIZU, S. 2004. Estimating hydration changes upon biomolecular reactions from osmotic stress, high pressure, and preferential hydration experiments. *Proceedings of the National Academy of Sciences of the United States of America,* 101**,** 1195-1199.
SHIMIZU, S. & MATUBAYASI, N. 2006. Preferential hydration of proteins: A Kirkwood-Buff approach. *Chemical Physics Letters,* 420**,** 518-522.
SHIMIZU, S. & SMITH, D. J. 2004. Preferential hydration and the exclusion of cosolvents from protein surfaces. *Journal of Chemical Physics,* 121**,** 1148-1154.

SHIMIZU, S., STENNER, R. & MATUBAYASI, N. 2017. Gastrophysics: Statistical thermodynamics of biomolecular denaturation and gelation from the Kirkwood-Buff theory towards the understanding of tofu. *Food Hydrocolloids,* 62**,** 128-139.

SINGH, L. R., DAR, T. A., HAQUE, I., ANJUM, F., MOOSAVI-MOVAHEDI, A. A. & AHMAD, F. 2007. Testing the paradigm that the denaturing effect of urea on protein stability is offset by methylamines at the physiological concentration ratio of 2 : 1 (urea : methylamines). *Biochimica Et Biophysica Acta-Proteins and Proteomics,* 1774**,** 1555-1562.

SMIATEK, J. 2014. Osmolyte effects: impact on the aqueous solution around charged and neutral spheres. *Journal of Physical Chemistry B,* 118**,** 771-782.

SMIATEK, J., HARISHCHANDRA, R. K., RUBNER, O., GALLA, H. J. & HEUER, A. 2012. Properties of compatible solutes in aqueous solution. *Biophysical Chemistry,* 160**,** 62-68.

SMITH, J. D., SAYKALLY, R. J. & GEISSLER, P. L. 2007. The effects of dissolved halide anions on hydrogen bonding in liquid water. *Journal of the American Chemical Society,* 129**,** 13847-13856.

SOMERO, G. N. 1986. Protons, osmolytes, and fitness of internal milieu for protein function. *American Journal of Physiology,* 251**,** R197-R213.

STREET, T. O., BOLEN, D. W. & ROSE, G. D. 2006. A molecular mechanism for osmolyte-induced protein stability. *Proceedings of the National Academy of Sciences of the United States of America,* 103**,** 13997-14002.

STUMPE, M. C. & GRUBMULLER, H. 2007. Interaction of urea with amino acids: Implications for urea-induced protein denaturation. *Journal of the American Chemical Society,* 129**,** 16126-16131.

TADEO, X., PONS, M. & MILLET, O. 2007. Influence of the Hofmeister anions on protein stability as studied by thermal denaturation and chemical shift perturbation. *Biochemistry,* 46**,** 917-923.

TIMASHEFF, S. N. 1993. The control of protein stability and association by weak interactions with water: how do solvents affect these processes? *Annual Review of Biophysics and Biomolecular Structure,* 22, 67-97.

TIMASHEFF, S. N. 1998. Control of protein stability and reactions by weakly interacting cosolvents: The simplicity of the complicated. *In:* DICERA, E. (ed.) *Advances in Protein Chemistry, Vol 51: Linkage Thermodynamics of Macromolecular Interactions.* San Diego: Elsevier Academic Press Inc.

TIMASHEFF, S. N. 2002. Protein-solvent preferential interactions, protein hydration, and the modulation of biochemical reactions by solvent components. *Proceedings of the National Academy of Sciences of the United States of America,* 99**,** 9721-9726.

TSAI, C. J., MAIZEL, J. V. & NUSSINOV, R. 2002. The hydrophobic effect: A new insight from cold denaturation and a two-state water structure. *Critical Reviews in Biochemistry and Molecular Biology,* 37**,** 55-69.

VENKATESU, P., LEE, M. J. & LIN, H. M. 2007. Thermodynamic characterization of the osmolyte effect on protein stability and the effect of GdnHCl on the protein denatured state. *Journal of Physical Chemistry B,* 111**,** 9045-9056.

VENKATESU, P., LEE, M. J. & LIN, H. M. 2009. Osmolyte counteracts urea-induced denaturation of alpha-chymotrypsin. *Journal of Physical Chemistry B,* 113**,** 5327-5338.

VENTOSA, A., NIETO, J. J. & OREN, A. 1998. Biology of moderately halophilic aerobic bacteria. *Microbiology and Molecular Biology Reviews,* 62**,** 504-544.

WEI, H. Y., FAN, Y. B. & GAO, Y. Q. 2010. Effects of urea, tetramethyl urea, and trimethylamine N-oxide on aqueous solution structure and solvation of protein

backbones: a molecular dynamics simulation study. *Journal of Physical Chemistry B,* 114**,** 557-568.
WILLIAMSON, M. P. 2013. Using chemical shift perturbation to characterise ligand binding. *Progress in Nuclear Magnetic Resonance Spectroscopy,* 73**,** 1-16.
WITHERS, P. C. & GUPPY, M. 1996. Do Australian desert frogs co-accumulate counteracting solutes with urea during aestivation? *Journal of Experimental Biology,* 199**,** 1809-1816.
WITTMAR, J., MEYER, S., SIELING, T., KUNTE, J., SMIATEK, J. & BRAND, I. 2020. What does ectoine do to DNA? A molecular-scale picture of compatible solute-biopolymer interactions. *Journal of Physical Chemistry B,* 124**,** 7999-8011.
YANCEY, P. H. 2001. Water stress, osmolytes and proteins. *American Zoologist,* 41**,** 699-709.
YANCEY, P. H. 2005. Organic osmolytes as compatible, metabolic and counteracting cytoprotectants in high osmolarity and other stresses. *Journal of Experimental Biology,* 208**,** 2819-2830.
YANCEY, P. H., BLAKE, W. R. & CONLEY, J. 2002. Unusual organic osmolytes in deep-sea animals: adaptations to hydrostatic pressure and other perturbants. *Comparative Biochemistry and Physiology a-Molecular and Integrative Physiology,* 133**,** 667-676.
YANCEY, P. H., CLARK, M. E., HAND, S. C., BOWLUS, R. D. & SOMERO, G. N. 1982. Living with water stress - evolution of osmolyte systems. *Science,* 217**,** 1214-1222.
YANCEY, P. H., RHEA, M. D., KEMP, K. M. & BAILEY, D. M. 2004. Trimethylamine oxide, betaine and other osmolytes in deep-sea animals: Depth trends and effects on enzymes under hydrostatic pressure. *Cellular and Molecular Biology,* 50**,** 371-376.
YANCEY, P. H. & SOMERO, G. N. 1979. Counteraction of urea destabilization of protein-structure by methylamine osmoregulatory compounds of elasmobranch fishes. *Biochemical Journal,* 183**,** 317-323.
YANCEY, P. H. & SOMERO, G. N. 1980. Methylamine osmoregulatory solutes of elasmobranch fishes counteract urea inhibition of enzymes. *Journal of Experimental Zoology,* 212**,** 205-213.
YANG, L. J. & GAO, Y. Q. 2010. Effects of cosolvents on the hydration of carbon nanotubes. *Journal of the American Chemical Society,* 132**,** 842-848.
YAO, W., WANG, K. Y., WU, A. D., REED, W. F. & GIBB, B. C. 2021. Anion binding to ubiquitin and its relevance to the Hofmeister effects. *Chemical Science,* 12**,** 320-330.
YAYANOS, A. A., DIETZ, A. S. & VANBOXTEL, R. 1979. Isolation of a deep sea barophilic bacterium and some of its growth-characteristics. *Science,* 205**,** 808-810.
YIN, M., PALMER, H. R., FYFE-JOHNSON, A. L., BEDFORD, J. J., SMITH, R. A. J. & YANCEY, P. H. 2000. Hypotaurine, N-methyltaurine, taurine, and glycine betaine as dominant osmolytes of vestimentiferan tubeworms from hydrothermal vents and cold seeps. *Physiological and Biochemical Zoology,* 73**,** 629-637.
YU, I. & NAGAOKA, M. 2004. Slowdown of water diffusion around protein in aqueous solution with ectoine. *Chemical Physics Letters,* 388**,** 316-321.
ZACCAI, G., BAGYAN, I., COMBET, J., CUELLO, G. J., DEME, B., FICHOU, Y., GALLAT, F. X., JOSA, V. M. G., VON GRONAU, S., HAERTLEIN, M., MARTEL, A., MOULIN, M., NEUMANN, M., WEIK, M. & OESTERHELT, D. 2016. Neutrons describe ectoine effects on water H-bonding and hydration around a soluble protein and a cell membrane. *Scientific Reports,* 6, 31434.
ZALAR, M., SVILENOV, H. L. & GOLOVANOV, A. P. 2020. Binding of excipients is a poor predictor for aggregation kinetics of biopharmaceutical proteins. *European Journal of Pharmaceutics and Biopharmaceutics,* 151**,** 127-136.
ZETTERHOLM, S. G., VERVILLE, G. A., BOUTWELL, L., BOLAND, C., PRATHER, J. C., BETHEA, J., CAULEY, J., WARREN, K. E., SMITH, S. A., MAGERS, D. H. &

HAMMER, N. I. 2018. Noncovalent interactions between trimethylamine N-oxide (TMAO), urea, and water. *Journal of Physical Chemistry B,* 122**,** 8805-8811.

ZHANG, N., LIU, F. F., DONG, X. Y. & SUN, Y. 2012. Molecular insight into the counteraction of trehalose on urea-induced protein denaturation using molecular dynamics simulation. *Journal of Physical Chemistry B,* 116**,** 7040-7047.

ZHANG, Y. J. & CREMER, P. S. 2010. Chemistry of hofmeister anions and osmolytes. *Annual Review of Physical Chemistry, Vol 61,* 61**,** 63-83.

ZOU, Q., BENNION, B. J., DAGGETT, V. & MURPHY, K. P. 2002. The molecular mechanism of stabilization of proteins by TMAO and its ability to counteract the effects of urea. *Journal of the American Chemical Society,* 124**,** 1192-1202.